




ADVERTIMENT. L'accés als continguts d'aquesta tesi queda condicionat a l'acceptació de les condicions d'ús establertes per la següent llicència Creative Commons:  <https://creativecommons.org/licenses/?lang=ca>

ADVERTENCIA. El acceso a los contenidos de esta tesis queda condicionado a la aceptación de las condiciones de uso establecidas por la siguiente licencia Creative Commons:  <https://creativecommons.org/licenses/?lang=es>

WARNING. The access to the contents of this doctoral thesis it is limited to the acceptance of the use conditions set by the following Creative Commons license:  <https://creativecommons.org/licenses/?lang=en>



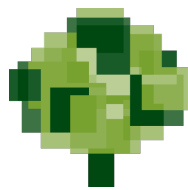
Process-based insights
into insect responses
to climate change:

Linking
microclimate,
ecophysiology,
and demography
in a butterfly model system

Maria Vives Ingla



UAB



CREAF



EXCEL·LÈNCIA
SEVERO
OCHOA

Universitat Autònoma de Barcelona
Centre de Recerca Ecològica i Aplicacions Forestals
PhD in Terrestrial Ecology

Process-based insights into insect responses to climate change

Linking microclimate, ecophysiology, and demography in a
butterfly model system

Doctoral Dissertation of:
Maria Vives Ingla

Advisors:
Prof. Jofre Carnicer Cols
Prof. Josep Peñuelas Reixach

September 2023



It is interesting to contemplate an entangled bank, clothed with many plants of many kinds, with birds singing on the bushes, with various insects flitting about, and with worms crawling through the damp earth, and to reflect that these elaborately constructed forms, so different from each other, and dependent on each other in so complex a manner, have all been produced by laws acting around us.

Charles Darwin

La naturaleza que me gusta definir como el tapiz de la vida, del que formamos parte, que nos entreteje y nos atraviesa. Y esto no es simplemente una frase poética. [...] Digo que el tapiz de la vida nos entreteje y nos atraviesa porque eso es lo que indica la más completa y actualizada evidencia científica. La naturaleza es fundamentalmente relaciones, es un construir y moler y rehacer siempre con los mismos materiales. Todas las personas que estamos aquí, y también los bacalaos, los tigres, las lombrices, los tomates que languidecen en el supermercado y las levaduras que levantan el pan, estamos hechos con los mismos átomos que se vienen tejiendo y destejiendo y retejiendo desde hace millones de años.

Sandra Díaz

En résumé, c'est un puzzle de centaines de millions de données différentes. Non pas une science hypothéticodéductive comme le disaient les philosophes d'autrefois. C'est une science d'assemblage de données multiples, dont la solidité est analogue à celle d'un tapis tissé de mille fils.

Bruno Latour



Agraïments

Aquesta tesi ha estat possible gràcies als fonaments assentats amb molta visió i compromís científics pel Jofre, el Constantí i el Josep que, després de força anys i la feina de moltes persones, han acabat consolidant un sistema d'estudi ric i robust. La tesi està impregnada de l'energia, la curiositat i l'entrega inacabables del Jofre, de la seva vocació per desgranar cada detall de la història sense perdre'n el fil principal. Gràcies per guiar-me en la complexitat i mantenir sempre una mirada ampla i oberta. El treball també recull el coneixement profund del Constantí en el sistema, que ha enriquit cada un dels capítols de la tesi i que ha permès que una pila d'investigadors disposem de sèries temporals excepcionals i imprescindibles. Del Josep, aquesta tesi s'endú una capa de saber fer senzill i pragmàtic que esmola les paraules i fa efectius tots els esforços. A tots tres, us dono les gràcies per la confiança, dedicació i empenta que m'heu donat.

També vull agrair aquesta tesi al Pol, per l'acollida i suport científics i humans. Gràcies per la teva generositat i per obrir-me les portes a tantes persones fantàstiques com el Chris, el Duncan, el Francesco, l'Ellie, el Marc, el Dongbo, la Beibei, la Sybille, el Roberto i l'Anna. Hi afegeixo també el meu amor cap a tota la xarxa del CREAM i, aquestes darreres setmanes, també de la UB, amb qui ens hem anat acompanyant en contextos constantment canviant i, de vegades, difícils. Especialment a l'Elena, la Txell, l'Alba, la Luciana, la Roser, la Mireia, l'Adrià (el Descals i el Barbeta), el Christian, el Quique, la Laura (la Blanquer i l'Escarmena), el Pepe, el Joan, la Tere, la Lucía, i moltes, moltes altres persones, contínuament d'arribada i de sortida. I encara dins l'àmbit acadèmic, també vull reconèixer totes aquelles iniciatives que contribueixen a construir una ciència més oberta, creïble, compartida i accessible. No vull deixar d'esmentar, també, que aquesta tesi s'ha finançat amb una beca FPU del Ministeri d'Universitats (FPU17/05869). En aquest sentit, agraeixo la feina de tantes persones que han permès que puguem doctorar-nos en unes condicions més dignes i que treballen perquè les tesis deixin de ser un pretext —encara massa sovint— de precarietat, abús i voluntarisme.

Finalment, vull donar les gràcies als meus pares per haver-me desvetllat el plaer d'intentar fer les coses bé i per educar-me en el pensament i l'art, en l'ètica i l'estètica. També al meu germà, pel seu suport incondicional, divertit i ple d'afecte i de música. Al Jordi, per la immensa complicitat i la vida compartida. Moltes gràcies pel teu acompanyament indispensable. A totes les amiguis, teixides per la pila d'anys de convivència, gaudi, escolta i dansa. A la meva família, especialment a la meva àvia, que m'omple de memòries i de bon viure. I a tota l'amalgama i suma d'esdeveniments, contribucions i influències que conflueixen en qualsevol treball i experiència humana.



Per acabar, voldria dedicar aquesta tesi al meu avi Manel, que de ben petita em preguntava què era la vida i amb qui m'hauria agradat seguir pensant respostes. També a la meva tieta Carme, de qui no ens vam poder acomiadar en la fatídica primavera del 2020. Per a ella, el compromís ecològic de la tesi, però també, la seva dimensió estètica. Finalment, també vull dedicar la tesi al meu futur nebot Nil i als altres napbufs de la seva generació —la Nina, l'Anna, el Biel, el Roger, la Bruna, la Lluna, el Xaloc... Tant de bo gaudiu d'una terra viva i habitable.

Barcelona,
setembre 2023



Abstract

Insects are in the warp and weft of the fabric of life on which we rely. Constituting 10% of animal biomass, insects play vital roles in ecological functions within terrestrial and freshwater ecosystems worldwide. However, many insect populations are experiencing declines, jeopardizing their significant contributions to both nature and human societies. These declines are primarily attributed to shifting land uses, habitat loss, agricultural intensification, and, as an increasingly influential factor, climate change.

Decades of research on the impact of climate change on insects have revealed that their responses are multifaceted, influenced by a complex interplay of processes across various scales. However, existing predictive models often overlook the underlying climatic and ecological processes that shape insect exposure and sensitivity. These models frequently aggregate climatic data on broad spatiotemporal scales that do not accurately reflect insects' climatic experiences, which are more tightly linked to the conditions measured in their microhabitats and host plants.

The objective of this thesis is to build more realistic predictive models that depict the current and future impacts of climate change on a well-known insect species—the green-veined white butterfly, *Pieris napi*—in the Mediterranean region. These models will be grounded in fundamental physiological and demographic processes, as well as climatic variations at relevant scales.

The initial chapters (Chapters 2 – 4) entail a combination of intensive field monitoring and experimental methodologies to characterise *P. napi*'s microclimatic exposure and the dynamics of their host plants across diverse populations. Additionally, I examine various phenotypic, physiological, and phenological traits of the butterfly species that determine their susceptibility to climate variations. Findings indicate that, in the northeast of the Iberian Peninsula, *P. napi* populations are predominantly influenced by summer drought. This region showcases a geographical mosaic of populations experiencing growth, stability, and decline. Notably, mid-elevation populations, that are not in decline, encounter more moderate and buffered microclimates than their lowland, declining counterparts. Moreover, these populations have continuous access to fresh host plants, unlike the lowland locations, where host plants wither in early summer and regenerate only in late summer. Consequently, declining lowland populations confront a period of food scarcity driven by summer climatic conditions. Wing size of *P. napi* shows a marked reduction during summer only in the declining populations, serving as an effective phenotypic biomarker of the different population vulnerability to summer impacts. Empirical observations highlight that the decline of certain *P. napi* populations stems from intricate interactions between the butterflies' physiological responses to microclimatic thermal exposure and the scarcity of host plants induced by drought.

In the subsequent chapters (Chapters 4 and 5), I employ the empirically collected data to parameterise two process-based models. These models aim to forecast the physiological and demographic responses of *P. napi* in the context of current and future climate change, facilitating the assessment of the contribution of

each identified process in shaping the species' responses. The first model employs the species' experimentally estimated thermal tolerance to compute heat-induced mortality in response to fluctuating microclimatic temperatures recorded in the field. Mortality rates caused by extreme thermal stresses are relatively low in declining lowland populations of *P. napi*, despite their limited access to microclimatic buffering. In contrast, a closely-related species, *P. rapae*, experiences much higher predicted thermal mortality due to its preference for adjacent open microhabitats characterised by extreme temperatures and microclimatic amplification processes. These outcomes underscore the pivotal role microclimatic mosaics and microhabitat choices play in mitigating the impacts of climate change on insects.

The data from previous empirical work are then utilized to build a matrix population model. This second model integrates *P. napi*'s vital rates across its life cycle, considering the effects of extreme microclimatic heat exposure and drought-induced scarcity of host plants on larval mortality and pupation. The model initially simulates present-day regimes of microclimatic heat extremes, drought, and their concurrent action (i.e. extreme hot-dry compound events). Results indicate that the existing declines in certain *P. napi* populations are primarily driven by drought-induced effects on host plants, corroborating prior field observations and highlighting the critical role indirect processes play in mediating insect responses to climate change. Subsequently, the model forecasts future regimes of extreme events under increasing global warming levels. These future scenarios anticipate a rise in the frequency of currently low-likelihood high-impact events relative to more moderate and recurrent extremes. Due to the nonlinear relationship between temperature and heat-induced mortality, simulations predict that under a global warming trajectory not aligned with the Paris Agreement, these low-probability, high-impact heat events will trigger more extensive and severe declines in *P. napi* populations. This effect could potentially surpass the impact of drought-induced plant scarcity.

In conclusion, this thesis underscores the value of employing process-based models that leverage field and experimental data to predict insect responses to climate change. The predictive models developed herein unravel the core underlying processes identified in empirical studies and quantify their individual and combined influences. Furthermore, these process-based models unveil an overlooked threat to insect populations: the disproportional escalation of low-likelihood high-impact extreme heat events. The generalizability of the thesis' findings and the utility of process-based models are subsequently discussed and contrasted with more commonly used correlative and coarse-grained approaches, which would not have been able to project the nonlinear impacts of these extraordinary events.

Resum en català

Els insectes constitueixen l'ordit i la trama del tapís de la vida del qual depenem. Representant el 10% de la biomassa animal, els insectes juguen rols vitals en el funcionament dels ecosistemes terrestres i d'aigua dolça arreu del món. Tot i així, moltes poblacions d'insectes estan en declivi, fet que posa en perill les seves contribucions significatives a la natura i a les societats humans. Aquests declivis s'atribueixen principalment als canvis recents en els usos del sòl, la pèrdua d'hàbitats, la intensificació agrícola i, de manera cada cop més important, el canvi climàtic.

Dècades de recerca sobre els impactes del canvi climàtic en els insectes han revelat que les seves respostes són polifacètiques i estan influenciades per un entramat complex de processos a diverses escales. Tot i així, els models predictius existents solen ometre els processos ecològics i climàtics subjacents que modulen la seva exposició i sensibilitat climàtiques. A part, aquests models sovint agreguen les dades climàtiques a escales espaciotemporals massa grans per a reflectir acuradament l'experiència climàtica dels insectes, la qual està més estretament lligada a les condicions mesurades en els seus microhàbitats i plantes hoste.

L'objectiu d'aquesta tesi es construir models predictius més realistes que il·lustrin els impactes actuals i futurs del canvi climàtic sobre una espècie d'insecte molt coneguda —la blanqueta perfumada, *Pieris napi*— a la regió Mediterrània. Aquests models es bastiran sobre processos fisiològics i demogràfics fonamentals, així com sobre variació climàtica mesurada a escales rellevants.

Els capítols inicials (Capítols 2–4) combinen metodologies tant de mostreig intensiu a camp com d'experimentació per a caracteritzar l'exposició microclimàtica de la *P. napi* i la dinàmica de les seves plantes hoste en diverses poblacions. A més a més, en aquests capítols també examino la variació de trets fenotípics, fisiològics i fenològics de l'espècie determinants de la seva susceptibilitat climàtica. Els resultats indiquen que, al nord-est de la Península Ibèrica, les poblacions de *P. napi* estan predominantment influenciades per la sequera estival. Aquesta regió presenta un mosaic geogràfic de poblacions en creixement, estables i en declivi. Notablement, les poblacions de muntanya mitjana, que no estan en declivi, tenen a l'abast microclimes més moderats i tamponats que les poblacions reculants de terra baixa. A més a més, les primeres tenen accés continu a plantes hoste fresques, a diferència dels indrets de terra baixa, on les plantes hoste es marceixen a principis d'estiu i no es regeneren fins a finals d'estiu. En conseqüència, les poblacions en declivi de terra baixa s'enfronten a un període d'escassetat d'aliments regulat per les condicions climàtiques estivals. La mida alar de la *P. napi* també mostra una reducció marcada durant l'estiu només a les poblacions estivals, fet que la converteix en un biomarcador fenotípic efectiu de la diferent vulnerabilitat que mostren les poblacions als impactes estivals. Així doncs, les observacions empíriques remarquen que el declivi d'algunes poblacions de *P. napi* resulta d'interaccions complexes i intricades entre les respostes fisiològiques de les papallones a l'exposició tèrmica microclimàtica i l'escassetat de plantes hoste que la sequera provoca.

En els capítols subseqüents (Capítols 4 i 5), utilitzo les dades recollides empíricament per a parametritzar dos models basats en processos. Aquests models tenen per objectiu predir les respostes fisiològiques i demogràfiques de la *P. napi* en el context actual i futur de canvi climàtic, i així facilitar la valoració de la contribució de cada procés identificat en la modulació de les respostes de l'espècie. El primer model utilitza la tolerància tèrmica estimada experimentalment per a computar la mortalitat induïda per altes temperatures en resposta a les temperatures fluctuants mesurades el camp a escala microclimàtica. Les taxes de mortalitat causades pels estressos tèrmics extrems són relativament baixes a les poblacions de terra baixa en declivi de *P. napi*, tot i el seu accés limitat a l'amortiment microclimàtic. En canvi, una espècie propera filogenèticament, la *P. rapae*, experimenta una mortalitat tèrmica més elevada a causa de la seva preferència per microhàbitats adjacents més oberts i subjectes a temperatures extremes i processos d'amplificació microclimàtica. Aquests resultats destaquen el rol central que els mosaics microclimàtics i la selecció de microhàbitat tenen en la mitigació dels impactes del canvi climàtic en els insectes.

Les dades dels treballs empírics anteriors també s'utilitzen per a construir un model matricial de poblacions. Aquest segon model integra les taxes vitals de la *P. napi* al llarg del seu cicle vital considerant els efectes de l'exposició microclimàtica extrema i de l'escassetat de planta hoste induïda per la sequera sobre la mortalitat larval i la pupació. El model inicialment simula els règims actuals de temperatures extremes microclimàtiques, de sequera i la seva acció combinada (esdeveniments extrems compostos de calor i sequera). Els resultats indiquen que els declivis presents en algunes poblacions de *P. napi* estan principalment conduïts pels efectes de la sequera sobre les plantes hoste, fet que corrobora les observacions de camp anteriors i en destaca el rol clau que els processos indirectes poden tenir a l'hora de modular les respostes dels insectes al canvi climàtic. Després, el model prediu la dinàmica de les poblacions en futurs règims d'esdeveniments extrems a nivells creixents d'escalfament global. Aquests escenaris de futur anticipen un creixement en la freqüència d'esdeveniments actualment de baixa versemblança i d'alt impacte en relació a esdeveniments extrems més moderats i recurrents. A causa de la relació no lineal entre la temperatura i la mortalitat induïda per altes temperatures, les simulacions prediuen que en trajectòries de canvi climàtic no alineades amb els Acords de París, aquests esdeveniments de baixa probabilitat i alt impacte poden desencadenar declivis severos i extensos a les poblacions de *Pieris napi*. Aquest efecte podria fins i tot excedir els impactes de l'escassetat de planta induïda per la sequera.

En conclusió, aquesta tesi subratlla el valor d'utilitzar models basats en processos que aprofiten les dades recollides a camp i experimentalment per a predir les respostes dels insectes al canvi climàtic. Els models predictius que hi he desenvolupat desgranen el conjunt de processos subjacents identificats en els estudis empírics i en quantifiquen la seva influència individual i combinada. A més a més, els models que he utilitzat destapen una amenaça a les poblacions d'insectes fins ara ignorada: l'escalada desproporcionada dels esdeveniments extrems de baixa versemblança i alt impacte amb el canvi climàtic. La generalitat dels resultats d'aquesta tesi i la utilitat dels models basats en processos es discuteixen i es contrasten amb les aproximacions correlatives de gra més groller més comunament emprades, les quals no haurien sigut capaces de predir els impactes no lineals d'aquests

esdeveniments tan extraordinaris.

Article references

- **Chapter 2:**

Carnicer, J., C. Stefanescu, M. Vives-Inгла, C. López, S. Cortizas, C. W. Wheat, R. Vila, J. Llusà, and J. Peñuelas. 2019. Phenotypic biomarkers of climatic impacts on declining insect populations: A key role for decadal drought, thermal buffering and amplification effects and host plant dynamics. *Journal of Animal Ecology* 88:376–391. Copyright © 2018, the Authors and Journal of Animal Ecology, John Wiley & Sons Ltd on behalf of the British Ecological Society. doi: 10.1111/1365-2656.12933.

- **Chapter 3:**

Vives-Inгла, M., C. Stefanescu, J. Sala-Garcia, and J. Carnicer. 2020. Plastic and phenological variation of host plants mediates local responses of the butterfly *Pieris napi* to drought in the Mediterranean basin. Pages 113–129 in C. Stefanescu and T. Lafranchis, editors. *Butterfly and moths in l’Empordà and their response to global change*. *Recerca i Territori*.

- **Chapter 4:**

Vives-Inгла, M., J. Sala-Garcia, C. Stefanescu, A. Casadó-Tortosa, M. Garcia, J. Peñuelas, and J. Carnicer. 2023. Interspecific differences in microhabitat use expose insects to contrasting thermal mortality. *Ecological Monographs* 93:e1561. doi: 10.1002/ecm.1561.

and the code and data to replicate the results can be found in Vives-Inгла, M., J. Sala-Garcia, C. Stefanescu, A. Casadó-Tortosa, M. Garcia, J. Peñuelas, and J. Carnicer. 2022. mvives-ingla/ecotones: Interspecific differences in microhabitat use expose insects to contrasting thermal mortality. Zenodo.

- **Chapter 5:**

Vives-Inгла, M., P. Capdevila, C. F. Clements, C. Stefanescu, and J. Carnicer. 2023. Novel regimes of extreme climatic events trigger negative population rates in a common insect. Under review in *Global Change Biology*.

The illustrations for the cover, back cover, and heading pages of the chapters are all in the public domain, and the credits of the works are:

- Introduction: Scroll Cover with Animals, Birds, and Flowers, Song dynasty (960–1279), China.
- Chapter 2: Papilio, 2022, Cesc Biosca, Catalonia.
- Chapter 3: Tapestry Picture, Qing dynasty (1644–1911), China.
- Chapter 4: Scroll Cover with Birds and Flowers, Song dynasty (960–1279), China.
- Chapter 5: Medallion, Qing dynasty (1644–1911), China.
- General Discussion: Panel with the five poisonous creatures, Ming dynasty (1368–1644), Wanli period (1573–1620), China.
- Main conclusions, cover, and back cover: Details from the The Unicorn Rests in a Garden (from the Unicorn Tapestries), 1495–1505, French (cartoon)/South Netherlandish (woven).

Contents

List of Figures	xvii
List of Tables	xix
1 Introduction	1
1.1 Insects, at the core of an unravelling <i>fabric of life</i>	3
1.2 Numerous intertwined processes modulate the impacts of climate change on insects	4
1.3 Process-based approaches require well-established model systems	8
2 Phenotypic biomarkers of climatic impacts on declining insects	21
2.1 Introduction	23
2.2 Materials and methods	25
2.2.1 Study species	25
2.2.2 Study zone	26
2.2.3 Population, climatic, and land cover modelling	26
2.2.4 Phenotypic biomarkers of population vulnerability	27
2.2.5 Common-garden experiment	29
2.2.6 Host plant microsite climatic measures	29
2.2.7 Thermal avoidance behaviour death time experiments	30
2.2.8 Plant trait measurements	31
2.3 Results	32
2.3.1 Climatic and population trends	32
2.3.2 Different population sensitivity to temperature impacts	33
2.3.3 Thermal avoidance behaviour death time experiments	36
2.3.4 Thermal stress during summer drought and microsite effects	37
2.3.5 Host plant resource dynamics	37
2.4 Discussion	39
3 Plastic host-plant variation mediating drought impacts	45
3.1 Introduction	47
3.2 Methods	48
3.2.1 Study system	48
3.2.2 <i>Pieris napi</i> abundance	48
3.2.3 Monitoring of host-plant traits and microclimatic conditions	50

3.2.4	Rain-induced plasticity in host-plant rhizomes	51
3.3	Results	52
3.3.1	Decadal trends and phenology of <i>Pieris napi</i>	52
3.3.2	Phenological and plastic variation of host plants	53
3.3.3	Plastic responses of <i>Lepidium draba</i> rhizomes to rain	55
3.4	Discussion	57
3.4.1	Phenological match between <i>Pieris napi</i> and its two host plants	57
3.4.2	The role of host-plant plasticity in mediating the impacts of drought	59
4	Interspecific differences in microclimatic thermal mortality	63
4.1	Introduction	65
4.2	Materials and methods	69
4.2.1	Study system	69
4.2.2	Oviposition behavior	69
4.2.3	Microclimatic and host-plant variation	70
4.2.4	Ecophysiological assays of heat tolerance	71
4.2.5	Statistical analysis	72
4.2.6	Predictions of thermal mortality in the field	73
4.3	Results	74
4.3.1	Interspecific differences in microhabitat selection	74
4.3.2	Interspecific differences in thermal exposure	74
4.3.3	Sources of thermal heterogeneity at fine scales	77
4.3.4	Host-plant variability	79
4.3.5	Interspecific differences in thermal strategies and mortality	79
4.4	Discussion	83
5	Novel extremes trigger insect declining rates	87
5.1	Introduction	89
5.2	Methods	93
5.2.1	Study system	93
5.2.2	Population matrices	94
5.2.3	Model parametrisation	94
5.2.4	Population projections	95
5.3	Results	100
5.3.1	Observed population growth rates	100
5.3.2	Elasticity analyses and key life stages	101
5.3.3	MPM validation and population forecasting	102
5.3.4	Impacts of extreme LLHI and compound events	103
5.4	Discussion	106
5.4.1	The impacts of LLHI events on insect populations	106
5.4.2	Process-based approaches to study extreme events impacts	108
5.5	Conclusions	111
6	General discussion	113
6.1	Unravelling the processes linking <i>Pieris napi</i> responses to climate change	115

6.1.1	The geographic mosaic of <i>Pieris napi</i> vulnerability to climate change	115
6.1.2	Microclimatic exposure and ecophysiological sensitivity of <i>Pieris napi</i> populations to climate change	116
6.1.3	The role of host plants in mediating climate impacts on <i>Pieris napi</i> populations	118
6.1.4	The relative contribution of extreme temperatures and drought on <i>Pieris napi</i> declines	123
6.1.5	Other processes mediating climate impacts on <i>P. napi</i> populations	125
6.2	Process-based models are useful, but are they usable?	128
6.2.1	Towards an integrative and predictive global ecology	128
6.2.2	The generality of <i>P. napi</i> predicted responses to climate change	129
6.2.3	Overcoming the challenges of consolidating a predictive global ecology	131
6.3	Potential improvements and lines of future research	132
7	Main conclusions	135
A	Chapter 2 - Supporting materials	139
A.1	Supplementary figures and tables	139
A.2	Phenotypic biomarkers of climatic stress	159
A.2.1	Habitat and behavioural thermal buffering, and host plant quality effect	159
B	Chapter 4 - Supporting materials	167
B.1	Characterisation of the host-plant microhabitats	167
B.2	Supplementary tables	169
B.3	Supplementary figures	172
C	Chapter 5 - Supporting materials	191
C.1	Supplementary figures and tables	191
C.2	MPM parametrisation	204
C.2.1	Model structure	204
C.2.2	Juvenile vital rates and growth chamber experiments	206
C.2.3	Adult vital rates	209
C.3	Demographic projections	210
C.3.1	Population projections	210
C.3.2	Net reproductive rates	213
C.3.3	Additional simulations	214
	Bibliography	217

List of Figures

1.1	Drivers of insect declines	5
1.2	The weave of processes shaping insect responses to climate change	7
1.3	<i>Pieris napi</i> study system	13
1.4	Demographic and climatic trends in the <i>Pieris napi</i> study system	14
1.5	A visual summary of the thesis' structure and contents	17
2.1	Climatic and butterfly abundance trends	34
2.2	Empirical trends in the phenotypic biomarker	35
2.3	Macroclimatic and microclimatic June temperatures	38
2.4	Annual variation in host-plant quality	39
2.5	Variation in leaf conductance of lowland host plants	40
3.1	A photograph of the green-veined white	49
3.2	Flight phenology of <i>Pieris napi</i>	53
3.3	Trends in <i>Pieris napi</i> abundance	54
3.4	Seasonal progression of host-plant phenology and condition	55
3.5	Microclimatic and host-plant variation across microhabitats	56
3.6	Resprout dynamics across microhabitats	57
3.7	Plastic responses of <i>Lepidium draba</i> resprouts	58
4.1	Microclimatic exposure, host plants, and thermal tolerance across ecotones	68
4.2	Interspecific differences in the microclimatic thermal regimes	76
4.3	Microclimatic mosaics and fine-scale processes	78
4.4	Soil and foliar water contents in host-plant microhabitats	80
4.5	Interspecific differences in thermal strategies and mortality	82
5.1	Low-likelihood high-impact extremes and their effects	92
5.2	Visual summary of the MPMs	99
5.3	Observed population growth rates	101
5.4	Elasticity analyses of the transition matrix	102
5.5	Observed and predicted R_0 at increasing global warming levels	104
5.6	Predicted effects of different extreme events	105
6.1	Vegetative dynamics of <i>Lepidium draba</i> 's summer resprouts	121
6.2	Drought effects on host-plant dynamics	122
6.3	Host-plant effects on <i>Pieris napi</i> 's wing size	123
6.4	Comparative analysis of insect TDT parameters	131

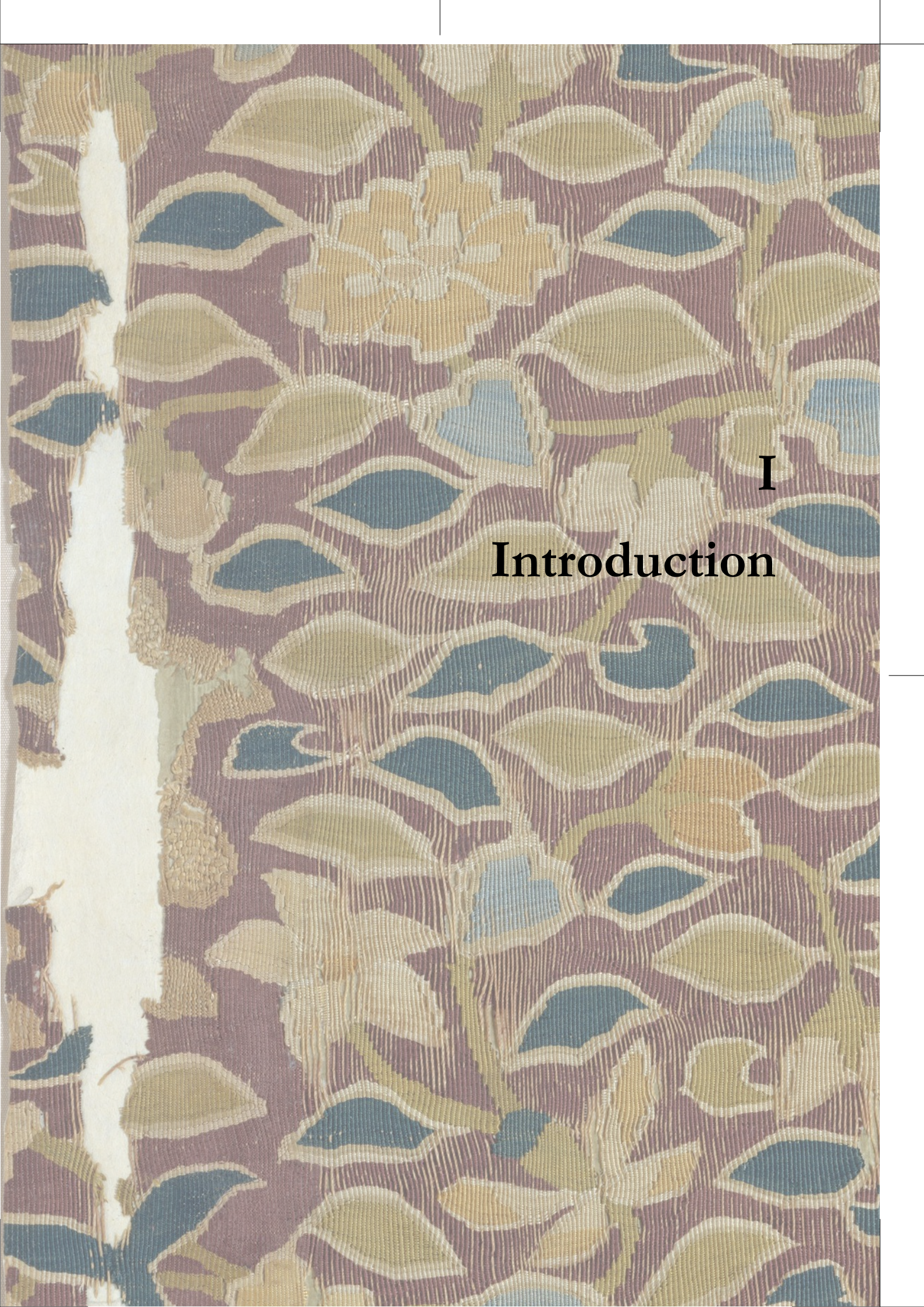
A1	Relation between summer rainfall and temperatures	140
A2	Photographs of the studied site in Ch. 2	141
A3	Wing landmarks	142
A4	Variation in <i>Pieris napi</i> wing condition	143
A5	Variation in mean daily temperatures	144
A6	June climatic conditions over 1994–2015	145
A7	June rainfall over 1997–2007	146
A8	Demographic trends over 1994–2015	147
A9	Effects of thermal treatment on development time	148
A10	Thermal death time curves for <i>Pieris napi</i>	149
A11	Monthly variation in <i>Lepidium draba</i> photosynthetic activity	150
A12	Relation between <i>Lepidium draba</i> phenology and plant quality	151
A13	Relation between butterfly body mass and temperature	152
A14	Definition of phenotypic biomarkers of climatic stress	160
A15	Simulations with the basic performance model	161
A16	Simulated threshold temperature in the basic performance model	162
A17	Simulations with habitat and behavioural buffering	164
A18	Simulations with host-plant stress	165
B1	Location of the studied populations	172
B2	Photographs of the studied microhabitats	173
B3	Vegetation cover of the microhabitats	174
B4	Daily patterns of behaviour of <i>Pieris napi</i> and <i>Pieris rapae</i>	175
B5	Microclimate in the open microhabitat of the lowland site	177
B6	Seasonal and microhabitat trait variation in <i>Lepidium draba</i>	178
B7	Seasonal and microhabitat trait variation in <i>Alliaria petiolata</i>	179
B8	Distribution and skewness of the measured microclimates	180
B9	Thermal heterogeneity at fine scales in the lowland site	181
B10	Reproductive output of the host plants	182
B11	Seasonal dynamics of the host plants	183
B12	Host-plant phenology	184
B13	TDT effects	185
B14	Oposing costs of acute and chronic thermal stress	186
B15	Predicted thermal mortality in the field	188
B16	Predicted development times in the field	189
C1	Mosaic of <i>Pieris napi</i> demographic trends	192
C2	Mean daily microclimatic temperatures	193
C3	Daily predation rates observed in the field	194
C4	Bootstrapped parameters of the transition matrix	195
C5	Projected increase in macroclimatic extremes	196
C6	Supplementary validation of the model	197
C7	The role of LLHI events on <i>Pieris napi</i> declining rates	198
C8	Impacts of extreme events on matrix elasticities	199
C9	Relation between realised fecundity and R_0	200

C10	Comparison between macroclimatic and microclimatic simulations	201
C11	Effects of increasing predation rates on predicted R_0	202

List of Tables

1.1	State of knowledge on the biology of <i>Pieris napi</i>	10
1.2	Main characteristics of the studied populations	19
2.1	OLS model for wing size	36
3.1	Summary of the models for host-plant quality	57
3.2	Summary of the models for foliar temperatures	58
4.1	Oviposition GLMMs models	75
4.2	Thermal death time GLMMs models	81
A1	Main attributes of the studied sites	153
A2	Number of butterfly sample sizes at each site	154
A3	Number of adults obtained in the experiments	154
A4	Summary of the installed data loggers	154
A5	Summary of the meteorological stations	155
A6	Sample size in host-plant stoichiometric analyses	155
A7	OLS models with a single climatic predictor	155
A8	OLS models with two climatic predictors	155
A9	OLS models with climatic and landcover predictors	156
A10	VIF values for the models with climatic predictors	156
A11	VIF values for the models with climatic and landcover predictors	157
A12	Effect sizes in the OLS model in wing size experiments	157
A13	Parameter estimates in the OLS model in wing size experiments	157
A14	Effect sizes in the OLS model in wing size experiments for both sites	158
A15	Parameter estimates in the OLS model in wing size models for both sites	158
A16	Buffering and amplification microclimatic effects	158
A17	Effect sizes in the OLS model in thermal tolerance experiments	158
A18	Parameter values in Fig. A15	162
A19	Parameter values in Fig. A17	163
A20	Parameter values in Fig. A18	166
B1	Microclimatic sensors	169
B2	Oviposition, microclimatic, and host-plant monitored variables	170
B3	Sample size for the TDT curves	171
B4	Oviposition census	171

C ₁	Probability of occurrence of extreme events	203
C ₂	Larval ages in the experiments of host-plant scarcity	204
C ₃	Transition matrices applied in each generation	204



I

Introduction



1.1 Insects, at the core of an unravelling *fabric of life*

Insects represent a major component of living organisms. With about 1 million named species and at least 4.5 million more still unidentified, insects comprise more than 60% of described animals and around a tenth of animal biomass (Bar-On et al., 2018; Stork, 2018; Zhang, 2013a,b). Due to (or resulting in) their great diversity of morphologies and lifestyles, insects are spread across the globe in almost all terrestrial and freshwater ecosystems, where they play numerous important functional roles as herbivores, pollinators, detritivores, parasites, predators, preys, ecosystem engineers, and dispersal agents, among others (Price et al., 2011; Seastedt and Crossley, 1984; Weisser and Siemann, 2007). Insects are thus in “the warp and weft” of the *fabric of life* on which we all depend (*sensu* Díaz, 2022; Díaz et al., 2019).

Despite the key functional roles insects play in most ecological networks of the biosphere, many insect populations have shown rapid declines during the last decades, raising social and scientific concerns (but see Althaus et al., 2021). Insects have gone through numerous large fluctuations since their origin more than 400M years ago (e.g. during glacial and interglacial periods, or after the expansion of human agriculture 10,000 years ago; Coope et al., 1997; Dennis, 1993; Elias, 1991; García-Berro et al., 2023; Wallberg et al., 2014; Webster et al., 2023). Yet, current declining trends are clearly caused by the acceleration in human activity during the past century (Díaz et al., 2019; Raven and Wagner, 2021; Wagner, 2020; Wagner et al., 2021b). Understanding the anthropogenic impacts on insect populations and reversing their declines has thus become of paramount importance to avoid the unravelling of insects’ important contributions to nature and human societies.

Most recent high-profile studies on the topic estimate an overall annual rate of decline in insect abundance around 1% (van Klink et al., 2020a,b; Wagner et al., 2021b). However, reported insect trends vary depending on the region, the temporal baseline of the study, the taxonomic lineage, and insect functional traits (Carnicer et al., 2012; Duchenne et al., 2022; Engelhardt et al., 2022; Høye et al., 2021; Melero et al., 2016; Stefanescu et al., 2011b; Sunde et al., 2023; van Klink et al., 2020a,b; Wagner et al., 2021a). For instance, declining trends have been mainly reported for terrestrial insects, while freshwater insects show increasing abundances in central Europe (Engelhardt et al., 2022). Decreases in abundance are also steeper for cold-adapted species and habitat specialists, although many widespread, common, and generalist species are reducing their abundances too (Melero et al., 2016; Stefanescu et al., 2011b; Wagner et al., 2021a). Overall, despite the fact that not all insect species are declining, the decreases reported for a considerable proportion of populations are already worrying.

The drivers of current insect declines, like in other biological groups, are associated with the increasing human demand for material commodities from nature (Díaz et al., 2019; Jaureguiberry et al., 2022). Concretely, these drivers are habitat loss and deterioration due to land abandonment, deforestation, and urbanisation; agricultural intensification and the increasing use of agrochemicals; pollution; invasive species; and current

climate change (Fig. 1.1; Dicks et al., 2021; Wagner, 2020; Wagner et al., 2021b). In Europe, where long-term surveys and natural collections enable more thorough and extensive assessments of populations trends (Kharouba et al., 2018; Warren et al., 2021), insect declines likely started more than a century ago, following the abandonment of traditional agriculture and the associated landscape changes (Dicks et al., 2021; Habel et al., 2019a,b; Raven and Wagner, 2021; Seibold et al., 2019; Warren et al., 2021). The consequences of the deep transformation in agroecosystems during the recent past are reflected in the steep declines of grassland and heathland butterflies observed in West Europe (Habel et al., 2016; van Strien et al., 2019; van Swaay et al., 2019; Warren et al., 2021). However, as the climate gets warmer and more extreme, the impacts of climate change on insects' trends are expected to rival the effects of land use changes and take a preeminent role in future declines (Engelhardt et al., 2022; Halsch et al., 2021; Harvey et al., 2023; Jørgensen et al., 2022b; Neff et al., 2022).

Crucially, while the role of climate change on insect declines is already acknowledged, our understanding of the underlying processes mediating its impacts on insect populations remains incomplete (Dicks et al., 2021). This knowledge gap is particularly pronounced for extreme climatic events, as they have received far less attention compared to the impacts of gradual changes in mean climatic variables on insect biology (Bastos et al., 2023; Buckley et al., 2023a; Halsch et al., 2021; Harvey et al., 2023; Jentsch et al., 2007; van de Pol et al., 2017; Wagner et al., 2021b). Understanding these underlying processes is fundamental for predicting insect population responses to climate change and its associated extremes. It also lays the groundwork for developing science-based conservation strategies to halt the current trends of insect decline (Buckley et al., 2023a; Urban et al., 2016; van de Pol et al., 2017). To contribute to addressing this pressing challenge, in this thesis, I aim to disentangle the complex weave of processes mediating the effects of climate change on a model insect species in the Mediterranean region and tailor predictive population models explicitly integrating these processes under current and future conditions of global warming.

1.2 Numerous intertwined processes modulate the impacts of climate change on insects

The acceleration in human activity has also caused the ongoing climatic change, which goes hand in hand with the current biodiversity crisis (Díaz, 2022; IPCC, 2021; Pettorelli et al., 2021; Turney et al., 2020). As a result, the mean global surface temperature has already warmed 1.1 °C relative to 1850–1900, triggering rapid changes in many aspects of the climate across the globe (IPCC, 2021). For instance, global warming has altered the global hydrological cycle and large-scale patterns of atmospheric circulation, affecting rainfall distribution, surface humidity, and terrestrial snow cover worldwide (Douville et al., 2021; Gulev et al., 2021). Besides the shifts in the mean values of climatic variables, observed changes in the climate also involve amplified variability, leading to an increased frequency, duration, and intensity of extreme climatic events (IPCC, 2021; Seneviratne

1.2. Numerous intertwined processes modulate the impacts of climate change on insects

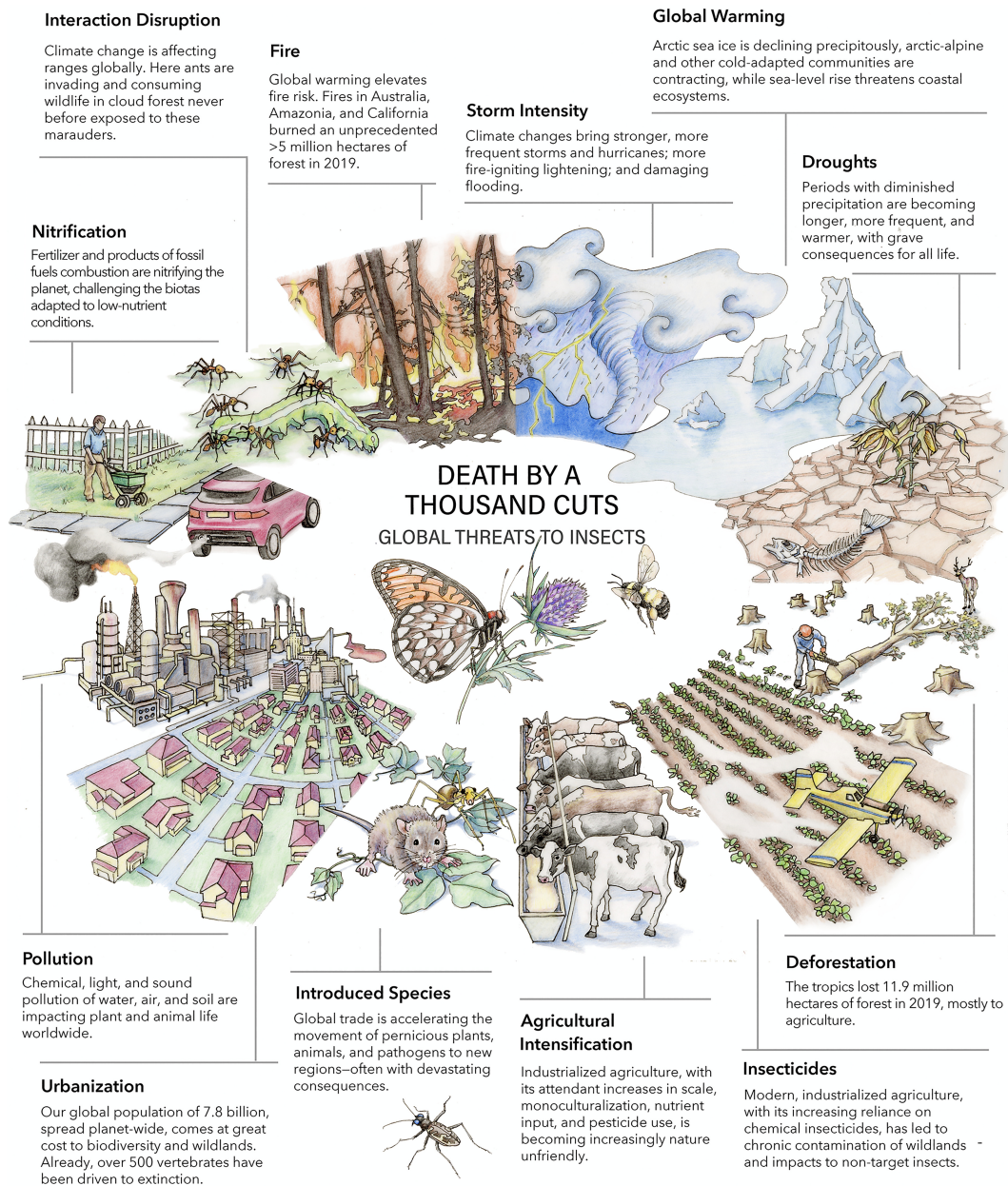


Figure 1.1: Multiple anthropogenic drivers threaten insect populations globally. Most of the drivers are associated with the acceleration of human activity over the past centuries and its increasing demand for natural resources. Featured insects: Regal fritillary (*Speyeria idalia*) (centre), rusty patched bumble bee (*Bombus affinis*) (centre right), and Puritan tiger beetle (*Cicindela puritana*) (bottom), all of them imperilled insects. This illustration is reproduced with the permission of the artist (Virgina R. Wagner) and was published in Wagner, D. L., E. M. Grames, M. L. Forister, M. R. Berenbaum, and D. Stopak. 2021. Insect decline in the Anthropocene: Death by a thousand cuts. *Proceedings of the National Academy of Sciences* 118:e2023989118.

et al., 2012, 2021). Importantly, the latest IPCC projections predict that climate change impacts will further intensify with every additional increment of global warming (IPCC, 2021).

The Mediterranean region, a European hotspot of insect diversity and endemism, is also one of the most vulnerable regions to climate change (Ali et al., 2022; Giorgi, 2006; IPCC, 2021; van Swaay et al., 2010). Surface temperatures are increasing in this area around 20% faster than the global mean, and precipitation is projected to decrease about 4% with every degree of global warming (Lionello and Scarascia, 2018). Dry and hot extremes are predicted to become particularly intense and common during Mediterranean summers—usually the harshest period for living organisms in this area—, with increasingly frequent compound hot droughts (i.e. concurrent dry and hot extreme events; Bastos et al., 2023; Bevacqua et al., 2021; Seneviratne et al., 2021; Simolo and Corti, 2022; Spinoni et al., 2020; Vogel et al., 2020). In fact, high temperatures and aridity, in conjunction with habitat loss, are the major forces of Mediterranean insect populations, a substantial fraction of which have undergone significant declines too (Bonelli et al., 2018; Colom et al., 2022; Herrando et al., 2019; Mingarro et al., 2021; Mora et al., 2023; Out-hwaite et al., 2022; Stefanescu et al., 2011a,b; Ubach et al., 2019; Zografou et al., 2014). Therefore, the Mediterranean region, where this thesis is developed, is at the forefront of climate change impacts on insects, reinforcing the urgent need to unveil the processes by which climate change affects insects and develop relevant predictive models of its impacts on natural populations.

Fingerprints of the impacts of current climate change on insect populations have been accumulating since the first reports on insects' range shifts in response to recent global warming (Boggs, 2016; Halsch et al., 2021; Harvey et al., 2023; Hill et al., 2021; Johnson and Jones, 2017; Parmesan, 1996, 2006; Parmesan and Yohe, 2003; Parmesan et al., 1999; Wilson et al., 2007). The reported impacts of current climate change on insects are highly heterogeneous and affect numerous ecological processes occurring at several interconnected levels, from genetic, physiological and behavioural levels, to population, phenological, species, and community levels (Angilletta 2009; Bradshaw and Holzapfel 2001; Caillon et al. 2014; Carnicer et al. 2011; Colom et al. 2021, 2022; Forister et al. 2018; Kingsolver et al. 2011; Nice et al. 2019; Palmer et al. 2017; Parmesan et al. 1999; Pincebourde et al. 2016; Stefanescu et al. 2003, 2011a; Suggitt et al. 2018; Ubach et al. 2022; Woods et al. 2015). Therefore, understanding climate change impacts on insects not only entails dealing with the multifaceted and multimetric nature of climate change but also with the multiplicity of interrelated ecological and evolutionary processes that are involved (Briscoe et al., 2023; Buckley et al., 2023a; Garcia et al., 2014; Lehmann et al., 2020; Yang et al., 2021). Such intertwined processes shape insect responses to climate change by affecting both the exposure and sensitivity of insects to the climate (Buckley, 2022; Carnicer et al., 2017; Dawson et al., 2011; Maino et al., 2016; Moritz and Agudo, 2013; Williams et al., 2008). In addition, these processes can directly link climate conditions with insects' biology (i.e. direct climate impacts), or transmit climate impacts indirectly, by affecting insects' resources or other interacting species. Furthermore, this complex weave of interrelated processes linking climate and insect responses often varies between populations at a local scale (Bennett et al., 2015; Nice et al., 2019; Parmesan and Singer, 2022), across the seasons (Dillon et al., 2016), and across insects' life stages (Brunner et al., 2023; Kingsolver et al., 2011; MacLean et al., 2016; Woods, 2013), producing heterogeneous mosaics of climatic stress and insect responses across species' ranges (Fig. 1.2).

1.2. Numerous intertwined processes modulate the impacts of climate change on insects

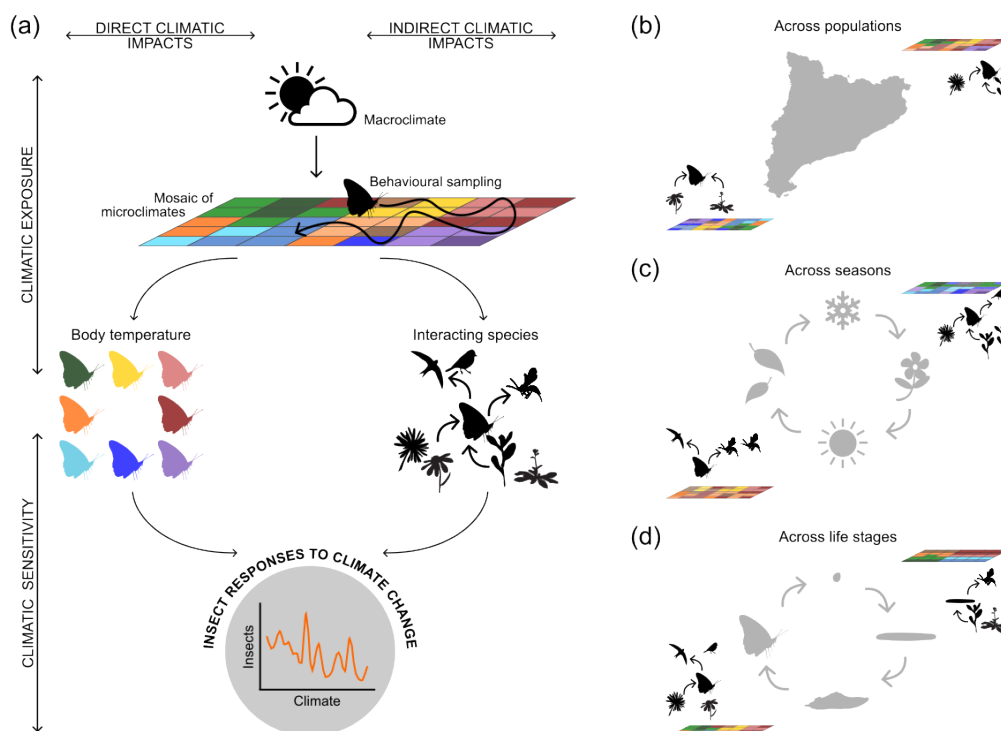


Figure 1.2: A complex weave of climatic and ecological processes shape insect responses to climate change. (a) Insect responses to climate change ultimately depend on the insect exposure to climate (top) and the sensitivity of insect performance to these climatic conditions (bottom). Multiple biotic and abiotic elements from the environment, like canopy shading and leaf evapotranspiration, can locally alter energy and water fluxes and create a mosaic of microclimatic conditions that deviate from the macroclimate. Insects are ectothermic animals with a typically small body size. Thus, their body temperature and climatic exposure results from the behavioural sampling and the use of the microclimatic mosaics produced at very fine scales in their habitats (top). The series of body temperatures experienced during the insect life cycle alter numerous of their physiological, phenotypic, and phenological traits that are responsive to temperature and determine insect population performance (bottom). Insect responses to the experienced climatic conditions during its life cycle represent direct impacts of climate change on insects (left). Additionally, varying macroclimatic and microclimatic conditions due to global warming can also affect the resources, predators, and other interacting agents of the insects, indirectly impacting insect populations (right). Furthermore, this complex weave of climatic and ecological processes mediating direct and indirect impacts of climate change on insects can vary across populations (b), across seasons (c), and across the life cycle of the insect. (b) For example, the local populations of an insect species can inhabit diverse landscapes with different local features and local biota, and thus be exposed to contrasting microclimatic mosaics and interact with other species. (c) Similarly, the various generations that a multivoltine insect produces across the year will face different microclimatic conditions and may find a distinct set of interacting species. (d) Finally, because many insects have complex life cycles and present different stages with contrasting sizes, mobility, and ecological requirements, they can inhabit various microhabitats with contrasting microclimatic mosaics and interact with different species across their life cycle.

Critically, most current predictive models of climate change impacts on insects do not address this complexity and ignore the important underlying ecological processes shaping insect responses (Briscoe et al., 2023; Buckley et al., 2023a; Maino et al., 2016; Urban, 2019; Urban et al., 2016, 2022). The vast majority of studies use correlative methods to establish associations between the climatic drivers and the insect responses (Ur-

ban et al., 2016). While these phenomenological approaches are useful to document the main patterns and observed changes, the methodologies typically employed are not valid for inferring causal relationships, which hamper our attributive and predictive capacity of current and future climate change effects on insects (Addicott et al., 2022; Arif and MacNeil, 2022; Buckley et al., 2023a; Ellner and Guckenheimer, 2006; Grainger et al., 2022; Urban et al., 2023). In this line, by excluding the fundamental ecological processes driving insect responses, the predictive capacity of correlative statistical models is limited to the observed range of climatic conditions (Buckley et al., 2023a; Ellner and Guckenheimer, 2006). Thus, although there are very good correlative models with a high predictive power, any extrapolation to climatic conditions outside this modelled range must be done with caution (Gustafson, 2013; Nice et al., 2019; Urban et al., 2023; van Bergen et al., 2020). This constraint is especially problematic if we want to predict future insect performance in extreme and novel climatic conditions (Maino et al., 2016; Urban et al., 2023). Another limiting issue of most current predictive models is that they aggregate the data at broad geographic, temporal, and taxonomic scales, failing to capture climatic and ecological variation at relevant finer scales, where the underlying processes occur (Briscoe et al., 2023; Dillon et al., 2016; Halsch et al., 2021; Kingsolver et al., 2011; Nice et al., 2019; Pincebourde and Woods, 2020; Pincebourde et al., 2016; Suggitt et al., 2017; Urban et al., 2023; Woods et al., 2015). For these reasons, many ecologists have prompted the development of more accurate predictive models of insect responses to climate change at relevant spatiotemporal scales that rely on the fundamental ecological processes producing these responses (i.e. process-based models, using Connolly et al. 2017 definition; Bastos et al., 2023; Briscoe et al., 2023; Ma et al., 2021; Maino et al., 2016; Urban, 2019; Urban et al., 2016, 2022, 2023; Yang et al., 2021). In this thesis, I parameterise both long-standing and emerging predictive models based on fundamental physiological and demographic processes benefitting from the comprehensive knowledge around a model insect species to predict its population responses to climate change.

1.3 Process-based approaches require well-established model systems

Parameterising process-based models requires high-quality, detailed information on the study system (Buckley et al., 2023a; Urban et al., 2022). For this reason, to obtain the key parameters of the predictive models employed in this thesis, I take advantage of a well-established study system comprising a model insect species at long-term monitoring sites of the north-east of the Iberian Peninsula. The studied butterfly species is the green-veined white (*Pieris napi* L. 1758), which is becoming a model system in insect thermal ecology and the study of physiological responses to climate-driven stresses, among other research areas. For instance, there are many studies regarding their physiological responses to temperature, drought, and food stresses, but also on their reproductive biology, their phenotypic and developmental plasticity, and, more recently, their genomic evolution and phylogeographic history (Box 1 and Table 1.1).

Pieris napi is a widespread and common butterfly across the palearctic region, with

a clear preference for humid and riverine habitats (Fig. 1.3a; García-Barros et al., 2013). The species finds in the Mediterranean region its southernmost and most climatically stressing distribution. In the Catalan territory, where this study is developed, *P. napi* has an abundant and ubiquitous presence, except in the most interior arid regions (Fig. 1.3b; Vila et al., 2018). Many of the populations in the region have been long monitored by the Catalan Butterfly Monitoring Scheme (CBMS), which provides weekly counts of butterfly abundance across established transects from March to September since 1993 (Pollard and Yates, 1993; Stefanescu, 2000). The analysis of the abundance data from the CBMS reveals that *P. napi* has a stable trend at a Catalan scale (Fig. 1.3c), yet this regional aggregation masks an heterogeneous mosaic of increasing, stable, and declining populations at a local scale (Fig. 1.3d). The declines in certain *P. napi* populations have been mainly observed in the lowlands and have been correlatively associated with increasing drought and heat impacts during late spring and summer (Fig. 1.4).

Box 1. Insects, butterflies, and the green-veined white as model systems

Insects' characteristics make them ideal model systems for the study of climate change impacts on living organisms. Due to their small size, ectothermic nature, and rapid life cycle, insects are highly responsive to environmental variation and easy to rear and manipulate in the laboratory (Hill et al., 2021; Price et al., 2011). Moreover, the shortness of their life cycles promotes the sampling of relatively long time series spanning numerous generations. All these traits, as well as insect's ubiquity and diversity, make them excellent candidates as model taxa in global change studies (Johnson and Jones, 2017).

Among insects, butterflies are one of the most popular and traditionally studied groups (Hill et al., 2021). Natural history collections and naturalist records have left useful information to assess butterfly presence more than a century ago (Habel et al., 2016; Kharouba et al., 2018). In addition, their relatively easy detection and identification have facilitated the establishment of citizen science programs that monitor their abundance in many parts of the northern hemisphere (Nice et al., 2019; Pollard and Yates, 1993; Stefanescu, 2000; van Swaay et al., 2008).

The green-veined white (*Pieris napi*, Pieridae) is one of the butterflies that has received more attention. It extends across many areas of Europe, Asia, North Africa, and North America (Tolman and Lewington, 2009), and because of its abundance and ordinary presence, is categorised as a least concern species in Europe (van Swaay et al., 2010). The species is characterised by the dark melanic bands in the ventral side of its hindwings and males emit a citric essence that can help their identification in the field (Tolman and Lewington, 2009). The species also presents numerous local morphs and sub-specific variants, complicating its taxonomic delimitation and the assessment of its phylogeographic history (Bowden, 1979; Chew and Watt, 2006). See Table 1.1 for a summary of the main characteristics and findings on the species spanning multiple biological fields, which consolidate the species as a model system in insect biology.

Table 1.1: A non-exhaustive summary of the research on *P. napi* biology.

Field	Main findings	Main references
Reproductive biology	<i>P. napi</i> females benefit from multiple mating (i.e. polyandry) in terms of lifetime fecundity and longevity. Males typically emerge earlier than females (protandry) and transfer a nuptial gift to females at mating, losing around 15% of their weight. After mating, females emit repellent pheromones (likely male-derived) to minimise the cost of female rematings by delaying them to times with decreased egg laying.	Bergström and Wiklund (2002); Bissoondath and Wiklund (1996); Forsberg and Wiklund (1989); Kaitala and Wiklund (1994); Karlsson et al. (1997); Välimäki et al. (2008); Wedell et al. (2002); Wiklund et al. (1993, 1998)
Host-plant use and oviposition behaviour	<i>P. napi</i> selects crucifer herbs from moist habitats to oviposit. Host-plant preference of the females is not associated with their habitat affiliation and does not lead to increased performance of the offspring. Moreover, <i>P. napi</i> larvae of some populations prefer small host plants or use their bottom leaves, a behaviour that has been related to micro-climatic conditions rather than plant condition.	Forsberg (1987); Friberg and Wiklund (2019); Friberg et al. (2015); Heinen et al. (2016); Ohsaki (1979); Shapiro (1979); Yamamoto (1983)
Predators, parasites, and specific parasitoids	Multiple vertebrate and insect predators, parasites, and parasitoids feed on <i>P. napi</i> individuals. Early life stages are mainly affected by insect predators and parasitoids, while bigger larvae are eaten by vertebrate predators. Predation pressure is thought to shape microhabitat and host-plant preference of the species.	Ohsaki and Sato (1994, 1999); Yamamoto (1981)

Field (cont.)	Main findings (cont.)	Main references (cont.)
Physiological responses to plant, heat, and drought stresses	<i>P. napi</i> larvae reared at high experimental temperatures (specially during extreme thermal treatments) has inferior efficiency of food conversion, leading to adults of small sizes, reduced immunity functions, decreased fecundity, but higher flying capacity. High temperatures in the laboratory also decrease host-plant quality by increasing C/N ratios and glucosinolates concentrations. However, simulated dry conditions have opposite effects on host plants, leading to adults with increased size and food conversion efficiency.	Bauerfeind and Fischer (2013a,b, 2014a,b); Degut et al. (2022); Kuczyk et al. (2021)
Seasonal polyphenism and developmental plasticity	<i>P. napi</i> produces several generations (2–5) across the seasons, except in the northernmost edge of its distribution. To adapt to this seasonality, larvae can undergo through at least two alternative development pathways depending on the temperature and photoperiodic conditions, and adults from different generations show contrasting phenotypes and behaviours. Larvae developing in the autumn wander for a longer time and lose more mass before pupating, after which they enter a winter dormancy stage. Subsequent adults emerge in spring, once the pupal diapause ends, and present the characteristic melanic bands in their hindwings. Larvae of the following generations directly develop (i.e. without diapausing) and the resulting adults present rounder and less melanic wings, which favours butterfly thermoregulation and dispersal capacity in the summer conditions.	Bowden (1979); Friberg et al. (2012); Karlsson and Johansson (2008); Kingsolver (1987); Kingsolver and Wiernasz (1987); Kivelä et al. (2015, 2017); Larsdotter-Mellström et al. (2010); Peñuelas et al. (2017); Shapiro (1977)

Field (cont.)	Main findings (cont.)	Main references (cont.)
Winter diapause	The photoperiod and temperature conditions determining winter diapause induction, duration, and termination in <i>P. napi</i> and its associated metabolic dynamics have been intensively examined. Both very low and very high winter temperatures affect diapause termination and the synchronisation in pupal eclosion. Moreover, high temperatures before the winter diapause period have negative fitness consequences for diapausing individuals, potentially becoming an added threat with increasing global warming.	Lehmann et al. (2016, 2017, 2018); Nielsen et al. (2022)
Local adaptations and clinal variation	<i>P. napi</i> populations show high plastic and genetic adaptive variation across elevations and latitudes in many functional and life-history traits, such as voltinism, diapause duration, post-winter development, maintenance vs reproductive traits, wing size and melanisation, and flight capacity.	Espeland et al. (2007); Günter et al. (2019, 2020a,b); Merckx et al. (2021); Peñuelas et al. (2017); Posledovich et al. (2015); Tuomaala et al. (2012)
Genomics	<i>P. napi</i> 's genome has been recently annotated and published, which revealed an unprecedented reorganisation of its chromosome structure relative to other lepidoptera and contributed to characterise the genetic basis of <i>P. napi</i> adaptive phenotypes and host-plant use. In addition, new genomic analyses are helping to clarify the taxonomic delimitation of <i>P. napi</i> -complex and its phylogeographic history.	Carnicer et al. (2023); Ge et al. (2023); Hill et al. (2019); Neethiraj et al. (2017); Pruischer et al. (2017, 2021)

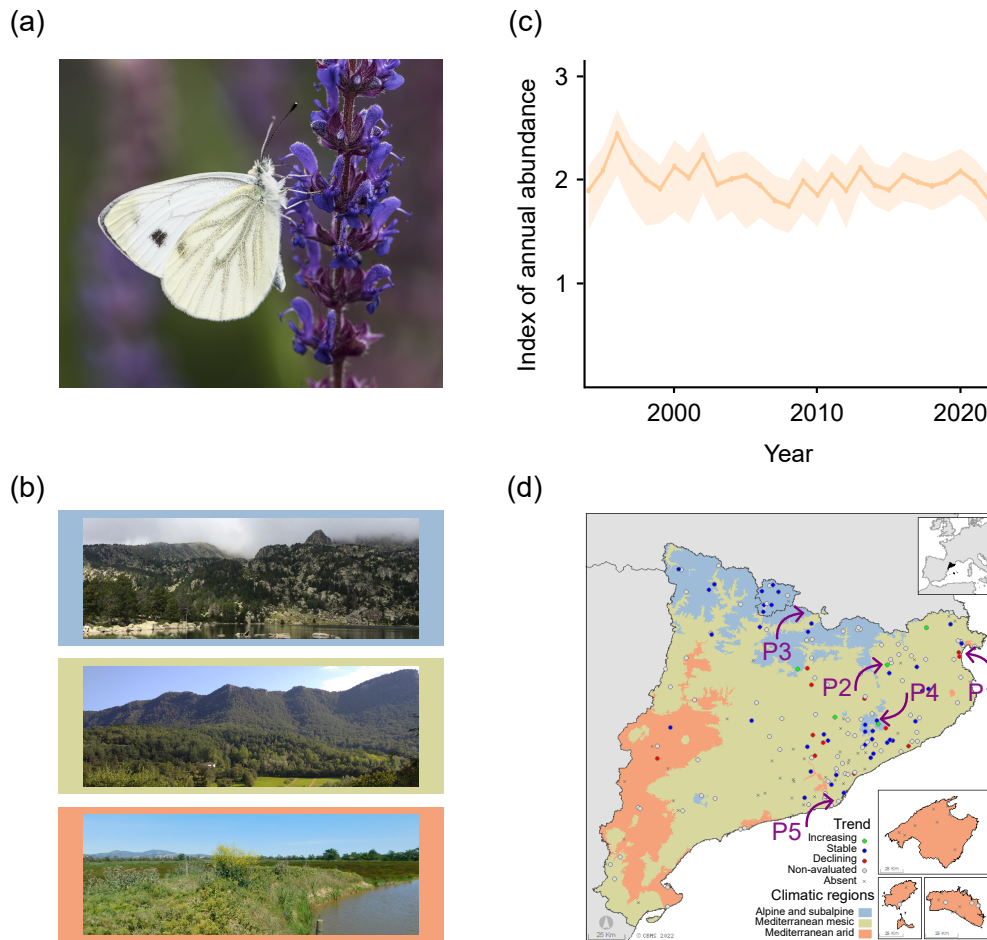


Figure 1.3: In this thesis, I quantify the impacts of extreme heat and drought on different intensively-monitored populations of the model species *Pieris napi*. (a) The butterfly is commonly known as the green-veined white due to the very characteristic melanic bands that it presents following its hindwing veins. Photograph provided by Vlad Dinca. (b) The green-veined white is a common and abundant butterfly in the Catalan territory, where it can be found from lowland, climatically-exposed areas (bottom, red square) to montane and high-elevation regions (mid, green square and top, blue square, respectively). Photographs by Jofre Carnicer and the author. (c) *Pieris napi* presents a stable trend at a regional, Catalan scale. Figure extracted and modified from the CBMS website (www.catalanbms.org). (d) At a local scale, the species presents a heterogeneous mosaic of increasing, stable, and declining populations. Purple arrows indicate the five intensively-monitored populations studied in this thesis (Table 1.2).

In this thesis, I aim to understand how drought and heat extremes are impacting *P.napi* populations in this climatically-stressed region and predict their increasing future impacts. To do it, I collect key information on the potential processes mediating these heat and drought impacts on a network of five intensively monitored populations placed across an elevation gradient and presenting contrasted demographic trends (Table 1.2). Combining direct measures in the field, with experimental estimates and computational calculations, I quantify several climatic and ecological processes directly shaping *P. napi* exposure and sensitivity to climate impacts, and indirectly, by affecting their host plants. The quantification of this complex weave of climatic and ecological processes

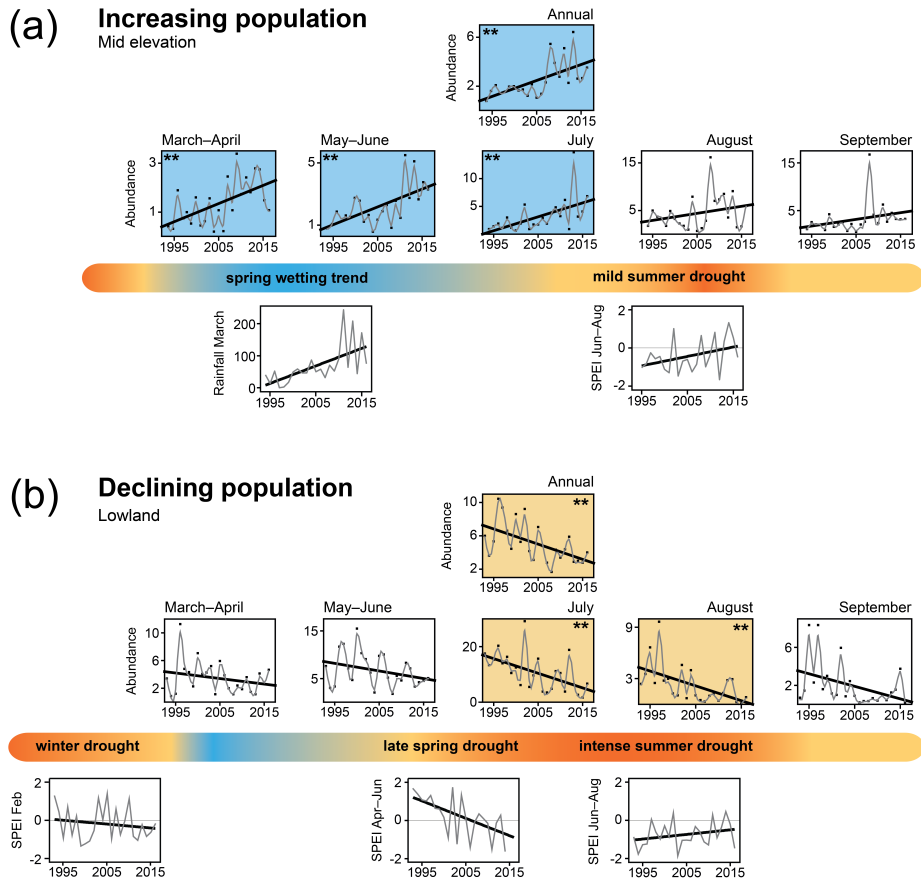


Figure 1.4: The multiannual trends in abundance of an increasing population (P_2 in Table 1.2) and a declining population (P_1 in Table 1.2) of *Pieris napi*. Using the CBMS demographic series, I calculated an standardised index of butterfly abundance for each year at an annual and a subannual scale by summing all the individuals counted during that period and dividing them by the number of monitoring weeks and the kilometres of the surveying transect. The subannual periods broadly correspond to the different generations the species produces during a year. (a) The mid-elevation population shows an annual positive trend, which results from the increase in butterfly abundance of the spring and early summer generations coinciding with a spring wetting trend (i.e. increasing march rainfall). (b) In contrast, the lowland population shows a multiannual declining trend associated with the decrease in abundance recorded for summer generations. In this area, late springs are becoming drier (lower and more negative values of the SPEI drought index between April and June) and summers have been affected by an intense, multidecadal drought (sustained negative values of SPEI drought index for summer months). Asterisks indicate statistically significant trends in butterfly abundance. SPEI drought index was calculated following Beguería and Vicente-Serrano (2017).

is conducted across the four chapters constituting the main body of the thesis. To give a general insight to the reader into the various quantified processes, I here briefly introduce them (and see Fig. 1.5 for a visual summary).

To quantify the local climatic exposure of the populations at a relevant scale, I complement local macroclimatic variables recorded from nearby standardised weather stations with fine-grained, microclimatic records at a microhabitat and a host-plant level. Temperatures at the microhabitats and surfaces where insects develop (i.e. the microcli-

mate) can deviate markedly from open, free-air, standardised measurements (the macroclimate) (Kearney et al., 2009a; Kingsolver et al., 2011; Pincebourde and Woods, 2020; Pincebourde et al., 2016; Potter et al., 2013; Suggitt et al., 2011; Woods et al., 2015). For instance, maximum temperatures under canopies are, on average, about 5 °C cooler than measurements at adjacent, open habitats (De Frenne et al., 2019), and the complexity of the microclimatic biophysics of leaves can produce steep thermal gradients at foliar surfaces —e.g. ~6 °C, when they are in the sun (Pincebourde and Suppo, 2016; Woods, 2013)— and heat leaves over the surrounding air more than 10 °C (Pincebourde and Woods, 2012). For this reason, I expect that microclimatic conditions recorded in this study system importantly modulate *P. napi* climatic exposure, in line with the findings from other insect species. Moreover, As insects' body temperature ultimately depends on their use of these microclimatic mosaics (Pincebourde et al., 2016; Woods et al., 2015), in the thesis I also quantify butterfly and larval thermoregulatory behaviours both in the field and the laboratory.

To characterise insects' sensitivity to the experienced thermal conditions, I measure several *P. napi* traits that are responsive to temperature and are known to affect insect performance. Specifically, I analyse the phenological variation in the flight periods of the populations; the phenotypic plasticity of morphological traits like wing size; larval developmental rates at varying temperatures; and heat tolerance to extreme thermal conditions. If populations are differently exposed to heat impacts, as I expect, then significant variation in these thermoresponsive traits should be observed.

These phenological, physiological, and phenotypic responses represent direct effects of climatic impacts on insects, which are typically better described than indirect impacts mediated by interacting species (Abarca and Spahn, 2021; Boggs, 2016; Boggs and Inouye, 2012). Yet, climate effects on food resources can also play a key role on the dynamics of natural populations (Gamelon et al., 2017; Lima et al., 2006; Stenseth et al., 2004). Because *P. napi* is an herbivorous insect that uses a relatively small set of herbaceous species as hosts (Ohsaki, 1979), I expect important additional indirect climatic effects on their population dynamics mediated by their host plants. With this aim, I also assess the parallel effects of heat and drought impacts on *P. napi* host plants by characterising their phenology and vegetative growth, and their morphological, physiological, and stoichiometric traits across the seasons.

The empirical quantifications of the processes mediating *P. napi* responses to heat and drought extreme impacts are primarily conducted in Chapters 2 and 3 of this thesis, with extensions in Chapters 4 and 5. In the latter two chapters, I also utilise all gathered data on this system to parametrise two different process-based models. These models predict the effects of extreme heat and drought exposure on key vital rates of the species (specifically larval mortality) and their overall population performance.

Chapter 2 focuses on characterising the multiannual trends of the studied populations and identifying the climatic factors driving them. Additionally, I quantify various microclimatic, host-plant, behavioural, and physiological processes that influence *P. napi* vulnerability to the identified climatic drivers. Ultimately, I investigate whether any insect

trait can serve as a phenotypic biomarker of its climatic vulnerability.

In Chapter 3, I delve into the seasonal dynamics of the host plants used by *P. napi* to assess the role of plant phenological and plastic variation in mediating butterfly responses to extreme drought impacts.

Chapter 4 addresses the consequences of fluctuating and sometimes extreme microclimatic temperatures recorded in the selected microhabitats on the survival of developing larvae. I compare the microclimatic exposure and thermal sensitivity of *P. napi* and *P. rapae*, another well-known butterfly of the same genus. The aim is to parametrise a recently (re)introduced dynamical model, the TDT model, which predicts the organism's probability of survival to cumulative heat injury based on the duration and intensity of heat stress.

In Chapter 5, I develop a process-based population model to investigate the effects of current and future heat and drought extremes on the seasonal population dynamics of the species. Utilising the field and experimental information and the vital rates estimated in the previous chapters, I parametrise a matrix population model (MPM) to predict the population performance under different regimes of extreme events at increasing global warming levels.

To wrap up, in the concluding chapter, I discuss the main contributions of this thesis, the generalizability and relevance of the results from the preceding chapters, as well as the limitations and potential improvements of the employed approaches.

1.3. Process-based approaches require well-established model systems

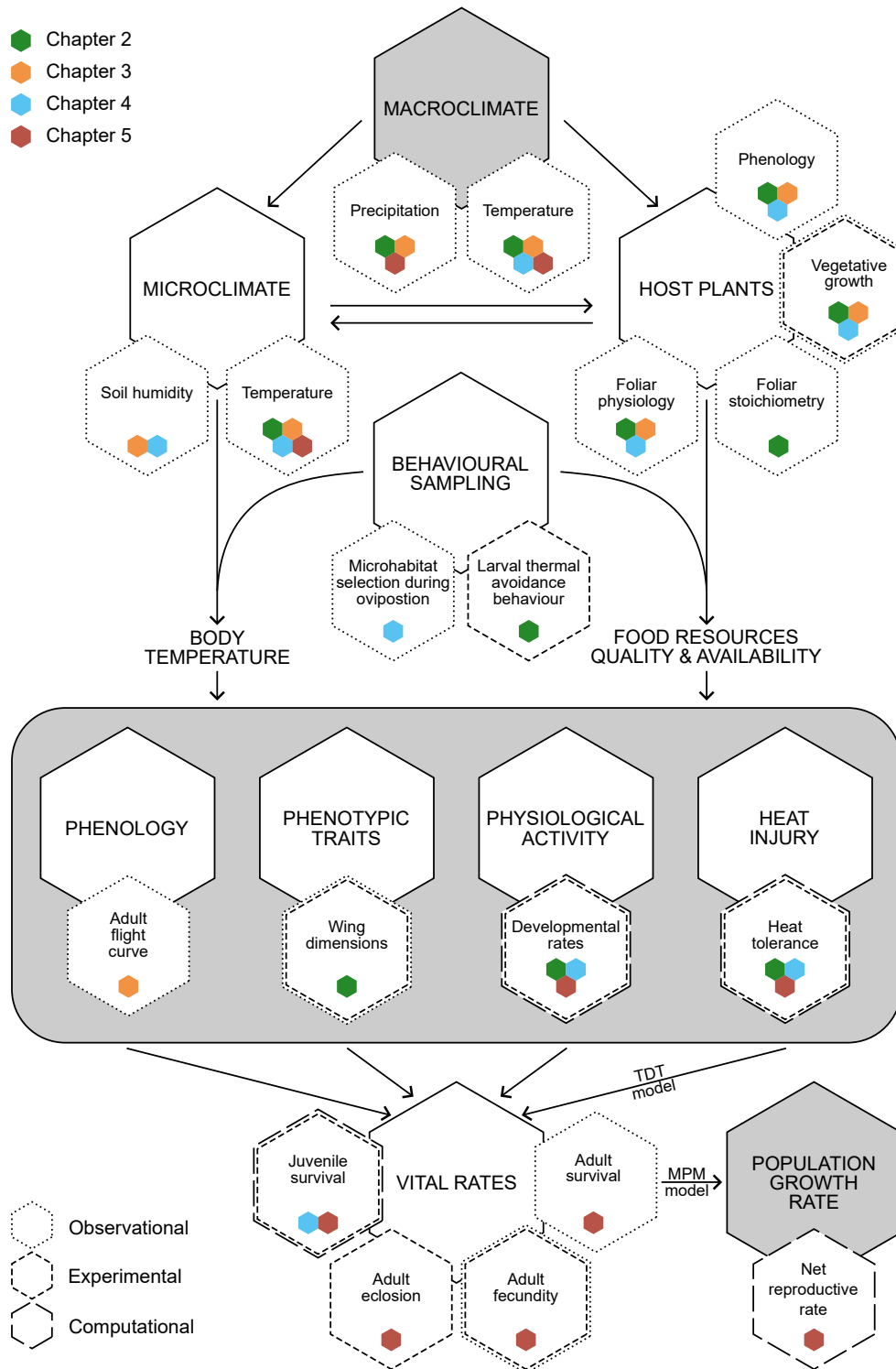


Figure 1.5: A visual summary of the complete set of climatic and biological parameters and variables estimated with the aim to predict macroclimatic warming effects (top grey hexagon) on *P. napi* population growth rates (bottom grey hexagon). Big, white hexagons indicate the different climatic and ecological dimensions quantified between the macroclimatic drivers and the population responses, whereas mid white hexagons specify which particular variables and parameters I estimate for each dimension. (Legend continues on next page).

I. INTRODUCTION

(Continuation of legend from Fig. 1.5). The coloured, small hexagons inside the mid hexagons indicate the chapters of the thesis where I estimate each variable, and the linetype surrounding the mid hexagons, the approach used for the quantification (either direct observations in the field, experimental estimations, or mathematical calculations from first principles). The dimensions above the grey rounded square represent climatic and ecological processes shaping *P. napi* exposure to climate, whereas the dimensions inside the grey square represent insect traits that are responsive to temperature and thus modulate insect sensitivity to climate. All these thermal responsive traits determine *P. napi* vital rates and population performance (below the grey square). In the thesis, I employ two distinct process-based predictive models parameterised with the gathered data: the thermal death time model (TDT model), which calculates larval survival based on *P. napi* tolerance to heat stresses of different intensity and duration, and the matrix population model (MPM model), which calculates the population growth rates based on *P. napi* vital rates across its life cycle.

Table 1.2: Main characteristics of the 5 model populations of *P. napi* that have been intensively monitored for this thesis. The latitude (°N) and longitude (°E) of each location is provided with the WGS 84 reference coordinate system. I developed most chapters with populations 1 and 2, and complemented the study with observations from other populations when possible. I indicate the populations used in each of the chapters with grey shades and provide between parentheses the code employed to name the population in the chapter. To ease readership, I continuously clarify through the chapters the references to a lowland declining population, or a mid-elevation non-declining population.

Population	Location	Mean elevation (m a.s.l)	Landscape	Chapter 2 (code)	Chapter 3 (code)	Chapter 4 (code)	Chapter 5 (code)
P ₁	El Cortalet, Aiguamolls de l'Empordà Natural Park (42.22, 3.092)	2 (lowland)	Coastal wetland	Yes (site 2)	Yes	Yes (site 2)	Yes (site 1)
P ₂	Can Jordà Zona Volcànica de la Garrotxa Natural Park (42.145, 2.511)	539 (mid-elevation)	Montane agroforest	Yes (site 3)	No	Yes (site 1)	Yes (site 2)
P ₃	Malniu, La Cerdanya, Catalan Pyrenees (42.454, 1.766)	2200 (high-elevation)	Subalpine woods	No	No	No	Yes (site 3)
P ₄	El Puig, Montseny Natural Park (41.801, 2.425)	1031 (mid-elevation)	Montane agroforest	Yes (site 4)	No	No	No
P ₅	Cal Tet, Delta del Llobregat Natural Spaces (41.306, 2.115)	1 (lowland)	Coastal wetland	Yes (site 1)	No	No	No



**Phenotypic biomarkers
of climatic impacts on
declining insect populations:
a key role for decadal
drought, thermal buffering
and amplification effects,
and host plant dynamics**





Abstract

Widespread population declines have been reported for diverse Mediterranean butterflies over the last three decades, and have been significantly associated with increased global change impacts. The specific landscape and climatic drivers of these declines remain uncertain for most declining species. Here, we analyse whether plastic phenotypic traits of a model butterfly species (*Pieris napi*) perform as reliable biomarkers of vulnerability to extreme temperature impacts in natural populations, showing contrasting trends in thermally exposed and thermally buffered populations. We also examine whether improved descriptions of thermal exposure of insect populations can be achieved by combining multiple information sources (i.e. integrating measurements of habitat thermal buffering, habitat thermal amplification, host plant transpiration, and experimental assessments of thermal death time (TDT), thermal avoidance behaviour (TAB), and thermally induced trait plasticity). These integrative analyses are conducted in two demographically declining and two non-declining populations of *Pieris napi*. The results show that plastic phenotypic traits (butterfly body mass and wing size) are reliable biomarkers of population vulnerability to extreme thermal conditions. Butterfly wing size is strongly reduced only in thermally exposed populations during summer drought periods. Laboratory rearing of these populations documented reduced wing size due to significant negative effects of increased temperatures affecting larval growth. We conclude that these thermal biomarkers are indicative of the population vulnerability to increasing global warming impacts, showing contrasting trends in thermally exposed and buffered populations. Thermal effects in host plant microsites significantly differ between populations, with stressful thermal conditions only effectively ameliorated in mid-elevation populations. In lowland populations, we observe a sixfold reduction in vegetation thermal buffering effects, and larval growth occurs in these populations at significantly higher temperatures. Lowland populations show reduced host plant quality (C/N ratio), reduced leaf transpiration rates and complete above-ground plant senescence during the peak of summer drought. Amplified host plant temperatures are observed in open microsites, reaching thermal thresholds that can affect larval survival. Overall, our results suggest that butterfly population vulnerability to long-term drought periods is associated with multiple co-occurring and interrelated ecological factors, including limited vegetation thermal buffering effects at lowland sites, significant drought impacts on host plant transpiration and amplified leaf surface temperature, as well as reduced leaf quality linked to the seasonal advance of plant phenology. Our results also identify multiannual summer droughts affecting larval growing periods as a key driver of the recently reported butterfly population declines in the Mediterranean biome.

2.1 Introduction

Declines in butterfly populations across diverse species over the last three decades have been described in the Mediterranean basin (Carnicer et al., 2012, 2013b; Melero et al., 2016; Stefanescu et al., 2004, 2011a,b; Wilson et al., 2005, 2007; Zografou et al., 2014). Negative

effects of land use changes and global warming have been proposed as the main drivers of the observed declining trends (Stefanescu et al., 2004, 2011a,b; Wilson et al., 2005, 2007). These negative demographic trends affect both habitat generalist and specialist butterfly species in the Mediterranean biome. The spatial diversity of most functional groups is negatively associated with increased temperatures and aridity (e.g. host plant use, dispersal capacity, habitat specialisation, and thermal niche groups; Stefanescu et al., 2011a,b). Furthermore, the available evidence suggests that global warming-induced population responses are intimately linked to complex interactions with habitat features and host plant dynamics (Bennett et al., 2015; Carnicer et al., 2013a, 2017; De Frenne et al., 2013; Merrill et al., 2008; Oliver et al., 2014, 2015; Suggitt et al., 2012). In line with this idea, it has been suggested that specific habitat attributes can modify global warming impacts on butterfly populations, triggering both positive and negative demographic responses. For example, it has been shown that the densification of forest habitats associated with land abandonment can cool local microclimates, buffering the impacts of global warming in some plant and insect populations and resulting in positive or neutral demographic responses to global warming (De Frenne et al., 2013; Nieto-Sánchez et al., 2015).

Populations inhabiting sites lacking effective habitat thermal buffering could experience increased negative impacts of extreme temperatures, resulting in substantial long-term demographic declines (Parmesan et al., 2000). In addition to the effects of habitat thermal buffering, the thermal exposure of butterfly populations can be crucially determined by other key processes, such as the seasonal variation of host plant transpiration and leaf water content during summer drought, the operation of thermal amplification processes in microhabitats, or the display of thermal avoidance behaviours in the insect larvae allowing the selection of cool microsites at the host plant (Carnicer et al., 2017). These key co-acting processes are often not measured, and their complex interactions remain poorly described. To understand the relative importance of all these processes, integrative studies combining multiple information sources in intensively studied populations are warranted.

Here, we provide an integrative study of the thermal exposure in four populations of *Pieris napi*, combining multiple sources of information (demographic and climatic data, phenotypic trait data, measurements of habitat thermal buffering, host plant traits, and experimental assessments of thermal responses). Furthermore, we explore whether temperature-responsive phenotypic traits can be applied as reliable biomarkers of the different vulnerability to increased temperatures in these intensively studied populations. Ample experimental evidence supports that diverse life-history and functional traits of butterflies are highly responsive to temperature variation and show predictable responses to extreme temperature treatments (Bauerfeind and Fischer, 2013a,b, 2014b; Jones et al., 1982; Nail et al., 2015; Sheridan and Bickford, 2011). In particular, wing and body size measures have been identified as traits highly responsive to temperature variation and climate change impacts (Atkinson, 1994; Atkinson and Sibly, 1997; Forster et al., 2012; Kingsolver, 2009; Nygren et al., 2008; Sheridan and Bickford, 2011; Talloen et al., 2009). Therefore, it is likely that an extensive quantification of plastic phenotypic traits in declining and non-declining natural populations could indicate their different vulnerability to warmer

conditions. In other words, if a specific morphological trait of a species is known to respond plastically and in a linear manner to thermal conditions, then we can potentially deduce, for specific populations, the exposure to these thermal conditions by quantifying its morphology. Moreover, if we measure extreme thermal conditions in a target population, which should induce a morphological response, and find non-altered biomarker values, we can suspect that the population is buffered from stressful conditions by micro-habitat effects.

In the Mediterranean region, summer drought periods and increased summer temperatures are tightly linked and significantly associated (Appendix A: Fig. A1). Therefore, during extreme summer drought periods, we expect phenotypic traits to be affected by extreme temperature impacts. In this context, those population sites lacking effective habitat thermal buffering effects should present a significant negative response in temperature-responsive biomarker traits. In contrast, we expect that populations characterised by effective microsite buffering mechanisms should present non-significant trends in temperature-responsive phenotypic biomarkers (see Appendix A.2 for a formal definition of the term biomarker and a simple mathematical framework supporting this definition).

To test this hypothesis and develop an integrative analysis of thermal exposure in a butterfly species, we address the following five research objectives using the green-veined white *P. napi* as a model species: (a) to analyse whether plastic phenotypic traits perform as reliable biomarkers of vulnerability to extreme temperature impacts in natural populations, by comparing phenotypic trait responses in four populations of *P. napi*; (b) to experimentally estimate thermal death time responses (thermal susceptibility z and critical thermal limit CT_{max}) and the thermal threshold for avoidance behaviour (TAB) for this model species, (c) to quantify thermal buffering in microsites, assessing whether they provide non-stressful thermal habitats only in specific localities; (d) to evaluate whether host plant resource dynamics qualitatively differ between the studied populations; and (e) to assess whether increased drought impacts could explain the reported long-term population declines in the selected model species.

2.2 Materials and methods

2.2.1 Study species

Pieris napi is a widely distributed Holarctic butterfly, common across most of North America and Europe, though only locally in North Africa. Throughout its distribution, it shows a clear preference for humid habitats, such as wetlands, riparian forests, and irrigated agricultural land. In Catalan lowland areas, there is a succession of four to five generations from early spring (March–April) to autumn (October–early November), with overwintering in the pupal stage. Maximum abundance is typically recorded in early summer, in coincidence with the peak of the third generation. This peak is followed by a

period of 1–2 months when abundance is much reduced, in coincidence with summer drought. Butterflies then reappear by the end of September, in what normally constitutes the last annual generation. In mountain areas, where the phenology is constrained by colder temperatures, a succession of three generations from April to September is the most common pattern. At most montane sites, abundance increases all over the season and reaches its maximum in the third and last annual generation. Eggs are laid singly on a wide range of wild Brassicaceae, *Lepidium draba* and *Brassica nigra* being the two most common host plants in lowland areas, and *Alliaria petiolata*, *Arabis glabra*, and *Cardamine pratensis* those mostly used in mountain habitats. Other secondary host plants have been recorded over the region (García-Barros et al., 2013).

2.2.2 Study zone

We studied two lowland declining populations (sites 1 and 2) and two mid-elevation non-declining populations (sites 3 and 4) in Catalonia, NE Spain. Sites 1 and 2 were located at two protected coastal wetlands (Delta del Llobregat and Aiguamolls de l'Empordà, 133 km apart). In contrast, sites 3 and 4 were located at higher elevations, also in natural protected areas (Zona Volcànica de la Garrotxa (503 m a.s.l.) and Montseny (1,031 m a.s.l.), 41 km apart). Mid-elevation sites were characterised by a heterogeneous mosaic of different habitat types, including open fields, small wetland and riverine areas, and temperate and evergreen forests. A more detailed summary of the geographic, climatic, and ecological attributes of the selected sites is provided in Table A1 and Fig. A2. To quantify long-term demographic trends, sites were surveyed from 1994 to 2012 as part of the Catalan Butterfly Monitoring Scheme (www.catalanbms.org) via weekly butterfly counts along fixed transect routes from March to September (a total of 30 recording weeks per year). All individuals seen within 2.5 m on each side and 5 m in front of the recorder were counted, using the standard methodology of the Butterfly Monitoring Schemes (Pollard and Yates, 1993; Schmucki et al., 2016). For site 1, demographic surveys were available only for 7 years distributed in two discrete periods [1994–1997 and 2007–2009]. An annual index calculated as the sum of weekly counts was used as the measure of population abundance at each season.

2.2.3 Population trends, climate and land cover data, and model selection approach

Climate factors and landscape use changes have been identified as the main drivers of long-term butterfly population trends in the Mediterranean biome (Stefanescu et al., 2011a,b). However, detailed models combining climatic and dynamic landscape data are still warranted to quantitatively assess the relative contribution of these two factors to long-term butterfly demographic declines. For this purpose, we compiled a database integrating butterfly annual abundance indices, monthly climatic rainfall and temperature data for the 1994–2012 time period (Domingo-Marimón, 2016), and land cover dynamics data for 1994–2012. To study landscape dynamics, aerial orthoimages (1:25,000) for

1993, 2001, 2006, and 2012 were digitised using *MiraMon*, a geographic information system (Pons, 2002). The images were provided by the Cartographic Institute of Catalonia (www.icgc.cat/). We selected a circular area (2 km of diameter) around the field transect sites and quantified the changes in the total surface (m²) of the following nine land cover types: wetland and continental water (L₁), dense forest (L₂), sparse forest (L₃), shrubland (L₄), grassland and herbaceous meadows (L₅), urbanised land (L₆), bare land (L₇), road and lane areas (L₈), and beach area (L₉). A continuous annual sequence of estimated land cover changes for 1994–2012 was obtained applying spline fits using *JMP* (SAS Institute Inc., 2012) and saving predicted values between consecutive orthoimages in the time series.

To analyse the observed temporal trends in the butterfly annual abundance of the four populations over 1994–2012, spline fits and ordinary least squares models (OLS) were implemented. Two model selection approaches were sequentially applied, first using only climatic variables (approach 1) and subsequently combining land and climatic variables in an integrated model (approach 2). The first modelling approach was simply used to reduce the large number of climatic variables analysed (a total of 28 monthly temperature and precipitation variables). In other words, we first selected monthly climatic variables significantly associated with the observed butterfly demographic trends (OLS stepwise approach; SAS Institute Inc., 2012), and then, we combined the selected climatic variables and dynamic landscape data in an integrated model selection approach. All possible models computable in each approach were contrasted in terms of their corrected Akaike's information criterion (AIC_c) and Bayesian information criterion (BIC), and the models with the lowest values were selected. The explanatory power of competing variables was contrasted by the stepwise selective approach and by comparing the estimates for the selected predictors (SAS Institute Inc., 2012). Digitised orthoimages were not available for site 4, precluding the inclusion of this site in the landscape modelling analyses. We included in the model selection approach monthly climatic variables of two consecutive years in order to account for the previous autumn growing period of winter-diapausing generations (i.e. current and previous year climatic data).

2.2.4 Phenotypic biomarkers of population vulnerability

In order to identify phenotypic traits that could perform as climate extreme biomarkers, butterfly populations were intensively sampled with weekly resolution during 2014 and 2015, covering the whole flying period (early spring to late autumn). Weekly samples were composed of a minimum of four males and four females. Supplementary samples were collected during seasonal abundance peaks. A total of 1265 butterflies were finally collected (see Table A2 for further details). The following phenotypic traits and their seasonal variance were quantified in the four selected populations: dry body mass, dry wing mass, wing size (i.e. length and area). Dry wing mass and wing area variables were significantly correlated and were considered synonymous descriptors ($R^2 = 0.40$; $P < 0.0001$). The same was true for dry body mass and wing area measures ($R^2 = 0.41$; $P < 0.0001$). In addition, we also quantified wing melanism, and whole-body $\delta^{13}C$, $\delta^{15}N$, %N, and

%C. However, these variables were not strongly related to climate variability and were discarded.

To quantify wing size (length and area), wing samples were photographed using standardised settings (fixed Nikon D7100 with a Sigma Macro objective at a height of 41.5 cm). The quantification was performed with *ButterflyPhotoGUI*, a MATLAB algorithm (developed by Hedrick, T., Kingsolver Lab, University of North Carolina), so that wing size corresponded to the number of pixels in the area defined by three fixed landmarks in the hindwing (tip of the vein M_1 , tip of the vein CuA_1 and the intersection of the veins CuA_1-CuA_2 , Fig. A3). The wing vein naming system applied is described in Wahlberg et al. (2014). In addition, wing length (mm) and area (mm^2) were measured independently in a subset of standardised photographs. All these measures (wing area in pixels, wing area in mm^2 , and wing length in mm) were strongly correlated and, thus, were considered related descriptors ($R^2 > 0.80$; $P < 0.0001$). Wing size was finally chosen to present our graphical results (i.e. *wing length* l in Fig. A3).

To track the impacts of extreme summer climatic conditions on wing size, we focused on the weekly variation of this trait during the spring, summer and autumn periods. To more precisely quantify the effect of climatic variables on phenotypic trait variability, we modelled the variation of wing size using ordinary least squares models (OLS) and introducing the following predictor variables: site, year (2014 or 2015), mean temperature during the larval and pupal growth period (25 days previous to the adult collection), accumulated rainfall previous to adult collection (60 days), mean relative humidity previous to adult collection (60 days), photoperiod (mean of 25 days previous to adult collection), and sex (male or female).

For each climatic variable, different possible temporal spans were assessed, ranging from 5 to 120 days (with a 5-day resolution), compiling subsets of related climatic variables. The climatic variables that were finally selected were characterised by higher correlation coefficients with the modelled variables (wing size) in multivariate correlation analyses (SAS Institute Inc., 2012). We selected the models and associated time spans that explained a greater fraction of the variation in the response variable. The modelling results with closely related variables were qualitatively similar (e.g. using a 20-day, 25-day, or 30-day time span resulted in qualitatively synonymous results).

The interactions between the predictor variables were examined, and significant interactions were retained. We have only considered simple, pairwise interactions in the models. We focused on the interactions that were strongly supported by the coefficient estimates (strong empirical signal in the models) and associated with a clear biological interpretation (e.g. site \times temperature and sex \times temperature interactions). Site \times temperature interactions were associated with diverging negative effects of elevated temperatures in lowland populations relative to mid-altitude sites. Temperature \times sex effects were consistent with sex-linked differences in body size observed in experimental thermal treatments (see below). In sum, we have applied a conservative approach in the management and inclusion of interactions, preferentially selecting a reduced number of interactions with a clear biological meaning. We excluded the first generation, that is, winter-diapausing indi-

viduals, from the modelling analyses. Photoperiod was calculated following Kirk (1994). We randomly collected both freshly emerged and older, worn individuals, and estimated adult age by quantifying wing condition state using an ordinal scale (Fig. A4). No significant effects of wing condition were observed on wing size models.

2.2.5 Common-garden experiment

To assess whether the selected biomarker traits were reliable predictors of direct temperature effects on the phenotype, we performed a common-garden split-brood experiment. Five female lines from the lowland site 2 were initiated, with eggs reared under photoperiod conditions inducing direct development (13:11L:D). The offspring (eggs) were divided into two temperature treatments (20 °C and 25 °C). As illustrated in Fig. A5, the 20 °C treatment corresponds to the observed mean daily temperatures in June or late August. In contrast, the 25 °C treatment corresponds to the warmest mean daily temperatures of June, July, and August in the study period (Fig. A5 and see Bauerfeind and Fischer, 2013a,b, 2014b, for additional experimental studies in this species).

Fresh leaves of the host plant species *Lepidium draba* were provided to the larvae *ad libitum*. A total of 143 adult individuals belonging to five different families were finally obtained (see Table A3 for detailed numbers). The experiment allowed testing the effects of treatment, sex, and family on wing size. The heritability of the measured traits was estimated using *MCMCglmm* (Aalberg Haugen et al., 2012; Hadfield, 2010). To assess putative differences between populations in plastic phenotypic responses between low-elevation and mid-elevation sites, 32 additional adult individuals, belong to mid-elevation site 3, were assessed in replicated experimental split-brood conditions (20 and 25 °C treatments, two female lines).

2.2.6 Host plant microsite climatic measures

Maximum summer temperatures often surpass the critical thermal limits of invertebrate ectotherms in multiple biomes (Sunday et al., 2014), and as a result, a key role of thermal buffering processes has been identified for population persistence (e.g. Ashton et al., 2009; Pateman et al., 2016; Suggitt et al., 2015; Sunday et al., 2014). Consequently, a robust evaluation of climate impacts on butterfly populations requires quantifying microclimatic thermal variability and habitat buffering effects at the host plant level during larval growth periods. In addition, the analysis of the temporal variation of host plant traits over the season allows the identification of critical periods of resource scarcity and changes in host plant quality. In the studied system, the dominant host plants were *Lepidium draba* at lowland wetland areas and *Alliaria petiolata* at mid-elevation sites. For *L. draba* and *A. petiolata*, six host plant microsites were selected at lowland and mid-elevation mountain ranges, respectively (see Table A4 for details). In each microsite, we installed an automatic temperature and humidity sensor (Lascar Electronics EL-USB-2- LCD) recording hourly climatic variability over 2014 and 2015. In the lowlands, *L.*

draba was mostly distributed in open microsites (open meadows and grassland areas) and more rarely under tree canopy and/or shrub cover. Egglaying by *P. napi* has been recorded on plants growing in both conditions. Four microsite sensors were therefore distributed in the most representative open meadow microsites, and two sensors were located at closed-canopy host plant microsites to quantify the effect of canopy cover on temperature and humidity records. An additional and commonly used host plant, *Brassica nigra*, was also present in lower numbers at lowland site 2 (inhabiting open microsites, along ditches). Two sensors were located at *B. nigra* microsites to quantify the observed trends for this host plant. At mid-elevation sites, a single dominant host plant (*A. petiolata*) was preferentially located and used for egg-laying at closed-canopy sites. However, a comparatively smaller number of host plants were distributed in open meadow and/or grassland microsites. Four sensors were located at the dominant and representative conditions (closed-canopy sites), and two additional sensors were located at the more unusual open grassland microsites. To contrast microsite climatic measures and standard measures, daily temperature and rainfall records were obtained from four meteorological stations located nearby the four surveyed transects (2–5 km) and at the same altitudinal range (Table A5). The automatic temperature and humidity sensors (Lascar Electronics EL-USB-2-LCD) were located at 25 cm height above the soil surface using metal stakes, and were protected from direct solar radiation by a plastic envelope sustained by a wire-mesh cylinder (installed 5 cm above the sensor and thus precluding the direct incidence of solar radiation). The sensors were surrounded by the host plant leaves and were also covered by abundant herbaceous vegetation (the herbaceous layer ranged between 50 and 120 cm of height). At closed sites, the sensors were in addition directly affected by the shadows of the surrounding shrubs and trees. The sensors estimated the air temperature, relative humidity and dew point with hourly resolution.

2.2.7 Thermal avoidance behaviour (TAB) and thermal death time (TDT) experiments

To avoid the exposure to critical thermal temperatures, butterfly larvae may display thermal avoidance behaviours (i.e. short movements to cooler microsites of the host plant). However, the thermal thresholds for these behaviours remain poorly quantified and experimentally studied in most butterfly species. We experimentally assessed thermal avoidance behaviour in 149 larvae of *P. napi* (last instar, site 2), assessing a total thermal range of 28–48 °C. Larvae were first placed on a leaf of a potted *A. petiolata* and acclimated at an ambient temperature of 22 °C for 5 min. Then, we experimentally raised leaf surface temperatures to a selected Celsius degree treatment (in the thermal range of 28–48 °C) using a 70 W light lamp and carefully controlling the leaf surface temperature with a HANNA HI935005N thermal sensor. Larval behaviour was recorded for 2 min, noting three types of responses: thermally neutral, thermally positive, and thermal avoidance movements to cooler microsites. For each Celsius-degree treatment, we assessed five to seven larvae. Each larva was used in a single thermal trial. A two-parameter logistic model was fitted to model the changes in the frequency of thermal avoidance behaviour $f(T)$ with increasing leaf surface temperature T :

$$f(T) = \frac{1}{1 + e^{-aT-b}} \quad (2.1)$$

where a is the growth rate of the function, and b is the thermal inflection point (°C) in which we observed a 0.5 frequency of thermal avoidance behaviours.

Thermal death time experiments (TDT) allow predicting from first principles when environmental temperatures may affect larval survival (Deutsch et al., 2008; Rezende et al., 2014). To assess the upper critical thermal limit (CT_{max}) in *P. napi*, we implemented a static thermal death time experiment with three static thermal treatments (40, 42, and 44 °C) (Rezende et al., 2014). We estimated CT_{max} and thermal susceptibility (z) from the equation:

$$T_{ko} = CT_{max} - z \log t \quad (2.2)$$

where t is the observed time to death of last instar *P. napi* larvae in static thermal experimental treatments, T_{ko} corresponds to the constant stressful temperature levels applied, CT_{max} is the temperature that would result in knockdown or death at 1 min ($\log t = 0$), and z is the constant of thermal susceptibility describing how thermal tolerance decays with the duration of the heat challenge. The experiment was implemented in 60 individuals from six family lines collected at site 2. Twenty individuals were assessed in each thermal treatment (40, 42, and 44 °C).

2.2.8 Plant trait measurements

To evaluate whether host plant resource dynamics qualitatively differed between populations, we quantified the weekly variation of leaf %N and leaf C/N. Previous empirical works have shown that nitrogen strongly determines butterfly host plant quality of mature leaves (Kaitaniemi et al., 1998; Mattson, 1980; Myers, 1985; Scriber and Slansky, 1981; Slansky and Feeny, 1977). Moreover, leaves containing less nitrogen constrain insect performance and reduce pupal mass in field experiments (Kause et al., 1999; Myers, 1985, but see Fischer and Fiedler 2000). Plant phenology and drought have been identified as key drivers of leaf nitrogen variation (Grant et al., 2014; Kause et al., 1999). Notably, drought and phenology should produce qualitatively different effects on the studied nitrogen-related traits (%N, C/N). In the case of phenology, a progressive reduction of the quantity of nitrogen in the leaves should be expected with plant maturation and leaf ontogeny due to the translocation of nitrogen-rich resources to flowers, fruits, and rhizomes (Jacobs, 2007; Kause et al., 1999). Overall, phenology should promote a progressive reduction of leaf %N and an increase in leaf C/N over the late spring and early

summer period. In contrast, in the case of drought-induced effects on plant ecophysiology, an increase in the quantity of nitrogen in the leaves could be expected (e.g. Bauerfeind and Fischer, 2013b; Grant et al., 2014; Valim et al., 2016). To perform the weekly leaf measurements, five plants were sampled per week and site, collecting five to eight leaves per plant for the analyses (Table A6). Seasonal trends for C/N ratio and %N were modelled applying ordinary least squares for linear trends and spline fits for nonlinear trends (SAS Institute Inc., 2012).

In order to achieve a more detailed assessment of plant responses to drought stress at lowland sites, monthly measures of leaf stomatal conductance and leaf surface temperatures were specifically conducted for plants *L. draba* and *B. nigra* (using a LICOR 6400 portable photosynthesis system). These measurements were restricted to open microsites and were conducted at midday (12.00–14.00) (Aiguamolls de l'Empordà wetlands, site 2). Four replicates were measured for each host plant species. The measurements were conducted in 2015, a year characterised by warm and dry summer conditions (Fig. A6). Stomatal conductance and leaf surface temperatures have been widely applied as integrated indicators of drought and heat stress in herbaceous plants (Annisa et al., 2013; Munns et al., 2010). Experimental evidence shows that leaf conductance and surface temperature show qualitatively different responses in heat treatments and soil drought experiments (Annisa et al., 2013). In conditions of abundant soil moisture, *Brassica* plants respond to strong air temperature stress with an increase in leaf stomatal conductance values, producing in turn positive leaf-to-air temperature differences (i.e. cooler leaf temperatures relative to air temperatures due to increased leaf transpiration; Annisa et al., 2013). In contrast, if plants experience combined soil water and air heat stress, which is probably more common in Mediterranean ecosystems, reduced leaf conductance values and negative leaf-to-air temperature differences are to be expected (i.e. higher leaf temperatures relative to air temperatures due to reduced leaf transpiration).

Photosynthetic rates (A) and stomatal conductances (g_s) were measured at a quantum flux density (PPFD) of $1080 \pm 19 \mu\text{mol m}^{-2} \text{s}^{-1}$ and ambient air temperature under a controlled CO_2 concentration of 400 ± 2 ppm. To conduct the measurements, one leaf was enclosed in a clamp-on gas-exchange cuvette of 2 cm^2 . We selected healthy leaves that were not affected by insect larvae consumption and/or fungal damage. Air flow through the dynamic cuvette was $732 \pm 0.05 \text{ ml min}^{-1}$. A LICOR 6400 XT (4647 Superior Street P.O. Box 4425 Lincoln, Nebraska USA) gas-exchange system was used.

2.3 Results

2.3.1 Climatic and population trends

Model selection analyses using only climatic data identified June rainfall of the current year as the best predictor of the interannual variation of *P. napi* abundance (Tables A7 and A8). An analysis of the temporal trends for this climatic predictor (June

rainfall) over 1994–2012 identified a decadal period of increasing drought (1997–2007, Fig. 2.1a). The observed decadal reduction in June rainfall was highly significant at the four sites (Fig. 2.1a). In line with the reported decadal trend of increasing summer drought stress, butterfly abundance at lowland sites significantly declined, paralleling the trend of June rainfall (Fig. 2.1b). As a result, lowland populations showed a sharp reduction of more than one order of magnitude with respect to the initial abundance numbers. In contrast, mid-elevation site populations remained fairly stable over the 1997–2007 drought period (Fig. 2.1c), and were therefore not paralleling June rainfall trends as observed at the lowland sites. After the decadal drought period, however, population at site 3 increased significantly ($R^2 = 0.38$, $P = 0.0024$, Fig. 2.1c), and this increase was significantly correlated to an abrupt increase in June rainfall during 2008–2012 ($R^2 = 0.38$, $P = 0.0028$). Lowland sites showed significantly lower June rainfall values during the 1997–2007 period (Tukey–Kramer test, $R^2 = 0.35$; $P = 0.0005$, Fig. A7).

The model selection approach combining climatic and land cover data reported that both types of variables significantly contributed to the reported demographic trends. Overall, however, the estimates of the models suggested a stronger and predominant effect for climatic variables in the reported trends (June rainfall, Tables A7 to A11. For landscape variables, significant negative effects of reduced meadow cover extent during 1994–2012 were detected at site 2. At mid-elevation site 3, a positive effect of increased wetland area was detected. Landscape data were not available for 2013–2015, and therefore, these years were excluded from the butterfly annual abundance models. Nevertheless, we examined the observed population trends for an extended period (1994–2015) and the results were fully consistent with the trends reported for 1994–2012 (Fig. A8). Mid-elevation site 4 showed a stable population trend (Fig. 2.1c), and no significant relationships with climatic variables in OLS models were observed for this site. Population abundances at low-elevation sites areas were higher (Fig. 2.1), presumably due to a much higher spatial density of host plants per unit of surface observed in these wetland areas.

2.3.2 Different population sensitivity to temperature impacts

The analysis of the environmental variation of wing size revealed significantly different trends between lowland and mid-elevation populations (Fig. 2.2a). Of note, these trends were significantly associated with increased summer temperature only at lowland sites (Fig. 2.2a). Consistent with this, OLS models identified the seasonal variation of temperature during the larval and pupal growth period (25 days previous to the adult emergence and collection) as the principal driver of diverging wing size seasonal trends and detected site \times temperature interactions (Table 2.1). The interactions between site and temperature were highly significant, reporting strong negative effects only at lowland sites (Table 2.1 and Fig. 2.2).

Consistent with the field observations, the common-garden splitbrood experiment demonstrated a significant link between temperature and wing size variation (Fig. 2.2b). Tables A12 to A15 summarise the results of the split-brood experiment. Significantly different wing size values were observed for the 20 °C and the 25 °C treatment, with reduced

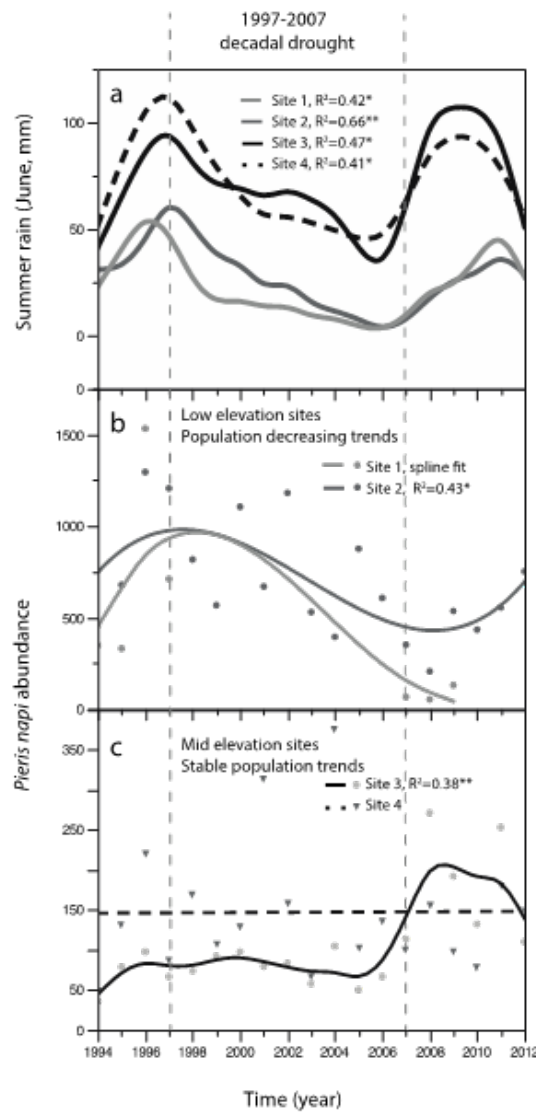


Figure 2.1: Climatic and butterfly demographic dynamics over the 1994–2012 period. (a) Annual variation of June rainfall at the four population sites. Significant linear rainfall trends are indicated in the 1997–2007 period. (b) Observed variation of butterfly annual abundance at lowland sites (Delta del Llobregat (1) and Aiguamolls de l’Empordà (2) protected wetlands). A significant polynomial and a spline fit are illustrated. (c) Observed variation of butterfly annual abundance at mid-elevation sites (Zona Volcànica de la Garrotxa (3) and Montseny Ranges (4) protected areas). Spline and linear fits were applied. When significant, the variance explained by the linear fit (R^2) is indicated.

wing lengths observed for the high-temperature treatment. In addition, we observed significant effects of sex and family, with females showing significantly lower wing sizes (Tables A12 to A15). The effect of the temperature treatment, however, was dominant and stronger than family and sex effects. Wing size heritability estimate reported by MCM-Cglmm models was 0.41 (CI = 0.12–0.76).

The observed wing sizes for the 25 °C treatment were similar to the observed range of

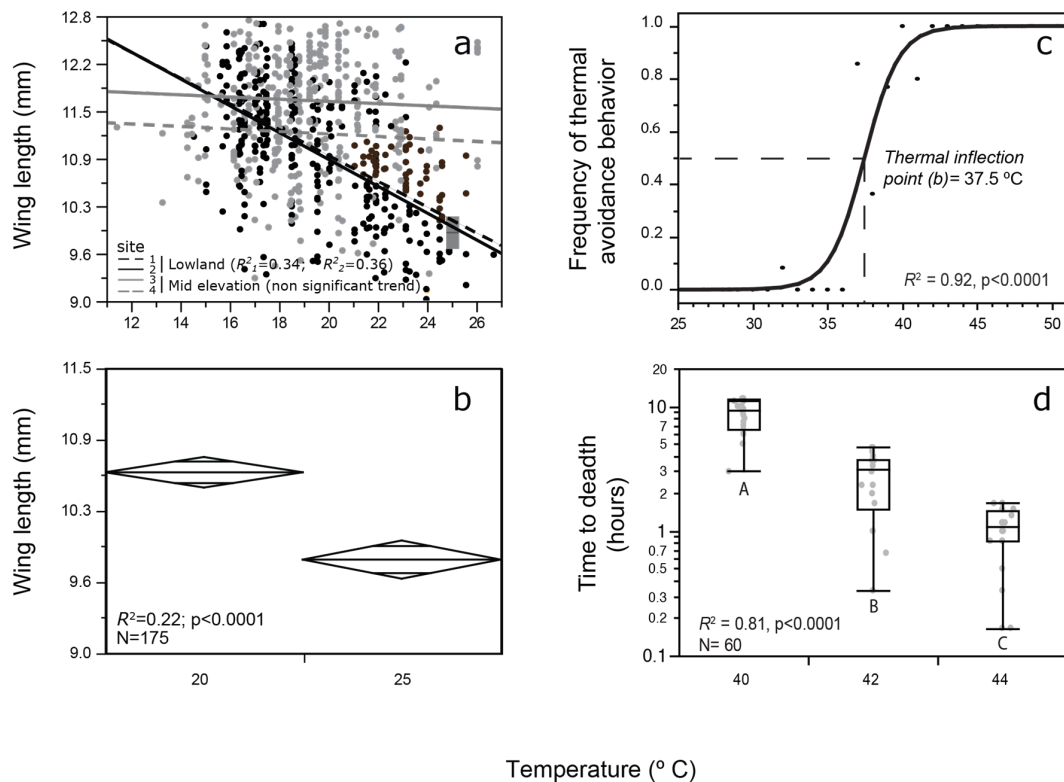


Figure 2.2: Observational (a) and experimental (b) trends in the selected phenotypic biomarker trait — wing size (mm)—. (a) Observed relationships between butterfly wing size and environmental temperature at the four sites. Black dots represent mid-elevation individuals. Grey dots represent low-elevation individuals. The grey square represents the mean wing size and the 95% confidence interval observed in the thermal stress experimental treatment (25°C), matching the field observational values (lines) at lowland sites. (b) Observed differences in wing size measurements between two experimental temperature treatments (20 and 25 °C). The line across each diamond represents the treatment mean. Diamond plots indicate the 95% confidence interval for each treatment (vertical span). We concluded that experimental and field results were in agreement, suggesting a key role of stressful temperatures at lowland sites in the reported wing size trends. (c) Estimated thermal inflection point for behavioural avoidance responses in last instars of *Pieris napi*. (d) Observed thermal death time (TDT) in static thermal treatments in last instar larvae of *Pieris napi*. The line within the box represents the median sample value. The ends of the box represent the 25th and 75th quantiles. Different capital letters indicate significantly different means (Tukey–Kramer test, $P < 0.0001$).

wing size values in the field dataset in the same range of temperatures (i.e. mean temperature during the growth period (25 days), Fig. 2.2a, grey square area). Significant effects of thermal treatment on larval developmental times were observed, as reported in Fig. A9 ($R^2 = 0.71$, $P < 0.0001$). Site effects were not significant (Tables A14 and A15). Mid-altitude sites showed more plastic responses to temperature in experimental treatments (Table A15), indicating that the flat trends in Fig. 2.2a were not related to a lack of thermally induced wing plasticity in mid-altitude populations.

2. PHENOTYPIC BIOMARKERS OF CLIMATIC IMPACTS ON DECLINING INSECTS

Table 2.1: Ordinary least squares model (OLS) of the variation of wing size. Values in bold highlight the principal effect of temperature variation and site×temperature interactions (negative in lowland, declining populations and positive at mid-elevation sites)

Wing size				
Model fit: $R^2 = 0.38$, $P < 0.0001$, $AIC_c = 18232.3$, $BIC = 18300.8$				
Term	Estimate	SE	t	P
Intercept	317368.16	190999.1	1.66	0.0970
Temperature (Temp)	-9164.388	1321.999	-6.93	<0.0001
Site 1	-13424.82	8506.542	-1.58	0.1150
Site 2	-23883.71	8205.615	-2.91	0.0037
Site 3	32545.087	10085.57	3.23	0.0013
Site 4	4763.4443	6388.543	0.75	0.4561
Sex (female)	-14702.02	2308.956	-6.37	<0.0001
Year	-153.3687	4089.377	-0.04	0.9701
Photoperiod	10464.797	5677.805	1.84	0.0657
Rainfall	764.4488	7598.182	0.10	0.9199
Relative humidity	2546.9183	2090.97	1.22	0.2236
Temp×site 1	-6824.945	1318.059	-5.18	<0.0001
Temp×site 2	-7078.373	1352.495	-5.23	<0.0001
Temp×site 3	4663.1566	1517.146	3.07	0.0022
Temp×site 4	9240.1615	1799.712	5.13	<0.0001
Temp×sex (female)	-1274.876	854.2187	-1.49	0.136

2.3.3 Thermal avoidance behaviour (TAB) and thermal death time (TDT) experiments

The results of the thermal avoidance behaviour experiment are shown in Fig. 2.2c. The observed behavioural response of thermal avoidance was well described by a two-parameter logistic model ($R^2 = 0.92$, $P < 0.0001$) with the following parameters: growth rate $a = 0.86 \pm 0.24$, thermal inflection point $b = 37.46 \pm 0.37$ °C. These results indicate a rapid shift to behavioural avoidance responses at temperatures above 37.5 °C in the last instar larvae of *Pieris napi*.

Fig. 2.2d synthesises the results of the static thermal death time experiments. Thermal death time experiments (TDT) reported an estimate of the temperature resulting in death at 1 min of exposure (CT_{max}) of 51 °C, and a thermal susceptibility constant (z) of 4.11 ± 0.33 (°C). The observed TDT relationships for 100% and 50% of mortality are illustrated in Fig. A10a. The thermal threshold for a time of exposure equal to the whole larval period was estimated in 32.5 °C (Fig. A10b). For a daily exposure of 6 hr to maximum daily temperatures (TE6h, 10 am–16 pm), the TDT curve indicated a thermal threshold of 34.5 °C (Fig. A10b). These thermal thresholds were achieved in warm summer days characterised by mean daily temperature ≥ 25 °C in 2014–2015 (Fig. A10c).

2.3.4 Thermal stress during summer drought and microsite effects

Analysis of meteorological data during 2014–2015 for the four population sites found that mean June maximum temperatures were in the range of 28–30 °C at three sites (1–3) and around 25 °C at site 4 (Fig. 2.3a). Maximum daily temperatures reached the experimental TDT thermal thresholds in warm summer days (i.e., for thermal values higher than the 75th quantile, Fig. 2.3a). Next, we examined whether host plant microhabitat buffering effects at the four sites could allow reduced maximum temperature values. Analysis of host plant microsite climatic data (2014–2015) revealed strong buffering effects only at mid-elevation populations (-5.2 ± 0.17 °C), and only for those plants located at closed microsites (Fig. 2.3b, green rectangles; Table A16). In contrast, in low-elevation sites we observed limited cooling effects of canopy cover at closed sites (-0.79 ± 0.32 °C, Fig. 2.3, Table A16). Open microsites were characterised by amplified mean maximum June temperatures (1.9 ± 0.18 °C in lowland sites and 3.04 ± 0.28 °C in mid-altitude sites; orange rectangles in Fig. 2.3b). The analysis of daily cycles of temperature variation showed that temperatures of warm summer days reached values higher than the experimental TDT thresholds for several hours in open sites (Fig. 2.3c). In contrast, these thermal values were not achieved in closed microsites of mid-elevation sites (most values < 30 °C, Fig. 2.3d). Overall, we conclude that significantly different thermal buffering effects were observed at lowland and mid-elevation sites, in line with the previously reported trends for butterfly demographic declines and for phenotypic biomarkers (wing size responses).

2.3.5 Host plant resource dynamics

The analysis of the seasonal patterns of host plant availability and quality (C/N ratio) revealed important differences between mid-elevation and lowland sites. Mid-elevation sites were characterised by a continuous availability of fresh *Alliaria petiolata* leaves during the whole summer period and, consequently, by more stable temporal C/N ratios (Fig. 2.4a). In contrast, at lowland sites, the leaves of the two host plants *Lepidium draba* and *Brassica nigra* presented a significant linear increase in the C/N ratio (indicating a progressive reduction of host plant quality with the advance of summer and plant phenology). This trend culminated in total leaf senescence at the end of June–early July (Fig. 2.4b).

Therefore, in contrast to mid-elevation sites, summer drought at the lowland sites produced a relatively large period (45–65 days) in which we observed a total absence of fresh leaves due to the complete senescence of the above-ground organs (leaves and shoots, corresponding to Julian days 190–235 —July 9–August 23— in Fig. 2.4b). In agreement with these observations, a significant reduction of leaf conductance values was observed during summer drought (Fig. 2.5). The observed values were below $0.2 \text{ mol m}^{-2} \text{ s}^{-1}$ (*B. nigra*: $0.176 \pm 0.034 \text{ mol m}^{-2} \text{ s}^{-1}$; *L. draba*: $0.137 \pm 0.021 \text{ mol m}^{-2} \text{ s}^{-1}$). These values

2. PHENOTYPIC BIOMARKERS OF CLIMATIC IMPACTS ON DECLINING INSECTS

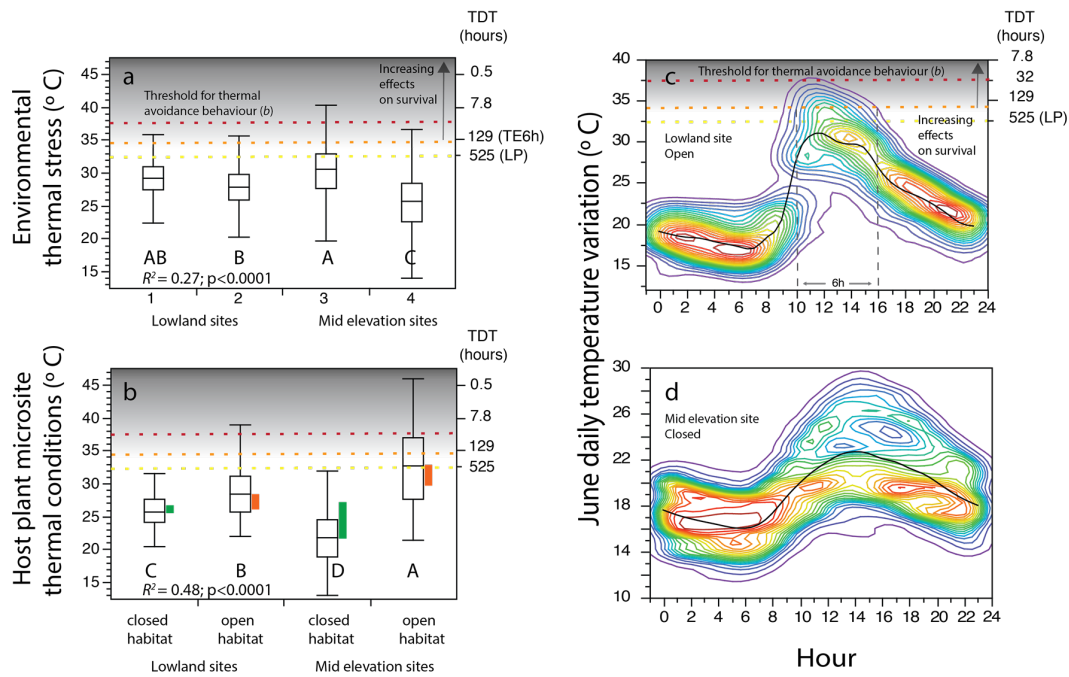


Figure 2.3: Comparison of June maximum temperature measurements (i.e. mean of the daily maximum temperatures during June) at standardised meteorological stations and at host plant microsites for 2014–2015. (a) Meteorological data. The line within the box represents the median. The ends of the box represent the 25th and 75th quantiles. The lines that extend from the box indicate the following distances: 25th quantile - $1.5 \times$ (interquartile range) and 75th quantile + $1.5 \times$ (interquartile range). The plane yellow dotted line indicates a thermal threshold of 32.5 °C calculated from the thermal death time (TDT) relationship, corresponding to a time of thermal exposure equivalent to whole larval period (LP, see Fig. A10). The orange dotted line indicates a 34.5 °C threshold, corresponding to the TDT for 6 hr of daily exposure to maximum temperatures over the larval period (TE6h). The red dotted line indicates the experimental threshold for thermal avoidance behaviour (TAB) of 37.5 °C. Different capital letters indicate significantly different means (Tukey–Kramer test). The grey surface area illustrates the logarithmic decrease in the thermal death time with linearly increasing temperatures. (b) Temperature–humidity host plant sensor data. Green rectangles indicate the observed habitat buffering effect in Celsius degrees at host plant microsites relative to standardised meteorological records. Orange rectangles indicate the observed thermal amplification of host plant microsites relative to standardised meteorological records. (c and d) Observed daily variation of June temperatures at two host plant microsites characterised by contrasting buffering trends (c, open microsite, lowland site; d, closed microsite, mid-elevation site). A spline fit (black line) indicates the mean trend observed. A smooth surface illustrating the density of data points is provided (total range of observed June temperatures). Red contour lines indicate maximum point density. The contour lines are quantile contours in 5% intervals (i.e. 5% of the temperature measurements are below the lowest—blue—contour, 10% are below the next contour. The highest—red—contour has about 95% of the thermal values below it).

matched the range of conductance values reported in water stress experiments for *Brassica* species in stressful conditions (Annisa et al., 2013; Guo et al., 2015). Complementary results for photosynthetic rates (A) and substomatal CO_2 concentrations (c_i) for *L. draba* are reported in Fig. A11.

In accordance with these trends, significantly higher temperatures at the leaf surface in relation to air temperature were recorded during the peak of summer drought (Tukey–Kramer test, *L. draba*: $R^2 = 0.64$, $P < 0.0001$; *B. nigra*: $R^2 = 0.56$, $P < 0.0001$, Fig. 2.4c

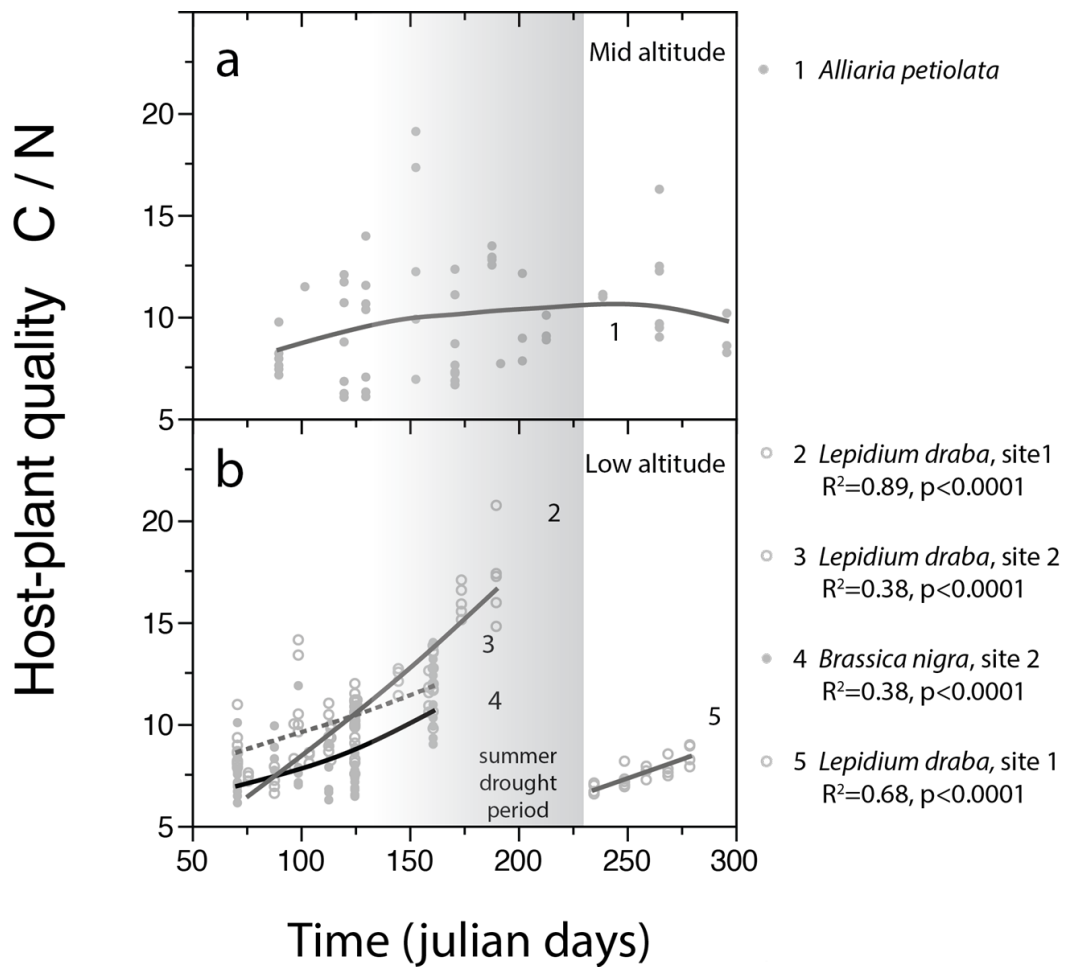


Figure 2.4: Observed annual variation of leaf host plant quality (C/N content ratio). Higher C/N ratio corresponds to lower host plant quality. (a) Observed trends at mid-elevation site 3. (b) Low-elevation sites 1 and 2. The grey surface area illustrates the summer drought period.

and d). Similarly, with the onset of summer season, midday leaf temperatures significantly increased (*L. draba*: $T_{June} - T_{May} = 14.5$ °C; *B. nigra*: $T_{June} - T_{May} = 14.4$ °C; Tukey-Kramer test: $P < 0.0001$). As a result, midday leaf temperatures in June reached 37.56 ± 0.35 °C in *B. nigra*, and 38.16 ± 0.52 °C, in *L. draba* (Fig. 2.5c and d). In summary, during the peak of summer drought, the results for lowland plants indicated significant reductions in leaf quality (increased C/N ratios), significantly reduced conductance values ($g_s < 0.2$ mol m⁻² s⁻¹) and significantly increased leaf surface temperatures.

2.4 Discussion

Our results indicate that a decadal trend of increased summer drought has triggered long-term declines of *P. napi* populations at lowland sites (Fig. 2.1). In contrast, the analysis of microclimatic conditions experienced by mid-elevation populations suggests a key role for habitat buffering processes in these sites. Mid-elevation populations presented significantly stronger thermal buffering effects in closed habitat microsites (a sixfold in-

2. PHENOTYPIC BIOMARKERS OF CLIMATIC IMPACTS ON DECLINING INSECTS

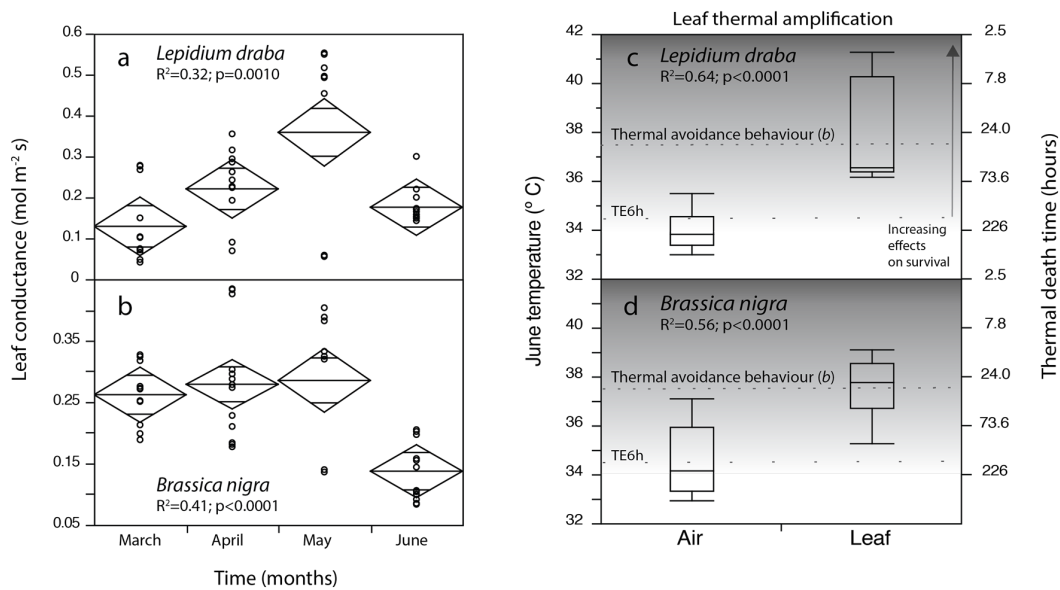


Figure 2.5: Observed monthly variation of leaf conductance for lowland plants *Lepidium draba* (a) and *Brassica nigra* (b). The line across each diamond represents the mean. The vertical span of each diamond represents the 95% confidence interval. Leaf conductance is linked to plant transpiration and leaf energy balance, and hence to the ability of the plant to cool itself under heat stress. (c and d) Observed midday June temperatures of the leaf surface of low-elevation host plants *L. draba* (upper panel) and *B. nigra* (lower panel). Temperatures were significantly higher than air temperatures synchronously recorded using LICOR 6400 portable photosynthesis system (indicated as *Air* in the panels). Expected thermal death time for *P. napi* is provided in the right axis for the amplified leaf surface temperatures. The line within the box represents the median sample value. The ends of the box represent the 25th and 75th quantiles. The grey surface area illustrates the logarithmic decrease in the thermal death time with linearly increasing temperatures.

crease), and as a result, individuals were characterised by comparatively larger butterfly wing sizes than butterflies from lowland populations exposed to similar conditions of environmental thermal stress without access to thermal buffering micro-refugia (Figs. 2.2 and 2.3). Moreover, a continuous availability of high-quality leaf resources with low C/N ratios was observed only at mid-elevation sites, in non-declining populations (Fig. 2.4). In contrast, lowland host plants showed a progressive seasonal reduction of leaf nitrogen content, possibly associated with the seasonal advance of the flowering and fruiting phenological cycle (Fig. A12). In line with this finding, previous studies have documented a decrease in crude protein and digestible fibre after flowering in *L. draba* (Jacobs, 2007). Finally, consistent effects of summer drought were observed in the leaf conductance of *L. draba* and *B. nigra*, the two lowland host plants, resulting in turn in significantly increased leaf surface temperature. In addition to these combined drought and leaf heat stress impacts, lowland populations also experience periods of host plant resource scarcity (during late July–August), which are in turn associated with a decrease in abundance due to pupal aestivation (Fig. 2.4). Overall, our results suggest that butterfly population vulnerability to long-term drought periods is associated with multiple co-occurring and interrelated ecological factors, including limited vegetation thermal buffering effects at lowland sites, significant drought impacts on host plant transpiration and amplified leaf

surface temperature, as well as reduced leaf quality linked to the seasonal advance of plant phenology.

June maximum daily temperature values recorded by host plant thermal sensors at open lowland microsites ranged from 22 °C to 42 °C (Fig. 2.3). Experimental studies in *Pieris* butterflies in thermally variable environments have been conducted (i.e. treatments of short-term heat stress exposure in daily cycles, mimicking natural daily variability). These treatments report strong negative effects on larval growth rates and consumption rates for temperatures above 39 °C (Kingsolver, 2000; Kingsolver et al., 2006). In addition, it has been recently reported that thermal conditions above 35 °C can significantly increase egg and young larvae mortality in other model species (Klockmann et al., 2017a). In line with this finding, we observed a significant negative effect of reduced larval size in thermal death time responses in *P. napi* (F ratio = 9.67, P = 0.031, Table A17, indicating a significantly increased susceptibility of younger larvae to thermal stress. In the case of *P. napi* habitats, we observed that at open lowland microsites a large percentage of the maximum daily temperature records (97.5%) were below 37.5 °C and more than 90% were below 35 °C (i.e. most of the values were not surpassing the thermal threshold of 34.5 °C estimated in TDT experiments for a daily exposure of 6 hr to maximum temperatures). Therefore, and according to the available experimental evidence in *Pieris* butterflies and other species, these thermal regimes should not necessarily impose a strong negative impact on the survival, consumption rates, and growth rates of larvae if conditions of optimal host plant quality and reduced leaf drought stress were simultaneously met (Kingsolver, 2000; Kingsolver et al., 2006). In line with these findings, we measured reduced leaf quality and water stress conditions in host plants at open lowland microsites during the summer period. We observed that in open exposed sites, amplified leaf surface temperatures and reduced transpiration could significantly increase host plant temperature (Fig. 2.4), surpassing the experimental thresholds estimated (i.e. TDT for TE6h and TAB). Of note, previous experimental works demonstrate significant interactions in combined heat stress and altered host plant quality treatments, often resulting in stronger negative impacts on butterfly larval growth rates (e.g. Jones et al., 1982; Kingsolver, 2000). In addition, pupal mass has been positively associated with fitness and total lifetime egg production in the genus *Pieris* (Jones et al., 1982; Wiklund and Kaitala, 1995). Consequently, direct negative impacts of body size reductions on population demography should not be discarded.

Our results also documented summer drought impacts on host plant ecophysiology. The observed reductions of leaf conductances at the peak of summer drought (values < 0.2 mol m⁻² s⁻¹) are in line with the quantitative values reported for *Brassica rapa* in comprehensive water stress experimental treatments (Fig. 2.5; Annisa et al., 2013; Guo et al., 2015). Under strong drought stress, host plants are expected to progressively reduce leaf water content and transpiration. This could potentially affect butterfly population demography because leaf water content is known to be an important factor for larval development (Scriber, 1977; Slansky and Feeny, 1977; Soo Hoo and Fraenkel, 1966). Moreover, leaf transpiration and leaf water content are key characters driving host plant selection by females in *Pieris* butterflies (Myers, 1985; Wolfson, 1980). The same is true for leaf nitro-

gen content, which also limits larval development and is a key trait in female host plant selection (Myers, 1985). Finally, leaf water and nitrogen content are generally positively correlated in *Brassica* host plants used by *Pieris* species (Mattson, 1980) and are also positively and significantly related to transpiration rates (Myers, 1985). On top of this, our results indicated a key role of decreased June rains on long-term population declines and in addition reported a significant reduction of leaf conductance in the transition from May to June at lowland areas (Fig. 2.5). Our study also highlights the potential importance of seasonal trends in leaf phenology, which in turn determine C/N content and host plant quality (Kause et al., 1999; Kriedemann, 1968). To our knowledge, these factors have been seldom considered as contributing factors determining butterfly population vulnerability to increased drought impacts.

Overall, this study identifies multiannual trends in summer drought as a primary driver of long-term demographic declines of *P. napi*. Crucially, nearly 70% of the butterfly species in this hot spot region for European butterflies are currently affected by significant population declines (Melero et al., 2016; Stefanescu et al., 2011a,b). Landscape changes and climatic drivers have been considered as the principal candidate drivers of these widespread declines, but their relative role and the ecological mechanisms implied are still poorly described for most of the species. In this context, our study clarifies the importance of summer drought as a key primary driver in *P. napi* in the studied populations and sheds some light into some of the ecological mechanisms implied (i.e. vegetation thermal buffering, phenology effects on plant quality, and changes in host plant water transpiration and leaf water content). It remains to be assessed whether these mechanisms could also apply to other populations of *P. napi* in Catalonia and to other butterfly species. In this regard, it is important to bear in mind that our analyses are restricted to abundant populations located in protected areas. The reported trends could possibly differ in lowland and mid-land populations currently affected by increased urbanisation pressures, intensified land use changes, pesticide management impacts and land abandonment (Stefanescu et al., 2011a,b). Moreover, the results do not describe the responses of *P. napi* populations that rely on other host plants in Catalonia (e.g. *Cardamine pratensis* and *Arabis glabra*). The host plant-specific mechanisms described in the paper may non-necessarily apply to these populations.

Finally, our study suggests that wing and body size measures are reliable phenotypic biomarkers of the geographic variability of thermal stress exposure in the studied populations, providing an indirect indicator of limited habitat thermal buffering conditions for these specific populations. In our field and experimental datasets, the percentage of reduction of wing size per degree Celsius (as defined in Forster et al., 2012) was in the range of 1–2% (regression slope for normalised experimental data: -1.56 ± 0.25 , $P < 0.0001$; regression slope for normalised field data: -1.80 ± 0.11 , $P < 0.0001$). This trend is consistent with the experimental slopes reported for body size–temperature relationships in other temperate butterfly species exposed to similar experimental thermal treatments (Forster et al., 2012, and see Fig. A13 for some examples). More detailed quantitative studies of the effects of thermal stress on survival and fecundity functions in this species are required to estimate the critical size values associated with negative effects on insect performance

and the associated thermal threshold (P^* and T^* values, see Appendix A.2 for further discussion). Moreover, we show that complementary analyses of host plant dynamics are highly informative and necessary, due to the multiple ecological processes that seem to be co-acting and interacting (Nygren et al., 2008; Talloen et al., 2009). In summary, this study indicates that phenotypic thermal biomarkers are informative as climatic stress indicators but should be complemented, whenever possible, by multitrait frameworks analysing host plant ecophysiological responses and by detailed microclimatic measurements.

Acknowledgements

Emili Bassols and Francesc Xavier Santaefemia provided support with permission management, scientific advice and key assistance during field work. Ty Hedrick and Heidi McLean provided guidance and help with the MATLAB PhotoGUI applications (Kingsolver Lab, University of North Carolina). Joel Kingsolver provided useful comments that largely improved the manuscript. Enrico Rezende and Mauro Santos provided technical advice in the experimental design of TDT experiments. Jordi Artola and Andreu Ubach provided invaluable help collecting *P. napi* samples at Can Jordà and lowland sites. Melodia Tamayo, Joaquim de Gispert, and Andreu Ubach contributed to the experimental work. Joan Llusà, Gerard Farré, and Daijun Liu helped with the plant photosynthesis measurements. Consorci per a la Protecció i Gestió dels Espais Naturals del Delta del Llobregat, Parc Natural de la Zona Volcànica de la Garrotxa, and Parc Natural Aiguamolls de l'Empordà provided logistic support. This research was supported by VENI-NWO 863.11.021, the Spanish Government grants CGL2016-78093-R, CGL2013-48074-P, and CGL201348277-P; the Catalan Government project SGR 2014-274; and the European Research Council Synergy Grant ERC-2013-SyG 610028 IMBALANCE-P. Additional funding was provided to CWW from the Knut and Alice Wallenberg Foundation (KAW 2012.0058) and the Swedish Research Council grant VR-2012-4001.





3

**Plastic and
phenological
variation of host
plants mediates
local responses of
the butterfly *Pieris napi*
to drought in the
Mediterranean basin**



3.1 Introduction

Global fingerprints of the effects of climate change on insect populations have already been reported (Boggs, 2016). The responses of insects to these climatic trends are, however, largely variable between species, geographic areas and even between populations of a particular species. Multiple processes that operate at the local scale can shape the climatic exposure and sensitivity of insect populations, modulating therefore their vulnerability to climatic impacts (see Carnicer et al., 2017, for a revision). Among the many mechanisms determining differential exposure to climate there are microclimatic variation produced by the interaction of macroclimatic conditions with biotic and abiotic elements of the environment (Woods et al., 2015), and plastic variation in thermoregulatory behaviour of insects. For example, Bennett et al. (2015) found that interpopulation variability in phenology, oviposition behavior, and the use of host plants and microhabitats in the butterfly *Euphydryas editha* produced a geographic mosaic of populations with different microclimatic and thermal exposures. This represented a case where complex local adaptation of the different populations of *E. editha* conferred them contrasting vulnerability in front of climate change.

Substantial progresses have been made to understand the underlying mechanisms driving the responses of insect populations to climate change. Nonetheless, most of the studies focus on the direct effects of climate on the phenology and the population dynamics of insects, modulated by insect's plasticity and local adaptations (Boggs, 2016; Carnicer et al., 2017). Other species that interact with the population of study may also be affected by climate change, however. Considering the additional indirect effects of climate change coming from the responses of insect's interacting species would, therefore, improve our understanding of the climatic impacts on insect populations. Phenological mismatches between insects and their host plants or nectar sources are one of the most common cases of study of the effects of climate change on plant–insect interactions (Donoso et al., 2016; Hindle et al., 2015; Singer and Parmesan, 2010). To our knowledge, the influence on insect populations of plastic responses to climate change in other plant traits different from phenology, however, have rarely been considered.

Our study assessed the potential role of host-plant plasticity on the mediation of the impacts of summer drought on a declining population of a drought-sensitive butterfly (*Pieris napi*) in the northwestern Mediterranean. A recent study that was partly carried out in Aiguamolls de l'Empordà Natural Park associated the long-term decline of this butterfly population with a decadal trend of increased summer drought (Carnicer et al., 2019). The study also identified diverse mechanisms operating at the local-scale modulating the effects of drought on the declining population. Detailed measurements of microclimatic conditions and of a phenotypic biomarker indicative of the thermal conditions during larval development (i.e. adult wing size) showed that the population lacked an effective thermal buffering from vegetation (Carnicer et al., 2019). Ecophysiological assays of larval heat tolerance of this population indicated that this thermal exposure was not necessarily lethal, conferring to host-plant quality and availability a crucial role in the butterfly declining trend. Here we describe the phenological cycle of *P. napi* and of its two

host plants in the area to assess their phenological match. We also quantify the variation of several host-plant traits crucially affecting plant quality and resource availability. More precisely, we analyze the variability of host-plant traits observed both in the field and in experimental assessments. Our main aim is to evaluate whether host-plant plasticity can effectively modulate the responses of this *P. napi* population to drought.

3.2 Methods

3.2.1 Study system

We studied the green-veined white butterfly *Pieris napi* (Fig. 3.1) and its two main host plants in a protected area (Aiguamolls de l'Empordà Natural Park, Catalonia) at the northeastern Iberian Peninsula. This butterfly is commonly spread across Eurasia, North Africa and North America (Vila et al., 2018), though it shows a clear preference for humid habitats. In Catalonia, it is found throughout the country except in its driest areas. The study site, located in a coastal wetland, holds one of the most abundant populations of *P. napi* in Catalonia, despite showing a negative trend. Adults can be detected in this area from late winter to autumn in four–five partially overlapped generations, except in late summer, when abundance is much reduced. Most eggs are individually laid on the leaves of *Lepidium draba* and *Brassica nigra*, although oviposition on other crucifers such as *Coronopus squamatus* has occasionally been observed too (Stefanescu, 1997).

The heart-podded hoary cress (*Lepidium draba*) is a perennial, rhizomatous herb usually found in ruderal areas and field margins with deep soil. Flowering individuals can be detected from March to June. Plants die back to the root crown after seed development (Jacobs, 2007) and all the aboveground parts completely disappear until new resprouts emerge from subterranean rhizomes in late summer and autumn. Its extensive, multi-branched rhizomes are notably capable of producing many new shoots, which can develop into large monocultural stands (Francis and Warwick, 2008). The black mustard (*Brassica nigra*), in contrast, is a cultivated, annual herb that has been naturalised in humid grasslands. Individuals complete their life cycle in late-spring–early-summer and no new plants can be found until the next growth season. At the study site, both plant species are present in a diversity of habitats, from open fields and wetlands to riparian forests and dense shrublands. The plants selected for oviposition by *P. napi*, however, usually grow in microhabitats presenting an intermediate degree of canopy closure (Vives-Inglà et al., 2023), in the margins of paths and irrigation canals protected by the surrounding vegetation (Stefanescu, 1997).

3.2.2 *Pieris napi* abundance

Weekly abundance of *P. napi* was recorded in the study site from 1993 to 2018, as part of the Catalan Butterfly Monitoring Scheme (CBMS, www.catalanbms.org). The CBMS



Figure 3.1: A green-veined white butterfly (*Pieris napi*) nectaring from a crucifer. *Pieris napi* lays most of their eggs on plants from the Brassicaceae family linked to humid habitats. Photograph: Vlad Dinca.

applies a standardised recording procedure (i.e. Pollard walks) consisting of weekly counts along fixed transects from March to September (30 weeks per year). The recorder counts all individuals of all butterfly species seen within 2.5 m on each side and 5 m in front of the trail (Pollard and Yates, 1993). For the current work, an index of weekly abundance of *P. napi* for each recording day was calculated as the number of butterflies seen divided by the length of the transect (in km). A LOESS analysis against Julian day including the data of all the years was then applied (neighborhood parameter $\alpha = 0.2$) to determine the mean phenology of *P. napi* at the study site. The analyses were conducted with R 3.6.1 (R Core Team, 2019) and were repeated for each year separately to assess phenological variation between years.

The phenological curves were divided into four generational periods: March–April, May–June, July, August–September. Additional abundance indices were then calculated at the annual and generational scales as the sum of weekly abundance indices of each period (i.e. the area under the phenological curve). General linear models were applied on the annual and on the four generational abundances against year to determine their decadal trend. The analyses were also repeated applying a polynomial fit.

3.2.3 Monitoring of host-plant traits and microclimatic conditions

Two local cohorts of *L. draba* (282 individuals) and *B. nigra* (39 individuals) were continuously monitored from March to October of 2017 every two weeks. Each monitoring date a total of 15 individuals of *L. draba* and 6 individuals of *B. nigra* were selected to measure their microclimatic conditions and several phenological, morphological and physiological traits. For each host plant species, the selection included individuals growing in different microhabitats in terms of canopy closure (3 individuals per microhabitat) and ensured that plants were randomly chosen without repetition to avoid pseudoreplication. Replicated foliar measurements were conducted in one apical, one medial and one basal leaf per plant.

Microclimatic measurements included canopy closure, the volumetric water content of the soil and the foliar temperature. The measurement of canopy closure (i.e. “the proportion of the sky hemisphere obscured by vegetation when viewed from a single point”, Jennings, 1999) consisted in visually estimating the per cent area occupied by the canopy assigning it to one of the cover classes defined by Daubenmire (1959) (0-5%, 5-25%, 25-50%, 50-75%, 75-95%, and 95-100%) and taking its midpoint. The ocular estimation was conducted in each one of the vertical and the four cardinal directions and the average value was kept. Five microhabitat categories were then defined based on the estimations of canopy closure: closed (C, mean closure of 40% for *B. nigra* and 60% for *L. draba*), semi-closed (SC, 55% for *L. draba*), semi-open (SO, 40% for *L. draba*), open (O, 20% for *B. nigra* and 0% for *L. draba*), and very open (OO, 0% and a very dry soil for *L. draba*). Soil humidity (%) was measured at three points near each plant using a DELTAT SM150 (Delta-T Devices Ltd, UK) soil-moisture sensor kit. Foliar temperature at its upper surface was measured using a wire K-type thermocouple probe (Omega SC-TT-KI-30-1M, Omega Engineering Ltd, UK) attached to a hand-held thermocouple thermometer (Omega HH503, Omega Engineering Ltd, UK, and HANNA HI935005N, Hanna Instruments Ltd, Spain). Average measurements (at least three records) were kept. The temperatures were measured between 10:00 and 16:00, and the time, wind and radiation conditions were recorded.

Foliar length, width, and chlorophyll content were measured in each monitored plant. Chlorophyll content was estimated as the mean of three measurements from a MINOLTA SPAD-502 (Konica Minolta Sensing, Spain) chlorophyll meter. Finally, leaves were severed and immediately weighed (fresh weight, FW) using a Pesola PJS020 Digital Scale (PESOLA Präzisionswaagen AG, witzerland) for calculating foliar water content. The leaves were oven-dried in the laboratory at 60 °C for two days to a stable weight (dry weight, DW). The ratio of foliar water content (to DW) was defined as $\frac{FW-DW}{DW}$. An independent phenological census for each microhabitat type was conducted selecting 15 individuals for each plant species. Plants were classified in one of four phenological stages: early vegetative (spring rosettes and young shoots before budding), reproductive (plants with buds, flowers, and/or fruits), senescent, and summer resprout (for *L. draba*). Summer resprouts of *L. draba* can represent a key resource for summer generations of *P.*

napi. A census of newly emerging resprouts of *L. draba* was thus conducted since July, when the first shoots grew from resprouting rhizomes. Five 25-cm quadrats were randomly placed in each microhabitat type. The total number of resprouts per unit area was counted (i.e. resprout density), and three resprouts per sampling quadrat were then randomly selected for measuring their heights and counting their total numbers of leaves.

Changes in the daily proportion of individuals at each phenological stage was assessed using LOESS smoothing in each species (neighbourhood parameter $\alpha = 0.5$). We also used LOESS regression between each host-plant variable and Julian day to assess the seasonal progression of plant quality for insect oviposition and hosting. The regression fit was applied separately to each species. The trends for *L. draba* variables were grouped by plant developmental period (i.e. flowering spring plants vs summer resprouts). Microclimatic and host-plant variables were also modelled against microhabitat type applying an ANOVA followed by a post-hoc Tukey HSD test with the emmeans package (Lenth, 2020). The distance between the different monitored microhabitats was short (i.e. less than 10 m for *B. nigra*, and less than 70 m for *L. draba*, except for the more open microhabitats which were 700 m apart from the others), suggesting no strong barriers to gene flow between microhabitats during reproductive and seed dispersal periods. Consequently, host-plant variation between microhabitats was therefore assumed to capture more strongly plastic responses in host-plant development to different microenvironmental conditions (e.g. light, soil humidity and temperature) rather than genetic variation between microhabitats. We evaluated the relative contribution of plant phenological stage and microhabitat (as a partial proxy of host-plant plasticity) on host-plant quality (i.e. foliar chlorophyll and water contents) by applying a two-way ANOVA. Significant interactions between phenology and microhabitat were included in the analyses. Foliar temperatures of host plants ultimately determine the thermal conditions experimented by the eggs and the growing larvae of *P. napi*. To assess the potential role of drought on the thermal conditions of the leaves a general linear model was also fitted on plant foliar temperature against soil humidity, canopy closure and plant height. All the analyses were conducted with R.

3.2.4 Experimental assessment of rain-induced plasticity in host-plant rhizomes

The availability of fresh resprouts of *L. draba* during summer and autumn can be determinant for the performance of *P. napi* late generations (August–October). Knowing the factors driving the resprouting capacity of *L. draba* rhizomes could thus shed some light into the local-scale mechanisms affecting host-plant availability and the population dynamics of *P. napi*. We hypothesised that summer rains could induce plastic development of adventitious buds of *L. draba* rhizomes into green new shoots favoring the recovery of late generations of *P. napi*. To assess this hypothesis, we performed a simple experiment of the plastic resprouting capacity of *L. draba* rhizomes in response to simulated summer rains.

Twenty-four rhizomes were collected at the study site on July 2017 and were divided

in three watering treatment groups (8 rhizomes per treatment) simulating three different scenarios of summer rainfall (T-5, T-10, T-75). T-5 simulated a dry July (5 mm month⁻¹, corresponding to the first quartile of July rain distribution for 1993–2016), T-10 corresponded to a moderately dry July (10 mm month⁻¹, second quartile of the rainfall distribution for this month in meteorological records). Finally, T-75 simulated an extremely wet July (75 mm month⁻¹, percentile 90). The length and the width of the rhizomes were measured before the transplant, and the initial adventitious buds they presented were counted. Each rhizome was then planted in a random pot in the laboratory with a standardised soil composition (45% of autoclaved peat, 45% of sand and 10% natural soil inoculum). Air temperature and radiation were continuously recorded using an LCpro+ System radiometer (ADC BioScientific Ltd., Hertfordshire, UK). Pots were watered twice per week and their positions were randomly modified. We recorded the height, the number and the length of the leaves of emerged resprouts. In addition, we measured soil humidity before and after watering, soil temperature and foliar chlorophyll. At the end of the experiment, fully-developed leaf samples were collected in order to measure their water content ($\frac{FW-DW}{DW}$).

3.3 Results

3.3.1 Decadal trends and phenology of *Pieris napi*

The annual surveys of the CBMS completely recorded the first three generations of *P. napi* at the study site (Fig. 3.2A). The first generation (G₁) was usually found between Julian day 60 (early March) and Julian day 120 (late April), the second one (G₂) on Julian days 140–180 (May–late June), and the third one (G₃) on Julian days 180–210 (July). During late July and August, the abundance of *P. napi* sharply decreased until late August and September, when the beginning of a fourth generation (G₄) was usually detected before the end of the CBMS survey. The phenological curves, however, greatly varied between years (Fig. 3.2). Adults in flight during late summer could be detected in some years, eventually conforming an August generation (e.g. 1997, Fig. 3.2B, and 2011, Fig. 3.2C). These years presented the wettest summers in the study site from 1993–2018 based on the annual SPEI index during June–August (a multi-scalar drought index calculated from data of local rainfall and temperature following Beguería and Vicente-Serrano (2017)). Dry years with low summer SPEI values, in contrast, presented a longer and sharper reduction of butterfly abundance during August (Fig. 3.2D), even affecting G₃ in July (Fig. 3.2E).

The data gathered by the CBMS during 1993–2018 confirmed a significant decline in annual abundance of the studied butterfly population (Fig. 3.3A). Significant negative trends at a generational scale could only be detected for summer generations (i.e. G₃ and G₄) while no significant trend was observed for G₁ and G₂ (Fig. 3.3B–E). The results of the polynomial fits were highly similar to the linear models and are thus not included.

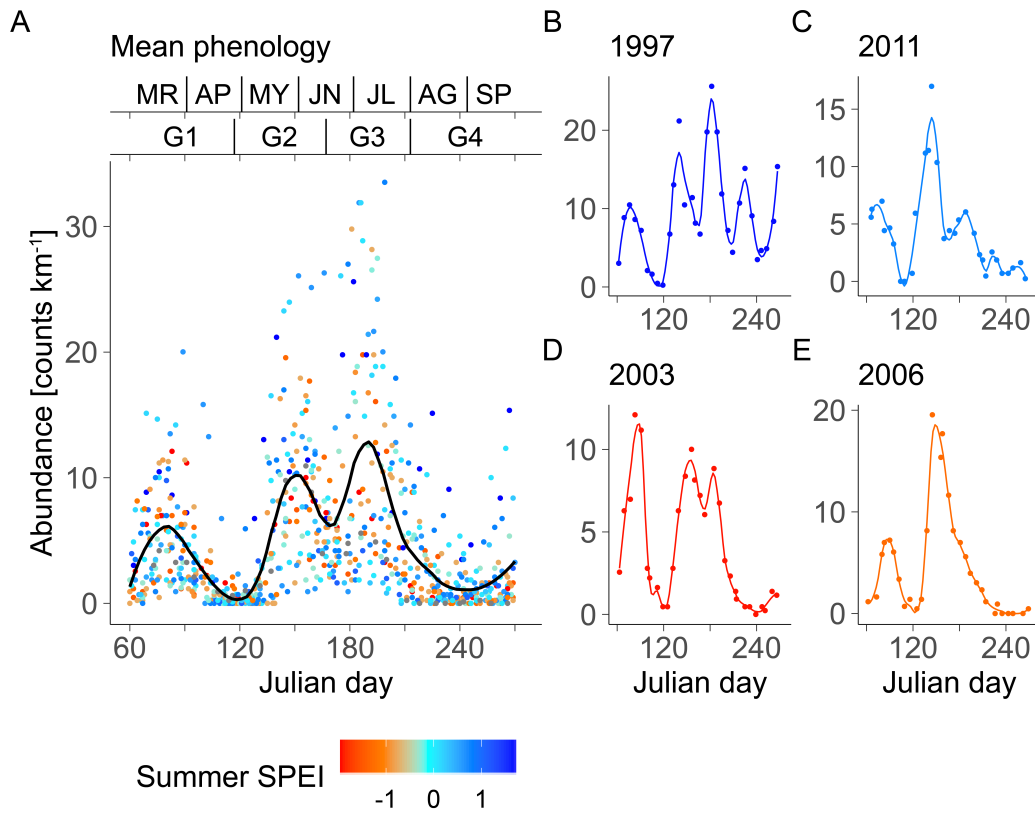


Figure 3.2: Flight phenology of *Pieris napi* in the study site. A: Mean phenological curve (black line) of the period 1993–2018. Each year is colored depending on the value of the SPEI drought index calculated for summer months (June–August) following Beguería and Vicente-Serrano (2017). Low, reddish values correspond to dry summers; while high, blueish values to summers with high rainfall and low temperatures. B, C: phenological curves of the years with two of the wettest summers. D, E: years with two of the driest summers. MR to SP, months from March to September; G1, first generation; G2, second; G3, third; and G4, fourth.

3.3.2 Phenological and plastic variation of host plants

Butterfly and host-plant phenologies recorded in 2017 were compared to assess their temporal match (Fig. 3.4). *Brassica nigra* had completely fructified (Fig. 3.4A) and *L. draba* had already started to senesce (Fig. 3.4B), during the peak of flight of G2 (around the Julian day 150, Fig. 3.4C). A parallel decay of foliar chlorophyll and water contents and an increase of foliar temperature were initiated in host plants at this time and maintained during the period of development of eggs and larvae from the G3 (Fig. 3.4D–F). The emergence of adults of G3 coincided with the senescence of *B. nigra* (Fig. 3.4A) and the complete absence of aboveground organs of *L. draba* (Fig. 4.4B). Eggs and larvae of G4, therefore, could uniquely rely on the appearance and availability of fresh, new resprouts of *L. draba*.

Microclimatic conditions (i.e. canopy closure, soil humidity and foliar temperature) significantly varied between the different microhabitats (Fig. 3.5A–F). Open microhabi-

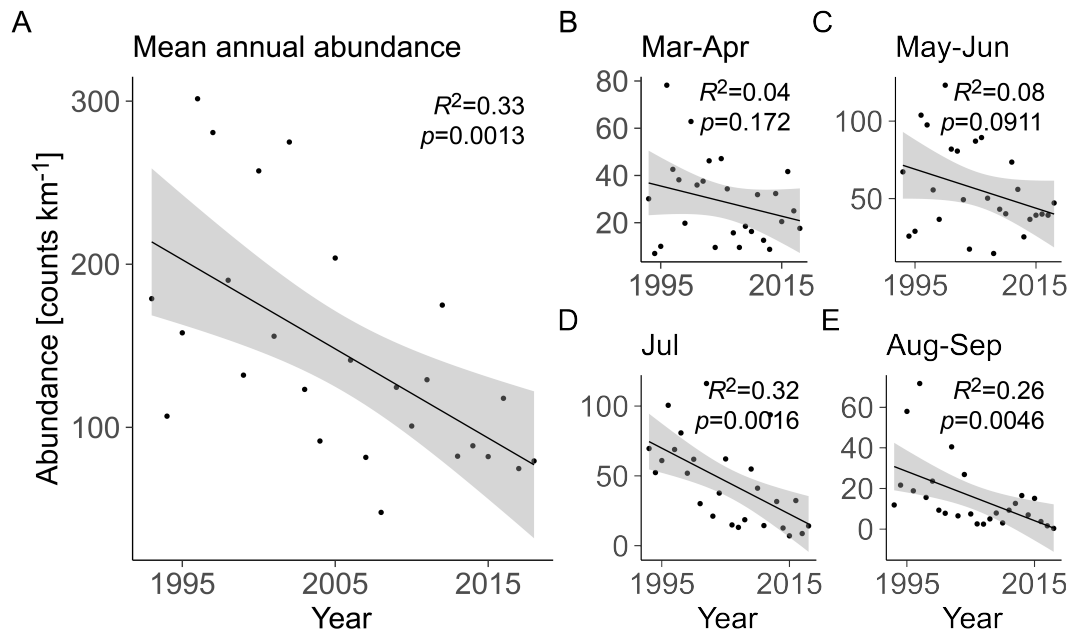


Figure 3.3: Linear trends of *Pieris napi* abundance in the study site. A: annual resolution, B: first generation, C: second generation, D: third generation, E: fourth generation.

tats presented higher temperatures (Fig. 3.5E and F) and drier soils (Fig. 3.5C and D). Host plants growing in these microhabitats accordingly presented significant differences in foliar traits associated with host-plant quality (Fig. 3.5G–J). Lower values of foliar water content were measured in open microhabitats (Fig. 3.5I and J), whereas foliar chlorophyll was inferior in closed microhabitats (Fig. 3.5G and H). *Lepidium draba* also showed contrasting patterns of summer resprouting between microhabitats (Fig. 3.6). The microhabitats that were more open presented significantly higher densities of resprouts, with more and longer leaves. Significant differences in microclimatic conditions and host-plant traits between microhabitats were also maintained during the resprouting period. The resprouts of *L. draba* appeared in mid-July, but they remained as short rosettes until September, when they notably grew in plant height, number of leaves and foliar length, coinciding with an increase of rainfall.

Both the plant phenological stage and the type of microhabitat strongly determined variation in host-plant quality across the whole year, as the results of the two-way ANOVAs indicated (Table 3.1). A greater relative contribution of phenology on the variation of either the chlorophyll or the water contents was however found in the majority of the analyses comparing the F value of both factors and its interaction. Foliar temperature of the two host plants significantly increased with the reduction of soil humidity (Table 3.2). Canopy closure also negatively influenced foliar temperature of both species while plant height only had significantly negative effects on *Lepidium draba*.

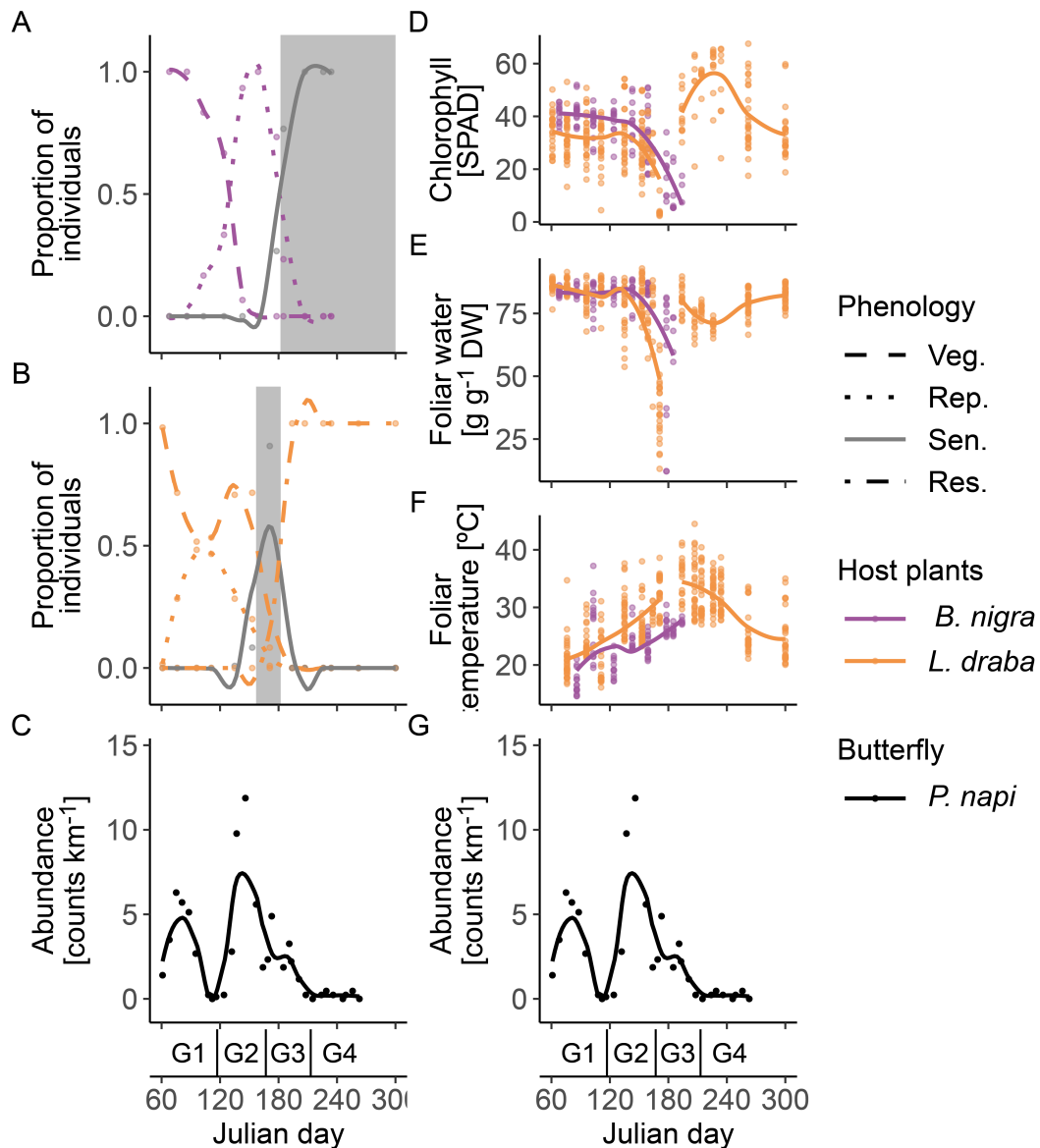


Figure 3.4: Seasonal progression of the phenology and quality of the host plants and the butterfly recorded in 2017. A: phenology of *Brassica nigra*. B: phenology of *Lepidium draba*. C, G: phenology of *Pieris napi*. The panel is repeated to facilitate the comparison between the seasonal trends. D, E and F: foliar traits associated with host-plant quality. The grey area indicates the absence of green host plant because of its senescence, corresponding to the period when non-senescent individuals are less than 50% of the total. Veg: vegetative plant, Rep: reproductive, Sen: senescent, Res: summer resprout. G1: first generation, G2: second, G3: third, G4: fourth.

3.3.3 Plastic resprouting of *Lepidium draba* in response to simulated rain

Summer rhizomes of *L. draba* showed significant responses to water treatments (Fig. 3.7). Higher water availability resulted in earlier resprouting responses (Fig. 3.7A) and increased resprout height (Fig. 3.7B). In addition, the interaction between water treatment and time

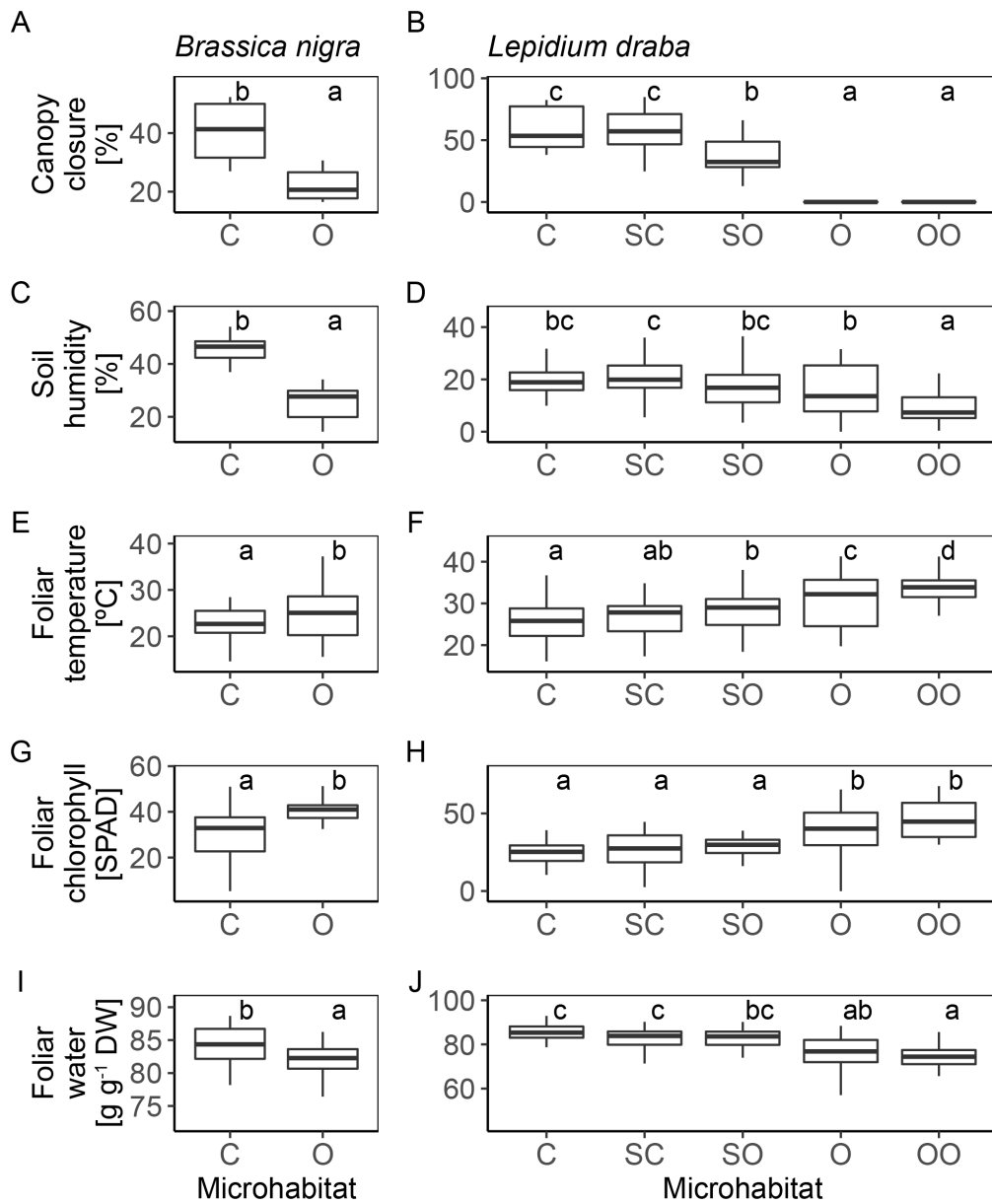


Figure 3.5: Variation in microclimatic conditions and quality of the two host plants between different microhabitats. Different letters indicate significant differences of the response variable between the microhabitat types in the Tukey HSD test. C, closed microhabitat; SC, semi-closed; SO, semi-open; O, open; and OO, very open.

($P < 0.0001$) in an ANCOVA model predicting resprout height was statistically significant, indicating higher growth rates with increased water availability (Fig. 3.7B). The initial number of resprouting buds were not differently distributed between treatments (one-way ANOVA $P = 0.17$). Confounding effects of this initial variable could thus be discarded. Different water treatments consistently originated different conditions of soil humidity (ANCOVA test $P < 0.0001$, $R^2 = 0.95$).

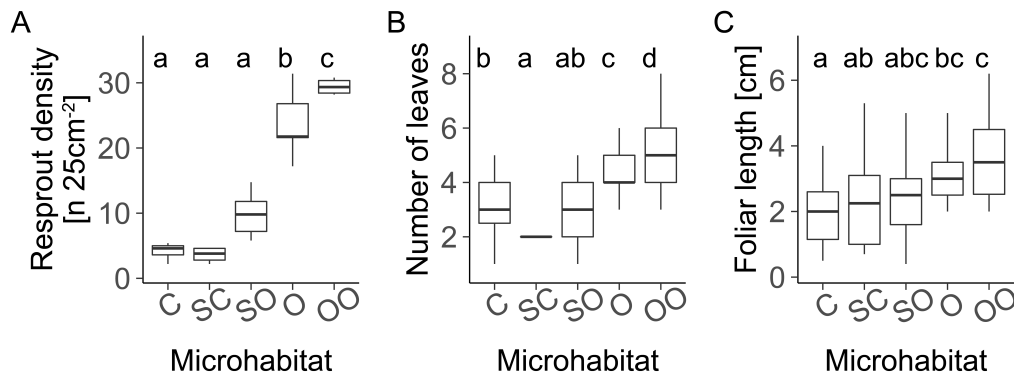


Figure 3.6: Resprout density (A), number of leaves (B), and foliar length (C) of the summer resprouts of *Lepidium draba* emerging in different microhabitats. Different letters indicate significant differences of the response variable between the microhabitat types in the Tukey HSD test. C, closed microhabitat; SC, semi-closed microhabitat; SO, semi-open microhabitat; O, open microhabitat; and OO, very open microhabitat.

Table 3.1: Two-way ANOVAs applied to foliar chlorophyll and water contents for the two host plants during all the monitoring period. R^2 , adjusted coefficient of determination of the model; df , degrees of freedom; and SS , sum of squares.

Species	Response	Explanatory	df	SS	F	P
<i>Brassica nigra</i>	Chlorophyll ($R^2 = 0.36$; $P < 0.0001$)	Microhabitat	1	1947	21.01	<0.0001
		Phenology	2	3866	20.87	<0.0001
		Microhabitat × Phenology	1	26	0.28	0.6002
		Residuals	102	9450		
<i>Brassica nigra</i>	Foliar water ($R^2 = 0.67$; $P < 0.0001$)	Microhabitat	1	845	14.48	0.0003
		Phenology	2	10435	89.44	<0.0001
		Microhabitat × Phenology	1	3	0.06	0.8117
		Residuals	90	5250		
<i>Lepidium draba</i>	Chlorophyll ($R^2 = 0.71$; $P < 0.0001$)	Microhabitat	4	13281	48.06	<0.0001
		Phenology	3	40236	194.16	<0.0001
		Microhabitat × Phenology	9	3612	5.81	0.0001
		Residuals	311	21484		
<i>Lepidium draba</i>	Foliar water ($R^2 = 0.77$; $P < 0.0001$)	Microhabitat	4	20957	38.98	<0.0001
		Phenology	3	126756	314.39	<0.0001
		Microhabitat × Phenology	9	1723	1.42	0.1766
		Residuals	310	41663		

3.4 Discussion

3.4.1 Phenological match between *Pieris napi* and its two host plants

Here we examined the temporal and spatial variation at the local-scale of the two host plants used by a declining population of the butterfly *Pieris napi*. Previous studies have associated the decline of the population with summer multidecadal drought (Carnicer et al., 2019). Our study confirmed that the negative trend in annual abundance of the

3. PLASTIC HOST-PLANT VARIATION MEDIATING DROUGHT IMPACTS

Table 3.2: General linear model of foliar temperature for the two host plants during all the monitoring period. R^2 : adjusted coefficient of determination of the model.

Species	Response	Explanatory	Estimate	Std. Error	<i>t</i>	<i>P</i>
<i>Brassica nigra</i>	Foliar temperature ($R^2 = 0.32$; $P < 0.0001$)	Intercept	26.35	1.38	19.1	<0.0001
		Soil humidity	-0.23	0.05	-5.0	<0.0001
		Canopy closure	0.15	0.05	2.9	0.0054
		Height	0.01	0.01	1.3	0.1835
<i>Lepidium draba</i>	Foliar temperature ($R^2 = 0.33$; $P < 0.0001$)	Intercept	35.65	0.72	49.5	<0.0001
		Soil humidity	-0.29	0.03	-9.7	<0.0001
		Canopy closure	-0.06	0.01	-5.7	<0.0001
		Height	-0.04	0.01	-4.6	<0.0001

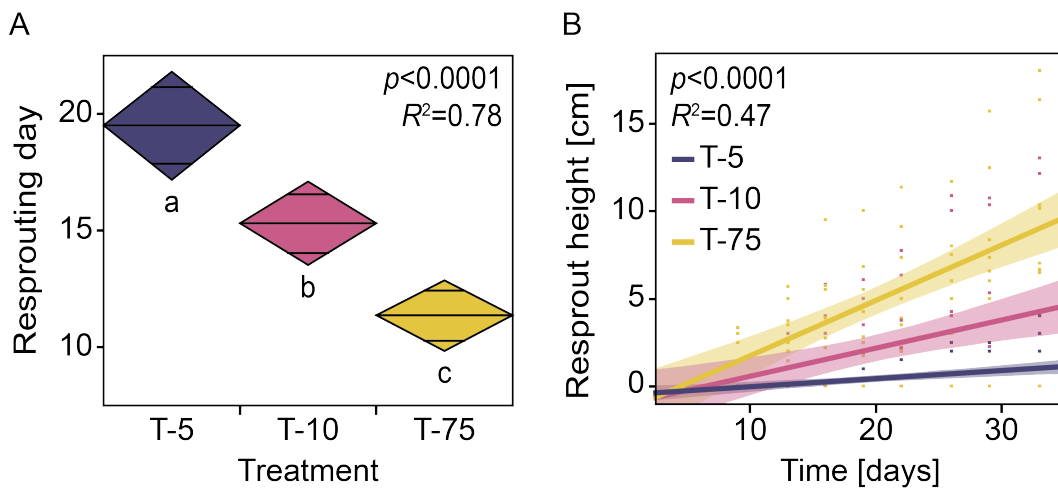


Figure 3.7: Experimental assessment of the plastic responses of summer rhizomes of *Lepidium draba* to simulated rains. A: Day of emergence of the resprouts between the three water treatments. Diamond plots indicate the 95% confidence interval for each treatment (vertical span) and the mean (midpoint line). Means that are not labelled by the same letter are significantly different. B: Temporal progression of resprout's height in the three water treatments. Slopes were significantly different (ANCOVA test). Water treatments: $5 \text{ L m}^{-2} \text{ month}^{-1}$ (T-5, purple), $10 \text{ L m}^{-2} \text{ month}^{-1}$ (T-10, pink), $75 \text{ L m}^{-2} \text{ month}^{-1}$ (T-75, yellow).

population persists (Fig. 3.3A). At a generational scale, a significant decreasing slope was only detected in the summer generations (i.e. G_3 and G_4), pointing to summer season as a key period for this population (Fig. 3.3). The phenological curve of the species in the study site indicated that the abundance of the butterfly is usually reduced in the second half of the summer (Fig. 3.2A). This reduction was especially sharp in the driest summers of the analyzed period (1993–2018), and could even affect the development of the July generation (G_3 , Fig. 3.2D and E). All these results give further support to summer drought as a key driver of the dynamics of the population.

Climate can drive the dynamics of insect populations both directly and indirectly due to its effects on other species that interact with the focal species (Boggs and Inouye, 2012). In our study system, the seasonal decrease in host-plant quality had been suggested to have a synergistic negative role on the mediation of the impacts of summer drought on the declining butterfly (Carnicer et al., 2019). Here we assessed how the phenological curves of *P. napi* and of the two host plants match in order to identify the periods when host

plants could have limiting and detrimental effects on butterfly performance (Fig. 3.4). While larvae from G₁ and G₂ had access to abundant and green host plants, we observed that later, summer generations grew in periods with resource of low quality (G₃) or low availability (G₄). The larval development of G₃ coincided with the senescence of host plants (Fig. 3.4A–C) and the drastic decay of their foliar chlorophyll and water contents (Fig. 3.4D and E). Both host plants completely disappeared after senescence until new resprouts of *L. draba* emerged. Summer resprouts, however, did not fully develop until September rains. The development of larvae of G₄, hence, was much more limited by host-plant availability than by quality.

The reduction of butterfly abundance in the second half of the summer, after the peak of flight of G₃, might be associated with this period of low availability of host plants. Roy and Thomas (2003) found that the seasonal cycle in the availability of host plants was likely representing an annual bottleneck for marginal populations of the Adonis blue butterfly (*Polyommatus bellargus*). We hypothesise that the scarcity of non-senescent host plants during late summer could similarly limit egg-laying opportunities of females of G₃ and/or increase the mortality of the derived larvae (G₄), resulting in the yearly reduction of butterfly abundance observed in this period (Fig. 3.2). It should be further examined, however, why this is one of the most abundant populations of Catalonia in spite of their possible annual bottlenecks. Another complementary and nonexclusive hypothesis would be that pupae of summer generations could plastically enter to a dormant state (i.e. estivation or summer diapause) until autumn, avoiding the period of more resource scarcity and climate stress. Although estivation in *P. napi* has never been described before, summer pupal diapause has been detected in Chilean and Spanish populations of the closely-related species *Pieris brassicae* (Benyamini, 1996; Held and Spieth, 1999). Both the lack of resources for oviposition and larval development (Benyamini, 1996) and the need to desynchronise the butterfly life cycle from its specialist parasitoid (Spieth, 2002; Spieth and Schwarzer, 2001) have been suggested as the reasons for these local adaptations. Experimental tests, rather than field observations (Spieth and Schwarzer, 2001), are further required to confirm or reject the estivation hypothesis in our studied population of *Pieris napi*.

3.4.2 The role of host-plant plasticity in mediating the impacts of drought on a declining population of *Pieris napi*

Most studies that consider plant–insect interactions in the assessment of climatic impacts on insect populations are conducted from a phenological point of view (i.e. the emerging phenological mismatches as a result of a change in climatic conditions) (see Donoso et al., 2016, for an example at the study site). Plastic responses to climate in other plant traits different from phenology, such as plant growth and foliar traits related to their quality as a food resource, could also exert significant effects, though. Here we monitored several traits related to the availability and quality of host plants to identify the role of host-plant plasticity in mediating the impacts of drought on a declining population of *Pieris napi*. Foliar chlorophyll and water contents, two host-plant traits usually associ-

ated to its quality for herbivorous insects (Scriber and Slansky, 1981), significantly varied between microhabitats (Fig. 3.5). These results suggest that both foliar traits plastically responded to shifts in microenvironmental conditions. Shifts in host-plant quality, however, were more strongly driven by phenological progression than by microhabitat (Table 3.1). We also found plastic variation in the resprouting dynamics of *L. draba*, which presented significant differences in resprout density, number of leaves and foliar length between microhabitats (Fig. 3.6). The resprouts remained, however, as short rosettes until late-summer rains, triggering their growth. In line with these observations, we observed significant differences in the emergence and growth of resprouts between the three watering treatments that simulated three summer rainfall regimes (Fig. 3.7), fully supporting the hypothesis that the development of *L. draba* resprouts plastically respond to summer rains.

Overall, the results suggest that both the phenological and plastic variation of its main host plants exert an important role in the mediation of local responses of *P. napi* to summer drought. We found that the development of G₃ coincided with the decay of quality of host plants, whereas larvae of G₄ could be limited by the availability of summer resprouts of *Lepidium draba*. The quality of host plants was most strongly affected by their phenological progression, while the availability and growth of resprouts plastically responded to summer rains. Our results suggest, therefore, that drought impacts on G₃ are mainly modulated by the variation in the phenological cycle of host plants. Drier and warmer conditions during late spring and early summer (May–June) could accelerate the phenological progression of host plants, advancing their decay in quality. These climatic conditions could also amplify temperatures at the foliar (Table 3.2) and microhabitat level, eventually supposing a situation of combined food and thermal stresses for larval development of G₃ (Carnicer et al., 2019; Vives-Inglà et al., 2023). Low quality of food resources can exacerbate the negative impacts of higher thermal conditions on larval growth, as previous experimental studies in *Pieris* butterflies have found (Bauerfeind and Fischer, 2013a; Jones et al., 1982; Kingsolver, 2000). Drought impacts on G₄, in contrast, are more likely mediated by plastic responses of the resprouts of *Lepidium draba*. Drier summers could slow down and postpone the emergence and growth of summer resprouts, affecting therefore the development of the late-summer generation.

Insect responses to climate impacts are shaped by multiple processes occurring at the local scale (Carnicer et al., 2017). Most of the studies in this line have described how microclimatic variability and plastic traits or local adaptation of insects can modulate their exposure and vulnerability to climate change. Other local-scale processes, such as host-plant responses to climatic variability, can also mediate climate impacts on insect populations but they have been, however, less studied. Here we reported diverse and co-occurring local-scale processes that involve host-plant responses to drought mediating the impacts of climate on a declining butterfly population. Interestingly, we reported how host-plant plasticity in traits different from phenology (i.e. rain-dependent growth of summer resprouts) can also mediate the indirect effects of climate in insects. The diverse mechanisms suggested here, furthermore, operated in a temporal sequence, affecting different generations. The effects of host plants on G₃ would be driven by the impacts of

early-summer drought on microclimatic conditions and host-plant phenology and quality, while G₄ would be influenced by the plastic responses of *L. draba* to late-summer drought.

Acknowledgements

Francesc Xavier Santaefemia and the Aiguamolls de l'Empordà Natural Park provided support with permission management, scientific advice and key assistance during fieldwork. We are grateful for the contribution to the field work of (in alphabetical order) Agnieszka Juszczak, Armand Casadó-Tortosa, Carlos López, Joaquim de Gispert, Katarzyna Bartnik, Meritxell Garcia and Sofía Cortizas. This research was supported by the Spanish Ministry of Science and Innovation through a doctoral grant (FPU17/05869) and the Spanish Ministry of Economic Affairs and Digital Transformation (CGL2016-78093-R).





4

**Interspecific differences
in microhabitat use
expose insects
to contrasting
thermal mortality**



Abstract

Ecotones linking open and forested habitats contain multiple microhabitats with varying vegetal structure and microclimatic regimes. Ecotones host many insect species whose development is intimately linked to the microclimatic conditions where they grow (e.g. the leaves of their host plants and the surrounding air). Yet microclimatic heterogeneity at these fine scales and its effects on insects remain poorly quantified for most species. Here we studied how interspecific differences in the use of microhabitats across ecotones lead to contrasting thermal exposure and survival costs between two closely-related butterflies (*Pieris napi* and *P. rapae*). We first assessed whether butterflies selected different microhabitats to oviposit and quantified the thermal conditions at the microhabitat and foliar scales. We also assessed concurrent changes in the quality and availability of host plants. Finally, we quantified larval time of death under different experimental temperatures (TDT curves) to predict their thermal mortality considering both the intensity and the duration of the microclimatic heat challenges in the field. We identified six processes determining larval thermal exposure at fine scales associated with butterfly oviposition behavior, canopy shading, and heat and water fluxes at the soil and foliar levels. Leaves in open microhabitats could reach temperatures 3–10 °C warmer than the surrounding air while more closed microhabitats presented more buffered and homogeneous temperatures. Interspecific differences in microhabitat use matched the TDT curves and the thermal mortality in the field. Open microhabitats posed acute heat challenges that were better withstood by the thermotolerant butterfly, *P. rapae*, where the species mainly laid their eggs. Despite being more thermosensitive, *P. napi* was predicted to present higher survivals than *P. rapae* due to the thermal buffering provided by their selected microhabitats. However, its offspring could be more vulnerable to host-plant scarcity during summer drought periods. Overall, the different interaction of the butterflies with microclimatic and host plant variation emerging at fine scales and their different thermal sensitivity posed them contrasting heat and resource challenges. Our results contribute to set a new framework that predicts insect vulnerability to climate change based on their thermal sensitivity and the intensity, duration, and accumulation of heat exposure.

4.1 Introduction

Vegetation cover locally modifies climatic conditions and generates a microclimatic regime that deviates from open, free-air, and standardised measurements (i.e. macroclimate; Geiger, 1950; Stoutjesdijk and Barkman, 2014). The absorption and reflection of solar radiation and the evapotranspirative cooling of forest canopies buffer macroclimatic temperatures and reduce thermal variation in the understory (Bramer et al., 2018; De Frenne et al., 2021; Zellweger et al., 2020). In contrast, in open areas with short and sparse vegetation, temperatures near the ground can be more extreme than those recorded at 2-m and shady conditions (i.e. thermal amplification; Carnicer et al., 2021; Stoutjesdijk and Barkman, 2014; Woods et al., 2015). Narrow ecotones that link open and forested habitats (hereafter termed open–closed ecotones) generate multiple microhabitats with

varying vegetal structure, potentially exposing the organisms they harbour to contrasting microclimatic conditions. Here we studied how interspecific differences in microhabitat use across ecotones shape the thermal exposure and the associated costs to survival of two closely-related butterflies.

Microclimatic variation determines the thermal experience of the organisms and has important effects on their thermal adaptations and performance (Franken et al., 2018; Kaiser et al., 2016; Kaspari et al., 2015; Pincebourde and Casas, 2019; Woods et al., 2022). The scale at which microclimatic measurements are relevant for organisms depends on their body size and mobility (Kingsolver et al., 2011; Pincebourde and Woods, 2020; Pincebourde et al., 2021). For butterflies, microclimatic variability at the landscape scale is pertinent in the adult stage, as they can easily fly and sample between alternative habitats (e.g. woodland vs grassland; Suggitt et al., 2011, 2012). In contrast, the area that eggs and larvae can use is much smaller (Courtney, 1986), and thus these less mobile stages will be more likely affected by the microclimatic variability inside their habitats. Larval stages may be more likely influenced by the microclimatic conditions of the air bath surrounding them (at less than ~ 1 m of distance, i.e. microhabitat), while the microclimate measured at the plant surfaces might be more important for eggs and small larvae (Kingsolver et al., 2011; Pincebourde et al., 2021; Potter et al., 2009; Woods, 2010, 2013). Microclimatic heterogeneity at these fine scales can be particularly high and comparable to that recorded at macroclimatic scales, but remains poorly quantified for most species (Pincebourde and Woods, 2020; Pincebourde et al., 2016).

The selection of microhabitat and host plant during butterfly oviposition will affect the growing environment of the offspring (Fig. 4.1a; Courtney, 1986; Doak et al., 2006; Forsberg, 1987; Gibbs and Van Dyck, 2009). On the one hand, we expect that shadier microhabitats will offer buffered microclimates, with dampened thermal variability and extreme values, while they are amplified in open areas exposed to direct radiation (Fig. 4.1a A–C). On the other hand, we also expect that microhabitat conditions could induce plastic shifts on many traits that define host plant quality, depending on their shade tolerance (Fig. 4.1a D–E; Poorter et al., 2019; Scriber and Slansky, 1981). Variation in host plant quality can interact with the microclimate experienced by the feeding larvae and influence their development in complex ways (Clissold and Simpson, 2015).

Butterfly responses to microclimatic exposure will depend on both their thermal exposure and thermal sensitivity (Carnicer et al., 2017). We hypothesise that the two studied butterflies will show diverging thermal adaptive strategies according to their microhabitat preferences and the associated thermal regime (Fig. 4.1a F–G). The probability of surviving heat stress depends on both its intensity and its duration (Rezende et al., 2014). This relationship can be synthesised by thermal death time (TDT) curves, where the critical temperature (T_{ko}) that an organism can tolerate linearly decreases with the logarithm of exposure time (t) following this equation:

$$T_{ko} = CT_{max} - z \log_{10} t \quad (4.1)$$

Therefore, thermal tolerance to a heat challenge not only depends on the upper critical thermal limit (CT_{max}) but also on the thermal sensitivity (z), which describes the required increase of temperature to decrease time to death one order of magnitude (Fig. 4.1b). The analysis of the TDT curves of 56 species of insects, bivalves, and fishes has pointed out that CT_{max} and z are positively and tightly associated (Rezende et al., 2014). Organisms with a high CT_{max} and z are more capable of surviving extreme temperatures, but their critical temperature (T_{ko}) rapidly decreases with exposure time (Fig. 4.1b, yellow). In contrast, low z values allow longer survival times at less intense but still stressful temperatures to the detriment of CT_{max} (Fig. 4.1b, blue). As a consequence of this trade-off, we expect that larvae growing in open microhabitats may show a thermotolerant strategy (high CT_{max} and z) to cope with the acute stresses of their highly-variable thermal regime (extreme temperatures for short times). In the same line, we would expect the opposite, thermosensitive strategy for species selecting shadier microhabitats with less intense temperatures but longer exposures (i.e. chronic stress).

To assess whether microhabitat variability in open–closed ecotones generates inter-specific differences in their thermal exposure and the associated costs to survival, we studied two model species of butterfly: *Pieris napi* L. 1758 and *P. rapae* L. 1758. These species were studied in two Mediterranean sites, which harbour populations of two host plants with contrasting tolerances to shade, *Alliaria petiolata* (shade-tolerant) and *Lepidium draba* (light-demanding). We first assessed whether the two butterfly species selected different microhabitats from the open–closed ecotones to oviposit and quantified the thermal exposure of their offspring both at the microhabitat and foliar scales. We also assessed concurrent changes in the nutritional quality and condition of host plants across ecotones. Then, we conducted ecophysiological assays of heat tolerance with the larvae of both species to estimate their TDT curves and determine their thermal sensitivity. Based on the experimental quantification of larval survival at different temperatures, we finally applied a dynamic model to predict thermal mortality in field microclimatic conditions.

4. INTERSPECIFIC DIFFERENCES IN MICROCLIMATIC THERMAL MORTALITY

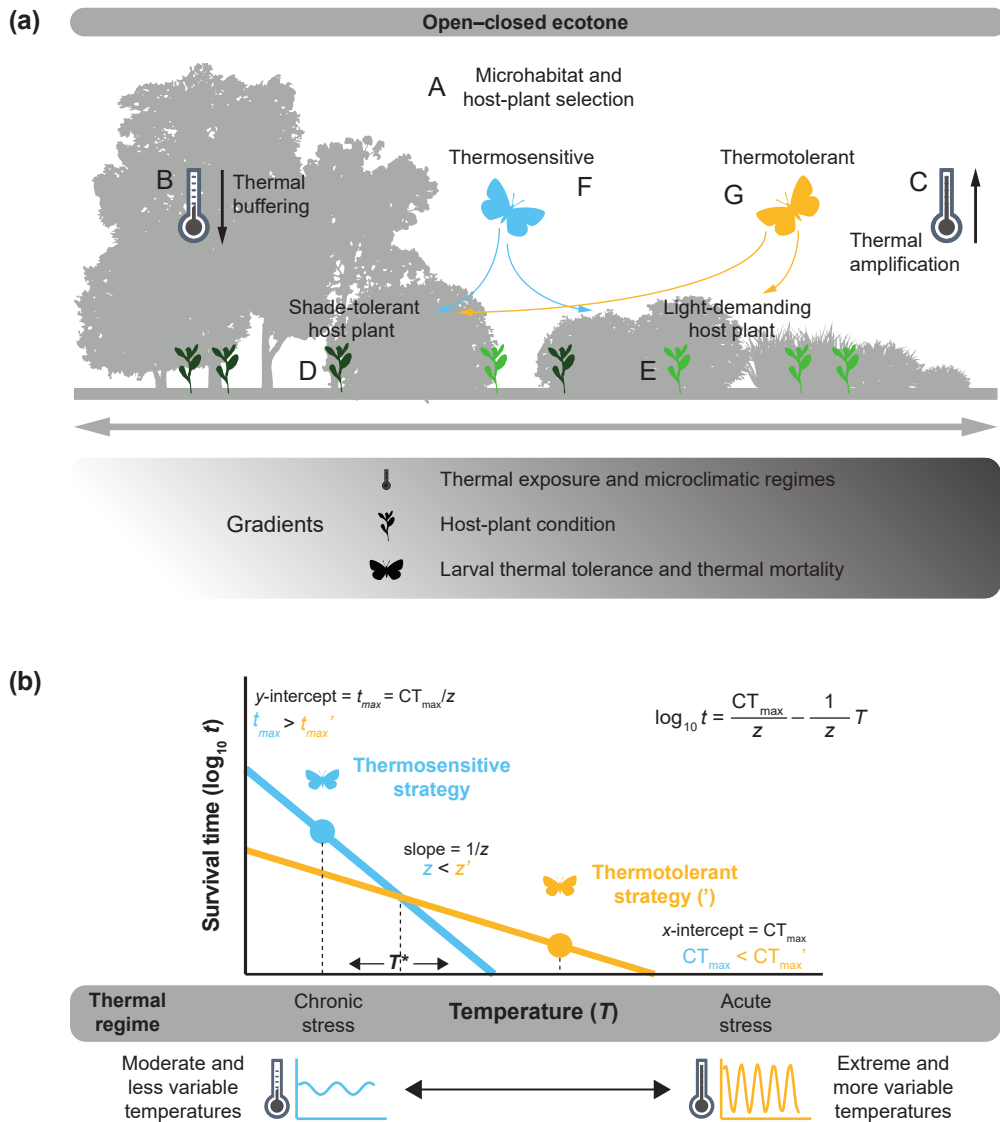


Figure 4.1: (a) Narrow ecotones that link open and forested habitats generate multiple microhabitats with distinct microclimatic regimes. Insects with contrasting thermal tolerances may select different microhabitats to oviposit, leading to large interspecific differences in thermal exposure of eggs and larvae. Moreover, host plants with varying shade tolerances may show different distributions, traits, and conditions across ecotones, synergistically affecting larval performance. Overall, concurrent gradients of both biotic and abiotic processes are produced across ecotones. (b) Thermotolerant and thermosensitive strategies are expected to evolve under different thermal regimes. The two strategies are characterised by different thermal death time (TDT) curves, reflecting an evolutionary trade-off between survival capacity at acute, extreme stresses (thermotolerant) and at chronic, less intense conditions (thermosensitive). Both species exhibit equal survival times at T^* , which represents the thermal threshold between these two alternative thermal strategies. Silhouettes used in this figure were obtained from rawpixel.com and phylopic.org.

4.2 Materials and methods

4.2.1 Study system

The thermal exposure of the two species, its impacts, and the concurrent variation in their host plants were studied in two protected areas of the north-eastern Iberian Peninsula, 50 km from each other (Appendix B: Figs. B1 and B2). The sites of study are part of a long-term monitoring network that provides data on butterfly abundance at a weekly resolution since 1994 (i.e. CBMS; Pollard and Yates, 1993; Stefanescu, 2000). They contain abundant populations of the green-veined white (*P. napi*) and the small white (*P. rapae*) that have been intensively studied since 2012 (Carnicer et al., 2019; Vives-Ingla et al., 2020). Site 1 is in a mid-elevation area (539 m a.s.l.; Can Jordà, La Garrotxa Volcanic Zone Natural Park) with a heterogeneous landscape of evergreen and deciduous woodlands, meadows, and natural ponds. Site 2 is in a coastal wetland (2 m a.s.l.; El Cortalet, Aiguamolls de l'Empordà Natural Park) surrounded by riparian deciduous forests, bush and bramble thickets, reed beds, and irrigated cropland. The landscape mosaic of both sites generates spatial gradients of vegetation cover between open and closed habitats and their transition zones (open–closed ecotones).

Pieris napi and *P. rapae* are partially syntopic species (i.e. they share some of the microhabitats for breeding). They co-occur in a wide range of habitats from the sea level to alpine regions, but *P. napi* is usually linked to shaded, humid sites while *P. rapae* is more common in dry, open areas. Both butterflies lay individual eggs on Brassicaceae species, such as *Alliaria petiolata* and *Lepidium draba*. However, *P. rapae* is a more generalist species and uses a greater diversity of host plants (Ohsaki, 1979).

The dominant host plant in the mid-elevation site is *Alliaria petiolata*. It is a biennial herb common in damp, shaded soils at the edges of deciduous and riverine forests. It can grow in highly contrasted environmental conditions, exhibiting considerable plasticity in different habitats (Cavers et al., 1979). Seedlings emerge during spring and early summer and persist as rosettes throughout the first year, until the next growing season when inflorescences are initiated. *Lepidium draba* is the dominant host plant in the lowland site. It is a perennial, rhizomatous herb and can be found in open areas and field margins (de Bolós and Vigo, 1990). Its extensive, multibranched rhizomes are notably capable of producing many new shoots, which can develop into large monocultural stands (Francis and Warwick, 2008).

4.2.2 Oviposition behavior

We assessed whether the differences in broad habitat preferences between the two butterflies (*P. napi* for humid areas and *P. rapae* for open habitats) led to different microhabitat selection for oviposition across open–closed ecotones. We tested this hypothesis by carrying out censuses of behaviour at the two study sites. Females were followed

and their behaviours recorded for periods of 45 min. The censuses fully covered the entire daily period of flight activity, between 9:00 and 19:00, and were conducted during summer. Oviposition was considered to occur when females that landed on a leaf were observed to curl their abdomen and remain in this position for at least three seconds. Egg-laying was visually confirmed in most of the cases. Species, hour, and microhabitat type (open, closed, or intermediate) were noted. Censuses were simultaneously performed in the various microhabitat types, balancing the time spent in each type. The temperature of the leaves where eggs were laid and their position (upper vs underside of leaves) were also recorded when possible using a wire K-type thermocouple probe (SC-TT-KI-30-1M, Omega Engineering Ltd, UK) attached to a hand-held thermocouple thermometer (HH503, Omega Engineering Ltd, UK, and HI935005N, Hanna Instruments Ltd, Spain) immediately after the female left the plant.

4.2.3 Microclimatic and host-plant variation

We assessed microclimatic conditions at both microhabitat and host-plant scales. For the measurements at the microhabitat scale, we installed fifteen standalone data loggers (EL-USB-2-LCD, Lascar Electronics, UK) in different microsites harboring host plants and where ovipositing females had been detected. Seven of the sensors were installed in the mid-elevation site, and the other eight in the lowland site (Tables B1 and B2). The sensors were programmed to record temperature (°C) and relative humidity (%) at hourly resolution and were placed 25 cm above the soil protected from direct solar radiation.

To quantify thermal exposure and trait variability of host plants, we monitored cohorts of 242 individuals of *A. petiolata* and 362 individuals of *L. draba* distributed in four representative categories of microhabitats found across the ecotones (open, semi-open, semi-closed, and closed). Each microhabitat category was assigned based on detailed measurements of the dynamics of the canopy and the ground cover by herbaceous plants (see Appendix B.1 and Figs. B2 and B3 for further details). Canopy closure was measured by visual inspection in the vertical and the four cardinal directions. The herbaceous layer was characterised both as herbaceous ground cover and as mean herb height using the point-intercept method. Closed and semi-closed microhabitats presented a mean canopy closure higher than 50%, while we defined semi-open and open microhabitats by their herbaceous layer, as trees and shrubs were less common there. We monitored the host plants in 2017, from March to September, and measured the same 14 microclimatic, phenological, morphological, and physiological traits every 15 days (Table B2).

Every monitoring day, we selected at least 16 host plants for each cohort (four individuals × four microhabitat types) ensuring that plants were randomly chosen, without repetition to avoid pseudoreplication. Microclimatic variables included several temperatures at soil, foliar, and air level and soil moisture. We used a penetration thermometer (HI98509, Hanna Instruments Ltd, Spain) to measure soil temperature at a depth of 10 cm. Soil surface temperature, air temperature above the host plant, and foliar surface temperature were measured using a thermocouple (see device and measurement details

in the section 4.2.2 *Oviposition behavior*). A minimum of three replicates were taken for each measurement. The temperatures were measured between 10:00 and 16:00, and the time, wind, and radiation conditions were recorded. We measured soil surface temperature near the host plants, replicating it in spots exposed to direct solar radiation and in the shade; air temperature, immediately above the host plant at a height of 1 m; and foliar temperature, on the upper and underside of the leaves. The volumetric water content of the soil (% by volume) was measured at three points near each plant using a DELTA-T SM150 (Delta-T Devices Ltd, UK) soil-moisture sensor.

The traits measured in host plants included phenology, stem length and foliar dimensions, density, and chlorophyll and water contents. These traits were selected because they have been associated with oviposition behaviour and offspring performance (Awmack and Leather, 2002; Gibbs and Van Dyck, 2009; Stefanescu et al., 2006; Wolfson, 1980) and are simple to measure. Foliar chlorophyll content is also an indicator of plant nutritional condition, photosynthetic capacity, and developmental stage (Curran et al., 1990; Everitt et al., 1985). We assessed plant phenological status by classifying the individuals in one of four phenological stages: spring early vegetative, reproductive, senescent, and summer late vegetative. A representative basal, medial, and apical leaf was chosen for each plant, and its state (green or senescent) was recorded. Chlorophyll content was estimated as the mean of three measurements from a SPAD-502 chlorophyll meter (Konica Minolta Sensing, Spain). Finally, leaves were severed and immediately weighed (fresh weight, FW) using a field digital scale (PJS020, PESOLA Präzisionswaagen AG, Switzerland), and then oven-dried in the laboratory at 60 °C for two days to a stable weight (dry weight, DW). Foliar water content was defined as $(FW - DW) / DW$. Foliar density was calculated as the ratio between DW and foliar length. When host plants were mature, we also counted the number of fruits per plant (siliques for *A. petiolata* and silicles for *L. draba*), as a proxy of plant reproductive performance between microhabitats and shade tolerance. A minimum of seven individuals were sampled for each microhabitat type.

4.2.4 Ecophysiological assays of heat tolerance

We implemented a static heat tolerance experiment using larvae of *P. napi* and *P. rapae* to determine whether they differ in their thermal strategies. If *P. napi* oviposits in more closed and buffered microhabitats than does *P. rapae*, as we hypothesised, the larvae of the former would exhibit a thermosensitive strategy, with lower values of z and CT_{max} . Females from both locations and species were captured and their offspring reared in growing chambers at 22 °C 13L:11D, with fresh and abundant host plants (*L. draba* and *A. petiolata*). The experiment was conducted on 210 larvae from 20 family lines (Table B3). Before the application of the thermal treatment, larvae were acclimated for 1 hour at constant 22 °C and deprived of food. We recorded the larval initial weight (g) and subsequently placed the larvae in individual plastic vials (diameter: 3.5 cm, height: 7 cm) that were submerged in a water bath programmed at a constant temperature (i.e. 40, 42, or 44 °C, depending on the treatment). These temperatures can be recorded in the field and are known to be stressful for both species (Kingsolver, 2000; von Schmalensee

et al., 2021a). The status of the larvae (alive or dead) was checked at regular time intervals (once every 30 min for the assays at 40 °C; every 20 min at 42 °C; and every 10 min at 44 °C), trading-off between accurate detection of time to death and potential thermal fluctuations associated with larval status checking. The air temperature inside the plastic vial was continuously recorded using a data logger with a 20-second resolution to have a more accurate estimate of the thermal exposure of the larvae and its temporal fluctuations during the treatment. The average temperature recorded with the data logger was used in the subsequent analyses, rather than the fixed, programmed temperature in the water bath (which was considered a less accurate proxy).

4.2.5 Statistical analysis

All data were analyzed using R 3.6.1 (R Core Team, 2019). We applied generalised linear mixed models (GLMMs) to determine whether the two butterfly species selected different microhabitats to oviposit. The final data set included a total of 7217 min of census, 139 ovipositions, and 43 ovipositing females (Table B4). The number of ovipositions observed per female was used as the response variable (model 1). We fitted the model using the *glmer* function of the *lme4* package (Bates et al., 2015) by maximum likelihood (Laplace approximation) and a Poisson error distribution with a log link function. The type of microhabitat, the species, and their interaction were added as fixed factors, and site, date, and period of the day of the census were treated as categorical, random factors. The logarithm of census duration was added as an offset term (i.e. a linear predictor without an estimated regression parameter to account for differences in sampling effort between censuses; Zuur et al. (2009)). We repeated the same modeling procedure using the number of ovipositing females per census as the response variable (model 2).

The seasonal dynamics of microclimatic conditions and host-plant traits were assessed by regressing LOESS models against ordinal day. To examine the spatial variation of these variables across the open–closed ecotones, an ANOVA testing for microhabitat type was applied followed by a post-hoc Tukey HSD test calculated using the *emmeans* package (Lenth, 2020). The analyses were performed for the entire sampling period and for specific phenological stages and seasons. The characterisation of the thermal regimes in different microhabitats and scales considered the absolute records at different levels (air, soil, leaves), thermal tendencies relative to macroclimatic conditions, and measures of dispersion (i.e. standard deviation and skewness). Daily records of macroclimatic temperatures were obtained from two meteorological stations near the study sites (Fig. B1). Microhabitat thermal offset was calculated as the difference of daily mean temperatures between data logger and standardised weather station measurements. We defined foliar thermal offset as the difference between the upper side foliar temperature and the synchronic air temperature above the host plant at 1 m height (also termed “thermal excess” in some studies; see De Frenne et al. (2021); Pincebourde and Woods (2012)). Daily standard deviation of temperatures recorded with the data logger was used as an indicator of the microclimatic temporal variability at the microhabitat scale, while we used daily SD of foliar temperatures in the same microhabitat as a measure of spatial thermal heterogeneity at finer scales.

To assess whether the two butterflies differ in their thermal strategy, we fitted a linear model of the logarithm of the time to larval death against the mean temperature recorded with the data logger during the static treatments for each species (i.e. TDT curve). We estimated z and CT_{max} from the regressed equations and we then tested whether the two species presented different slopes by fitting an ANCOVA of the effect of temperature, species, and their interaction on \log_{10} of larval survival time. Additional general mixed linear models were also fitted for each species on log of time to larval death with thermal treatment ($^{\circ}\text{C}$), larval weight (g), and site as fixed factors and family within site as a random factor.

4.2.6 Predictions of thermal mortality in the field

The semilogarithmic link between knockdown times and temperature during a heat challenge (i.e. TDT curve) can be estimated experimentally for different levels of mortality (e.g. time where 100% or 50% of larvae were dead), resulting in parallel lines with the same slope (z). From these parallel curves, we can define how mortality rate (and, hence, survival probability) changes with exposure time for any constant temperature (Rezende et al., 2020b). We obtain in this way temperature-specific survival curves, which are mathematically related and collectively define the thermal tolerance landscape of the species (Rezende et al., 2014, 2020a,b). In the field, organisms are exposed to variable temperatures and their survival responses are the result of shifts between temperature-specific curves. Therefore, if we know how temperature changes during a specific period, we can predict the survival probability under field conditions by summing up the infinitesimal changes in the survival rate that occurred during that period (Rezende et al., 2020b).

Here we adapted the methods and scripts developed by Rezende et al. (2020a,b) to numerically predict the daily thermal mortality throughout the year for the larvae of both *Pieris* species in the different microhabitats. Microclimatic field conditions during the whole year were obtained from the thermal records of the data loggers. For each sensor, we calculated the mean thermal series of all the recorded years (Table B1) and estimated the thermal profile at 1-min resolution of each day by non-linear interpolation between consecutive hours (Rezende et al., 2020b). Daily thermal mortality was predicted from March to September (both included), to capture the period of higher thermal stress (i.e. summer). We predicted larval survival in the dynamical field conditions based on the TDT curves, by bootstrapping the time of death of 35 larvae per species in each of the three experimental treatments (i.e. 40, 42, or 44 $^{\circ}\text{C}$, total sample size = 210). Bootstrapped data was then used to estimate the tolerance landscape of each species with a resolution of 0.001 of survival probability (see Rezende et al., 2020b, for further details). From this relationship between survival and time at constant temperatures, we calculated the daily mortality curve at a 1-min resolution for each species, day, and microclimatic sensor by numerical approximation Rezende et al. (2020b).

We defined daily thermal mortality as the maximum mortality ($1 - \text{survival probability}$) of the day and calculated, with these daily values, the cumulative mortality during

development (using a rolling window of 30 days from March to September). We then averaged cumulative mortality for the periods where it exceeded 0.01 (i.e. mostly in summer) to summarise the peaks of thermal mortality for each species in each microhabitat. Finally, we assessed how thermal mortality would change if we consider that larvae can avoid acute thermal stress on the leaves by actively moving to shadier parts of the plant (thermal avoidance behavior, TAB; Carnicer et al., 2019). This was done by truncating daily thermal profiles at fixed TAB thresholds (none, 35, 37.5, 40, 42.5, and 45 °C) and repeating the whole numeric procedure with the truncated thermal profile. These thresholds were obtained from previous experimental observations of thermal avoidance behaviours for the genus *Pieris* (Carnicer et al., 2019). We performed 100 bootstrap replicates per threshold to have an estimate of the uncertainty associated with the predictions.

4.3 Results

4.3.1 Interspecific differences in microhabitat selection

Results of the GLMM analyses applied on the number of ovipositions per female (model 1) and on the number of ovipositing females (model 2) were very similar (Table 4.1). Both *P. napi* and *P. rapae* distributed their eggs unequally across the open–closed ecotones (model 1: microhabitat $\chi^2 = 13.1$, $df = 2$, $P = 0.0015$). However, the microhabitats selected by females differed between the two butterflies (model 2: microhabitat \times species $\chi^2 = 21.2$, $df = 2$, $P < 0.0001$). *Pieris napi* preferentially selected host plants from the microhabitats with intermediate vegetation covering (which include the semi-open and semi-closed microhabitats, Fig. 4.2a). Concretely, predictions from model 1 indicated that the number of eggs laid in these microhabitats was six and three times higher than in closed and open microhabitats, respectively. In sharp contrast, *P. rapae* mainly laid eggs in the open microhabitats (in model 1, open microhabitats received 99% of *P. rapae* ovipositions). Closed microhabitats were rarely selected by either species, but a few ovipositions of *P. napi* were observed. The oviposition pattern did not present relevant differences between sites, as the variance estimated for this random factor was much lower than the other effects in both models (model 1: $sd_{site} = 0.02$, $sd_{date} = 1.47$, $sd_{period} = 1.77$; model 2: $sd_{site} = 0.23$, $sd_{date} = 0.7$, $sd_{period} = 1.26$).

4.3.2 Interspecific differences in thermal exposure

Foliar temperature recorded during oviposition differed between both species (with thermal differences in the range 5–10 °C in the leaf underside, where most eggs were laid, Fig. 4.2b). The thermal regimes characterised throughout the monitoring campaign varied between microhabitats in the same line. Daily maximum temperatures recorded with the data loggers were, respectively, a mean of 6 and 2 °C lower in the semi-closed and semi-open microhabitats than in the open areas, where *P. rapae* oviposits (Fig. 4.2c). A

Table 4.1: Generalised linear mixed models of the number of ovipositions per female and the number of ovipositing females per census. Results from the type III Wald χ^2 analysis of deviance of the fixed effects. Marginal R^2 for GLMMs (including only fixed effects) were calculated following Nakagawa et al. (2017) with the version 0.9.2 of the *performance* package (Lüdtke et al., 2021). Abbreviations: *df*, degrees of freedom

Model	Response variable	Fixed effect	χ^2	<i>df</i>	<i>P</i>
Model 1 ($R^2_{GLMM} = 0.23$)	Ovipositions per females	Microhabitat type	13.1	2	0.0015
		Species	0.3	1	0.5576
		Microhabitat type \times Species	60.7	2	<0.0001
Model 2 ($R^2_{GLMM} = 0.14$)	Ovipositing females per census	Microhabitat type	6.1	2	0.0474
		Species	1.3	1	0.2475
		Microhabitat type \times Species	21.2	2	<0.0001

similar pattern was found for temperatures recorded at the upper surface of the leaves (Fig. 4.2d), which were measured during the period of highest insolation (10–16h) and when most eggs are usually laid (Fig. B4).

Canopy cover of the closed and semi-closed microhabitats from the mid-elevation site diminished mean daily temperatures of the understory an average of 3 °C relative to mean macroclimatic conditions (Fig. 4.2e). In contrast, the buffering capacity of lowland vegetation was much lower, and the largest offsets from macroclimatic mean temperatures were observed in the open and semi-open microhabitats (daily mean temperatures 1–2 °C higher than meteorological records). Besides the higher air temperatures at the microhabitat scale, leaves in the open microhabitats of the lowland site were additionally subject to important thermal amplification processes that could elevate foliar temperatures up to 10 °C higher than the air above the host plant (Fig. 4.2f). Overall, the structure of the open–closed ecotones largely determined the microclimatic processes that operated in the different microhabitats, modifying the thermal exposure of the host plants. Microhabitat and foliar temperatures could exceed 40 °C in the open microhabitats (Fig. 4.2b–d), especially in the lowland site during summer (Fig. B5), while temperatures remained below 40 °C in semi-closed and semi-open microhabitats of both sites across the seasons (Figs. B6 and B7).

Temperatures in closed and semi-closed microhabitats were more constant throughout the day and were more homogenous across this type of microsite (Fig. 4.2g–h). Open microhabitats presented instead the most variable daily thermal profiles (Fig. 4.2g), with more positively skewed distributions (i.e. more extreme values in the upper side of the thermal distribution, Fig. B8a). Thermal heterogeneity at fine spatial scales was also higher in the open microhabitats, which was calculated as the SD of the temperatures recorded on the upper- and underside of the leaves in each microhabitat on a daily basis (Fig. 4.2h).

4. INTERSPECIFIC DIFFERENCES IN MICROCLIMATIC THERMAL MORTALITY

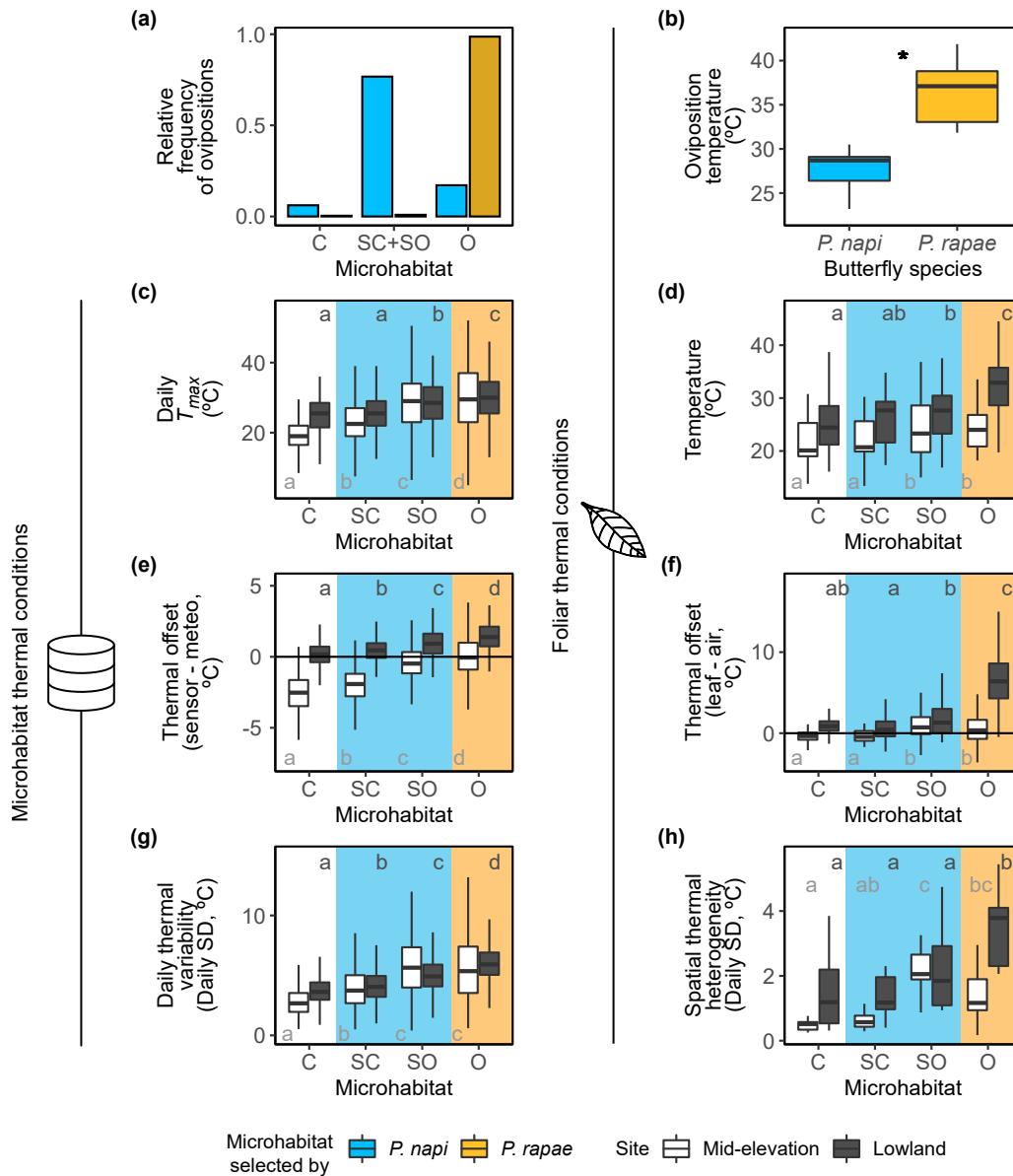


Figure 4.2: Interspecific differences in the thermal regime that eggs and larvae are exposed to, both at microhabitat (c, e, and g) and foliar (b, d, f, and h) scales. (a) Relative distribution of ovipositions for each species across the open–closed ecotones. (b) Foliar temperature during oviposition at the underside. (c) Daily maximum temperatures recorded with the data loggers. (d) Foliar temperatures at the upper side during host-plant monitoring. (e) Thermal offset calculated as the difference of the mean daily temperatures between the microhabitat and the macroclimate. (f) Foliar thermal offset calculated as the instantaneous difference of foliar and air temperatures above the host plant at 1 m height. (g) Daily temporal variability (standard deviation, SD) of the temperatures recorded at microhabitat scale. (h) Thermal heterogeneity of foliar temperatures in the same microhabitat and time. Different letters indicate the microhabitats with $P < 0.05$ in pairwise Tukey HSD tests of the response variable for each site (light grey for the mid-elevation site, and dark grey for the lowland site). The lower and upper hinges of the box represent the 1st and the 3rd quartiles respectively (Q_1 , Q_3); its inner line, the median; and the length of the box, the $IQR = Q_3 - Q_1$. (Legend continues on next page).

(Continuation of legend from Fig. 4.2). Lower whisker represents the smallest value $\geq Q_1 - 1.5 \times IQR$; and the upper whisker, the biggest value $\leq Q_3 + 1.5 \times IQR$. Outliers are not shown. Coloured areas in the panels C–H indicate the microhabitats selected by each species (i.e. blue: *P. napi*; orange: *P. rapae*) to facilitate interspecific comparisons. C, closed; SC, semi-closed; SO, semi-open; and O, open microhabitat.

4.3.3 Sources of thermal heterogeneity at fine scales

All the thermal variables measured at the host-plant level (i.e. excluding air temperatures at the microhabitat scale recorded with the data loggers) were strongly correlated in pairwise correlations for each site and microhabitat type ($R^2 = 0.81 \pm 0.16$; and $P = 0.0042 \pm 0.0198$, which summarise the mean \pm sd of the R^2 and P values obtained in the correlation tests). Nevertheless, there were notable differences between leaves, soils, and the air in the open microhabitat of the lowland site, where thermal heterogeneity was higher (Figs. 4.3 and B9).

Soil in the open microhabitat of the lowland site was warmer and drier than in the other microhabitats (Figs. 4.3 and 4.4a), especially during summer (Fig. 4.4c). Soil surface reached temperatures higher than 45 °C when exposed to full radiation (i.e. soil thermal amplification, Fig. 4.3c). Going up from the soil, air temperature rapidly decreased with height following a hyperbolic sine function (i2 in Fig. 4.3). In this line, basal leaves of the host plants from open microhabitats were 2–7 °C warmer than apical leaves (i1 in Fig. 4.3), while basal leaves in semi-open and semi-closed microhabitats could reach inferior temperatures than apical leaves (i.e. soil cooling effect, Fig. 4.3b). This thermal difference between leaves could be recorded in spring plants of *Lepidium draba*, which were > 40 cm height. In contrast, leaves of summer resprouts (< 5 cm height) presented the highest temperatures and the lowest thermal heterogeneity (daily SD of foliar thermal records, Fig. B5c–d).

Fine-scale thermal heterogeneity was also detected between sides of the same leaves. In intermediate ranges of microhabitat air temperature (i.e. 20–35 °C), foliar underside temperatures were 1–3 °C cooler than upper parts of the leaves exposed to direct radiation in open microhabitats (Fig. 4.3d). However, at higher air temperatures (i.e. > 35 °C), thermal differences between foliar upper and underside vanished (Fig. 4.3e). In these conditions leaves could be 10 °C warmer than air temperature above the host plant (Fig. 4.3f). The effects of foliar height and foliar side on thermal heterogeneity were putatively associated with radiative heating and sensible heat fluxes from the soil and with processes of stomatal closure of the leaves.

4. INTERSPECIFIC DIFFERENCES IN MICROCLIMATIC THERMAL MORTALITY

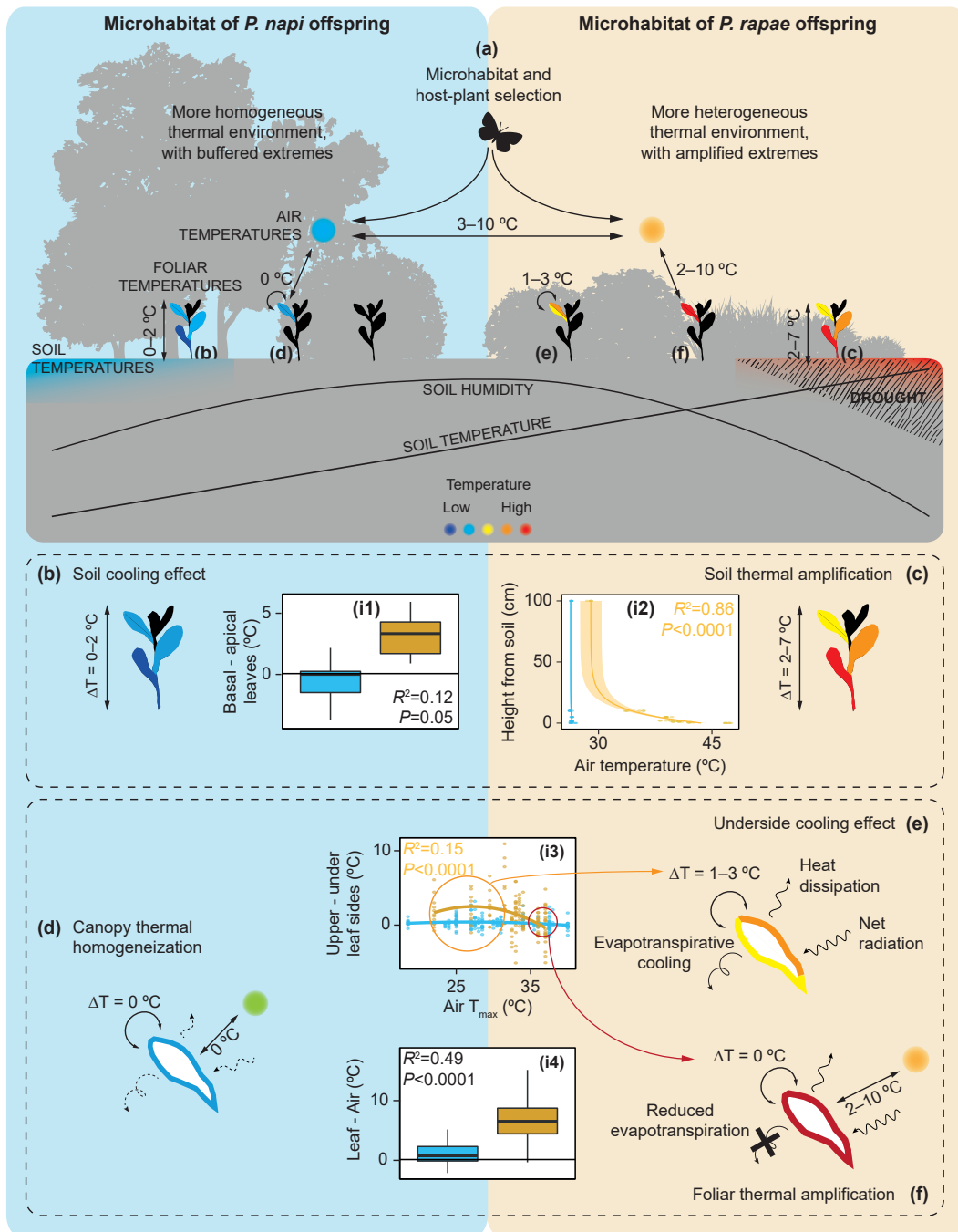


Figure 4.3: A visual summary of the diverse microclimatic mosaics and processes at fine scales quantified in the lowland site. Blue areas (left) indicate microhabitats preferentially selected by *P. napi*, and orange areas (right), by *P. rapae*. Observed thermal differences between the air, host plants, and soil allowed the identification of six processes determining larval thermal exposure: butterfly oviposition behaviour (a); the influence of soil cooling effects (b) and soil thermal amplification on basal leaves (c); canopy thermal homogenisation (d); leaf underside cooling by active stomatal conductance (e); and foliar thermal amplification by reduced stomatal conductance (f). Detailed thermal data is reported in the four insets providing evidence for these processes (i1–i4). (a) Air temperatures in the semi-open and semi-closed microhabitats where *P. napi* oviposits reach about 3–10 °C inferior values and are less variable than in open microhabitats (ovipositing microsities of *P. rapae*). (Legend continues on next page).

(Continuation of legend from Fig. 4.3). Open microhabitats are more thermally heterogeneous at fine scales, with notable thermal differences between leaves, soil, and the air. (b) Temperatures at the soil surface influence the heat balance of basal leaves, such that basal leaves in the semi-closed microhabitat can be cooler than apical leaves (i1). (c) Soil thermal amplification in the open microhabitat warms the lower air layers and creates steep thermal gradients with height (i2), which can be also detected between basal and apical leaves (ii). (d) Canopy shading in more closed microhabitats cools leaves and air, resulting in similar temperatures in the leaf upper- and undersides (i3 and i4, results in blue). (e) When temperatures in open microhabitats were moderately warm (around 25 °C), we observed that stomatal conductance and evapotranspiration cooled foliar undersides 1–3 °C in relation to the upper sides, which are more directly exposed to radiative heating (i3, orange line). (f) However, in dry and warm conditions (> 35 °C), high radiative heating from the soil and reduced evapotranspiration linked to leaf stomatal closure can bring leaves 10 °C warmer than the air (i4, orange). Black lines in the soil are added for illustrative purposes and represent the patterns of variation of soil temperature and humidity across the ecotone that we observed in Figs. 4.4 and B1b. More detailed results of thermal heterogeneity at fine scales can be found in Figs. B5 and B9.

4.3.4 Host-plant variability

Open–closed ecotones also induced changes in host-plant traits, paralleling variation in thermal exposure (Figs. 4.4, B6, and B7). Host plants in open microhabitats had smaller leaves with lower ratios of water content (i.e. less water per mg of foliar dry weight, Fig. 4.4d). Variation in foliar chlorophyll content and fruit production depended on the shade tolerance of the host plant. *Lepidium draba* (lowland site) presented higher chlorophyll contents and produced more fruits in open microhabitats, while plants in closed and semi-closed microhabitats did not reproduce sexually and had thinner leaves, with low chlorophyll contents. On the contrary, chlorophyll content and fruit production for *A. petiolata* in the mid-elevation site was lowest in the open microhabitat (Fig. B10).

Foliar water and chlorophyll contents decreased in both host plants (Fig. 4.4e–f and Fig. B11) as they senesced after fructification during late spring and early summer (ordinal days 140–180). Only non-flowering first-year rosettes (*A. petiolata*) and summer rhizome resprouts (*L. draba*) remained in midsummer after senescence (Fig. B12). First-year rosettes of *A. petiolata* notably coexisted in June with the reproductive stage of second-year individuals. In contrast, there was no temporal overlap between reproductive *L. draba* plants and new summer resprouts, leading to a period of scarcity of fresh host plants lasting 2–3 weeks.

4.3.5 Interspecific differences in thermal strategies and mortality

Time to larval death and experimental temperatures were associated in semilogarithmic curves for both species (Fig. 4.5a), presenting a steeper slope (25% more negative) for *Pieris napi* (species × temperature $P = 0.0085$ in the ANCOVA model, which explained a 76% of the variance). The estimated intersection point of the two TDT curves was located at $T^* = 41.2$ °C. Above this threshold, *P. rapae* exhibited greater survival than *P.*

4. INTERSPECIFIC DIFFERENCES IN MICROCLIMATIC THERMAL MORTALITY

napi, while the opposite was true for inferior temperatures (Fig. 4.5a). As predicted, the estimates (\pm SE) of thermal tolerance z and CT_{max} were higher for *P. rapae* ($z = 5.10 \pm 0.24$ °C; $CT_{max} = 53.48$ °C) than for *P. napi* ($z = 4.10 \pm 0.26$ °C; $CT_{max} = 51.08$ °C). In the general mixed linear models considering more factors than temperature, strong effects were also found for larval weight (Table 4.2), with smaller larvae presenting lower survival times. Concretely, an increase of 0.1 g in larval weight would cancel out the effects of an increase of 1 °C in temperature (i.e. the former would provoke an increase of 30–50% in survival times, while the later would decrease them by 30–50%, Fig. B13).

Interspecific differences in the TDT curves and the predicted thermal mortality in the field were in agreement with the pattern of microhabitat selection of the two species. Daily mortality was higher for the thermosensitive *P. napi* (Fig. B14) when thermal stresses were more acute (more intense heat challenges, mainly found in open microhabitats). In contrast, more constant thermal regimes, with less extreme but longer thermal heat challenges (i.e. chronic stress), were deadlier for *P. rapae*. Daily thermal mortality from March to September was usually low (< 0.01), although it could reach values around 0.4 in the open microhabitats during the warmest days ($< 15\%$ of the days, Fig. B15a).

The accumulation of low daily mortalities for a period similar to larval development

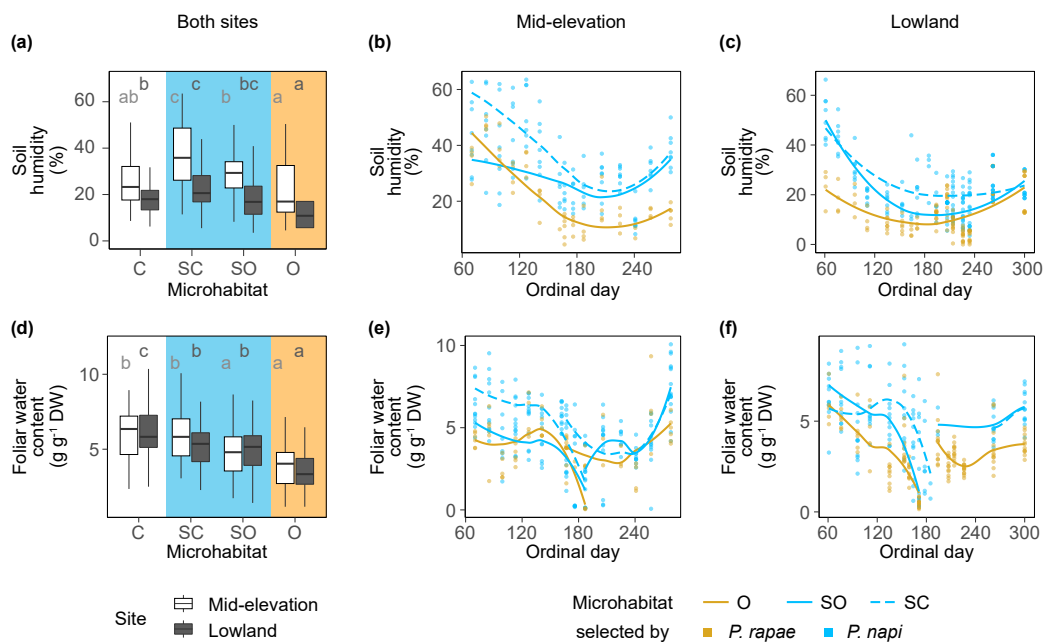


Figure 4.4: Spatial and seasonal variation in the soil humidity (a–c) and foliar water content (d–f) of the host plants measured during the monitoring campaign. (a and d) Variation across open–closed ecotones. Different letters indicate the microhabitats with $P < 0.05$ in pairwise Tukey HSD tests of the response variable for each site (light grey for the mid-elevation site, and dark grey for the lowland site). (b, c, e, and f) Seasonal cycle of the soil humidity (b–c) and the foliar water content (e–f) measured in different microhabitats types monitored in the mid-elevation (b and e) and lowland (c and f) sites. Open microhabitats (mainly selected by *P. rapae*) are represented in yellow; and semi-open and semi-closed microhabitats (mainly selected by *P. napi*), in blue. C, closed; SC, semi-closed; SO, semi-open; and O, open microhabitats.

time (i.e. 30 days) could exert considerable thermal pressure on natural populations (cumulative mortality > 0.8 during the summer in the open microhabitats). However, the estimates indicated that thermal mortality would be importantly reduced if larvae conducted thermal avoidance behaviours (Fig. B15b). Mean thermal mortality during the development was around 0–0.2 in semi-open and semi-closed microhabitats (Fig. 4.5b), and an average of 15% lower for *P. napi* than for *P. rapae* (Fig. 4.5c). The opposite pattern was found in the open microhabitats, where mean thermal mortality during development was 15% higher for *P. napi* than for *P. rapae* and ranged between 0.4 and 0.8. Thus, by laying its eggs on semi-open and semi-closed microhabitats, *P. napi* eludes a high thermal mortality. In contrast, *P. rapae* selects the microhabitats with the most intense heat challenges, exposing its offspring to deadly thermal stresses that it can withstand better than *P. napi*.

Table 4.2: General linear mixed model of the time to larval death for each species. Results from the type III Wald χ^2 analysis of deviance of the fixed effects. Marginal R^2 for GLMMs (including only fixed effects) were calculated following Nakagawa et al. (2017) with the version 0.9.2 of the *performance* package (Lüdtke et al., 2021). Abbreviations: *df*, degrees of freedom

Model	Fixed effect	χ^2	<i>df</i>	<i>P</i>
<i>Pieris napi</i> ($R^2_{GLMM} = 0.75$)	Temperature (°C)	194.0	1	<0.0001
	Larval weight (g)	5.7	1	0.0166
	Site	1.6	1	0.2051
<i>Pieris rapae</i> ($R^2_{GLMM} = 0.8$)	Temperature (°C)	476.1	1	<0.0001
	Larval weight (g)	9.4	1	0.0022
	Site	1.9	1	0.1691

4. INTERSPECIFIC DIFFERENCES IN MICROCLIMATIC THERMAL MORTALITY

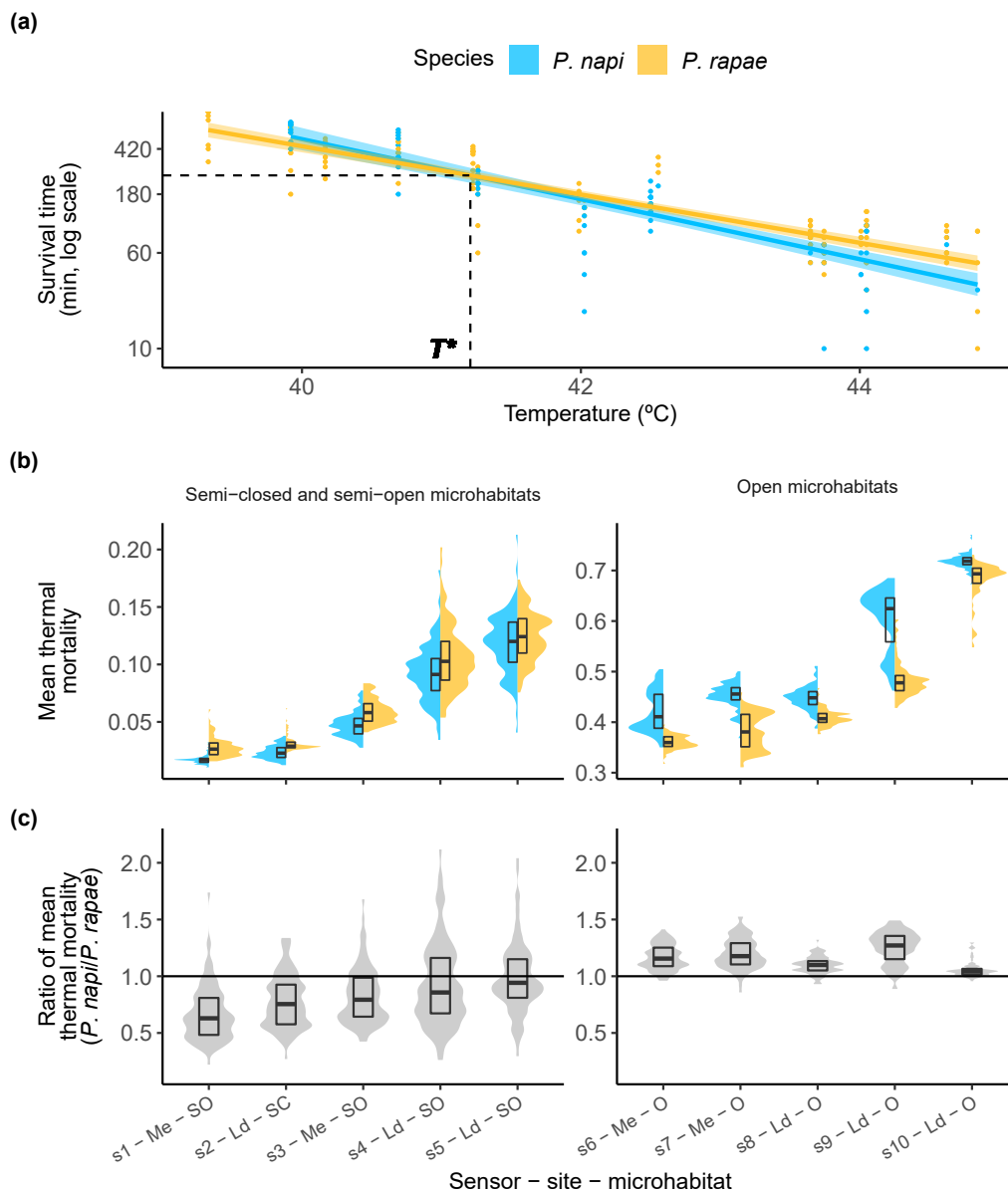


Figure 4.5: (a) Thermal death time (TDT) curves for *P. napi* and *P. rapae*. The dashed lines indicate the intersection point between the two TDT curves, representing the temperature at which both species show equal survival times. (b) Interspecific differences of mean thermal mortality during development for the periods where 30-day cumulative mortality was equal or higher than 0.01. Coloured areas represent the density functions of the mean thermal mortality in the 100 bootstrap replicates for each species and each data logger (each temporal series of microclimatic temperatures). The lower and upper limits of the boxes represent the 1st and the 3rd quartiles of mean thermal mortality and, their inner line, the median. (c) Interspecific ratio ($P. napi / P. rapae$) of mean thermal mortality during development observed in each microhabitat. For both species, estimated mortality was lower in their preferred microhabitats: *Pieris napi* showed inferior mortalities in semi-open and semi-closed microhabitats (left panels) but higher in open microhabitats (right panels). Microhabitats with a cumulative mortality inferior to 0.01 during the whole period (March–September) are not shown. Me, mid-elevation; Ld, lowland sites. C, closed; SC, semi-closed; SO, semi-open; and O, open microhabitats.

4.4 Discussion

Our work quantified the microclimatic and host-plant conditions of the microhabitats where two butterfly species lay their eggs and assessed their potential impacts on the offspring. We conducted the study with two model species from an extensively-studied family of butterflies in the ecotones between forested and open habitats of two protected areas. We combined field census of butterfly behavior, detailed measurements of the microclimate in the selected microhabitats, and an experimental characterisation of the thermal tolerance of the larvae, to computationally predict the thermal mortality in the field. Many studies stress the need to consider temperatures at the microclimatic scale to better understand the thermal ecology of the species and their responses to global warming (Bramer et al., 2018; Pincebourde and Woods, 2020; Woods et al., 2015). As far as we know, mortality associated with microclimatic variation has been very occasionally assessed (Kaiser et al., 2016; Kingsolver, 1979; Potter et al., 2009; Woods et al., 2022). For the first time, here we predicted the mortality derived from microclimatic temperatures considering both the intensities and the duration of the thermal exposures, and their cumulative effects (Rezende et al., 2020b).

The two butterflies selected the same host-plant species from different microhabitats to oviposit: *Pieris napi* laid most of their eggs in semi-open and semi-closed microhabitats, and *P. rapae*, in open ones (Table 4.1 and Fig. 4.2). These results indicate that habitat choice preceded host-plant selection, as has long been proposed (Courtney, 1986; Dennis, 2010; Porter, 1992) and as has been found for this pair of species (Friberg and Wiklund, 2019; Ohsaki, 1982; Ohsaki and Sato, 1999). Ovipositing females generally use multiple cues following a spatially-structured and hierarchical process, from coarse to finer scales. Determining which specific cues influenced oviposition decisions is beyond the scope of our study, but both microclimatic and host-plant factors could have had a role. Ohsaki (1982) associated *P. napi* and *P. rapae* oviposition decisions with the different light conditions of the microhabitat, and Forsberg (1987) suggested that *P. napi* in Sweden actively oviposited in small plants to favour higher microclimatic temperatures. Other studies related oviposition decisions of *P. rapae* with host-plant qualities. Visual stimuli (mainly the colour or the greenness of the plant) have a key role when females are searching for a host plant (Myers, 1985; Tsuji and Coe, 2014), although olfactory cues likely influence pre-alightment decisions too (Renwick and Radke, 1988). After landing on host plants, chemical, and nutrient status of the plants were found to be decisive (Hern et al., 1996). For example, leaves with higher water and nitrogen content and with high transpiration rates are more frequently accepted to oviposit (Myers, 1985; Wolfson, 1980). In our study, all of these factors varied between the selected microhabitats (Figs. 4.2 and 4.4).

Microhabitat preferences observed in the field matched interspecific differences in the TDT curves determined in the laboratory and in the predicted thermal mortality in the field (Fig. 4.5). *Piers napi* presented a more thermosensitive strategy, with lower survivals under acute stresses, but higher under longer subextreme challenges. Accordingly, its mean thermal mortality during development was approximately 15% higher than *P. rapae* in open microhabitats, where heat challenges are more extreme, but 15% lower than

P. rapae in their selected microhabitats. Petersen (1954) already proposed that, as a result of interspecific competition, *P. napi* would have specialised in developing in shaded environments, where thermal regimes are cooler and host plants have thinner leaves than in the dry, open habitats selected by *P. rapae*. But later research suggested that competition between Pierids is unlikely to be driving their habitat segregation (Courtney, 1986), and that escape from parasitism is a more likely driver in the case of *P. napi* and *P. rapae* (Ohsaki and Sato, 1999). Regardless of the ultimate cause driving this habitat differentiation, specialisation in fresh and humid habitats or dry and hot habitats usually comes with different costs and benefits. For example, studies with other butterflies have shown that specializing in hot environments can select higher fecundities and adult survival at the expense of larval survival (Karlsson and Wiklund, 2005). In this line, our results also predicted that larval survival in open microhabitats is lower (Fig. 4.5), and previous studies found that *P. rapae* laid more eggs but smaller ones than *P. napi* (Ohsaki, 1982).

In this study we also identified six processes (a–f in Fig. 4.3) modulating the thermal exposure of the two species at very fine scales, and hence their thermal mortality. The first one is microhabitat selection by adult butterflies, which strongly determines the thermal exposure of the larvae. Thermal differences between open and intermediately-covered microhabitats were in the range of 3–10 °C for diurnal temperatures at the foliar and air levels (Figs. 4.2 and 4.3a). These results are in agreement with the thermal differences between more open and closed habitats of herbivorous insects reported in other studies (Ashton et al., 2009; Friberg et al., 2008; Merckx et al., 2015; Ohsaki, 1982; Suggitt et al., 2012). Daily temperatures in open microhabitats also presented higher variation, with more extreme temperatures. Then, heat and water fluxes at fine scales create very different microclimatic mosaics between the selected microhabitats (Fig. 4.3b–f). In open microhabitats, processes like soil and foliar thermal amplification can raise foliar temperatures 10 °C relative to the air (Fig. 4.3c and f; Carnicer et al., 2021; Pincebourde et al., 2021; Woods et al., 2022), or evapotranspiration can cool the foliar underside 3 °C relative to the upper side (Fig. 4.3e). These processes create a more heterogeneous thermal mosaic than that found in semi-open and semi-closed microhabitats, where soil cooling and canopy shading homogenise temperatures (Fig. 4.3b and d). Our predictions of thermal mortality were based on the thermal series extracted from the data loggers, which represent air temperatures at the microhabitat level. But larvae might be more dependent on temperatures at the foliar level, especially at their initial stages (Pincebourde et al., 2021; Woods, 2013). The high fine-scale thermal heterogeneity in open microhabitats could potentially expose larvae of *P. rapae* to more acute thermal stresses than those we predicted, but could also offer more opportunities for behavioural thermoregulation (by moving to the foliar underside [Fig. 4.3e], or to a cooler leaf or plant [Fig. 4.3c]). Although thermal heterogeneity was lower in summer in the lowland, some leaves presented temperatures that could reduce thermal mortality. For example, if larvae avoided thermal exposures > 40 °C, cumulative mortality during development would be importantly reduced (Figs. B5 and B15). Thermal avoidance behaviours have been reported for the larvae of *P. napi* (Carnicer et al., 2019) and *P. rapae* (Kingsolver and Gomulkiewicz, 2003).

The microclimatic exposure during the development of insects will simultaneously

affect other physiological and demographical rates besides larval survival (Braschler et al., 2021; Diamond et al., 2013; Kingsolver et al., 2011; von Schmalensee et al., 2021a), which can influence the larval mortality patterns described here. For example, different microclimatic regimes can lead to shorter or longer larval development times due to nonlinear changes of development rates with temperature (thermal performance curves; Greiser et al., 2022; von Schmalensee et al., 2021a, Fig. B16). These variations in the development time would in turn modulate the time of exposure to microclimatic lethal stresses. Moreover, our results indicated that smaller larvae were more sensitive to heat challenges (Table 4.2 and Fig. B13). TDT curves in this study were built with all the larvae, so predictions of thermal mortality assumed a constant weight during the whole development. However, as larvae grow, they would become more tolerant, suggesting that plastic and evolutionary changes in growth rates and thermal performance curves could play a key role on larval thermal mortality. Further studies should consider how growth dynamically modifies thermal tolerance landscapes during development, and the parallel effects of microclimatic regimes on growth, development, and mortality. The differences between the microclimatic regimes of the microhabitats where the two species lay their eggs led to contrasting patterns of thermal mortality of the offspring. Despite being more thermosensitive, the offspring of *P. napi* were predicted to present higher survivals than *P. rapae* (Fig. 4.5) due to the thermal buffering provided by the microhabitats with intermediate cover (Fig. 4.2). Our results feed the growing literature on the key role that vegetation cover may play in buffering thermal macroclimatic stresses (Carnicer et al., 2019; De Frenne et al., 2021; Zellweger et al., 2020). However, many studies on butterflies indicate that other species-specific requirements, such as host plant condition and availability, should be met in these microhabitats to successfully buffer macroclimatic impacts (Ashton et al., 2009; Bennett et al., 2015; Carnicer et al., 2019; Kaiser et al., 2016; Nieto-Sánchez et al., 2015; Stefanescu et al., 2011b; Suggitt et al., 2011, 2012). For example, in summer in the lowland site, *L. draba* plants reduced their foliar water and chlorophyll contents until their complete senescence (Figs. 4.4 and B11), which would likely interact with the microclimatic impacts on larval development (Clissold and Simpson, 2015). We suggest that the different adaptive strategies of the species and their different oviposition behaviours pose different challenges to the populations. With the current microclimatic conditions, *P. napi* may not be as threatened by thermal exposure as *P. rapae*. However, the decay and disappearance of *L. draba* during the summer in the lowlands might have more negative impacts on *P. napi* because they rely on fewer host-plant species than *P. rapae*, which are more likely to find other host plants in a better condition during this period (Carnicer et al., 2019; Vives-Inglá et al., 2020).

Our study assessed both the thermal exposure and the thermal sensitivity of two species to predict the associated mortality using a dynamic model calibrated with physiological information from the experiments and simulated with the microclimatic regimes recorded in the field. Previous assessments of the vulnerability of organisms to global warming usually compared their experimental upper thermal limits with maximum temperatures recorded in the field (Duffy et al., 2015; Pincebourde and Casas, 2019; Sunday et al., 2014; Woods et al., 2022). However, this approach overlooks the time-dependent effects of thermal tolerance and the cumulative nature of heat injury (Jørgensen et al.,

2021; Rezende et al., 2020b), which may underestimate the vulnerability of organisms to global warming (Huey and Kearney, 2020). We predicted larval thermal mortalities applying the tolerance landscape framework, which allowed us to adopt a more realistic approach by considering their thermal sensitivity to both the duration and the intensity of microclimatic thermal exposures (Rezende et al., 2014, 2020b). This new framework can offer new insights on the role of climate change in the declines reported for many insect species around the globe (Didham et al., 2020; Wagner et al., 2021b, and all the references therein), also in our study area (Colom et al., 2022; Herrando et al., 2019; Melero et al., 2016; Stefanescu et al., 2011b; Ubach et al., 2021). Predictive models of ecological responses to climate change should incorporate information of climatic exposure at relevant scales and capture the key processes shaping organisms' sensitivity and performance in the dynamic thermal conditions they experience in nature.

Acknowledgements

Carlos López, Sofía Cortizas, Joaquim de Gispert, Katarzyna Bartnik, and Agnieszka Juszcak contributed to the field and experimental work. Roger Vila provided insightful comments that improved the manuscript. Emili Bassols provided support with permission management, scientific advice and key assistance during fieldwork. Parc Natural de la Zona Volcànica de la Garrotxa and Parc Natural Aiguamolls de l'Empordà provided logistic support. This research was supported by the Spanish Ministry of Science and Innovation through a doctoral grant (FPU17/05869); the Spanish Ministry of Economic Affairs and Digital Transformation (CGL2016-78093-R and CGL2013-48074-P); the Catalan Government (SGR-2017-1005); and by Nederlandse Organisatie voor Wetenschappelijk Onderzoek (863.11.021).

5

**Novel regimes of extreme
climatic events trigger
negative population
rates in a
common
insect**





Abstract

The IPCC predicts that events at the extreme tail of the probability distribution will increase at a higher rate relative to less severe but still abnormal events. Such outlier events are of particular concern due to nonlinear physiological and demographic responses to climatic exposure, meaning that these events are expected to have disproportionate impacts on populations over the next decades (so called low-likelihood, high-impact events - LLHI). Because such events are historically rare, forecasting how biodiversity will respond requires mechanistic models which integrate the fundamental processes driving biological responses to our changing climate. Here we built a matrix population model (MPM) from long-term monitored populations of an insect model species in a Mediterranean area. The model simultaneously integrates the effects of extreme microclimatic heat exposure and drought-induced host-plant scarcity on early life stages, a key methodological step forward because these understudied life stages are usually very susceptible to extreme climatic events. This model for the first time allows us to forecast the demographic impacts that extreme LLHI events will have on an organism with a complex life cycle. We find that juveniles were the life stage with the largest relative contribution to population dynamics. In line with field observations, simulated population rates in current climatic regimes were importantly determined by drought impacts, producing a regional mosaic of non-declining and declining populations. The simulations also indicated that, in future climate scenarios not meeting the Paris Agreement, LLHI heat extremes triggered regionally-widespread and severe declines in this currently abundant species. Our results suggest that LLHI events could thus emerge as a critical new—but overlooked—driver of the declines in insect populations, risking the crucial functions they perform in agro and natural ecosystems. We suggest that process-based and whole-cycle modelling approaches are a fundamental tool with which to understand the true impacts of climate change.

5.1 Introduction

The latest IPCC projections predict that, as the climate warms, the distribution of extreme events will change (IPCC, 2021; Seneviratne et al., 2021). However, not all extreme events will increase at the same rate; events closer to the tails of climatic distributions, will increase relatively more than less severe events (Seneviratne et al., 2012, 2021; Simolo and Corti, 2022; Sutton, 2018; Zscheischler et al., 2018). For instance, the frequency of hot temperature extremes will very likely increase nonlinearly with global warming, with larger percentage increases for rarer and very extreme events than moderate extreme temperatures (e.g. those that occur several times a year; IPCC, 2021; Seneviratne et al., 2021; Simolo and Corti, 2022; Vogel et al., 2020). These rarer extreme events are known as *low-likelihood, high-impact events* (LLHI events, hereafter)—or *black swan* events in the financial literature (Taleb, 2007)—because, despite having a much longer return period, they can have profound consequences on ecological and social systems (Fig. 5.1a). LLHI events can stem from extreme anomalies of single climate variables (e.g. a LLHI thermal

event), or from the simultaneous and successive occurrence of extreme events of different types (e.g. a compound hot-dry event; Bastos et al., 2023; Seneviratne et al., 2021; Zscheischler et al., 2018). Over the next decades, emerging novel regimes of extreme events are predicted to render a disproportionate increase in both single and compound LLHI events, potentially becoming a new but unexplored threat for biodiversity conservation (Fig. 5.1b). However, the ecological impacts of LLHI events on biological populations are still poorly understood (but see Anderson et al., 2017), and they currently represent a key research frontier in global change biology (Bastos et al., 2023; Bevacqua et al., 2021; Buckley et al., 2023a; Jentsch et al., 2007; van de Pol et al., 2017; Wood et al., 2023; Zscheischler et al., 2018).

LLHI events can have strong impacts on animal and plant populations through direct and indirect effects (Fig. 5.1c). Directly, by pushing organisms to stressful conditions beyond their tolerance and triggering nonlinear physiological responses (e.g. heat-induced mortality). Indirectly, LLHI events may affect key food resources (Johansson et al., 2020; Maron et al., 2015; van Bergen et al., 2020) or modify top-down controls in the trophic web exerted by predators, parasites, or other biological agents (Harvey et al., 2020). Although such events may last only a few days, their stressing effects can persist during a considerable proportion of the organisms' life cycles, with important consequences for their populations (Ma et al., 2021). Moreover, these impacts can combine during a compound event, with potentially larger effects than in single events occurring separately (i.e. interactive effects; Zscheischler et al., 2018).

Predicting natural population responses to the growing impacts of LLHI events with correlative approaches is usually problematic, given their scarcity in historical climatic records (Buckley et al., 2023a; van de Pol et al., 2017). Thus, to understand and predict the impacts of extreme events on populations we need process-based models explicitly integrating the underlying demographic mechanisms, such as Matrix Population Models (MPMs; Buckley et al., 2023a; Herrando-Pérez, 2013; Urban et al., 2016; van de Pol et al., 2017). While there have been many recent advances to mechanistically predict how climate variation affects key vital rates such as developmental time or juvenile mortality, the attempts to upscale these physiological effects and model the consequent population responses are still relatively scarce (Greiser et al., 2022; Jørgensen et al., 2022b; Kearney and Porter, 2020; Kearney et al., 2018; Kingsolver, 2000; Kingsolver and Buckley, 2017; Rezende et al., 2020b; Vives-Inglá et al., 2023; von Schmalensee et al., 2021a). MPMs represent mathematical summaries of populations' life cycle, allowing us to predict the impacts of extreme climatic and LLHI events on populations using a process-based and integrative approach (e.g. Capdevila et al., 2016; Davis, 2022; Jenouvrier et al., 2009, 2015; Logofet and Salguero-Gómez, 2021; Pardo et al., 2017). If we know how LLHI events impact the vital rates included in the MPM, we can simulate the behaviour of the population under different regimes of extreme events (Fig. 5.1a; Capdevila et al., 2016; Jenouvrier et al., 2009, 2015; Pardo et al., 2017). Specifically, MPMs can be simulated on different sequences of extreme events of varying intensities (LLHI or not) and types (single and compound, Fig. 5.1b). Thus, with MPMs, we can quantify the direct and indirect effects of extreme climatic impacts on populations, and the interactive effects of compound events.

Finally, MPMs allow modelling the varying impacts of extreme events across the different stages of the organisms' life cycle (Fig. 5.1c). By determining the key life stages of the population, these models identify the mechanisms driving population declines and assist the development of informed conservation strategies (Caswell, 2001; Kerr et al., 2020; Kingsolver et al., 2011; Ma et al., 2021; McDermott Long et al., 2017; Radchuk et al., 2013).

The use of MPMs in global change ecology has often been limited by the quantity of experimental and fine-grained observational data they require. Here, we use a long-term, consolidated study of a model insect to parametrise an MPM and predict their population responses to extreme LLHI events (Carnicer et al., 2019; Vives-Inгла et al., 2020, 2023). Because of their ectothermic nature and short life cycles, insects are generally very sensitive to changing environmental conditions and are often used as model organisms to study the physiological and demographic impacts of climate change (Hill et al., 2021; Johnson and Jones, 2017; Price et al., 2011). Furthermore, understanding insect responses to climate change is of major importance, as they perform key ecosystem functions, such as pollination, soil formation, pest control, decomposition, and nutrient cycling (Seastedt and Crossley, 1984; van der Sluijs, 2020; Weisser and Siemann, 2007). During the last decades, many insect populations have shown significant and rapid declines (van Klink et al., 2020a,b; Wagner, 2020); and it is becoming increasingly apparent that, among all other drivers of insect trends, climatic change will take a preeminent role in the coming years (Dicks et al., 2021; Jaureguiberry et al., 2022; Neff et al., 2022; Wagner et al., 2021b).

Here we analyse a unique long-term high-resolution demographic and physiological data set for the Mediterranean populations of the butterfly *Pieris napi* exposed to hot, dry, and compound hot-dry extreme events (Carnicer et al., 2019; Stefanescu et al., 2011b; Vives-Inгла et al., 2023). With this information, we first build MPMs and identify the key stages and vital rates for the population performance using an elasticity analysis on the matrices. Then, we reproduce the observed demographic dynamics under the current regimes of extreme climatic events to validate our model. Finally, we project the population under different scenarios of global warming with an increasing proportion of single and compound LLHI events, and quantify the separate and interactive effects of extreme heat and drought.

5. NOVEL EXTREMES TRIGGER INSECT DECLINING RATES

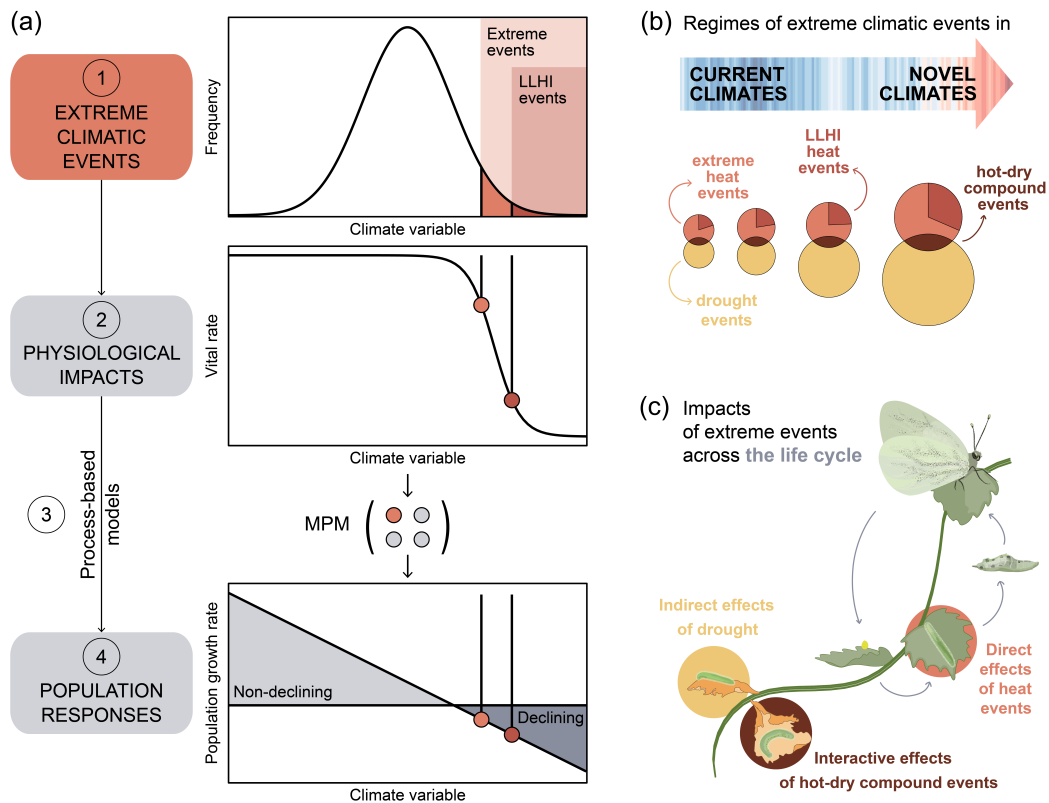


Figure 5.1: Matrix population models (MPM) and the effects of low-likelihood, high-impact extreme events (LLHI events) on insect ecophysiology and demography in future global warming scenarios. (a) 1. Climate change will progressively increase the frequency and intensity of extreme LLHI events (dark-red square). 2. Extreme events often trigger negative, nonlinear responses on key insect vital rates, such as individual survival and reproduction, potentially affecting population performance. 3. Process-based models like MPMs allow the quantitative integration of multiple climatically-induced ecophysiological effects on vital rates providing, as a predictive output, the expected population growth response. 4. MPMs enable the prediction of declining and non-declining population responses of insects to the increasing impacts of extreme LLHI events. (b) A diagram illustrating the non-proportional increase in the frequency of LLHI events expected with ongoing global warming and the associated emergence of novel climatic regimes (IPCC, 2021). Several types of extreme events are represented. The growing size of red circles represents the predicted increase of extreme heat events by the IPCC. Similarly, lower, ochre circles represent drought events, which will also increase progressively in novel climates in some regions of the globe (IPCC, 2021). Note that inside the red circles, increasing dark red portions highlight the non-proportional increase of strong LLHI heat events predicted in novel climates. Finally, brown areas of the intersecting red and ochre circles illustrate the expected increase of compound hot-dry events. Further methodological details can be found in Appendix C: Fig. C5, Table C1, and Appendix C.3. (c) Extreme climatic events impact insects across their life cycles and through multiple pathways including direct and indirect effects, and their combined action. Red circle: direct effects of extreme heat on insect physiological rates in multiple stages of the life cycle (egg, larvae, pupae, and adult). Ochre circle: indirect effects of drought on insects by reducing host-plant availability. Brown circle: interactive effects of direct (extreme heat) and indirect (drought-induced plant scarcity) impacts triggered by compound hot-dry events.

5.2 Methods

5.2.1 Study system

Our model species for the MPM demographic analyses is the green-veined white (*Pieris napi* L. 1758), a very common and widespread butterfly throughout the Holarctic region (Tolman and Lewington, 2009). It is an extensively-studied species, with much research focusing on their physiological responses to thermal, drought, and food stresses (Bauerfeind and Fischer, 2013b, 2014b; Carnicer et al., 2019; Degut et al., 2022; Günter et al., 2020a; Kuczyk et al., 2021; Shapiro, 1979; Vives-Inglà et al., 2023; von Schmalensee et al., 2021a, 2023), which consolidate the species as a model to study climate change impacts on insects. We have studied the climate-induced declines of this model species over the last three decades in the north-east of the Iberian Peninsula. This location is a European hotspot of butterfly diversity and endemism, and a global hotspot of climate change impacts associated with the increasing frequency of hot events, dry events, and hot-dry compound events (Giorgi, 2006; Lemus-Canovas and Lopez-Bustins, 2021; Newbold et al., 2020; Seneviratne et al., 2021; Simolo and Corti, 2022; Stefanescu et al., 2011a; van Swaay et al., 2010; Vogel et al., 2020). To study their population dynamics in this area, we used a unique long-term demographic series (1993–2018) from the Catalan Butterfly Monitoring Scheme (CBMS, www.catalanbms.org, Pollard and Yates, 1993; Stefanescu, 2000). The species currently shows a geographic mosaic of demographic trends (Fig. C1), with some populations increasing or remaining stable in climatically-buffered areas, and declining populations often located in more exposed, lowland sites (Fig. 5.2a; Carnicer et al., 2019; Vives-Inglà et al., 2020, 2023). To parametrise the MPM for the species, we complemented these demographic series with detailed observational and experimental information regarding the phenology of the adults; the developmental rates and the thermal tolerance of the immature stages; their microclimatic exposure; and the seasonal cycles of their host plants from one declining and one non-declining population (see below and Appendix C.2; Carnicer et al., 2019; Vives-Inglà et al., 2020, 2023).

Pieris napi is multivoltine in the study area. Populations display each year an initial spring generation when hibernating pupae end their diapause, followed by multiple subsequent generations that directly develop during summer. They typically produce a total of three consecutive generations in colder, mid-elevation areas (Fig. 5.2a, left panel), and can reach up to four or five generations in warmer, lowland Mediterranean areas (Carnicer et al., 2019; Vives-Inglà et al., 2020). The demographic declines observed in these lowland populations have been associated with increased summer droughts (Carnicer et al., 2019). More specifically, previous field studies have shown that drier soil conditions during summer induce an earlier decay of the host plants used by these populations (Vives-Inglà et al., 2020). The developing larvae of the third annual generation during dry summers are thus exposed to an important reduction of food availability (Fig. 5.2a, right panel; Carnicer et al., 2019; Vives-Inglà et al., 2020, 2023), negatively affecting population growth rates.

5.2.2 Population matrices

To simulate the population consequences of different regimes of extreme LLHI events we used MPMs. These models are mathematical summaries of the population life cycle represented in a transition matrix (A) containing the probabilities of any individual of a given size, age, or stage class to transition into any other class (Caswell, 2001). The transition matrix allows to predict the structure of the population at any time (i.e. n_t , the distribution of their individuals in different classes) given the vector with their previous structure (n_{t-1}) (Caswell, 2001, Eq. (5.1)):

$$n_t = A \times n_{t-1} \quad (5.1)$$

The transition probabilities included in A are calculated from the vital rates across the life cycle of the modelled organism. We parameterised the MPM of *P. napi* following the matrix structure recently proposed by Kerr et al. (2020). The model classified individuals into adults and juveniles, and subdivided these two stages by their age in days. The juvenile stage included the egg, larval, and pupal states. Therefore, A was compounded by four submatrices (Eq. (5.2)) representing juveniles surviving but not transitioning to adults (A_{JJ} juvenile stasis submatrix, hereafter); juveniles surviving and transitioning to adults (A_{JM} , juvenile transition submatrix); and the adult survival (A_{MM}) and adult fecundity submatrices (A_{MJ}).

$$A = \begin{pmatrix} A_{JJ} & A_{MJ} \\ A_{JM} & A_{MM} \end{pmatrix} \quad (5.2)$$

The elements of these submatrices were calculated from the following vital rates: juvenile survival (j_x), juvenile maturity (e_x), adult survival (s_x), and adult fecundity (f_x). A more detailed mathematical description is provided in Appendix C.2 (see also Kerr et al., 2020).

As the species produces several generations per year, we built two separate transition matrices representing spring and summer generations to capture the differences in the mean microclimatic conditions and vital rates during their development. All the analyses to parametrise the model and the subsequent demographic projections were performed in the R environment version 4.3.0 (R Core Team, 2023).

5.2.3 Model parametrisation

Transition probabilities

The submatrices of juvenile stasis (A_{JJ}) and juvenile transition (A_{JM}) included the estimates on juvenile survival (j_x) and the probability of pupal eclosion (e_x , the probability of transition from the juvenile to the adult stage conditioned on juvenile survival).

We estimated these parameters experimentally in growth chambers programmed under both spring and summer mean microclimatic temperatures and light conditions inducing direct development (i.e. without pupal diapause, 13:11 L:D, Fig. C2). To account for juvenile predation and parasitism (which was prevented in the growth chamber experiments), we added an extra 5% of daily juvenile mortality, obtaining similar probabilities for an egg to become an adult to those reported in the field ($\sim 7-10\%$) (Fig. C3; Cappuccino and Kareiva, 1985; Doak et al., 2006; Forsberg, 1987; Keeler et al., 2006; Yamamoto, 1981). For the A_{MJ} and A_{MM} submatrices, we obtained adult fecundity (f_x) and survival rates (s_x) from published quantifications for this species both in field and laboratory conditions (Brooks et al., 2017b; Friberg et al., 2015; Kerr et al., 2020; Larsdotter-Mellström et al., 2010; Ohsaki, 1980; Pick et al., 2019; Välimäki et al., 2006; Wiklund et al., 1993). We checked that the resulting matrices were primitive, irreducible, and ergodic. This means that no portion of the life cycle is isolated; any individual can go from any class to every other class; and that projections of the matrix will always exhibit the same asymptotic outcome regardless of the initial conditions (Otto and Day, 2011; Stott et al., 2010). A visual representation of the parameters finally compounding the transition matrices can be found in Fig. C4.

Extreme event impact

We simulated extreme heat events on a daily basis and a microclimatic scale. We defined extremely hot days as days where maximum microclimatic temperature (T_{max}) exceeded 35°C , and categorised them as LLHI hot days if $T_{max} > 40^\circ\text{C}$ (i.e. a less frequent but higher-impact extreme event) (Fig. 5.2b red circle). To simulate the direct impacts of heat days on the species, we multiplied the juvenile survival and eclosion by a thermal mortality variable (k) that depended on T_{max} . Thermal mortality values were quantified both in the non-declining and declining model populations combining the experimental thermal death time curves of the larvae (TDT curves) and field microclimatic records (Carnicer et al., 2019; Rezende et al., 2014, 2020b; Vives-Inglá et al., 2023). To estimate drought effects on insect vital rates, we conducted a complementary growth chamber experiment under the same summer microclimatic and light conditions, but limited host-plant availability (see Section 5.2.3 *Transition probabilities*). With these experimental estimates, we modelled the reduction in the juvenile survival rates and eclosion time due to the impacts of summer drought on host-plant availability (Fig. 5.2b, ochre circles). A detailed description of the parametrisation of the extreme climatic events is provided in Appendix C.2.2.

5.2.4 Population projections

We projected the dynamics of the populations between consecutive generations in different seasonal regimes of extreme climatic events with the *project* function from the *popdemo* R package, version 1.3-1 (Stott et al., 2012). We simulated the different transition periods between generations that a representative lowland, declining population and a

mid-elevation, non-declining population typically show across the year. The projections started with an initial vector of 1 recently-emerged reproductive adult (i.e. n_0 with 1 adult of age 1, and 0 individuals of the other stages) and lasted 70 days to give enough time to the simulated population to complete the whole life cycle, when the adults from the subsequent generation emerged (i.e. around 20–50 days, depending on microclimatic exposure (Carnicer et al., 2019; Vives-Inгла et al., 2023; von Schmalensee et al., 2021a)).

The first transition between generations thus simulated the period from reproductive adults that emerge in early spring after winter dormancy to the developing larvae and the subsequently emerging adults in May–June ($R_{0,1}$ in Fig. 5.2a). We conducted these simulations with the A_{spring} matrix, estimated from growth chamber experiments reproducing spring thermal conditions (20 °C treatment). For the subsequent transitions, we used the summer A matrices (estimated from the 25 °C experimental treatment), which included the A_{summer} , to simulate mild, standard summers (experimentally estimated with enough fresh host plants), and $A_{drought}$, to simulate the impact of extremely dry summers (estimated with host-plant scarcity experiments). In line with field observations, $R_{0,2}$ in the non-declining population was always simulated with the A_{summer} matrix (mild summers), while the simulations of $R_{0,2}$ in the declining population included both mild and dry summers. The use of these two matrices in the summer simulations of the declining population depended on the probability of occurrence of a dry summer ($P_{drought}$) extracted from the estimates of the IPCC-WGI for the Iberian Peninsula (frequency of 1-in-10-year soil moisture drought for the June to August period; IPCC, 2021; Seneviratne et al., 2021). The final transition period in the declining population ($R_{0,3}$) was always simulated with the dry-summer matrix ($A_{drought}$). In this summer period, observational studies indicate that host plants are usually very scarce and affected by drought (Carnicer et al., 2019; Vives-Inгла et al., 2020). See Appendix C.3 for a detailed description of the procedures.

To simulate the impacts of heat events, we built a sequence of daily hot events for each simulation (Fig. 5.2b). Based on estimated probabilities for extreme heat events (P_{35} and P_{40}), the simulations alternatively selected between a day with usual maximum temperatures (i.e. $T_{max} < 35$ °C), an extremely hot event ($T_{max} > 35$ °C), or an LLHI hot event ($T_{max} > 40$ °C). For the present-day period simulations (reproducing the 1993–2018 rates), the probabilities of occurrence of heat events (P_{35} and P_{40}) were calculated from the field microclimatic records taken in sheltered microhabitats selected by *P. napi* females to oviposit (Table C1 and Appendix C.2; Vives-Inгла et al., 2023; von Schmalensee et al., 2023). For the simulations in future global warming levels (GWL), the probabilities of extreme heat events (P_{35} and P_{40}) were increased based on the predictions of the last IPCC report for the Iberian Peninsula (see Appendix C.3.1). To integrate the impacts of the sequence of daily heat events in the simulations, we calculated the thermal mortality value (k) for each daily event and applied it to the juvenile rates of the transition matrices (see Section 5.2.3 *Extreme event impacts*). Compound hot-dry events were simulated as dry summer periods with extremely hot days ($T_{max} > 35$ °C, Fig. 5.2b).

We performed 10,000 projections per each transition period between generations to account for the environmental stochasticity in the occurrence of extreme events. In each

replicate, we built a transition matrix sampling directly from the physiological data (non-parametric bootstrap) to also account for the variation and uncertainty in the estimated vital rates. We guaranteed that all the bootstrapped matrices maintained their primitivity, irreducibility, and ergodicity (Otto and Day, 2011; Stott et al., 2010). We repeated this procedure for the simulations in present-day climatic conditions (1993–2018 period, GWL-0.85) and three future scenarios of global warming (GWL-1.5, GWL-2, and GWL-4). The GWL-0.85 scenario corresponded to an increase in global surface temperatures of 0.85 °C relative to 1850–1900 recorded during 1995–2014, covering the period of the field demographic series of the species (Chen et al., 2021; IPCC, 2021). For the future scenarios, two of them were in line with the Paris Agreement goals (GWL = +1.5 °C and +2 °C), and the other consisted in a high-emissions scenario with ineffective climate policies (GWL = +4 °C) where LLHI events increased disproportionately (Fig. C5; Chen et al., 2021; IPCC, 2021). The different scenarios were defined by different regimes of extreme hot days and dry summers (i.e. different P_{35} , P_{40} , and $P_{drought}$) based on the projections compiled by the IPCC (Table C1 and Fig. C5; Gutiérrez et al., 2021; IPCC, 2021; Iturbide et al., 2021; Seneviratne et al., 2021). See Appendix C.3 for further details on population projections.

Elasticity analysis

We first conducted an elasticity analysis of all the bootstrapped matrices to identify the demographic transitions and associated life stages that contributed the most to the population performance. An elasticity analysis of a transition matrix involves calculating, for each parameter of the matrix, the relative change in fitness produced by an infinitesimal, relative change in that parameter (Caswell, 2001; Metcalf and Pavard, 2007). This analysis enables the quantification of the relative contribution of each matrix component to population growth. We calculated the elasticity of the asymptotic finite rate of population increase (λ_{day}) to all the parameters of each daily matrix (i.e. 70 daily matrices \times 10,000 simulations \times 5 transition periods \times 4 GWL, Fig. 5.2b3). We then summed the elasticities for each submatrix, which represent four main vital processes: juvenile stasis (A_{JJ}), juvenile transition (A_{JM}), adult survival (A_{MM}), and adult fecundity (A_{MJ}).

Net reproductive rates (R_0)

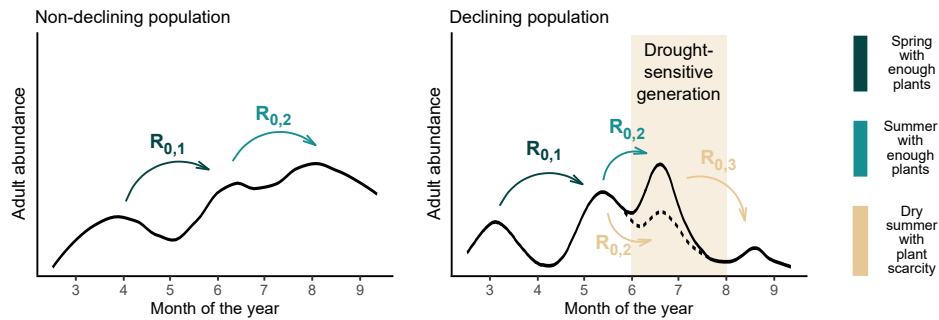
To estimate the population performance in the different seasonal and climatic scenarios, we calculated the transient net reproductive rate (R_0) in each of the 10,000 bootstrap replicates conducted per scenario. Net reproductive rates represent the mean lifetime production of offspring per female of the population, and give a rate of demographic increase per generation and an indicator of population persistence ($R_0 > 1$ for growing populations, and $R_0 < 1$ for declining ones) (Caswell, 2009). Based on its classical definition (Caswell, 2009; Lotka, 1934; Rhodes, 1940), we approximated the transient R_0 as the sum of all adult individuals of age 1 produced in the simulated population until the

end of the first generation (the shaded areas of the population curves in Fig. 5.2b3). This calculation corresponds to the expected lifetime offspring production of the adult of age 1 compounding the population at the beginning of the simulation.

We used the predicted R_0 for three different objectives. Firstly, we compared the predicted R_0 in current levels of global warming (GWL-0.85) with the observed R_0 . This was done in order to validate our MPM and give mechanistic support to the hypothesis that summer drought is currently driving population declines. The model populations are part of the Catalan Butterfly Monitoring Scheme, which provide standardised, weekly counts of the adult butterfly of the species detected along a fixed transect from March to September. From this data, we calculated the observed R_0 in each year by summing all the weekly counts during one flying peak of adults and dividing it by the sum of counts of the preceding flying peak (see Appendix C.3.2). We also calculated interannual growth rates (λ_{annual}) of the populations by summing all the individuals counted during one year and dividing it by the counts of the preceding year.

Secondly, we used the predicted R_0 of the future scenarios to forecast the performance of the population in different global warming levels and the associated regimes of extreme climatic events. Finally, the predicted R_0 were also used to quantify and compare the impacts of extremely (non-LLHI) hot days, LLHI hot days, droughts, and their combined effects. The effects of each type of extreme event on *P. napi* was quantified by extracting the median $\ln R_0$ of the simulations where, stochastically, no event occurred, from the median $\ln R_0$ of the simulations where only that particular type of event occurred.

(a) Observations



(b) Predictions

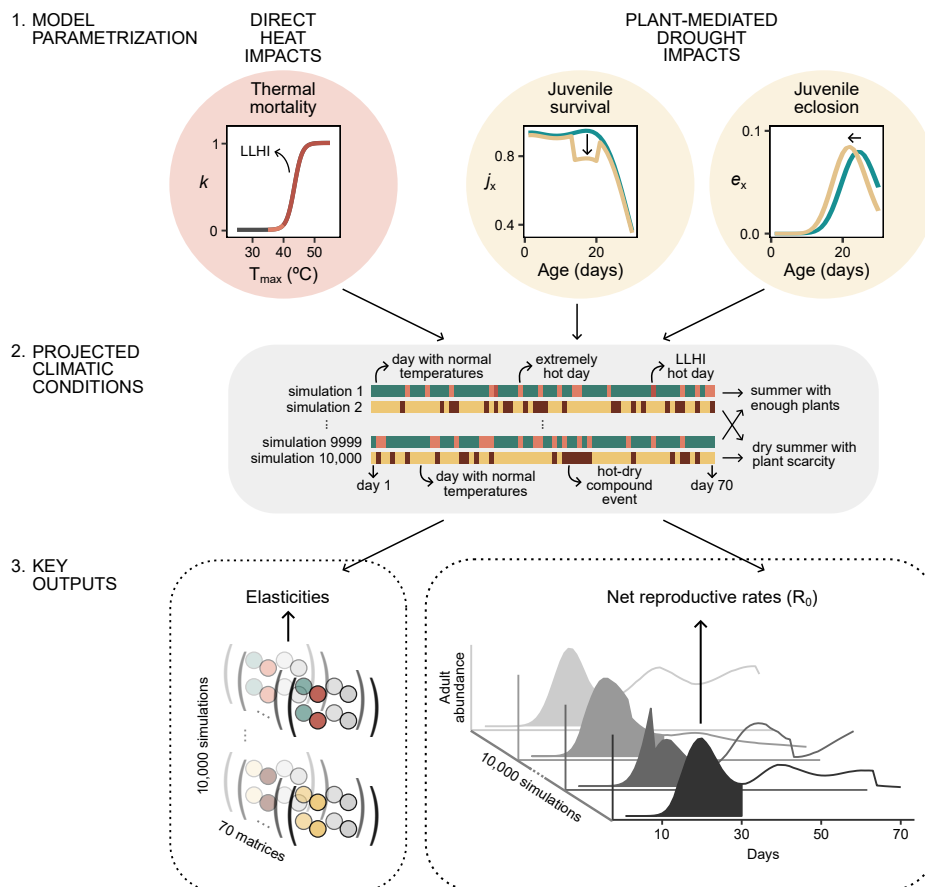


Figure 5.2: Visual summary of the methods. (a) The observed adult flight curves of a typical non-declining population (left) and a declining population (right) of the model species. The populations display several consecutive generations (peaks of the curve) per year. Non-declining populations usually show a continuous increase in the total number of individuals across the three consecutive generations, and are typically located at mid-elevation sites. In contrast, declining populations are typically located in lowland areas and display four or five generations across the annual cycle. (Legend continues on next page).

(Continuation of legend from Fig. 5.2). In lowland areas, the abundance of the third generation flying between June–July importantly decreases during dry summers, which induce an earlier die-off of the host plants (dotted curve in the ochre rectangle). The arrows between consecutive generations represent the net reproductive rates (R_0) calculated from observed adult abundances or simulated with the MPM model. (b) 1. Model parametrisation. The impacts of hot days (red circle) and dry summers (ochre circles) on the populations were introduced by modifying the juvenile parameters of the MPM. Using thermal death time curves (TDT curves) for the species and microclimatic records from the field, we calculated the nonlinear response of thermal mortality (k) to maximum daily microclimatic temperature (T_{max}). Note the substantial increase in k when $T_{max} > 40$ °C (i.e. a LLHI hot day, represented in dark red). We estimated the impacts of drought-induced plant scarcity on juvenile survival (j_x , central circle) and the probability of adult eclosion (e_x , right circle) rearing the offspring of female butterflies captured from the field in growth chamber experiments with either fresh or drought-stressed host plants (green and ochre curves, respectively). See Appendix C.2 for further details. 2. Projected climatic conditions. We simulated the dynamics of the population between consecutive generations in different climatic scenarios (a global warming level of 0.85, 1.5, 2, and 4 °C). The three types of extreme-event impacts on the vital rates (circles in b1) were stochastically integrated in the simulations depending on their probability of occurrence. Each simulation lasted a maximum of 70 days and included an entire reproductive cycle for one generation. The probability of extreme summer drought occurrence, based on IPCC predictions for the Mediterranean area in the different warming levels, determined mild (green bars) or dry (ochre bars) summer conditions in each climatic scenario. Heat impacts were simulated on a daily scale and included extremely hot days ($T_{max} > 35$ °C, light-red stripes) and LLHI hot days ($T_{max} > 40$ °C, dark-red stripes). Heat events during the simulations conducted with dry conditions were considered compound hot-dry events (brown stripes). We conducted 10,000 simulations per transition period. See Appendix C.3 for further details. 3. Key outputs. Each simulation produced 70 daily matrices including the basal transition matrix built directly from experimental data when no extreme event occurred (non-parametric bootstrap) and the matrices integrating the impacts of extreme events on juvenile stages (matrices with ochre and red circles). We conducted an elasticity analysis on each of these matrices to identify the life stages that more importantly determine population dynamics. With the MPMs, we also predicted the R_0 in each simulation by summing all the newly-eclosed adults produced during the first replicated generation (shaded area of the flying curve). We used R_0 to infer increasing ($R_0 > 1$) or declining ($R_0 < 1$) population responses in the different global warming scenarios. See Appendix C.3 for further details.

5.3 Results

5.3.1 Observed population growth rates

Interannual growth rates calculated from field records of the monitored populations showed, for the period 1993–2018, both increasing ($\lambda_{annual} > 1$) and decreasing ($\lambda_{annual} < 1$) values. Population dynamics between years was highly variable, with some years doubling individual abundance or reducing it by a half ($\sim 20\%$ of the years, Fig. 5.3).

During the studied period, the lowland population declined in abundance, losing an average of 3% of its individuals annually (geometric mean of $\lambda_{annual} = 0.97$). Yet, during spring, the population generally grew and the second annual generation of the population, which flies during May–June, used to be more abundant than the preceding one

($R_{0,1} > 1$ in Fig. 5.3). In contrast, during late summer, the population was strongly reduced almost every year (geometric mean of $R_{0,3} = 0.25$). The preceding net reproductive rate ($R_{0,2}$) in early summer, which corresponds to the production of a drought-sensitive generation, included values both higher and lower than 1, and showed a decreasing trend ($P = 0.014$ and $R^2 = 0.2$ in a linear model of the logarithm of $R_{0,2}$ against year). Thus, years where this drought-sensitive generation declined in abundance relative to the preceding generation, instead of growing, became more common in the later period.

The mid-elevation population increased in abundance (average annual increase of 6%). In this population, each generation used to be more abundant than the preceding one, especially the third generation (geometric mean of its $R_{0,2} = 2.62$).

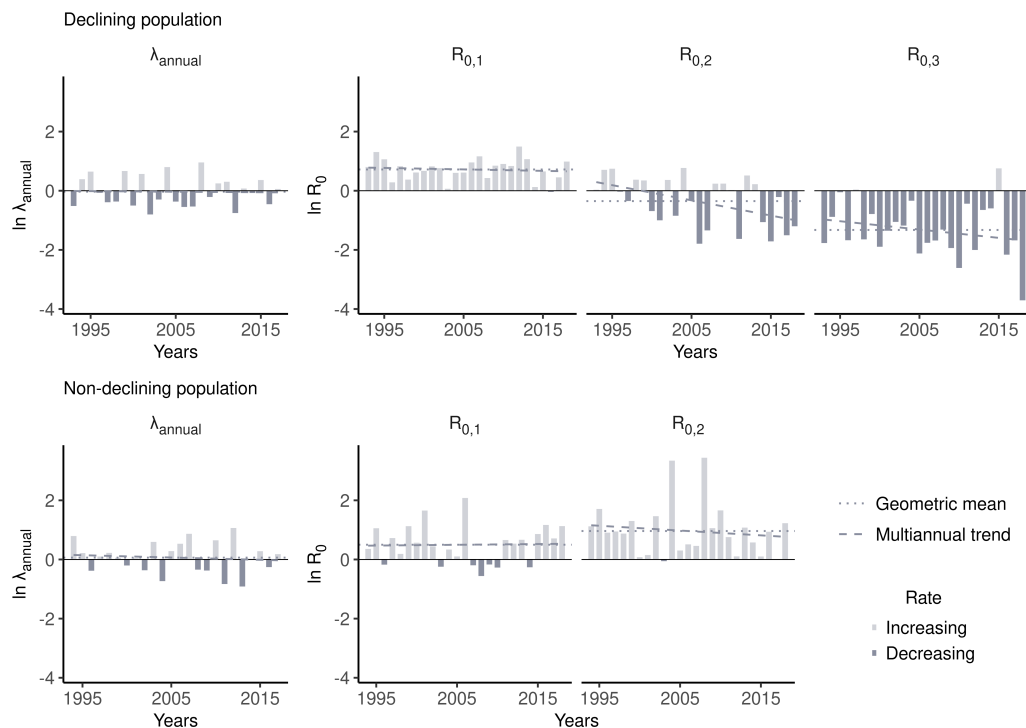


Figure 5.3: Interannual growth rates (λ_{annual}) and net reproductive rates (R_0) of one declining and one non-declining model population of *Pieris napi* at a logarithmic scale calculated from field data during 1993–2018. The logarithm of the geometric mean (dotted line) and a linear multiannual trend (dashed line) are also shown. Note that values > 0 or < 0 represent an increasing or a decreasing growth rate, respectively.

5.3.2 Elasticity analyses and key life stages

In line with field observations, the spring transition matrix (A_{spring}) we built from experimental and bibliographic data had an increasing asymptotic finite rate of population growth ($\lambda_{\text{day}} = 1.02$). For summer matrices, λ_{day} had also an increasing value in the matrix with enough fresh host plants (A_{summer} , $\lambda_{\text{day}} = 1.02$), but a decreasing one in the matrix for dry summers (A_{drought} , $\lambda_{\text{day}} = 0.99$). We found that juvenile stasis (i.e. the

transition probability that a juvenile survives and remains in this stage) was the vital process that most contributed to the fitness (λ_{day}) of the population for the three types of matrices (Fig. 5.4). With a much lower contribution, adult survival was the second matrix component that most contributed to the population growth.

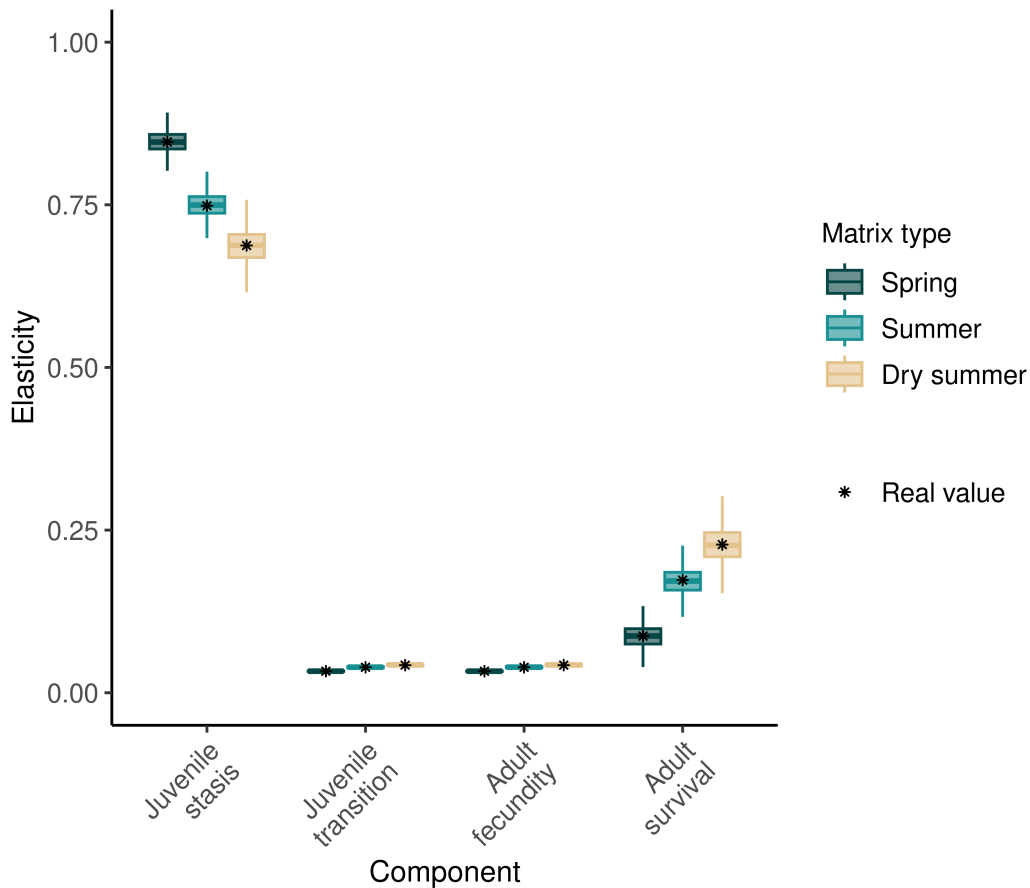


Figure 5.4: Relative contribution of each matrix component to the finite rate of population increase (λ_{day}). We calculated the elasticities for all the parameters of all the bootstrapped matrices and summed them by their main component (i.e. the four submatrices constituting the transition matrices). Boxplots are built from the median elasticities of the 70 daily matrices that each simulation contained, while the asterisks indicate the elasticities for the matrices built from the original, non-bootstrapped data. The lower and upper hinges of the box represent the 1st and the 3rd quartiles respectively (Q_1 , Q_3); its inner line, the median; and the length of the box, the $IQR = Q_3 - Q_1$. Lower whisker represents the smallest value $\geq Q_1 - 1.5 \times IQR$; and the upper whisker, the biggest value $\leq Q_3 + 1.5 \times IQR$. Outliers are not shown.

5.3.3 MPM validation and population forecasting

Observed and predicted distributions of R_0 during the study period (i.e. GWL-0.85) substantially overlapped, which validated the use of this MPM to predict the performance of *P. napi* in different climatic scenarios (Figs. 5.5 and C6). In the GWL-0.85 scenario, the values corresponding to a decreasing R_0 ($R_0 < 1$) were mainly replicated in the simulations with drought-induced plant scarcity (during the summer period of the declining population). In contrast, the simulations that only included the effects of thermal

mortality associated with microclimatic heat events generally led to increasing R_0 (green shades in Fig. 5.5).

With a global warming level in line with the Paris Agreement (GWL-1.5 and GWL-2), the MPM models predicted that R_0 would be slightly reduced (a 5–15% reduction in the median R_0 relative to the GWL-0.85 scenario). We found more important reductions and increased variability of R_0 in the high-emissions scenarios (GWL-4). These results are associated with the increasing frequency of heat events, as pronounced reductions in R_0 were observed in the seasonal scenarios where we did not augment the probability of drought (e.g. a 50% reduction in the median $R_{0,3}$). Notably, the projected reductions in R_0 strongly affected the currently non-declining population (Fig. 5.5). In the GWL-4 scenario, the median $R_{0,1}$ of this population went from 1.42 (a population increase of 42%) to 0.68 (a population decrease of 32%).

5.3.4 Impacts of extreme LLHI and compound events

In Fig. 5.6a we summarised the effects of each type of extreme event on the drought-sensitive generation of the declining population of *P. napi* ($R_{0,2}$, see Fig. C7 for the effects in other seasons). The impacts of extreme heat events increased with global warming level, due to the rising frequency of extremely hot days (red bars in Fig. 5.6a). The decreases in $R_{0,2}$ were higher in the simulations where these extremely hot days included at least one LLHI hot event ($T_{max} > 40^\circ\text{C}$, dark-red bars). Furthermore, the $\ln R_{0,2}$ diminished with the number of LLHI hot days (Fig. 5.6b) but remained stable when plotted against the number of non-LLHI hot days (i.e. $35 < T_{max} < 40^\circ\text{C}$, Fig. C7). These results indicate a key role of the non-proportional increase of LLHI events in driving the projected strong declines of the species under novel regimes of extreme events.

Dry summers without extremely hot events (ochre bars) had more negative impacts on $R_{0,2}$ in all climatic scenarios than summers with extremely hot days but enough plant availability (Fig. 5.6a). While several non-LLHI hot days are usually produced during summer simulations, more than 90% of the simulations in GWL in line with the Paris Agreement produced no or just one LLHI hot day per month (Fig. 5.6c). In these conditions, the effects of drought-induced plant scarcity were higher than thermal mortality associated with extreme heat exposure. Yet, in the high-emission scenario (GWL-4), 1 in 6 summers produced 2 or more LLHI hot days per month (Fig. 5.6c), leading to a decreasing $R_{0,2}$ ($\ln R_{0,2} < 0$), and equaling or surpassing the effects of drought-induced plant scarcity (arrows at 2 and 3 LLHI hot days month⁻¹, respectively, *vs.* the arrow at 0 in Fig. 5.6b).

Overall, the MPM predicted the most negative impacts when both heat and drought events co-occurred (larger brown bars in Fig. 5.6a). The sum of the separate effects of extremely hot and drought events (dashed bar in Fig. 5.6a) led, however, to more negative impacts than those directly predicted from the simulations with compound hot-dry events (i.e. an extra decrease of 25–30% in R_0 , brown bars). These results indicate a compensatory interaction between the two types of extreme events, which is also denoted by

5. NOVEL EXTREMES TRIGGER INSECT DECLINING RATES

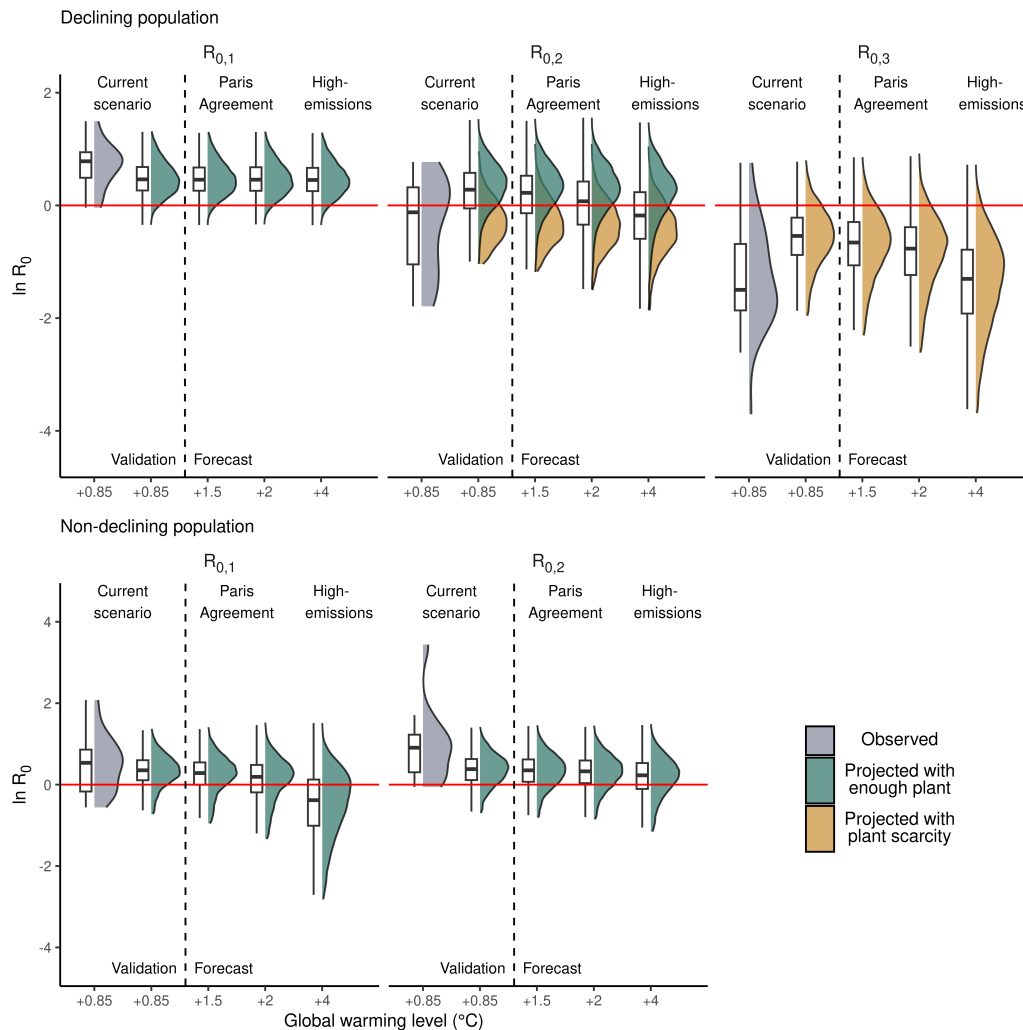


Figure 5.5: Distribution of the logarithm of the net reproductive rates (R_0) observed in a declining and a non-declining model population during 1993–2018 (grey shades), and the predicted R_0 in different seasonal and climatic scenarios (coloured shades). The predicted values of R_0 were predicted from the 10,000 bootstrap replicates performed for each climatic scenario defined by different frequencies of hot days and dry summers. The distributions placed at the left of the dashed line represent the observed and predicted R_0 at current climatic conditions ($\text{GWL} = +0.85^\circ\text{C}$), and their comparison enables MPM validation. The distributions at right of the dashed line represent predicted R_0 at future global warming levels meeting the Paris Agreement ($\text{GWL} = +1.5$ and $+2^\circ\text{C}$) or not ($\text{GWL} = +4^\circ\text{C}$). Ochre simulations indicate dry summer and plant scarcity conditions, and are differentiated from simulations of mild summers with enough plant availability (green). Boxplots summarise the distribution of the complete set of 10,000 simulations for each climatic and seasonal scenario. The lower and upper hinges of the box represent the 1st and the 3rd quartiles respectively (Q_1 , Q_3); its inner line, the median; and the length of the box, the $IQR = Q_3 - Q_1$. Lower whisker represents the smallest value $\geq Q_1 - 1.5 \times IQR$; and the upper whisker, the biggest value $\leq Q_3 + 1.5 \times IQR$. Outliers are not shown.

the tendency to converge, as the number of LLHI hot days per month increased, of the simulations with enough plant availability and those with plant scarcity (Fig. 5.6b).

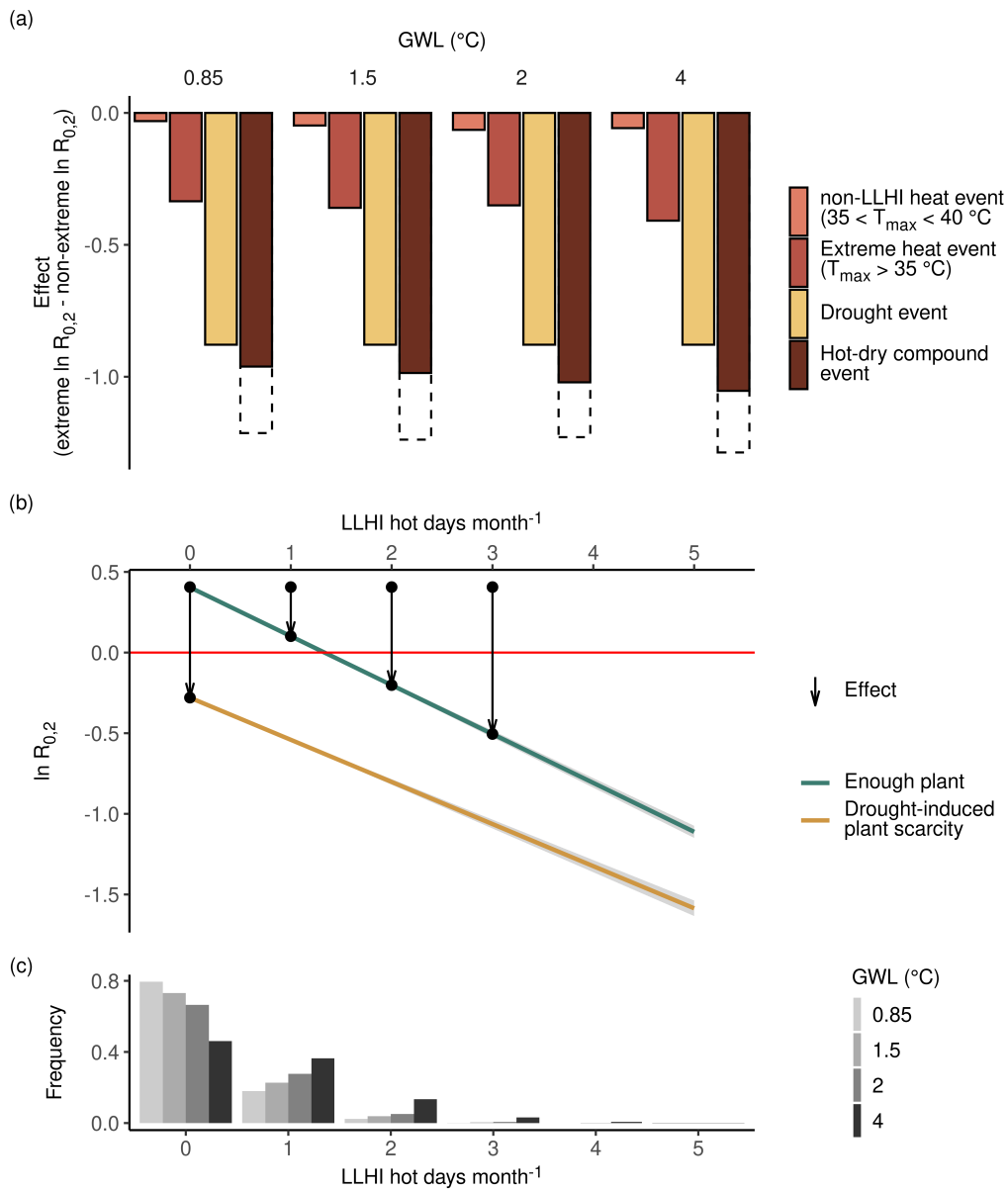


Figure 5.6: The effects of different extreme events on R_0 . (a) Effects of each type of extreme climatic event quantified by subtracting the medians of the logarithmic net reproductive rates of the simulations where no extreme event occurred from the simulations where the extreme event occurred. Non-LLHI heat events: simulations where only extreme, non-LLHI heat events occurred ($35 < \text{daily } T_{max} < 40$ °C). Extreme heat events: simulations where only heat events occurred (both LLHI and non-LLHI). Drought events: simulations with drought but no heat events (daily $T_{max} < 35$ °C). Hot-dry compound events: simulations with co-occurring drought and heat extreme conditions (both non-LLHI and LLHI). The dashed column represents the sum of the effects of the extreme heat and drought events when they occurred separately. Dashed columns ending before the coloured column indicate that the interactive effects are synergistic, while coloured columns ending before the dashed column ones are indicative of compensatory interactions of the two effects. (b) Linear fits of the logarithmic net reproductive rates with the number of LLHI events occurring during the first 30 days of the simulations, in enough plant (green line) or drought-induced plant scarcity conditions (ochre line). (Legend continues on next page).

(Continuation of legend from Fig. 5.6). The ochre line at LLHI events month⁻¹ > 0 thus represents the predicted $\ln R_0$ when hot-dry compound events occur. Arrows represent the effects that the different extreme events have on $\ln R_0$. The left arrow indicates the effects of a dry summer with no LLHI heat event; and the next arrows, a summer with at least one LLHI heat event but no drought. (c) Frequency of stochastic simulations with 0 to 5 LLHI hot days during the first 30 days in each climatic scenario. All the analyses only include the simulations of the key generation of the declining population.

5.4 Discussion

5.4.1 The impacts of LLHI single and compound events on insect populations

Climate change and the associated increase in extreme climatic events are important drivers of insect declines worldwide, yet the underlying mechanisms remain poorly understood (Dicks et al., 2021; Halsch et al., 2021; Wagner, 2020; Wagner et al., 2021b). This is especially true for those extreme events placed further at the tails of climatic distributions (*low-likelihood*, *high-impact* or *black-swan* events), whose rare occurrence complicates the statistical study of their effects from historical records. Previous studies have associated extreme climatic events with strong changes in insect population growth rates, but without specifically considering LLHI single and compound events (Harvey et al., 2020; Johansson et al., 2020; Oliver et al., 2015; Palmer et al., 2017; Ubach et al., 2022; van Bergen et al., 2020). Despite being extreme events of much lower frequency, LLHI events are expected to have more detrimental impacts on natural systems than more recurrent but less harmful extreme events (Seneviratne et al., 2021; Sutton, 2018; Zscheischler et al., 2018). Our study clearly supported this expectation and predicted, for the first time, the impacts that single and compound LLHI events would have on an insect model species.

We found that the occurrence of LLHI hot and dry events was determinant to predict declining net reproductive rates of *P. napi* populations ($R_0 < 1$; Figs. 5.6 and C7). Despite not being tested in our study, the key role of LLHI events found is likely extensive to other insects and animals. For example, Anderson et al. (2017) showed that around 5% of the insect, mammal, and bird analysed populations displayed statistically improbable and strong abundance crashes, often related with successive extreme climatic events (i.e. compound events). Generalised LLHI impacts on insects would be of particular concern because many ecosystem functions —such as pollination, macrodecomposition, and trophic linking between primary producers and consumers— depend on insects (Weisser and Siemann, 2007). In addition, the latest IPCC projections predict that, as climate changes, LLHI events will increase further than less severe extreme events (IPCC, 2021; Lemus-Canovas and Lopez-Bustins, 2021; Seneviratne et al., 2021; Simolo and Corti, 2022; Vogel et al., 2020), potentially emerging as an overlooked threat for insect populations (Jørgensen et al., 2022b; Malinowska et al., 2014; Soroye et al., 2020; Warren et al., 2021; Zscheischler et al., 2018). Overall, our findings give an ecological perspective on the consequences of increasing LLHI single and compound events in novel climates,

complementing recent climate research that highlights their expected crucial role in the future (Bastos et al., 2023; Bevacqua et al., 2021; Seneviratne et al., 2021; Zscheischler et al., 2018).

Negative, indirect effects of drought on population dynamics through reducing host-plant availability have been described for other butterfly species (Ehrlich et al., 1980; Johansson et al., 2020; McLaughlin et al., 2002; Singer and Parmesan, 2010; van Bergen et al., 2020). In fact, extreme droughts are behind many crashes in insect abundance (Carnicer et al., 2011; Oliver et al., 2015; Palmer et al., 2017; Shure et al., 1998) and are one of the most important driving forces of butterfly dynamics in the Mediterranean climates (Crossley et al., 2021; Donoso et al., 2016; Forister et al., 2018; Herrando et al., 2019; Stefanescu et al., 2011a; Ubach et al., 2022; Uhl et al., 2022). In the model system we used to parametrise the MPM, previous studies empirically linked the negative trends of the declining populations of *P. napi* to drought-induced plant scarcity in summer (Carnicer et al., 2019; Vives-Inгла et al., 2020). Our simulations gave full support to this drought-driven process, as predicted values for R_0 in the present-day climatic conditions (GWL-0.85) were more similar to observed when drought-induced plant scarcity was included (Fig. 5.5).

In relation to the microclimatic heat impacts, our results showed that the physiological effects of extremely hot days not exceeding the 40 °C threshold were not lethal enough to produce a conspicuous response at the population level (Fig. 5.6a and Fig. C7). This contrasted with LLHI hot days ($T_{max} > 40$ °C), which rapidly led to declining R_0 as the number of events per month increased, especially when coinciding with a dry summer (compound hot-dry events, Fig. 5.6). These results indicate that LLHI hot events have a disproportionate impact on population performance despite their lower frequency. The disproportionate impacts of LLHI hot days relative to non-LLHI hot days are associated with the nonlinear responses of larval mortality to microclimatic thermal exposure (Fig. 5.2b; Carnicer et al., 2019; Jørgensen et al., 2022b; Rezende et al., 2014, 2020b; Vives-Inгла et al., 2023). Nonlinear and threshold-like physiological responses are usual triggers of the sometimes-unexpected impacts of extreme climatic events on insects and other biological systems (Buckley et al., 2023a; Jørgensen et al., 2022b; Koons et al., 2009; Ma et al., 2021; Ørsted et al., 2022; van de Pol et al., 2017). For example, in the case of the unprecedented episodes of forest mortality recorded during recent extremely hot-dry events (Adams et al., 2017; Allen et al., 2010; Anderegg et al., 2016), the biphasic curve of the leaf cuticular conductance of plants in response to temperature has been identified as a likely underlying mechanism of the tree hydraulic failure (Cochard, 2021). These processes underpin the ecological relevance that LLHI single and compound events will have as they become more frequent in novel climates, potentially emerging as a new driving mechanism of insect declines.

In our study system, LLHI heat events are still infrequent in current conditions (Fig. 5.6c and Table C1), and long-term declining trends are only found in those populations more affected by drought and hot-dry events in the lowlands (Figs. 5.3 and 5.5). However, in future scenarios of global warming, especially in those that do not meet the Paris Agreement (GWL-4), our simulations indicate that the disproportionate increase in LLHI hot

days will also negatively affect currently buffered populations (Fig. 5.5). Thus, if greenhouse gas emissions are not reduced fast enough to meet the Paris Agreement, our results predict a shift from the current situation characterised by a geographic mosaic of increasing, stable, and declining population trends (Fig. C1), to a scenario with a higher and pervasive risk of regional butterfly declines and extinction. This situation of widespread shrinkages of butterfly populations could likely lead to a worse scenario if it prompted an associated reduction of the potential rescue effects between connected populations (Brown and Kodric-Brown, 1977; Hanski, 1999), a process that has not been modelled in our study.

Moreover, our results have relevant implications in other areas of the globe beyond the Mediterranean region. For example, the increase in LLHI hot days is expected to be especially disproportionate relative to background conditions in the tropics (Seneviratne et al., 2021; Simolo and Corti, 2022; Vogel et al., 2020). This is a disturbing prediction because tropical areas are estimated to host 85% of global insect diversity (Stork, 2018), while, at the same time, insect trends in this region are far less described (Finn et al., 2023). Climate change impacts have already been quantified for some tropical insects (e.g. Janzen and Hallwachs, 2019; Salcido et al., 2020), which generally present a narrow thermal safety margin (Deutsch et al., 2008; Hoffmann et al., 2013; Rezende and Bozinovic, 2019; Sunday et al., 2014) and a high degree of specialisation (Forister et al., 2015). Therefore, LLHI hot events in the tropics might have as severe impacts on insect populations, if not more, than those predicted in the present study.

5.4.2 Process-based approaches to study extreme events impacts on insects

Our study quantified the impacts of extreme events on a model insect species by explicitly representing the demographic processes in a MPM ultimately determining its population dynamics. As previous studies have shown, MPMs provide a sound mathematical framework to predict population responses to extreme climatic events (Capdevila et al., 2016; Davis, 2022; Flockhart et al., 2015; Herrando-Pérez, 2013; Jenouvrier et al., 2009, 2015; Morris et al., 2008; Pardo et al., 2017). In comparison to correlative approaches where the underlying mechanisms connecting drivers to the responses are usually obscure, with MPMs we were able to distinguish the effects of extreme events of different nature and intensity. In particular, our simulations quantified distinct specific processes triggered by different climatic drivers affecting insects both directly (heat effects on larval mortality) and indirectly (effects of drought-induced plant mortality on juvenile survival and eclosion). Disentangling the effects of this complex net of processes can be rarely done with descriptive, correlative methods (Connolly et al., 2017; Ellner and Guckenheimer, 2006; Grainger et al., 2022). For this reason, process-based models calibrated with experimental and field data are critical to improve our understanding and predictive capacity of climate change impacts on insects (Buckley et al., 2023a; Ma et al., 2021; Maino et al., 2016; Urban et al., 2016; van de Pol et al., 2017; Yang et al., 2021), although they may come with some other limitations, such as their high-quality data requirements.

With our MPM we were also able to quantify the combined effects of compound hot-dry events (Fig. 5.6). Notably, the decline in the median R_0 was about 20–35% inferior in the simulations including compound events than the sum of the two types of events occurring separately (Fig. 5.6a). These results indicated a positive, compensatory interaction (i.e. antagonism) between heat and drought events, likely stemming from an earlier mean date of pupal eclosion in the drought-induced plant scarcity simulations that reduces the time of exposure of the juveniles to high thermal mortality rates (Fig. 5.2b1 and Appendix C.2.2). Although compensatory interactions between multiple drivers of ecological change are far less reported than synergies, they are also common (Darling and Côté, 2008; Jactel et al., 2019). The positive interaction found in our study emerges from the impacts we integrated in the MPM (heat and drought effects on juvenile survival and eclosion). Therefore, while this interaction is capturing one plausible process, other effects and pathways of interaction between the two stressors that were not modelled in our study could also occur in the field. For example, the microclimatic heat exposure of the larvae on their host plants can increase due to thermal amplification feedbacks when soil and plant evapotranspiration is reduced by summer drought (Carnicer et al., 2019, 2021; Cochard, 2021; Pincebourde and Woods, 2012; Vives-Inгла et al., 2023; Wood et al., 2023). Similarly, during dry summers, limited access to fresh host plants could also increase the thermal sensitivity of the larvae, making them more vulnerable to heat challenges (Huey and Kingsolver, 2019). These positive feedbacks were not explicitly modelled, as heat and drought impacts were included separately in our simulations, and could have changed the overall sign of the interaction between the two stressors (e.g. from antagonism to synergy).

Another relevant outcome of MPMs is the identification of the vital rates and associated life stages that contribute relatively more to population growth rates. In correlative approaches, the identification of key life stages is inferred by considering climate drivers at a subannual scale and detecting the period with the highest statistical signal (McDermott Long et al., 2017; Ubach et al., 2022). Again, this inference is especially unclear when different life stages overlap temporally and multiple climatic drivers in a single model are considered. We found the highest elasticity values for the components of the juvenile stasis submatrix (i.e. the probability of juveniles surviving and remaining in the same stage, Fig. 5.4). Thus, juveniles, the life stage that is receiving the impacts of extreme events in our models, importantly contribute to population dynamics. The use of MPMs on insects is still scarce. Yet, comparative studies including insect MPMs found that short-lived organisms presented higher elasticities of population growth rates to survival than to reproductive rates, in line with our results (Morris et al., 2008). A key role of early life stages on insect performance have also been found in similar MPMs built for closely-related species (Kerr et al., 2020) and in other experimental studies on butterflies (Carnicer et al., 2019; Klockmann and Fischer, 2017; Vives-Inгла et al., 2023).

The high elasticities found for the juveniles in our MPM reinforce the idea that low-detectability and understudied life stages should not be ignored, and that climate change responses of insects should be assessed across their whole life cycle (Brunner et al., 2023; Kingsolver et al., 2011; Logofet and Salguero-Gómez, 2021; MacLean et al., 2016; Nguyen

et al., 2019). In this line, our model could be further improved by integrating the additional impacts that extreme drought and microclimatic heat exposure have on adult, pupal, and egg survival, or the carry-over effects of larval heat stress on adult parameters (Degut et al., 2022; Donoso et al., 2016; Flo et al., 2018; Harvey et al., 2020, 2023; Karlsson and Wiklund, 2005; Klockmann et al., 2017b; Ma et al., 2021; MacLean et al., 2016; Murphy et al., 1983). Adding these additional impacts could produce even more severe declines than those predicted in this study, but a preliminary analysis suggests that juveniles would still be the stage with higher elasticities in our MPM (Fig. C8).

The variation in the population growth rates ultimately depend on both the absolute change in the underlying vital rate and its relative contribution to the population growth rate (i.e. the elasticity). Therefore, having a low relative contribution to population growth rates does not necessarily imply being a less important regulating factor of the population, if the vital rate shows high interannual fluctuations (Logofet and Salguero-Gómez, 2021; Romanov and Masterov, 2020). For instance, early demographic life-table studies on Pierid butterflies associated population fluctuations to changes in the realised fecundity of the females more frequently than to larval mortality (Courtney, 1986; Dempster, 1967, 1983; Hayes, 1981; Kingsolver, 1989; Warren et al., 1986). Specifically, they attributed explosions in butterfly abundance to years with good weather during the oviposition season; and population crashes, to years with a more limited availability of time for oviposition. In our study, although we found low elasticity values for reproductive rates, adult survival rates —the other key determinant of realised fecundity— accounted for around one fifth of the contribution to population growth (Fig. 5.4). Moreover, despite not modelling the impacts of extreme events on adult fecundity, the realised fecundity in the different bootstrap replicates substantially varied and was positively associated with increasing net reproductive rates (Fig. C9).

Most of these seminal demographic studies were conducted in temperate climates; and the experiments used to parametrise adult fecundities in our MPMs, too. In other climatic regions —such as in the Mediterranean— where sunny, clear days are more frequent, adult females are likely less limited than in temperate locations, and other life stages could be equally or more important (Ubach et al., 2022). In this line, our MPM could be further improved by including adult vital rates parameterised with field data from Mediterranean populations. This addition could help to understand the overall contribution of different life stages and vital rates on population dynamics, and the variation of their contribution across latitudinal and climatic axes.

The predictive potential of our MPM could also benefit from the simulation of the overwintering generations and the additional impacts of increasing thermal extremes during autumn and winter (Lehmann et al., 2017; Nielsen et al., 2022; Ubach et al., 2022). For instance, modelling approaches including this overwintering generation would enable the prediction of long-term trends of the populations from the net reproductive rates between consecutive generations calculated in our study. Overall, despite these potential improvements, our study provides a methodological step forward to forecast in a process-based way the demographic impacts of extreme climatic variability on organisms with complex life cycles.

5.5 Conclusions

Humans are thinning the *fabric of life* on which we all depend (*sensu* Díaz, 2022) by exploiting natural resources, changes in land use, polluting the environment, displacing species worldwide and, more recently, by warming the climate (Jauregui et al., 2022). These anthropogenic pressures are complex and multifaceted, leading to intricate ecological responses (Lehmann et al., 2020; Yang et al., 2021). Understanding and forecasting the future of biodiversity in the novel conditions of the Anthropocene require more realistic models that integrate the fundamental mechanisms driving biological responses (Buckley et al., 2023a; Maino et al., 2016; Urban et al., 2016). In this study, the use of process-based models allowed us to predict the impacts of these newly emerging stressors (LLHI events) on the populations of a model butterfly species. Moreover, we did it by explicitly including the least-studied life stages (juveniles), which are often determinant for population dynamics. If the processes modelled in our study also take place in other species, LLHI single and compound events will likely have a key role on future insect declines as the climate changes. Crucially, our simulations suggest that the disproportionate increase of LLHI events in high-emissions scenarios could affect previously-buffered and stable populations, increasing regional extinction risks. Overall, the study predicts the high impacts that novel regimes of extreme events emerging in high-emission scenarios might have on insect populations and the important ecosystem functions they sustain, providing new evidence of the need to keep global warming within the Paris Agreement goals.

Acknowledgements

The authors thank Roberto Molowny-Horas for his initial methodological and computational advice. The authors are also very grateful to Jordi Artola and the other CBMS volunteers that have been taking weekly records of butterfly abundance during the past 30 years. We also want to thank Andreu Ubach and Melodía Tamayo for their help in the larval growth chamber experiments. The warming stripes in the arrow of Fig. 5.1b were created by the climatologist Ed Hawkins and archived under a CC BY-SA 4.0 licence. *Pieris napi* life cycle in Fig. 5.1c was illustrated by Maria Argentí Bosch (Vertex creacions, @maria.vertex). M.V.-I. was supported by a doctoral grant from the Spanish Ministry of Science and Innovation (FPU17/05869 and EST21/00301). P.C. was supported by the European Union-Next Generation EU Maria Zambrano Program (ZAMBRANO 21-26), C. C. was supported by NERC grants NE/T006579/1 and NE/T003502/1, J.C. was funded by PID2020-117636GB-C21 and TED2021-132007B-I00 grants, butterfly monitoring at the study sites was funded by the Catalan Government.



6

General discussion



6.1 Unravelling the processes linking *Pieris napi* responses to climate change

6.1.1 The geographic mosaic of *Pieris napi* vulnerability to climate change

In this thesis, I investigated the climatic and ecological processes mediating the impacts of extreme heat and drought on the populations of a common and well-known butterfly in the north-west of the Mediterranean basin. Because most studies on insect responses to climate change use correlative phenomenological methods, the underlying mechanisms linking climatic drivers to insect responses are usually unknown (Urban et al., 2016). Yet, unravelling the fundamental processes producing these responses remains a key knowledge gap for building relevant predictive models of current and future impacts of climate change on insect populations (Buckley et al., 2023a; Urban, 2019; Urban et al., 2016; Yang et al., 2021). With the aim to contribute to this key challenge, I intensively characterised the different processes shaping *P. napi* exposure and sensitivity to climate variation in five contrasted populations (Chapter 1: Table 1.2). Specifically, combining field and experimental observations, I quantified the microclimatic exposure of the juveniles at their microhabitats and host plants; the plastic and seasonal variation of their host plants; and the variation in different *Pieris napi* phenotypic, phenological, behavioural, and physiological traits that are responsive to temperature (Fig. 1.5). The extensive empirical descriptions conducted in the first three chapters of this thesis were then used to parametrise process-based predictive models of the physiological and demographic responses of *P. napi* populations to increasing drought and heat impacts (Chapters 4 and 5).

After decades of research on climate change impacts on insects, it is evident that insect responses to climate change are heterogeneous and nuanced by multiple, interrelated processes occurring at fine scales (Bennett et al., 2015; Buckley et al., 2023a; Kingsolver and Buckley, 2017; Kingsolver et al., 2011; Nice et al., 2019; Parmesan and Singer, 2022; Pincebourde et al., 2016; Suggitt et al., 2018; Woods et al., 2015). In this same line, I found that climate impacts differed among the populations monitored in this thesis, producing a geographic mosaic of climate stress and *P. napi* vulnerability across the Catalan region. Summer rainfall was the most important driver of population abundance identified in Chapter 2. Therefore, part of the reported geographic heterogeneity of *P. napi* vulnerability to climate change likely owes to the differences in the local climate and their different trends of change with global warming. For instance, the local climate at the lowland sites, where *P. napi* shows the steepest declines, is much drier than in montane sites (Figs. 1.4 and 2.1). Yet, these two type of populations are also differently coupled to climate variation (Tables A7 and A8), meaning that the variability in their responses to the climate not only stems from their different positions along the climate altitudinal gradient, but also from the variability in the underlying weave of processes linking the climatic drivers with the biological responses.

In the following lines, I discuss the main findings of this thesis in the context of current literature knowledge. I first elaborate on the underlying processes shaping the heterogeneous mosaic of *P. napi* vulnerability to climate change based on the findings from the empirical studies (Chapters 2 to 4). I group the processes into two categories: the microclimatic and ecophysiological processes mediating direct climate impacts on *P. napi* (discussed in Section 6.1.2), and the indirect climate impacts on *P. napi* mediated by their host plants (discussed in Section 6.1.3). Then, I discuss the relative contribution of these two processes in driving *P. napi* declines based on the outcomes of the process-based models I employed (Section 6.1.4). I end the first section of the discussion briefly commenting on other plausible processes putatively mediating *P. napi* responses to climate that were not assessed in this thesis (Section 6.1.5). In the following section, I discuss the generalizability of the findings of this thesis and how process-based models contribute to the understanding and prediction of ecological responses to global change (Section 6.2). I finally close this thesis by discussing future potential improvements in the process-based approaches employed and stating the main conclusions that can be extracted from all this work (Section 6.3 and Chapter 7).

6.1.2 Microclimatic exposure and ecophysiological sensitivity of *Pieris napi* populations to climate change

Microclimate ecology, the science that studies how fine-grained deviations in the climate relative to background atmospheric conditions affect living organisms, has gained renewed global attention in the past years (Bramer et al., 2018; Geiger, 1950; Kemppinen et al., 2023; Pincebourde et al., 2016; Potter et al., 2013; Stoutjesdijk and Barkman, 2014; Woods et al., 2015). Microclimate crucially connects macroclimate and ecophysiology, and its study has consequently consolidated as “an inseparable part of ecology and biogeography” (Kemppinen et al., 2023). Recent improvements in data acquisition and processing have enabled the measurement of the microclimate in virtually all biomes of the world to address a wide range of ecological questions at the relevant spatiotemporal scales (Carnicer et al. 2021; Gril et al. 2023; Jucker et al. 2020; Kaspari et al. 2015; Kearney 2019; Lembrechts et al. 2021a,b; Ma et al. 2023; Maclean et al. 2021; Man et al. 2023; Pincebourde and Suppo 2016; Porter et al. 1973; Senior et al. 2019; von Oppen et al. 2022; Wild et al. 2019; Zellweger et al. 2019). This thesis is grounded in the resurgent advances in microclimate ecology in insects, whose small size links them more tightly to the conditions measured on the surfaces and inside the tissues of their hosts than to the atmospheric measurements obtained from standardised weather stations (Pincebourde and Woods, 2020; Pincebourde et al., 2021; Potter et al., 2013).

In Chapters 2 to 4 of this thesis, I characterised the microclimatic exposure of *P. napi* populations at the microhabitat and host-plant levels. The lowland locations not only had a drier climate, but also presented a less forested landscape, with sparser and less developed vegetation than in montane areas. The lowland, declining populations of *P. napi* thus had a much limited access to the microclimatic thermal buffering typically provided by canopy cover (Figs. 2.3 and 4.2). There is extensive literature documenting how forest

canopies are buffering climate change impacts by cooling and reducing thermal variation in the understory (Carnicer et al., 2021; De Frenne et al., 2013, 2019, 2021; Lenoir et al., 2017; Suggitt et al., 2018; Zellweger et al., 2020). Here, besides the thermal buffering capacity of canopy cover, I also described five more microclimatic processes determining insect thermal exposure at a finer, host plant scale (Fig. 4.3). These processes included soil cooling and soil thermal amplification effects, mainly influencing basal leaves of the host plants, but also the thermal homogenisation of host-plant microclimatic temperatures under canopies, and the complex interactions between soil water content, host-plant evapotranspiration, and foliar temperatures. Plant evapotranspiration cooled leaf undersides when soil humidity and air temperature remained in a permissive range (i.e. underside cooling effect). But, when extreme temperatures and drought induced stomatal closure and halted evapotranspiration, leaf temperatures sharply increased, a process we named foliar thermal amplification (Figs. 2.5 and 4.3f).

To understand the consequences that these interpopulation differences in microclimatic exposure would have on *P. napi* physiology, I experimentally estimated its larval sensitivity to heat stress. Results from Chapter 2 suggested that, despite having access to less buffered microclimates, larval survival in the lowland declining populations should not be necessarily compromised, as their estimated thermal limits were rarely exceeded in host-plant microhabitats (Fig. 2.3). Yet, this chapter also documented that thermal tolerance limits were significantly surpassed during reduced plant evapotranspiration, associating drought impacts in the declining populations of *P. napi* with these foliar amplification effects, among other processes (Fig. 2.5). In Chapter 4, I found that *P. napi* females mainly select partly-sheltered microhabitats, where the higher soil humidity and canopy shading usually maintain foliar temperatures below 35 °C (Fig. 4.2). Combined with the thermal avoidance behaviours described for *P. napi* larvae (Fig. 4.2), it is therefore unlikely that foliar amplification processes have an important contribution to the drought-induced declines of *P. napi* in the lowland populations, at least in the current climatic conditions. Impacts of extreme foliar temperatures due to thermal amplification processes would be rather expected for its congener, *P. rapae*, which selects open microhabitats to oviposit, as found in Chapter 4. Yet, the species presents a stable trend in almost all the population of the Catalan region¹, probably because their thermal and seasonal strategies are better adapted to cope with extreme heat stress (Fig. 4.5 and see von Schmalensee et al., 2023).

Independently of the higher or lower survival costs of microclimatic stress for *P. napi* larvae (which are further discussed in Section 6.1.4), the differences in the thermal exposure between populations clearly had marked effects in other butterfly phenotypic, physiological, and phenological traits. For example, butterflies from summer generations of lowland populations had lower wing sizes and body mass as a result of a higher thermal exposure (Fig. 2.2). The relation between environmental temperatures and wing size was found at a macroclimatic scale but is likely the result of the microclimatic experience during larval development, which would explain why wing size of the thermally-buffered

¹Population trends of *Pieris rapae* in the Catalan region can be consulted in www.catalanbms.org/en/species/piepra/

mid-elevation populations is uncoupled from macroclimatic temperatures. Summer individuals from the lowland populations also presented less melanic wings (results included in Peñuelas et al., 2017) and inferior development times, as predicted with a process-based thermal performance model in the appendix of Chapter 4 (Fig. B16; von Schmalensee et al., 2021a). Furthermore, the differences observed in the local phenology between the populations (Fig. 5.2) likely stem from the variation in their respective microclimates. Such a phenological effect was not explicitly tested in this thesis, but has been reported in other *P. napi* populations (Greiser et al., 2022; von Schmalensee et al., 2021a). Overall, these different traits that are responsive to the experienced microclimatic can have complex implications for butterfly vital rates across its life cycle and influence their microclimatic exposure itself (Kingsolver and Huey, 2008). For instance, faster development rates could reduce *P. napi*'s larval mortality by decreasing their time of exposure to parasitoids and predators (Ohsaki and Sato, 1999), but also result in smaller adult butterflies with lower fecundities than those individuals developed at cooler temperatures (Degut et al., 2022; Kingsolver and Huey, 2008). Butterfly wing size, wing melanism, and behavioural thermoregulation also affect the heat balance of the adults, determining their flight activity time and realised fecundity (Bladon et al., 2020; Buckley and Kingsolver, 2012; Kingsolver, 1983, 1988; Kingsolver and Buckley, 2015, 2017).

The changes observed in wing and body size as a result of varying temperatures were also tested experimentally, confirming that phenotypic plasticity had a higher contribution than heritability to size variation (Table 2.1 and Fig. 2.2). These results were in line with the classical rule in physiology between body size and temperature (Forster et al., 2012; Kingsolver and Huey, 2008), and supported the use of size as a phenotypic biomarker of the different microclimatic regimes populations are exposed to. For instance, the stable size found for butterflies in the mid-elevation, non-declining populations across the seasons successfully indicated the strong buffering of the microclimate experienced by these populations. Therefore, while microclimatic-induced variation in wing size might not be the underlying process driving the declines reported in some *P. napi* populations, it effectively distinguishes the populations receiving the highest climatic impacts and is thus a useful biomarker of *P. napi* vulnerability to climate stress.

6.1.3 The role of host plants in mediating climate impacts on *Pieris napi* populations

Climate effects on *P. napi* local host plants were the other group of ecological processes mediating *P. napi* responses to increasingly dry and hot conditions evaluated in this thesis. Herbivorous insects establish intimate and complex interactions with their host plants, yet indirect impacts of global warming on insects mediated by their interaction counterparts are possibly less studied than direct impacts (Abarca and Spahn, 2021; Boggs, 2016; Boggs and Inouye, 2012). One of the most documented impacts of global warming on plant–insect interactions are the varying climatic effects on the phenologies of the two partners and the emergence of phenological asynchronies (Donoso et al., 2016; Memmott et al., 2007; Parmesan, 2007; Thackeray et al., 2010). The effects of these

phenological mismatches induced by climate change are well understood for plants, but less is known on the insect counterpart (Abarca and Spahn, 2021; Bewick et al., 2015). Global warming effects on plant phenology, but also on plant physiology, growth, and stoichiometry, impact the availability and quality of insects' food resources, with relevant effects on insect performance. Food availability is an important determinant of butterfly abundance (Curtis et al., 2015), and climate effects on limiting resources can strongly shape population dynamics (Bewick et al., 2015; Gamelon et al., 2017; Lima et al., 2006; Stenseth et al., 2004). Yet, negative impacts of climate change on butterflies through limiting host-plant availability have been documented for just a few species (Boggs and Inouye, 2012; Ehrlich et al., 1980; Johansson et al., 2020; McLaughlin et al., 2002; Singer and Parmesan, 2010; van Bergen et al., 2020).

In this thesis, I monitored in different *P. napi* populations a diverse set of physiological, phenological, stoichiometric, and growth traits determining the quality and availability of their host plants across the seasons (Chapters 2 to 4). I found key differences in the host plant species used by the different *P. napi* populations that could importantly shape *P. napi* vulnerability to climate change across the Catalan region.

In addition to being exposed to more intense summer droughts and having less effective microclimatic buffering, declining populations in the lowlands also relied on less stable food resources. *Lepidium draba* and *Brassica nigra*, the two main host plants in the lowlands, complete their life cycles between May and June. Associated with the ending of their life cycle, these two host plants show a progressive increase in their foliar C/N stoichiometric content and decline of their foliar water and chlorophyll contents (Figs. 2.4, 3.4, and 4.4). After a period of complete plant scarcity, new resprouts of *L. draba* usually emerge in mid or late summer (Fig. 6.1). In Chapter 3, I experimentally determined the plastic growth responses of *L. draba* resprouts to soil water content, which explained why these resprouts remain small and do not grow until autumn rains revert soil summer drought (Fig. 3.7). In the case of *B. nigra*, subsequent plantlings do not emerge until the following growing season in spring. Therefore, the late spring and summer generations of *P. napi* lowland populations are exposed to a period of low-quality host plants (during plant senescence) followed by a period of host-plant scarcity (during plant absence).

Significantly, the extension of this resource-limiting period is subject to the influence of the local climate. Warm and arid conditions during the late spring are likely to accelerate the phenological senescence of the host plants (as depicted in Fig. 6.2), whereas droughts occurring in late summer can postpone the growth of *L. draba* resprouts (as discussed in Chapter 3). In contrast, *P. napi* populations situated at mid elevations, which do not exhibit decline, maintain consistent year-round access to fresh leaves of *Alliaria petiolata* —their primary host plant in these specific locations— with steady levels of foliar C/N, water, and chlorophyll contents (Figs. 2.4 and 4.4).

In Chapter 5, I also quantified in growth chamber experiments of *P. napi* the effects of plant scarcity in offspring development. Larvae with limited access to fresh host plants had a 17% lower daily survival rate than larvae in control conditions. Additionally, host-plant scarcity during the last stages of larval development also advanced the pupation of

6. GENERAL DISCUSSION

the larvae (Fig. 5.2). Pupation advancements due to limiting food resources have been also observed in field experiments for this species (von Schmalensee et al., 2021a) and other insects (McLaughlin et al., 2002; Parmesan and Singer, 2022; Shafiei et al., 2001). Furthermore, adults emerging from larvae exposed to limited food resources had smaller wings than larvae fed ad libitum (Fig. 6.3). Therefore, reduced wing sizes observed in the summer generations of the lowland, declining populations of *P. napi* could also be capturing the effects that drought-induced plant scarcity has on this trait, reinforcing its use as a phenotypic biomarker of climatic impacts (Chapter 2). Several studies have assessed the effects of climatic-induced changes in host-plant quality on *P. napi* larval and adult performance in the laboratory (Bauerfeind and Fischer, 2013a,b; Kuczyk et al., 2021). Yet, to my knowledge, this is the first study that finds —combining field, experimental, and modelling approaches— climatic impacts on *P. napi* populations through the effects of both low resource quality resulting from host-plant senescence and low resource availability.

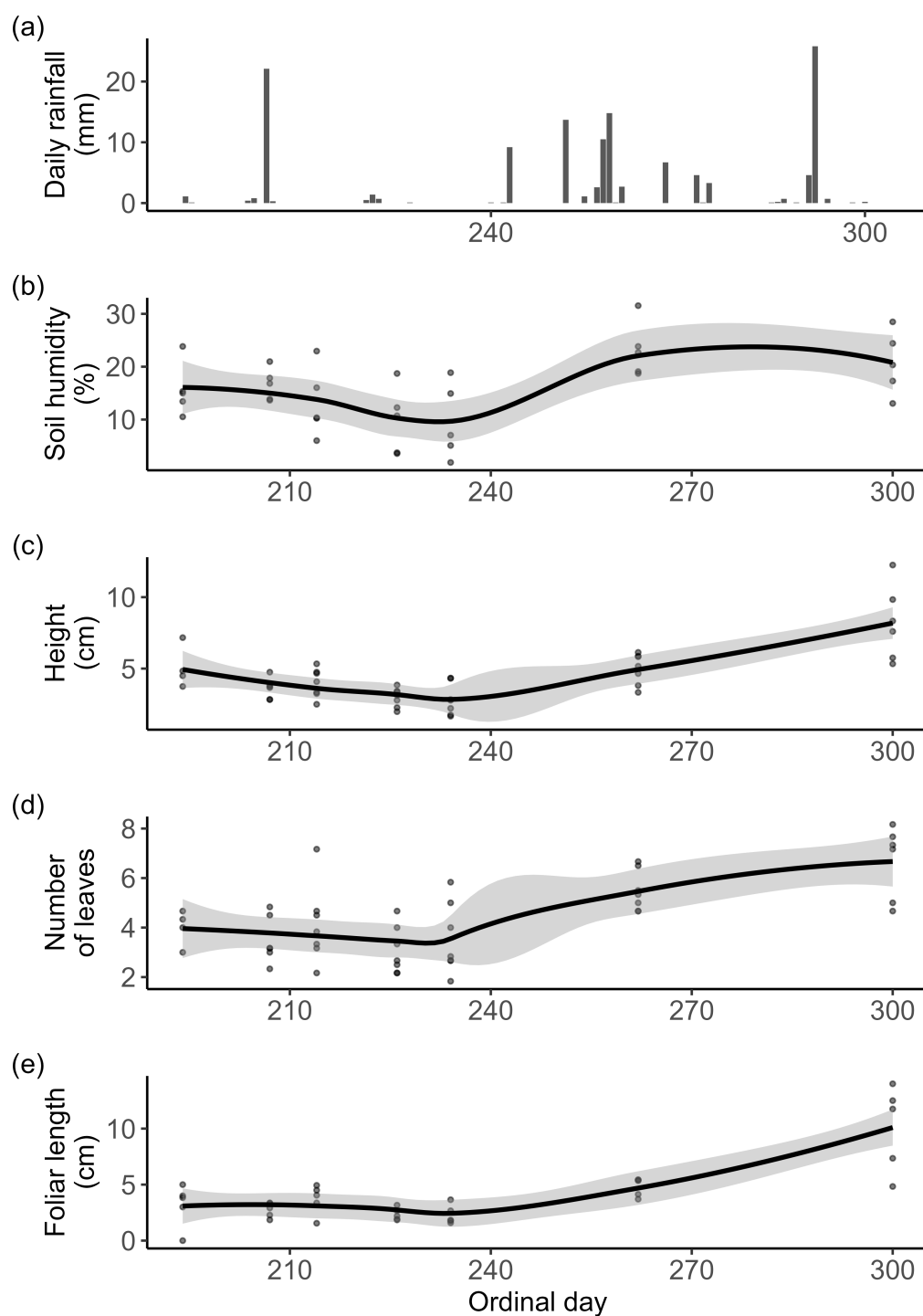


Figure 6.1: Vegetative dynamics of *L. draba* summer resprouts in the lowland, declining population. (a) Daily rainfall recorded from a nearby weather station in 2017. (b–e) Soil humidity, plant height, number of leaves, and foliar lengths of *L. draba* summer resprouts during the monitoring campaign conducted in 2017 (see methods from Chapter 3 for further details).

6. GENERAL DISCUSSION

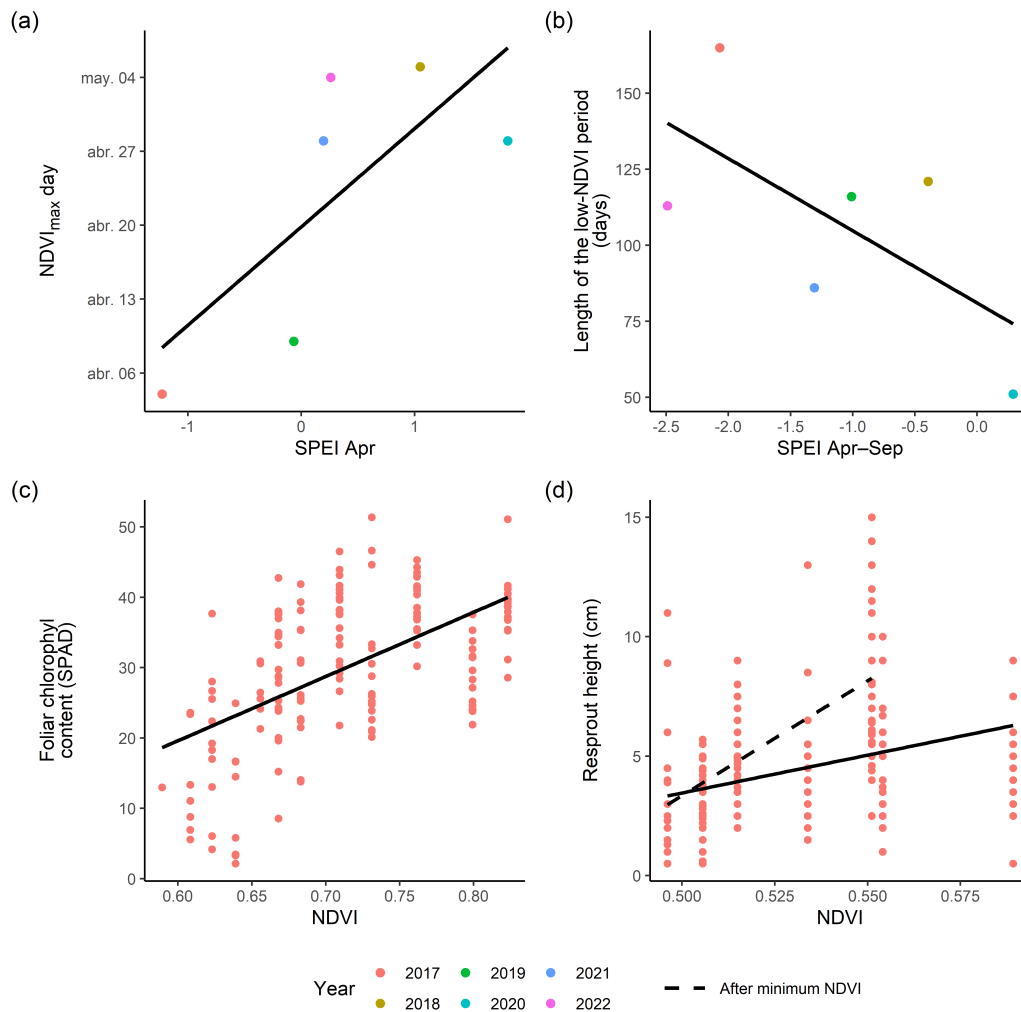


Figure 6.2: Drought effects on host-plant vegetative dynamics. (a) Relation between the spring day showing maximum values of the normalised difference vegetation index (NDVI) calculated in a 10-m pixel covering an area with abundant *L. draba* in the lowland site using optical satellite images (Sentinel-2) and the SPEI drought index during April calculated for that area following Beguería and Vicente-Serrano (2017). Note that drier springs (more negative SPEI values) are associated with earlier peaks of NDVI, after which host plants start to senesce. (b) Relation between the length of the period with low values of NDVI (NDVI < 0.6) and the SPEI values between April and September. Moister springs and summers are associated with shorter periods of low vegetation density. (c) The calculated NDVI in the 10-m pixel during 2017 is positively associated with the foliar chlorophyll contents recorded for *L. draba* spring plants in this area. The positive relation indicates that higher values of NDVI are representative of the period where foliar chlorophyll content reaches their maximum during *L. draba* maturation, and that lower NDVI values capture the subsequent process of host-plant senescence until NDVI reaches values around 0.6. (d) NDVI is also positively associated with the height of the summer resprouts emerging in mid July, especially for height measurements conducted after NDVI reaches its lowest value at the end of August (dashed line).

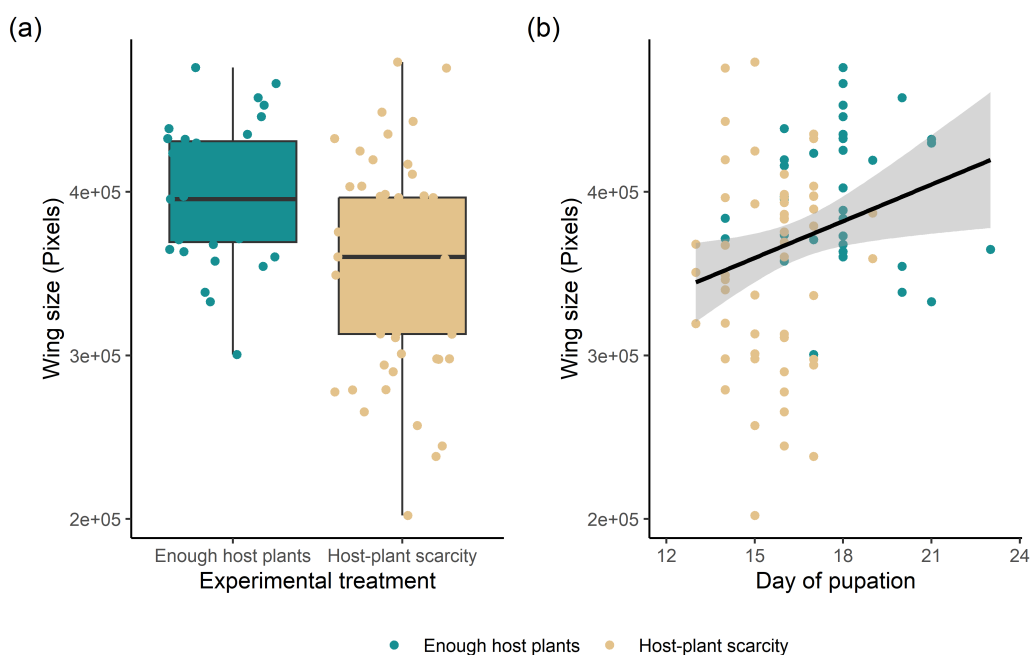


Figure 6.3: Experimental effects of host-plant scarcity during larval growth on *P. napi* wing size. (a) Larvae exposed to plant scarcity in growth chamber experiments (see Appendix C.2.2) produced adults with smaller wings. (b) The pupation advancement of individuals with limited access to food resources was positively associated with reduced wing sizes.

6.1.4 The relative contribution of direct impacts of extreme temperatures and plant-mediated impacts of drought on *Pieris napi* declines

The empirical study of the direct and indirect processes mediating climate impacts on *P. napi* populations indicated that summer thermal microclimatic exposure would not be necessarily harming provided the access to fresh host plants is guaranteed (Chapter 2 and discussion above). Therefore, observational studies conferred to host plants a key role in the drought-driven declines observed in some *P. napi* populations (Chapters 2 and 3). To test this hypothesis and predict the relative contribution of these two processes in the responses of *P. napi* populations to climate change, I applied two process-based models parameterised with the data gathered in the field and experimental observations (Chapters 4 and 5).

Firstly, in Chapter 4, I predicted the larval mortality caused by extreme thermal exposure in the fluctuating microclimatic temperatures recorded in the field. The dynamic model I employed used the thermal death time curves (TDT curves) experimentally obtained from *P. napi* to calculate the accumulated larval heat injury throughout the day and the associated daily survival probability. In the microhabitats where *P. napi* offspring develop, daily survival probabilities to the recorded microclimatic exposure were gener-

ally high (survival ≥ 0.99 in 96% of the simulations with the summer microclimatic temperatures recorded in the lowland site and 99% of the mid-elevation site simulations). These values supposed that the mean cumulative thermal mortality during larval development oscillated between 0.01–0.17 in the lowland site and 0.0003–0.06 in the mid-elevation site in summer (Fig. 4.5; 95% prediction intervals of the mean cumulative thermal mortality per simulation). Thus, the predicted thermal mortality was higher in the lowland declining site than in the mid-elevation non-declining site, but still, it was reasonably low.

In Chapter 5, I integrated in a matrix population model (MPM) the direct impacts of extreme microclimatic temperatures on larval survival (TDT predictions) and the indirect impacts of drought through host-plant scarcity on larval development (growth chamber experiments). I then used the MPM to calculate the effects that these two types of climatic impacts have on *P. napi* population growth rates and infer which of these two processes were more likely driving the declines observed in some populations. The simulations that included the indirect impacts of drought mediated by host-plant scarcity had more negative effects on the population growth rates of summer generations than the direct impacts of current regimes of extreme microclimatic temperatures (Fig. 5.6). Furthermore, the declining growth rates observed in the lowland populations could only be replicated when drought-induced plant-scarcity effects were simulated (Fig. 5.5). In line with empirical observations, these results provide mechanistic support to the key role that the host plants play in the drought-driven declines in the studied *P. napi* populations, adding new evidences for this underreported impact of climate change in butterfly populations (Boggs and Inouye, 2012; Ehrlich et al., 1980; Johansson et al., 2020; McLaughlin et al., 2002; Singer and Parmesan, 2010; van Bergen et al., 2020).

The key importance of host plants in mediating climate impacts on *P. napi* populations does not mean that thermal mortality has no relevant effect on population performance. In fact, in the MPMs, the most severe impacts on population growth rates were predicted for the simulations including compound hot-dry events, which triggered both direct thermal impacts of extreme heat and indirect plant-mediated drought impacts on *P. napi* vital rates (Figs. 5.5 and 5.6). Furthermore, the relatively low importance of thermal mortality on *P. napi* population dynamics is only due to the microclimatic buffering provided by the sheltered microhabitats selected by the species (Fig. 4.5). If the buffering capacity of the vegetation in these partly-covered microhabitats was limited due to reduced soil moisture or drought-induced canopy-cover dieback — a plausible scenario with increasing global warming (Davis et al., 2019; De Frenne et al., 2021; IPCC, 2021)—, thermal mortality resulting from extreme heat exposure would likely be as or more important than drought-induced plant scarcity. For instance, the predicted daily thermal mortality for *P. napi* in the open microhabitats increased by a mean factor of 72 the daily mortalities predicted in their partially-sheltered microhabitats (mean factor of increase = 16 in the declining populations, and 141 for the currently non-declining population, Fig. 4.5). Moreover, MPM simulations projected in macroclimatic warming conditions (i.e. without accounting for the microclimatic buffering of thermal extremes in *P. napi* microhabitats) predicted more severe declines in *P. napi* populations as the climate

warms than forecasts at a microclimatic scale, especially for the currently non-declining and more effectively sheltered population (Fig. C10).

Besides the putative reduction of the microclimatic buffering capacity of vegetation cover in the coming decades, ongoing global warming is projected to trigger a nonlinear increase in the frequency of hot and dry extreme events (IPCC, 2021; Seneviratne et al., 2021). Specifically, the frequency of rarer but more extreme thermal events will increase relatively more than moderate extreme temperatures (IPCC, 2021; Seneviratne et al., 2021; Simolo and Corti, 2022; Vogel et al., 2020). In Chapter 5, I predicted the damaging effects that the projected disproportionate increase of these low-likelihood high-impacts (LLHI) events in novel climates will have on *P. napi* populations. The results indicated that, despite not having a key role in the current *P. napi* declines, extreme heat events will emerge as a new important global-change stressor if greenhouse gas emissions are not halted fast enough, equaling the effects of drought-induced host-plant scarcity (Fig. 5.6).

Altogether, these results reinforce the usefulness of developing process-based models at a relevant microclimatic scale to better understand and predict insect responses to climate change (Buckley et al., 2023a; Ma et al., 2021; Urban, 2019; Urban et al., 2016; Yang et al., 2021). The initial chapters of this thesis used observational and experimental approaches to identify the processes that possibly drive population declines in the selected populations of *Pieris napi*. Subsequently, the process-based models employed in this thesis enabled the prediction of *P. napi* population dynamics in novel regimes of extreme events (Chapters 4 and 5). Methodological approaches failing to capture the underlying processes linking the climatic driver with the response can be hardly used to predict responses to climatic conditions outside the range of observed climate, a very relevant limitation when predicting responses to extreme climatic conditions and emerging novel climates (Buckley et al., 2023a; van de Pol et al., 2017). Moreover, some of the predicted effects of climate change on *P. napi* populations stemmed from nonlinear processes, such as the rapid acceleration of the heat failure rates at increasingly stressful temperatures (Jørgensen et al., 2022b) or the complex interactions between water availability and microclimatic feedbacks (Carnicer et al., 2021; Davis et al., 2019; Pincebourde and Woods, 2012; von Arx et al., 2013), which are rarely captured by the linear statistical approaches usually employed (Buckley et al., 2023a; Maino et al., 2016; Urban et al., 2016). In addition, with the process-based models employed in this thesis I could also simulate and compare the relative effects of the different putative processes mediating climate change impacts on *P. napi*. Specifically, I could identify the process more importantly driving current *P. napi* declines but also anticipate the future risks associated with the intensification of currently milder impacts.

6.1.5 Other processes mediating climate impacts on *P. napi* populations

Together with the numerous climatic and ecological processes quantified in this thesis, other processes that could not be covered might also shape *P. napi* responses to cli-

mate change. For instance, the observed population growth rates in the summer generations of the declining population were more negative than predicted with the MPM in the current climatic conditions (Fig. 5.5), which might suggest that additional impacts could be missing from the model. Some of the potentially missing processes were already commented in the respective discussions of each chapter, such as the impacts that heat and drought events can also have in the egg, pupal, and adults stages (Chapter 5); or the complex feedbacks between drought, plant physiological status, microclimatic exposure, larval growth, and thermal tolerance (all chapters). Yet, here I provide a brief discussion of other processes that could be further studied in the future.

Chapter 3 and personal communications with Constantí Stefanescu —the responsible of the CBMS monitoring during the last 30 years in the lowland location I most studied in this thesis— speculated on the possibility that *P. napi* pupae from the declining, lowland population aestivate during the harsher summer conditions. This hypothetical mechanism would enable the summer generations of *P. napi* to avoid the detrimental impacts of the recurrent host-plant scarcity reported in this population. Moreover, it could explain the sharp reduction in butterfly numbers annually observed after the peak of the July (third) generation and why predicted growth rates with the MPMs in this period are generally higher than the estimated rates from observed adults (Fig. 5.5). Previous attempts to experimentally induce summer diapause in *P. napi* individuals of this population have failed (Christopher Wheat and C. Stefanescu, personal communications). Yet, future modelling efforts explicitly including a dormant stage in the summer MPMs (Ellner and Guckenheimer, 2006; Flockhart et al., 2015; Paniw et al., 2017, 2020; Radchuk et al., 2013; Rees et al., 2006) could provide new promising insights into this issue.

Pupal aestivation has been detected in other *Pieris* species, such as *P. melete* (a sister species of *P. napi* in Asia, with very similar ecological requirements and previously included in the *P. napi*-complex; Ge et al., 2023) and in some Iberian populations of *P. brassicae* (Held and Spieth, 1999; Spieth, 2002; Spieth and Schwarzer, 2001; Spieth et al., 2011; Xiao et al., 2006; Xue et al., 1997). The summer diapause confers to these species a third developmental strategy that is triggered and controlled independently of its winter counterpart (Held and Spieth, 1999; Xue et al., 1997). In both cases, despite being widespread species, the faculty of undergoing a summer dormancy period is only present in a fraction of their populations. This plastic behaviour has been associated, in the case of *P. melete*, with the synchronisation of the butterfly generations with the annual cycle of its host plants and the avoidance of summer thermal extremes (Xiao et al., 2006; Xue et al., 1997). For *P. brassicae*, populations undergoing summer diapause are restricted south of the Pyrenees, where this facultative response enables the species to synchronise generations in areas producing a high number of generations per year (6–9) while desynchronizing their population dynamics from the life cycle of its specific parasitoid (Spieth and Schwarzer, 2001; Spieth et al., 2011). Notably, the reduced geographic scope of this local adaptation in *P. brassicae* does not result from an insufficient gene flow or low heritability of the trait, but rather from the maladaptive effects that summer diapause would have in populations with a slightly shorter growing season where aestivation costs would likely exceed its potential benefits (Spieth et al., 2011).

In the case of *P. napi*, preliminary genetic and genomic analyses with the studied populations suggest extensive gene flow and frequent gene dispersal following riverine networks (COI, Illumina, and Radseq analyses, Roger Vila, Jofre Carnicer, Javier Sala-Garcia, C. Wheat, unpublished data). Therefore, as in the case of *P. brassicae*, the potential presence of this summer facultative behaviour in just a few lowland populations could be the result of a strong local selective pressure and the possibly maladaptive effects of upriver gene flow. Indeed, growth chamber experiments found evidence for local adaptations to low temperatures and winter diapause on Pyrenees and mid-elevation Catalan populations of *P. napi* despite the extensive gene flow (J. Carnicer, unpublished data).

The example of *P. brassicae* points to another summer stressor that could affect *P. napi* populations but that has not been explicitly monitored in this thesis: the seasonal dynamics in the predatory and parasitoid pressures on the species (Spieth et al., 2011; Stefanescu et al., 2022). Natural enemies could have played an important role in shaping *P. napi* adaptations (such as their host-plant use; Ohsaki and Sato, 1994, 1999; Yamamoto, 1981) and regulate their population dynamics (Courtney, 1986). For instance, two specific parasitoids of *P. napi* young larvae — *Cotesia rubecula* (Braconidae: Microgastrinae) and *Hyposoter ebeninus* (Ichneumonidae: Campopleginae)— have been found in the most studied lowland population of this thesis, although other tachinid flies and ichneumonid wasps are also likely present there and in other Catalan populations (C. Stefanescu, personal observations). In addition, eggs from the lowland populations are known to be regularly parasitised by a *Thrichogramma* wasp (Liana Greenberg and C. Stefanescu, ongoing research).

Despite not being specifically studied in this thesis, the MPMs developed in Chapter 5 included a daily rate of parasitism and predation based on field estimates from other *P. napi* populations (Fig. C3). The additional set of simulations with varying parasitism rates still conferred a key role to drought-induced plant scarcity and extreme heat in driving declining populations rates, yet it also indicated that increasing parasite rates would make the situation worse (Fig. C11). Whether herbivore populations are more importantly regulated by bottom-up or top-down processes is a long-standing classical debate in ecology (Cornell et al., 1998; Hairston et al., 1960; Keeler et al., 2006; Kempel et al., 2023; Murdoch, 1966). Both processes are likely to be relevant in our study case, and further assessments of their relative contributions and potential feedback between demography and species interactions could be made by modelling tritrophic (or community-wide) interactions in structured populations models like MPMs (Hoover and Newman, 2004; Paniw et al., 2023).

Finally, other drivers of global change could interact with the climate-driven processes covered in this thesis. For example, the effects of changing land uses, urbanisation, and land abandonment on *P. napi* microhabitats and the associated microclimatic and host-plant conditions (Dennis, 2010; Merckx et al., 2021; Mingarro et al., 2021; Nieto-Sánchez et al., 2015; Stefanescu et al., 2011a,b; Ubach et al., 2019); the effects of soil nitrification on host-plant quality and the surrounding microclimate (Klop et al., 2015; Merckx et al., 2015; WallisDeVries and van Swaay, 2017); or the direct impacts of insecticide and herbicide use on *P. napi* and other interacting species (Azpiazu et al., 2019; Fontaine et al.,

2016; Forister et al., 2016).

6.2 Process-based models are useful, but are they usable?

6.2.1 Towards an integrative and predictive global ecology

Developing process-based forecasting tools with a sound mathematical and biological basis is of critical importance for having a more accurate predictive capacity of insect — and biodiversity — responses to global change (Briscoe et al., 2023; Buckley et al., 2023a; Maino et al., 2016; Urban et al., 2016). Poor progresses have still been made to halt climate change and the other anthropogenic drivers of biodiversity loss (Díaz et al., 2019; Jaureguiberry et al., 2022). This worrying situation reinforces the urgent need to consolidate a robust ecological forecasting science that can predict the potential benefits for human and nature well-being of changing our societies. Recent improvements in this line set the basis towards the maturation of an integrative and predictive ecological science, which will require, as climate science did in the past decades, global coordinated efforts to establish a common scientific agenda and shared infrastructures (Urban, 2019; Urban et al., 2016, 2022). However, process-based models are data hungry. Their parameterisation requires high-quality, fine-grained, and multisource data on the system, and their use, quantitative and computational skills (Briscoe et al., 2023; Urban, 2019; Urban et al., 2016, 2022). This central limitation brings the following question: despite the usefulness and the critical importance of crafting more sophisticated process-based models, how usable are they?

In this thesis, I used two different process-based models to predict *P. napi* population responses to climate change. I selected *P. napi* as a study species for several reasons. First, it is an insect, whose small size, ectothermic physiology, and short life cycles makes them very responsive to changing environmental conditions and thus an ideal model organism to study biological responses to climate change (Hill et al., 2021). Second, *P. napi* itself is a model species among insects and butterflies, with much information regarding numerous aspects of their biology (Table 1.1 and Section 1.3; Bauerfeind and Fischer, 2013a; Degut et al., 2022; Günter et al., 2020a; Hill et al., 2019; Lehmann et al., 2018; Ohsaki and Sato, 1999; Peñuelas et al., 2017; von Schmalensee et al., 2023; Wiklund et al., 1993, among others). Third, *P. napi* is a very common and widespread butterfly in the Catalan region, where I contributed to consolidate a well-established monitoring system in different populations of the species (Peñuelas et al., 2017). All these aspects favoured my access to a considerable amount of high-quality data for a well-known species, at relevant local scales, and for a long period relative to its life cycle. Specifically, this thesis benefitted from two 25-year abundance series at a weekly resolution —representing around 5,000 working hours each (C. Stefanescu, personal communications)—; 180,000 hourly microclimatic records; 1,000 h in sampling campaigns in the field; and more than 325 h of experimentation. All these tasks represent more than 190,000 h —excluding the sensor records, more

than 10,000 h (i.e. more than one year)— added to the time spent in the collection, processing, and publication of the data I gathered from bibliography (Chapter 5). Therefore, given the time and the multiple types of data I needed for this particular study case, is it reasonable to pursue a global assessment of biodiversity responses to climate change with a process-based approach?

It is quite evident that it will not be feasible to obtain the same amount of high-quality data gathered in this thesis and parametrise process-based models for a substantial fraction of global populations, especially with the celerity we should. Yet, this constraint does not invalidate the need and the feasibility of developing a better predictive ecological science based on first principles. The usability of process-based models to predict ecological responses to global stressors will indeed depend on the generality of the outcomes from these more carefully modelled systems (Urban et al., 2016, 2022). In Section 6.1.3 of this discussion, I already emphasised the success and the usefulness of the process-based models employed in this thesis. These models relied on local, fine-grained climatic and biological data —one of the keystones for developing relevant and realistic predictive models (Briscoe et al., 2023; Buckley et al., 2023a)—, yet their strength may have simultaneously compromised the generalisability of their outcomes. In other words, recognizing the extreme vastness and richness of the tapestry of life, to what extent the deep understanding of a few sparse, small knots will help to anticipate its unravelling? In the following lines, I discuss the extendibility of the findings of this thesis to other *P. napi* populations, insect species, and living organisms, and some practical ways forward that have been proposed to overcome these model limitations and consolidate a robust predictive global ecology.

6.2.2 The generality of *P. napi* predicted responses to climate change

The outcomes of any process-based model depend on the parameters of the model (in this case defined by insects' sensitivity to changing conditions) and the conditions of simulation (defined by insects' exposure). Therefore, although insects' climatic exposure and sensitivity largely vary across many scales and dimensions, the findings of this thesis will apply to those populations and species whose model parameters and conditions are similar enough to prevent any significant difference in the outcome of the predictions. For instance, the predictions of thermal mortality and population growth obtained from the lowland, declining population of *P. napi* (Chapters 4 and 5) likely apply to other Catalan and Mediterranean populations of the species with limited access to microclimatic buffering and relying on summer-fading host plants. Similarly, results from the mid-elevation, non-declining populations are likely extensible to other *P. napi* populations with wetter, temperate climates and agroforestral landscapes that offer milder microclimates and year-round fresh host plants.

Expanding the geographic scope, many studies in other *P. napi* populations have found close resemblances with the key characteristics shaping the butterfly responses to climate change I studied in this thesis. For instance, *P. napi* populations from Southern

Sweden also select partly-shaded microhabitats to oviposit, exposing their offspring to colder and less variable microclimates than *Pieris rapae* (Fig. 4.2; Friberg and Wiklund, 2019; von Schmalensee et al., 2023). Moreover, these comparative studies also found that *P. napi* had a higher thermal sensitivity and a lower survival at high temperatures than its congener (Fig. 4.5; von Schmalensee et al., 2023). In Japan, these two species also show similar differences (Ohsaki, 1979, 1982). Therefore, although there might be important differences between *P. napi* populations worldwide (e.g. in their phenologies, host plants, and local climates and adaptations), the similitudes in the key traits shaping their climatic exposure and sensitivity suggest that the process-based models developed in this thesis could be easily reconfigured for other populations.

Following the same argumentative line, the results of this thesis shall not be extensive to species ecologically or phylogenetically divergent. Yet, species with similar ecological traits and requirements, microclimatic exposures, life histories and phenological cycles, and biotic interactions could benefit from the work developed in this thesis. For example, to identify which butterfly species could have similar microclimatic exposures to those quantified in this thesis, we could compare the butterfly affiliations to more open or closed microhabitats with the recently-proposed TAO index (Ubach et al., 2019). The CBMS provides a TAO index for 160 butterflies based on their recorded abundances across the Catalan territory and groups them in 10 different categories. Taking into account the number of butterflies in the same category, 9% of the species have the same TAO affiliation as *P. napi*, and 16%, the same as *Pieris rapae*. Therefore, the microclimatic buffering and amplification processes reported in this thesis could putatively apply to at least 25% of the Catalan butterflies².

The effects on heat-induced mortality resulting from similar microclimatic exposures would however depend on butterflies' thermal sensitivity (i.e. the TDT curve of the species). A comparative analysis with insect TDT data gathered by Jørgensen et al. (2022a,b) indicates that the parameters of *P. napi*'s TDT curve estimated in this thesis falls inside the interquartile range of observed parameters for other species, and is thus more representative of insect's thermal tolerance than *P. rapae*, whose estimated parameters are more outlying (Figs. 4.5 and 6.4). Furthermore, butterflies having similar microclimatic exposures, thermal sensitivities, and life histories to *P. napi* are likely to show analogous relative changes in population growth rates as global warming increases the frequency of extreme LLHI heat events (Chapter 5), especially in those regions where LLHI events are expected to increase relatively more (e.g. in the Tropics and the Mediterranean area; IPCC, 2021; Simolo and Corti, 2022).

²The TAO index for the different butterflies found in Catalonia can be checked in www.catalanbms.org/en/especies/

6.2. Process-based models are useful, but are they usable?

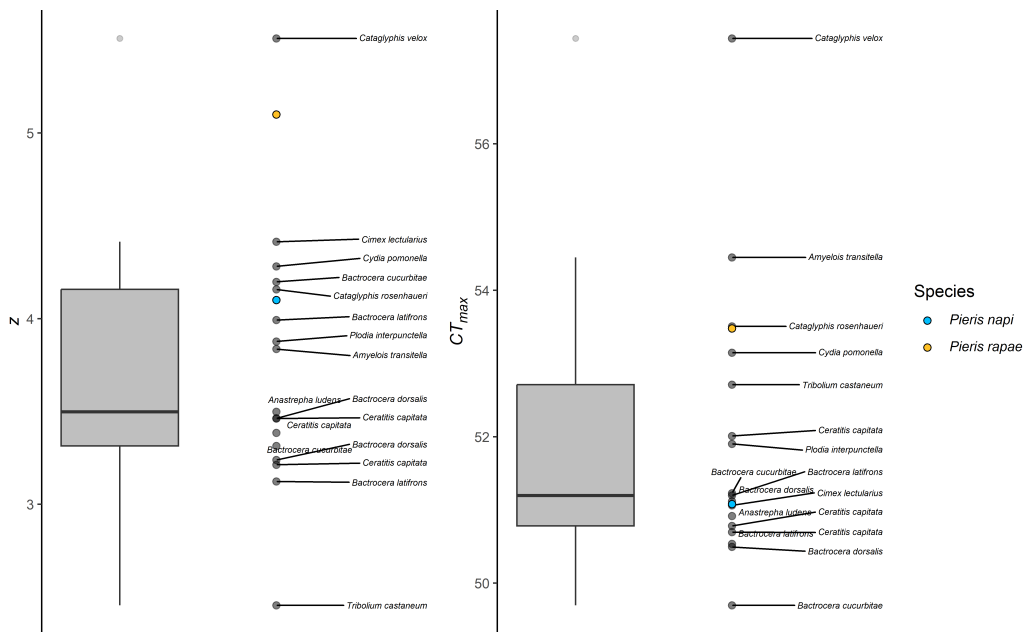


Figure 6.4: Comparison of the parameters of the thermal death time curves (TDT curves) for *Pieris napi* (blue), *P. rapae* (yellow), and 12 other insect species (grey; data gathered from Jørgensen et al., 2022a,b). (a) Thermal sensitivity parameter (z), (b) Maximum critical temperature (CT_{max}). The boxplots at the left part of the panels summarise the distribution of the 12 insect dots. Boxes represent the interquartile range ($IQR = Q_3 - Q_1$). The lower whisker represents the smallest value $\geq Q_1 - 1.5 \times IQR$; and the upper whisker, the biggest value $\leq Q_3 + 1.5 \times IQR$.

6.2.3 Overcoming the challenges of consolidating a predictive global ecology

These examples illustrate the key utility that comparative macroecological studies will have for filling the gaps of the missing parameters of process-based models for understudied species (Urban et al., 2016). The appropriate data to parametrise realistic predictive models is still lacking for the vast majority of species, hindering the consolidation of a predictive ecological science based on first principles and operable for all species and ecosystems (Urban et al., 2016). Yet, in the process of leveraging this missing information, data from key traits of less studied species can also be estimated from correlative studies assessing trait variation with phylogenetic distance and the covariation of multiple sets of traits along main axes (i.e. multivariate trait continua; Bielby et al., 2007; Carnicer et al., 2012, 2013b; Dapporto and Dennis, 2013; Díaz et al., 2016; Jeschke and Kokko, 2009; Wright et al., 2004). For instance, a first step towards the consolidation of a predictive butterfly ecology could start by developing a limited number of process-based models for a reduced set of species representative of basic functional and phylogenetic groups (Carnicer et al., 2013b; Melero et al., 2022; Stefanescu et al., 2011a), complementing correlational studies covering the whole set of species monitored by citizen science programmes (Colom et al., 2022; Melero et al., 2016, 2022; Stefanescu et al., 2011b; Ubach et al., 2022).

These approaches would help to estimate the parameters governing the key biological processes underlying ecological responses to climate change. Yet, to obtain relevant and realistic outcomes, these process-based models should be simulated with climatic information at relevant temporal and spatial scales (Briscoe et al., 2023; Buckley et al., 2023a). Macroclimatic data is already accessible worldwide, but it has been repeatedly shown that most organisms and ecological processes are more tightly linked to climatic conditions at finer scales. While obtaining microclimatic data for the vast majority of organisms is still challenging, a myriad of new methods developed in the last years are increasingly filling this information gap with both in-situ and modelling tools (Buckley et al., 2023b; Gril et al., 2023; Kearney and Porter, 2017; Kempainen et al., 2023; Lembrechts et al., 2021a,b; Maclean et al., 2021; Man et al., 2023; Pincebourde and Casas, 2006).

Consolidating a predictive global ecology could further benefit from iterative modelling schemes that continuously indicates the most important data needs (e.g. based on parameter sensitivity; Urban et al., 2016, 2022); the simulation of virtual sets of traits and microclimates to identify the most vulnerable species (Urban et al., 2016); and the development of flexible and accessible models that can accommodate to general modelling needs, such as hybrid correlative-mechanistic approaches (Buckley et al., 2023a; Urban et al., 2016).

Therefore, despite developing a predictive global ecology will be an enormous endeavour, the many improvements developed until the day suggest that this effort might be both feasible and worth doing. Comparable global efforts boosted the forecasting capacity of climate science in the past decades (Urban, 2019), and there are already many successful cases of increasing predictive capacity through process-based modelling in multiple ecological fields such as tree hydraulics and drought-induced tree mortality (Anderegg et al., 2015a,b; Cochard, 2021; De Cáceres et al., 2021; Mantova et al., 2022), species distribution modelling (Buckley et al., 2010, 2023a; Urban et al., 2023), population ecology (Caswell, 2001; Jenouvrier and Visser, 2011; Jenouvrier et al., 2014, 2015; Paniw et al., 2023; Rees and Ellner, 2009), and biophysical and thermodynamic biology (Briscoe et al., 2023; Buckley et al., 2023b; Kearney and Porter, 2017; Maino et al., 2016; Pincebourde and Woods, 2012). Overall, while a predictive global ecology built on process-based models could overcome many of the shortcomings of correlative approaches, the first also comes with other epistemological limitations, such as the reductionism of an inherently complex nature, that should be kept in mind (Levins, 1966).

6.3 Potential improvements and lines of future research

In previous sections I already discussed other possible processes mediating *P. napi* responses to climate change that could be further explored in the field (Section 6.1.5) and some practical ways forward to extend the outcomes of this thesis to other study systems (Section 6.2.2). Yet, the process-based models I employed could also be fine-tuned and complemented with new features in the future.

The dynamical model I used to predict heat-induced mortality based on the TDT curves of *P. napi* already represents an important step forward to translate experimentally-determined thermal tolerances into insect's performance in nature. Specifically, it enables the shift from a threshold approach — where the risk of suffering significant heat injury in the field is assessed by comparing the upper thermal tolerance limits with the maximum environmental conditions (Sunday et al., 2014, and Fig. 2.3)— to one that captures the additive, time-dependent, and cumulative effects of heat injury in fluctuating thermal conditions (Rezende et al., 2020b, and Fig. 4.5). The TDT approach has gained resurgent attention in thermal ecology in the past decade and is consolidating as a robust framework to assess ectotherm responses to stressful temperatures (Bigelow, 1921; Bigelow and Esty, 1920; Huey and Kingsolver, 2019; Jørgensen et al., 2021, 2022b; Ørsted et al., 2022; Rezende and Santos, 2012; Rezende et al., 2011, 2014, 2020b; Santos et al., 2011). However, it could be further improved by integrating in a common dynamical model the effects on insects' performance of temperatures fluctuating in permissive as well as stressful ranges (Jørgensen et al., 2021; Ørsted et al., 2022). Nonlinear effects of varying temperatures on insect performance are captured by thermal performance curves (TPC), and there have been some recent advances to combine them in a common modelling framework with TDT curves (Jørgensen et al., 2021; Ørsted et al., 2022). This combined TPC-TDT framework would enable, for instance, to assess the role of insects' homeostatic capacity at permissive temperatures in buffering the damaging impacts of thermal stress through the repair of the heat injury (Jørgensen et al., 2021; Ørsted et al., 2022).

Another potential line of future work could focus on integrating the effects of organism size on the modelled responses. For instance, in this thesis I showed that both extreme thermal exposure and drought-induced plant scarcity during larval development produce significant decreases in adult size (Figs. 2.2 and 6.3), which are likely to have relevant effects on adult fecundity and survival (Degut et al., 2022). Moreover, smaller larvae are also more vulnerable to heat challenges than larger ones (Table 4.2). Therefore, future modelling efforts could benefit from additionally integrating the dynamic increase in size in the TPC-TDT framework (von Schmalensee et al., 2021a), and also from the addition of a size covariate in the structured population models I employed, shifting from a matrix population model (MPM) to an integral projection model (IPM; Ellner and Guckenheimer, 2006; Rees and Ellner, 2009).

Finally, to fine-tune the predictive accuracy of *P. napi* responses to climate change, the models I used in this thesis could be complemented with other biophysical models predicting insects' body temperature based on their thermoregulatory behaviours across the microclimatic mosaics (Buckley et al., 2023b; Kearney and Porter, 2020; Kearney et al., 2009b; Woods et al., 2015, and see Fig. 2.2 for larval thermal avoidance behaviours and Fig. 4.2 for adult microhabitat sampling). Further improvements could also try to interconnect current models predicting physiological and population responses with process-based models addressing other key dimensions of ecological responses to climate change (Buckley et al., 2023a; Urban et al., 2016, 2022). For instance, by integrating multispecific interaction networks into population models to predict community-wide responses (Brodie et al., 2018; Paniw et al., 2023), by considering dispersal and meta-population dy-

6. GENERAL DISCUSSION

namics (Brown and Kodric-Brown, 1977; Hanski, 1999), or addressing the evolutionary and plastic feedbacks on insects' adaptive traits (Buckley and Huey, 2016; Kearney et al., 2009a; Kingsolver and Buckley, 2017).

To conclude, combining multiple sources of detailed information and approaches is critical to understand, as I did in this thesis, the complex set of interlacing processes that weave the rich *fabric of life* we rely on. The efforts needed to predict how the human unravelling of various fabric strands will propagate through this interwined tapestry are titanic, but the advancements made until the day make the challenge worthwhile.



Main conclusions



Chapter 2

- The demographic dynamics of *Pieris napi* populations in the Catalan territory are tightly linked to summer drought conditions, forming a heterogeneous geographic mosaic of increasing, stable, and declining populations.
- The empirical quantifications conducted in the field show that the vulnerability of *P. napi* populations to increasing drought and heat climate change impacts is shaped by multiple interrelated ecological processes occurring at local and microclimatic scales. Specifically, non-declining *P. napi* populations benefit from effective microclimatic buffering provided by their selected microhabitats and the year-round availability of host plants in good condition. In contrast, declining *P. napi* populations have limited access to microclimatic buffering effects and the availability of fresh host plants is interrupted during summer.
- The experimental determination of the thermal death time curve for *P. napi* suggests that their larvae would withstand the microclimatic temperatures on most days, except when thermal amplification feedbacks raise foliar temperatures of their host plants beyond their thermal tolerance limits.
- *Pieris napi* wing size plastically varies with temperature, showing only a marked size reduction in the summer generations of the lowland declining populations. Therefore, *P. napi* wing size can be used as a reliable phenotypic biomarker of the geographic variation in *P. napi* population exposure to climate change impacts.

Chapter 3

- The intense monitoring of host plants reveals that drought's indirect impacts on declining *P. napi* populations are mediated by the plant's plasticity in their phenological cycle and vegetative growth.
- Drought impacts *P. napi* populations sequentially. First, late spring and early summer droughts accelerate the host-plant die-off, exposing the third generation of *P. napi* to a period of low-quality food resources. Then, late summer drought postpones the development of host-plant autumn resprouts, exposing the fourth generation of *P. napi* to a period of resource scarcity.

Chapter 4

- Combined field, experimental, and modelling analyses reveal how thermal adaptations and heat-induced mortality coherently vary with the differences in the microhabitat use and microclimatic exposure of *P. napi* and its sister species *Pieris rapae*.

- *Pieris rapae* selects open microhabitats to oviposit, where microclimatic temperatures are higher, more extreme, and subject to foliar and soil thermal amplification processes. In agreement, they present a thermotolerant adaptive strategy, allowing the species to have higher survival rates than its counterpart during an acute heat challenge.
- The partially-covered microhabitats where *P. napi* lays their eggs offer, instead, a more thermally-buffered and homogeneous microclimate that can be better withstood by this thermosensitive butterfly than by *Pieris rapae*.
- Thermal mortality values predicted from thermal death time curves and microclimatic field series offer a robust assessment of insect vulnerability to increasing heat impacts based on the intensity, duration, and accumulation of heat stress at relevant scales.

Chapter 5

- Matrix population models enable the prediction of *P. napi* population growth rates based on the probabilities for any individual of the population to transition through all the stages of its complex life cycle.
- The elasticity analysis on the transition matrices indicates that early life stages can play crucial roles in insect population dynamics despite being usually neglected in the studies of climate change impacts on insects due to their low detectability.
- The projection of the matrix population model at present-day regimes of extreme heat and drought events indicates that current declines observed in some *P. napi* populations are driven by drought impacts on their host plants, validating previous field observations and offering new evidence of the critical role that indirect processes can have in mediating insect responses to climate change.
- The non-proportional increase in the frequency of low-likelihood high-impact extreme climatic events relative to milder extremes is predicted to produce more severe and regionally-widespread declines of *P. napi* populations as the climate changes, potentially emerging as a new and overlooked climatic threat for biodiversity.

Appendix A

Chapter 2 - Supporting materials

A.1 Supplementary figures and tables

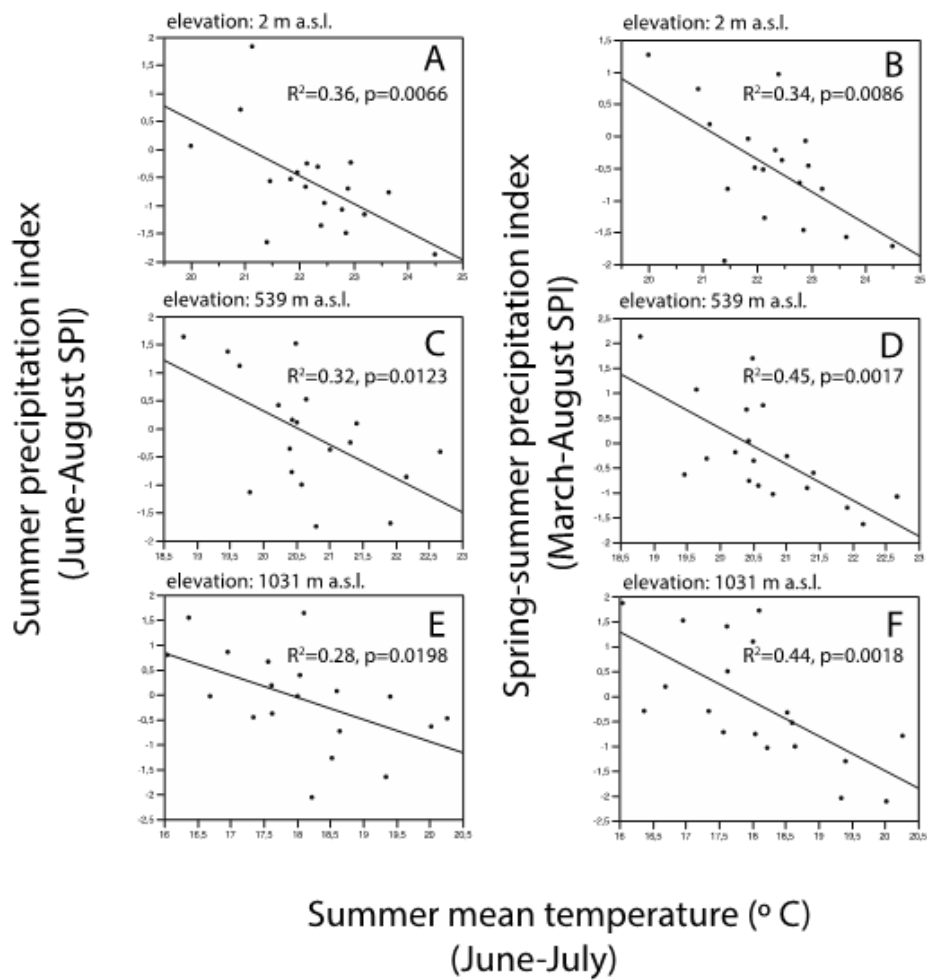


Figure A1: Observed relationships between seasonal rainfall (summer, spring–summer rains) and summer monthly temperatures (June–July) for three sites located at different elevations over the studied period (1994–2012). Water availability was estimated applying the standardised precipitation index (SPI).

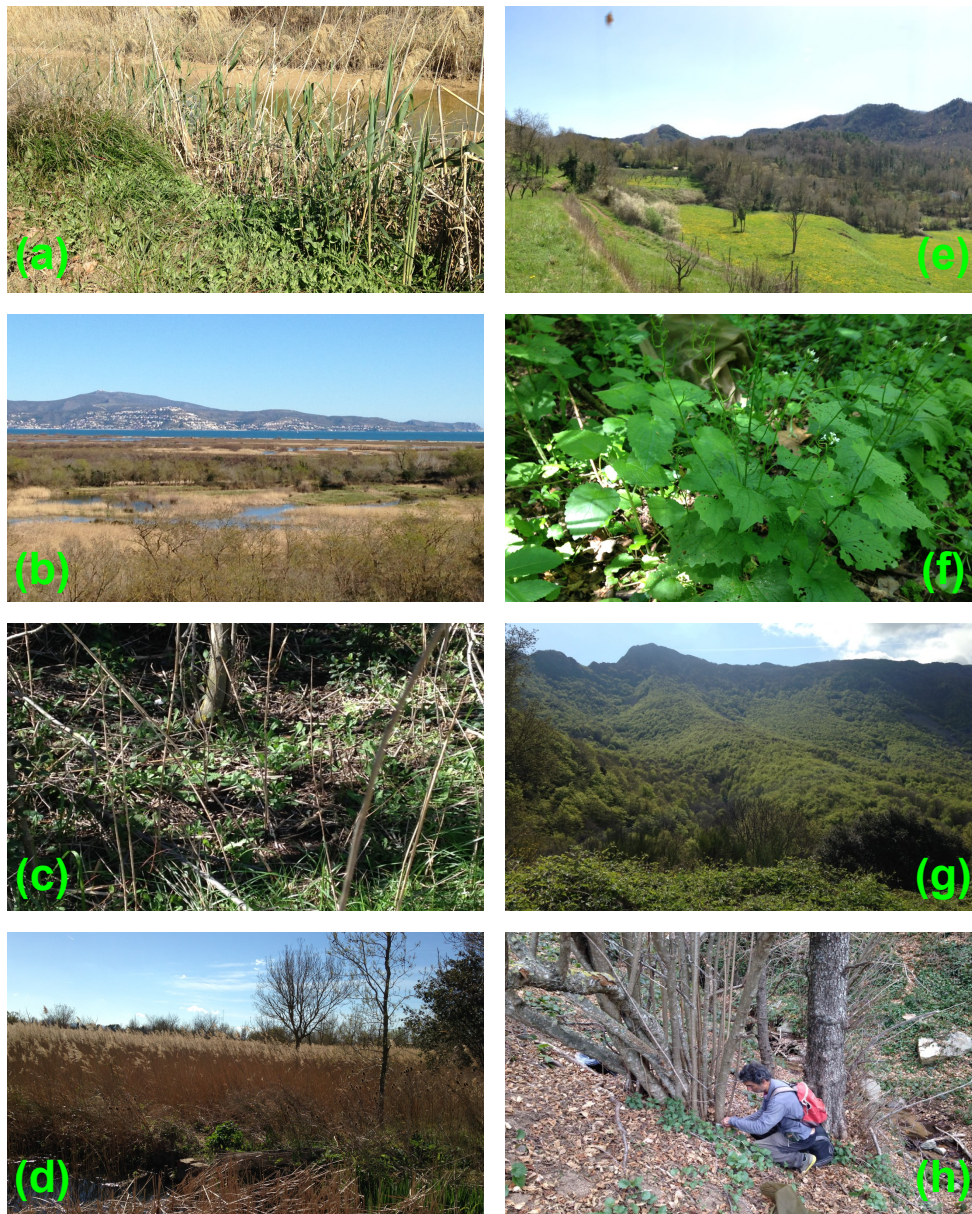


Figure A2: Photographs of the four sites inhabited by the studied *P. napi* populations. (a) Site 1. Lowland wetlands. Population of *Lepidium draba*. Delta del Llobregat Natural Park. Early spring (March). (b) Site 2. Lowland wetlands. Aiguamolls de L'Empordà Natural Park. Landscape view. Early spring (March) (c) Site 2. Lowland wetlands. Aiguamolls de L'Empordà Natural Park. Population of *Lepidium draba*. Early spring (March). (d) Site 2. Lowland wetlands. Population of *Brassica nigra*. Early spring (March). (e) Mid elevation site 3. Landscape view. Natural Park of the Zona Volcànica de la Garrotxa. Can Jordà. (f) Mid elevation site 3. Flowering plant of *Alliaria petiolata*. Late spring (May). (g) Mid elevation site 4. Montseny Natural Park. Landscape view. (h) Mid elevation Site 4. Population of *Alliaria petiolata*. Early spring (March).

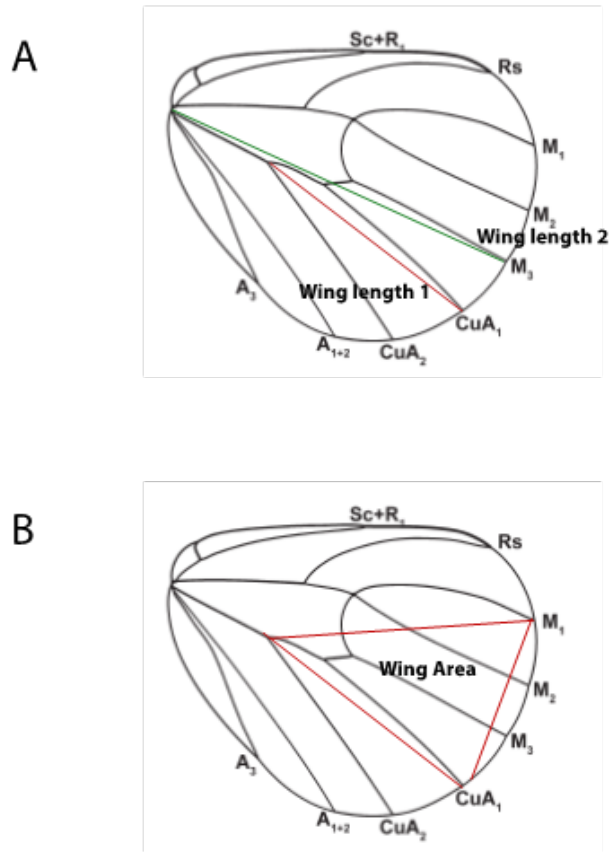


Figure A3: Landmarks used for the quantification of wing length, area, and melanism.

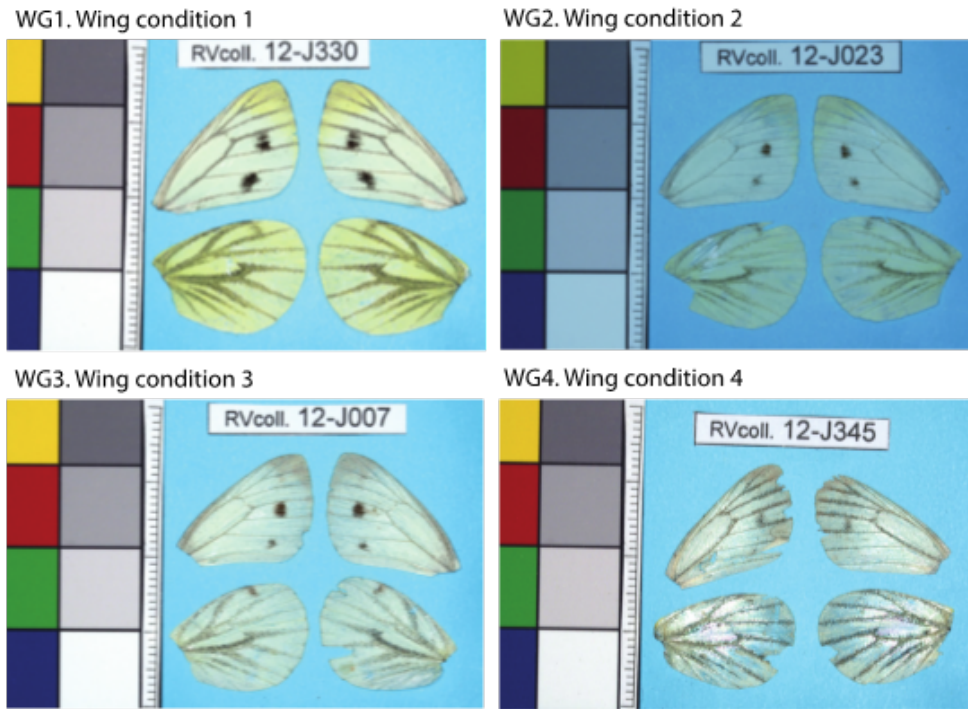


Figure A4: Observed variation in wing condition in *Pieris napi* samples.

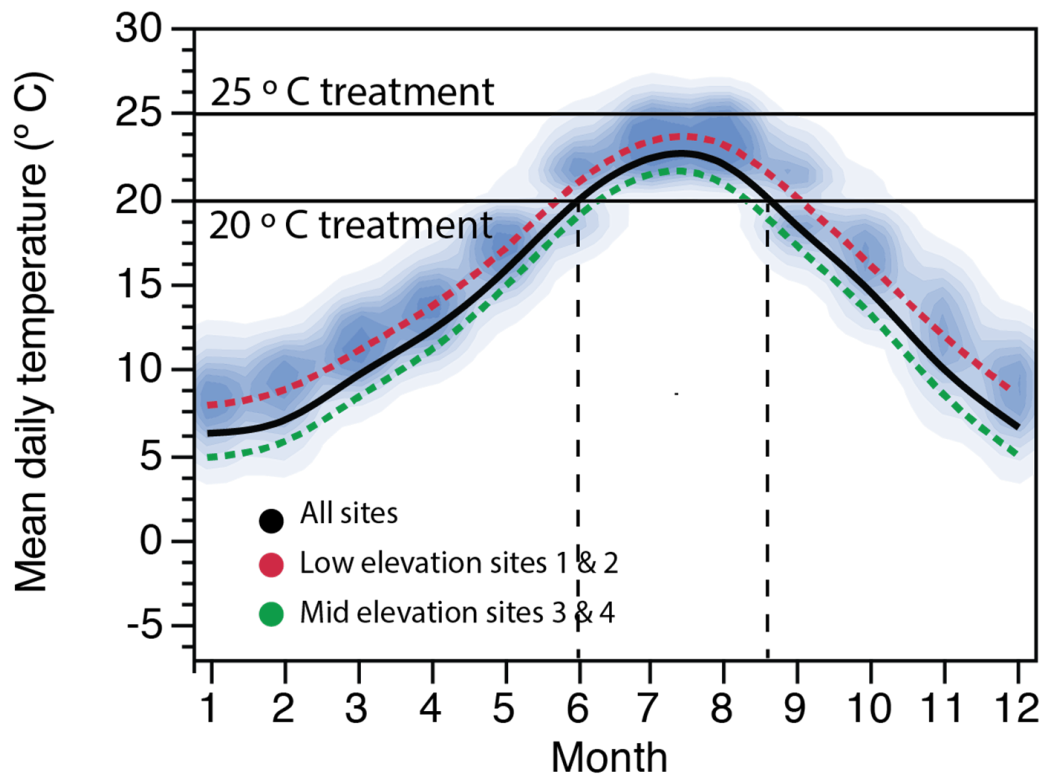


Figure A5: Observed variation in mean daily temperature (2014–2015). Early and late summer conditions correspond to a mean temperature of 20 °C. Warm summer days show mean daily temperatures around 25 °C or even higher values.

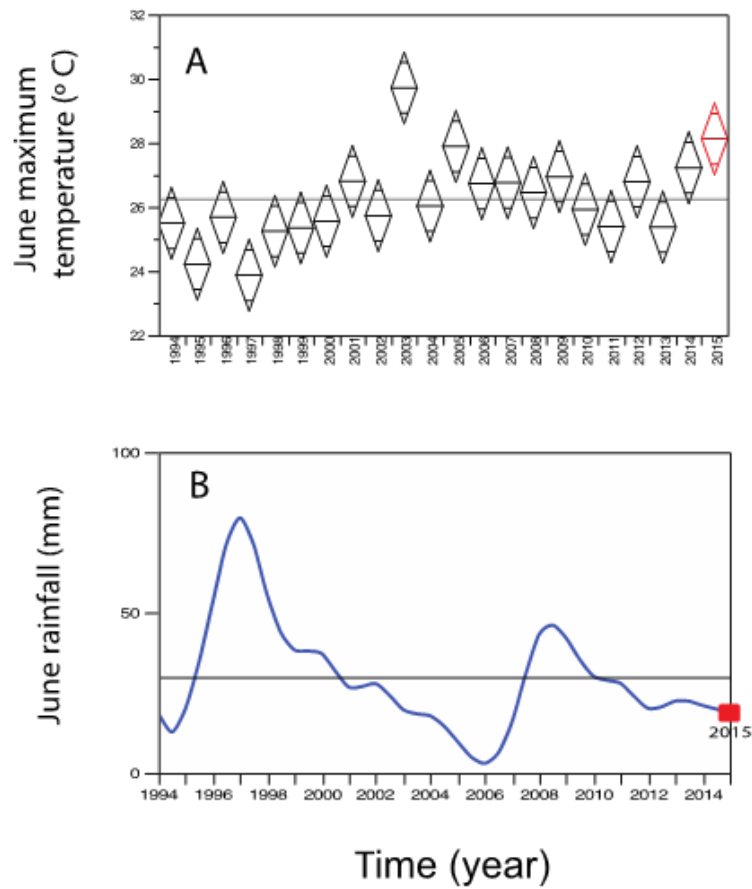


Figure A6: Comparison of June maximum temperatures (A) and June rainfall (B) over 1994–2015 recorded at the location of the LICOR6400 measurements (leaf stomatal conductance and leaf surface temperature, Aiguamolls de l'Empordà wetlands, lowland site 2). The year 2015 was the second warmest of the series and was also characterised by reduced rains (values below the mean for the 1994–2015 time period). Horizontal lines indicate the mean value for the 1994–2015.

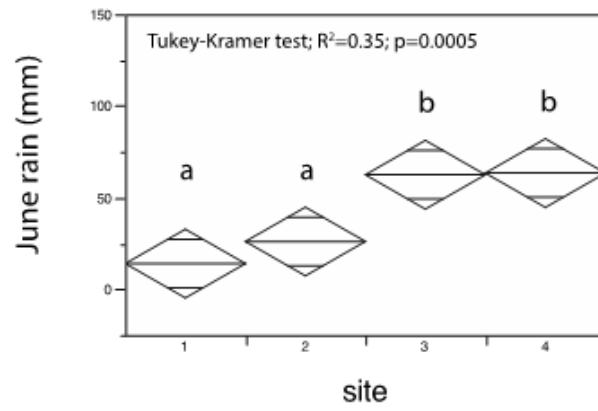


Figure A7: Comparison of June rain values recorded at the three sites over the 1997–2007 decadal drought period. The line across each diamond represents the June rainfall mean for each site. The vertical span of each diamond represents the 95% confidence interval for each site.

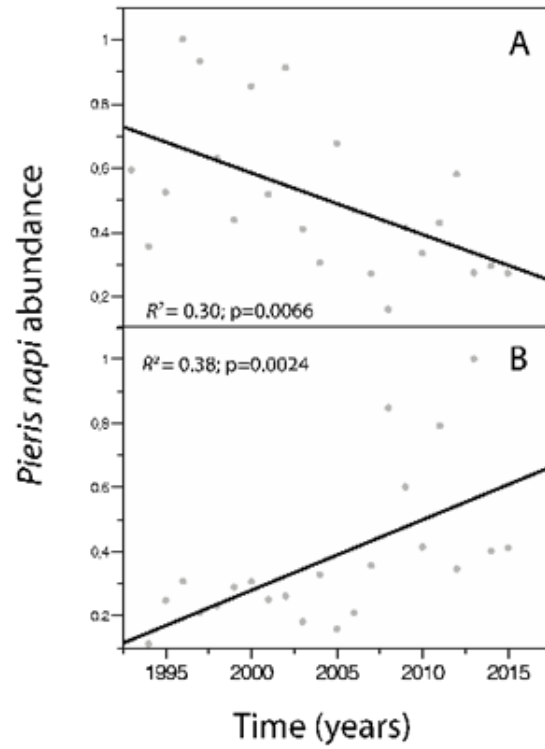


Figure A8: Observed significant demographic trends for 1994–2015 at sites 2 (A) and 3 (B). Site 4 maintained a stable and non-significant population trend during 1994–2015 (not shown), in line with the trends reported in Fig. 2.1.

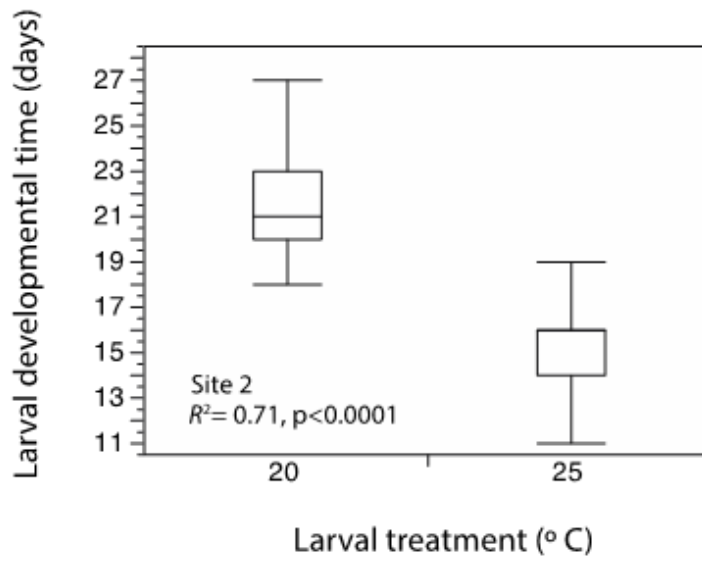


Figure A9: Observed effects of rearing temperature (20, 25 °C) on larval developmental time.

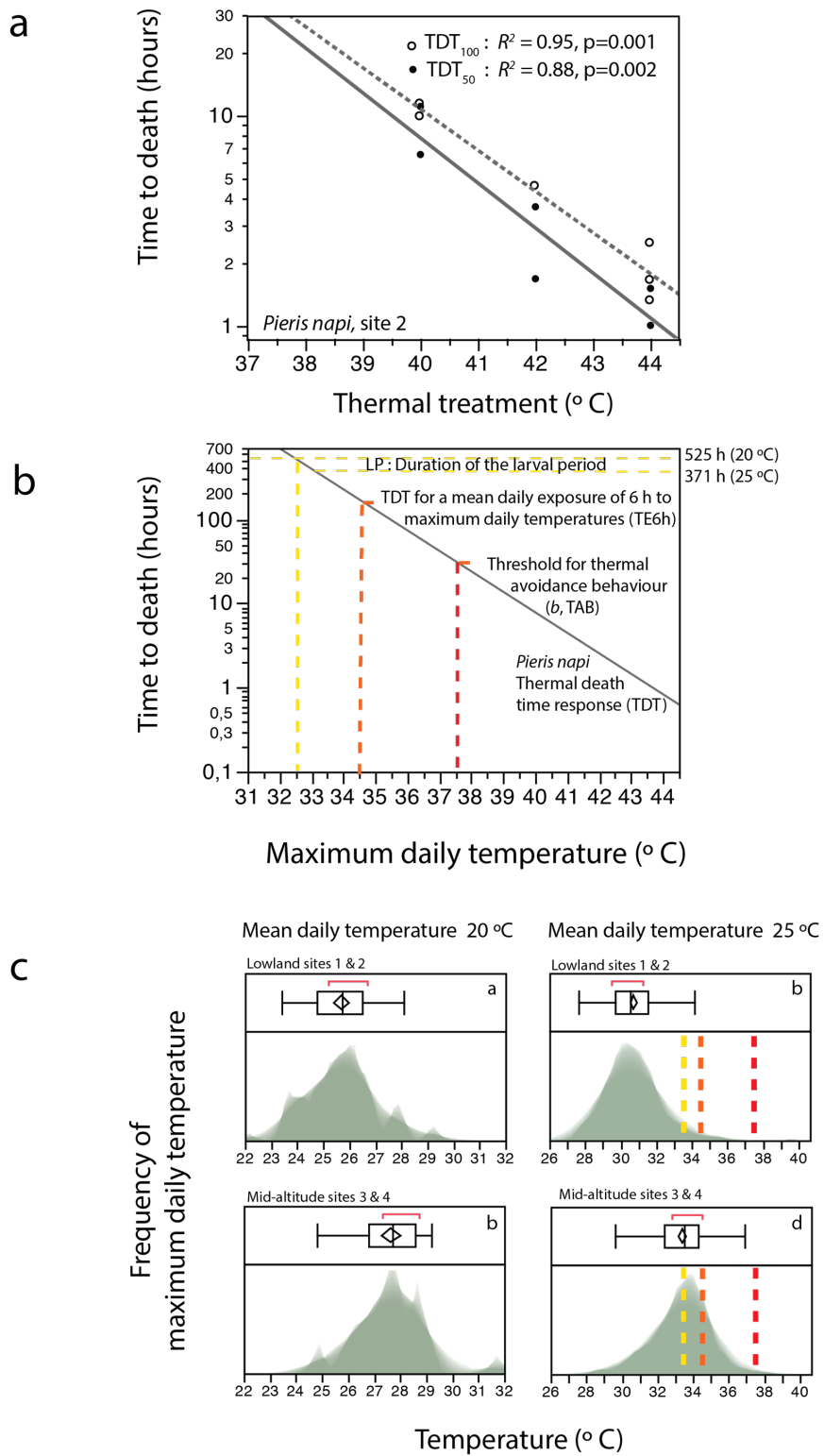


Figure A10: Legend on next page.

(Legend from Fig. A10). Thermal death time (TDT) relationships. a) Observed TDT fits for 100% of larval mortality and 50% of larval mortality (Rezende et al., 2014). b) Thermal thresholds for the duration of the larval period (LP, yellow line), and a mean daily exposure of 6h to stressful, maximum daily temperatures (TE6h, orange line). The thermal threshold for behavioural avoidance behaviour is also illustrated (red dotted line). c) Observed variation of maximum daily temperatures in summer days characterised by mean daily temperatures of 20 °C (panels a and b) and by mean daily temperatures of 25 °C (panels c and d). The thermal thresholds for LP, TE6h and TAB are indicated. The vertical line within the box represents the median sample value. The diamond describes the mean and the upper and lower 95% of the mean. The left and right sides of the diamond represent the upper and lower 95% of the mean. The ends of the box represent the 25th and 75th quantiles. The red bracket outside of the box identifies the most dense 50% of the observations. The lines that extend from each side of the box indicate the following distances: 25th quantile - 1.5×(interquartile range) and 75th quantile + 1.5×(interquartile range). A shadowgram is illustrated, overlaying multiple histograms with different bin widths.

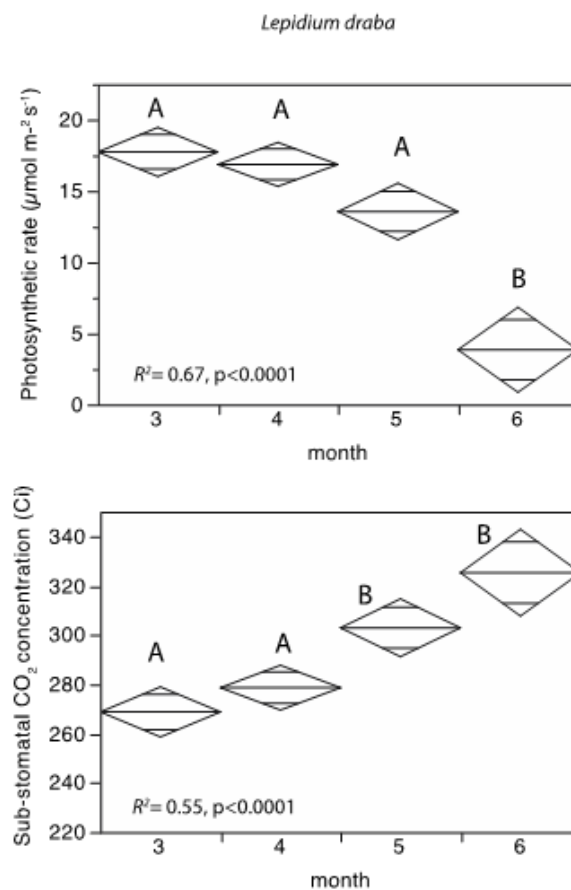


Figure A11: Observed monthly variation of leaf photosynthetic rates and sub-stomatal CO₂ concentration for the lowland plants *Lepidium draba*. The line across each diamond represents the mean. The vertical span of each diamond represents the 95% confidence interval for each treatment.

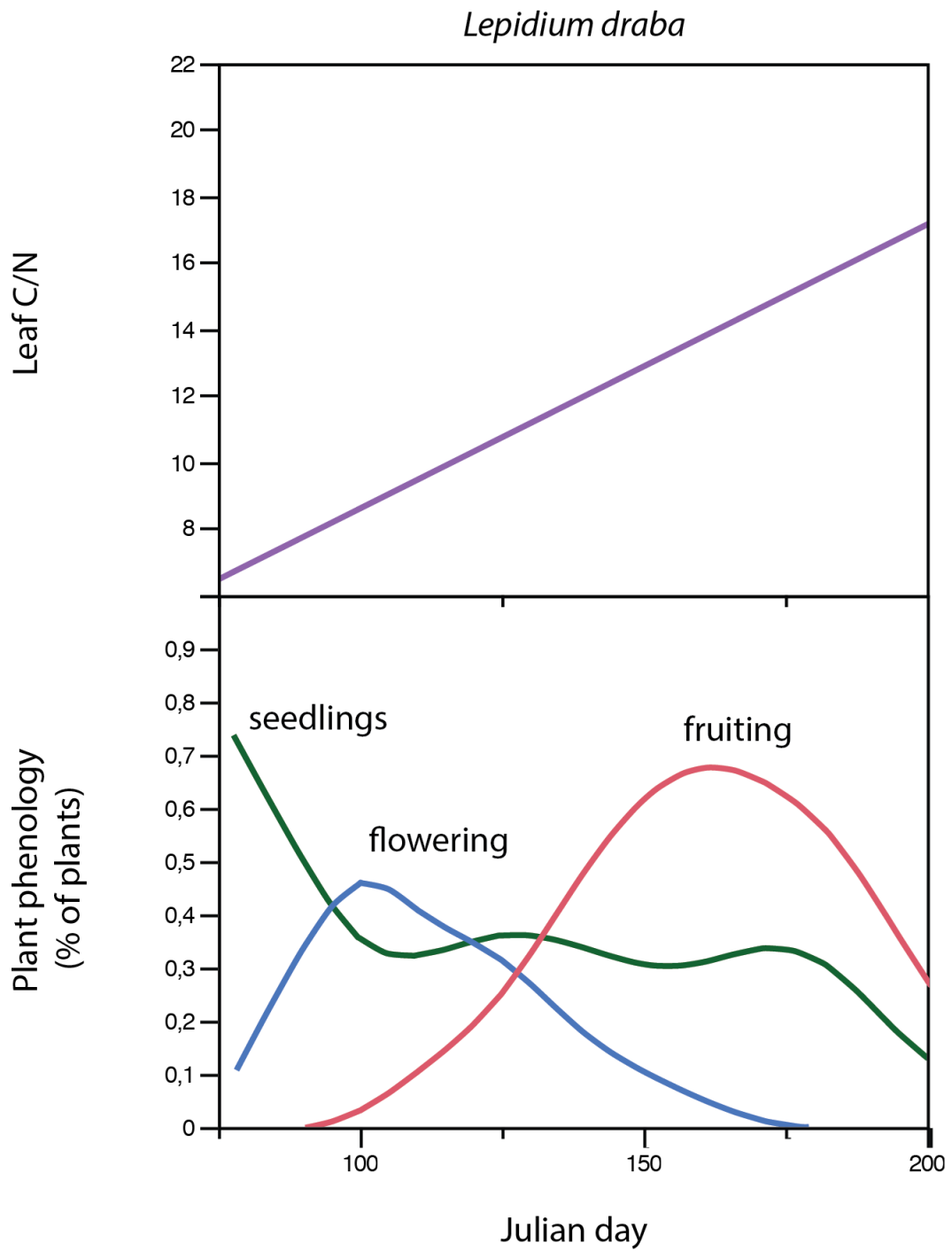


Figure A12: Observed temporal relationships between leaf C/N content and plant phenological change (*Lepidium draba*, lowland population, site 1).

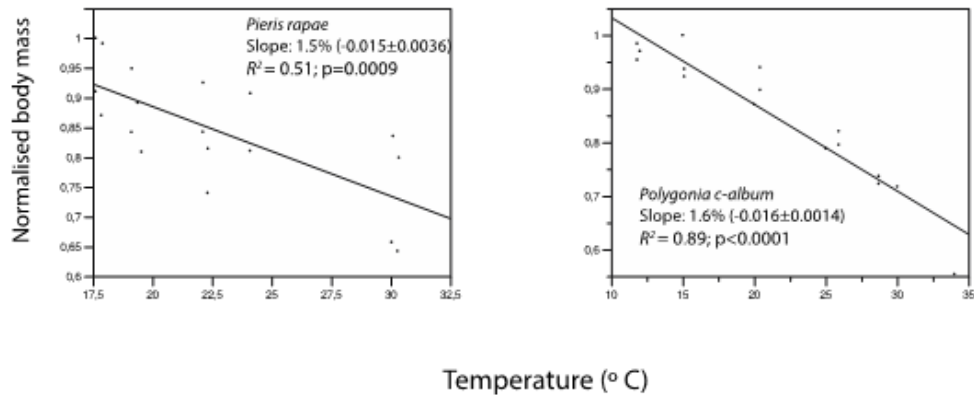


Figure A13: Observed relationships between normalised body mass and temperature in other temperate butterfly species (data extracted from Forster et al., 2012).

Table A1: Summary of the climatic, geographic, field sampling and ecological attributes of the four studied sites.

Site	Name	Latitude (°)	Longitude (°)	Mean elevation (m a.s.l.)	CBMS transect length (m)	Surveyed period	Habitat types	Mean annual temperature (°C)	Mean annual rainfall (mm)
1	Cal Tet, Delta del Llobregat	41.304160	2.116594	1	2928	7 years (1994–1997, 2007–2009)	Wetland, open fields, shrublands, riparian, and pine forests (<i>Pinus pinea</i>)	16	659
2	Cortalet, Aiguamolls de l'Empordà	42.223897	3.091586	2	4296	19 years (1994–2012)	Wetland, open fields, shrublands, riparian forests	15	628
3	Can Jordà, Parc Natural Zona Volcànica de la Garrotxa	42.144163	2.510836	539	1672	19 years (1994–2012)	Open fields, deciduous and evergreen oak forests (<i>Quercus ilex</i> , <i>Q. robur</i> , <i>Q. petraea</i> , <i>Q. pubescens</i>), beech forests (<i>Fagus sylvatica</i>)	12	1100
4	El Puig, Parc Natural del Montseny	41.800216	2.425547	1031	2017	19 years (1994–2012)	Open fields, deciduous and evergreen oak forests (<i>Q. ilex</i> , <i>Q. robur</i> , <i>Q. pubescens</i>), beech forests (<i>Fagus sylvatica</i>)	10	983

Table A2: Number of butterfly samples collected at each site. Numbers in brackets for 2015 indicate the number of samples used for isotopic analyses.

Site	Number of butterfly samples		
	2014	2015	TOTAL
1	168	164 (70)	332
2	169	190 (90)	359
3	269	137 (78)	406
4	90	78 (32)	168
Total number	696	569 (270)	1265

Table A3: Number of adult individuals obtained for each family line.

Female (code)	Number of butterflies in the Fi
Site 2	
Female 1 (AEC8)	27
Female 2 (AED1)	33
Female 3 (AED2)	25
Female 4 (AED3)	27
Female 5 (AED4)	31
Site 3	
Female 6 (CJ1)	8
Female 7 (CJ3)	24
Total number	175

Table A4: Summary of the LascarElectronics EL-USB-2-LCD sensors located a host plant microsites.

Sensor	Habitat type	Host plant
Lowland sites		
1	closed	<i>Lepidium draba</i>
2	closed	<i>Lepidium draba</i>
3	open	<i>Lepidium draba</i>
4	open	<i>Lepidium draba</i>
5	open	<i>Lepidium draba</i>
6	open	<i>Lepidium draba</i>
7	open	<i>Brassica nigra</i>
8	open	<i>Brassica nigra</i>
Mid-elevation sites		
9	closed	<i>Alliaria petiolata</i>
10	closed	<i>Alliaria petiolata</i>
11	closed	<i>Alliaria petiolata</i>
12	closed	<i>Alliaria petiolata</i>
13	open	<i>Alliaria petiolata</i>
14	open	<i>Alliaria petiolata</i>

Table A5: Summary of the meteorological stations. From the links, we obtained the following climatic variables: daily mean, maximum, and minimum temperature, relative humidity, solar radiation, atmospheric pressure, wind strength and direction, rainfall.

Meteorological stations	Link to the data	Distance to the CBMS transect (km)	Elevation (m.a.s.l)
El Prat (site 1)	Link to the data	2.04	8)
Sant Pere Pescador (site 2)	Link to the data	3.37	4
Olot (site 3)	Link to the data	2.96	433
Viladrau (site 4)	Link to the data	5.15	953 m

Table A6: Number of samples of each host plant species in the stoichiometric analyses (%C and %N).

Species	Sample size
Lowland populations	
<i>Lepidium draba</i>	146
<i>Brassica nigra</i>	72
Mid-elevation populations	
<i>Alliaria petiolata</i>	73

Table A7: OLS models with the single selected climatic predictor.

Population	Climatic predictors	Estimate	<i>t</i>	<i>P</i>	<i>R</i> ²	<i>AIC_c</i>	<i>BIC</i>
Site 2 (Lowland)	Summer rainfall (June)	8.80 ± 3.10	2.84	0.0113	0.32	271.42	272.65
Site 3 (Mid-elevation)	Summer rainfall (June)	1.26 ± 0.34	3.65	0.0020	0.44	207.15	209.16

Table A8: OLS models selecting two climatic predictors. OLS models are shown for populations having complete demographic time series (1994–2012) and also showing significant populations trends (sites 2 and 3).

Population	Climatic predictors	Estimate	<i>t</i>	<i>P</i>	<i>R</i> ²	<i>AIC_c</i>	<i>BIC</i>
Site 2 (Lowland)	Summer rainfall (June)	11.94 ± 2.96	4.03	0.0010	0.52	268.24	269.17
	Previous autumn temperature (October)	155.33 ± 61.19	2.54	0.0219			
Site 3 (Mid-elevation)	Summer rainfall (June)	1.67 ± 0.30	5.49	<0.0001	0.66	200.86	201.78
	Autumn temperature (November)	10.43 ± 3.22	3.23	0.0052			

Table A9: OLS models combining climate and dynamic landcover data.

Population	Predictors	Estimate	<i>t</i>	<i>P</i>	<i>R</i> ²	<i>AIC_c</i>	<i>BIC</i>
Site 2 (Lowland)	Summer rainfall (June)	8.71 ± 2.37	3.67	0.0023	0.75	259.50	259.61
	Previous autumn temperature (October)	187 ± 46	4.04	0.0011			
	Grassland and herbaceous meadow cover	3.34E-3 ± 8.94E-4	3.74	0.0020			
Site 3 (Mid-elevation)	Summer rainfall (June)	1.44 ± 0.21	6.68	<0.0001	0.85	189.09	189.19
	Autumn temperature (November)	6.63 ± 2.37	2.79	0.0138			
	Wetland and continental water cover	5.80E-3 ± 1.33E-3	4.36	0.0006			

Table A10: Variance inflation factors (VIF) associated to the reported coefficients in Table A8. VIF values higher than 5 units indicate possible effects of collinear predictor variables in the standard errors of the estimated coefficients. All observed VIF values were lower than 5 units and associated to small design standard errors relative to the standard error in the coefficients.

Population	Climatic predictors	Coefficient standard error	VIF	Design standard error
Site 2 (Lowland)	Summer rainfall (June)	2.96	1.40	0.01
	Previous autumn temperature (October)	61.19	1.25	0.27
Site 3 (Mid-elevation)	Summer rainfall (June)	0.30	1.21	0.01
	Autumn temperature (November)	3.22	1.21	0.08

Table A11: Variance inflation factors (VIF) associated to the reported coefficients in Table A9. VIF values higher than 5 units indicate possible effects of collinear predictor variables in the standard errors of the estimated coefficients. All observed VIF values were lower than 5 units and associated to small design standard errors relative to the standard error in the coefficients.

Population	Climatic predictors	Coefficient standard error	VIF	Design standard error
Site 2 (Lowland)	Summer rainfall (June)	2.37	1.40	0.01
	Previous autumn temperature (October)	46	1.25	0.27
	Grassland and herbaceous meadow cover	8.94E-4	1.2	5.21E-6
Site 3 (Mid-elevation)	Summer rainfall (June)	0.21	1.21	0.01
	Autumn temperature (November)	2.37	1.39	0.09
	Wetland and continental water cover	1.33E-3	1.16	4.96E-5

Table A12: Summary of the OLS model analysing the effects of treatment, sex, and family on butterfly wing size (mm) in the split-brood common garden experiment (20 vs 25 °C) for site 2.

Model fit: $R^2 = 0.32$, $P < 0.0001$, $AIC_c = 3447.31$				
Variable	df	Sum of squares	F ratio	P
Thermal treatment	1	9.677E10	35.90	<0.0001
Sex	1	2.842E10	10.54	0.0015
Family	4	6.680E10	5.27	0.0006

Table A13: Parameter estimates of the OLS model for the split-brood common garden experiment for lowland individuals (site 2). The model describes the effects of treatment (20 and 25 °C), sex and family on wing size variation (length, mm).

Term	Estimate	Std Error	t ratio	P	Lower 95CI	Upper 95CI
Intercept	399760.14	4550.64	87.85	<.0001	390759.13	408761.15
Treatment [20]	27642.77	4613.46	5.99	<.0001	18517.52	36768.02
Treatment [25]	-27642.77	4613.46	-5.99	<.0001	-36768.02	-18517.52
Sex [Female]	-14395.60	4433.10	-3.25	0.0015	-23164.11	-5627.08
Sex [Male]	14395.60	4433.10	3.25	0.0015	5627.08	23164.11
Female [AEC8]	16739.70	8991.73	1.86	0.0649	-1045.58	34525.00
Female [AED1]	-24545.58	8287.69	-2.96	0.0036	-40938.31	-8152.84
Female [AED2]	27841.75	9351.96	2.98	0.0035	9343.93	46339.56
Female [AED3]	-21064.05	9120.41	-2.31	0.0225	-39103.88	-3024.21
Female [AED4]	1028.17	8696.17	0.12	0.9061	-16172.51	18228.86

Table A14: Summary of the OLS model for the split-brood common garden experiment considering both lowland (site 2) and mid elevation individuals (site 3). The model describes the effects of site, treatment (20 vs 25 °C), family and sex on wing size.

Model fit: $R^2 = 0.37$; $P < 0.0001$, $AIC_c = 4248.05$				
Variable	df	Sum of squares	F ratio	P
Site	1	567174780.77	0.2114	0.6463
Temperature[Site]	2	169582508213	31.6022	<.0001
Family[Site]	5	56797751889	4.2338	0.0012
Sex	1	30618217610	11.4116	0.0009

Table A15: Parameter estimates of the OLS model for the split-brood common garden experiment for lowland and mid elevation individuals (site 2 and 3). The model describes the effects of treatment (20 and 25 °C), sex and family on wing size variation (length, mm).

Term	Estimate	Std Error	t ratio	P	Lower 95CI	Upper 95CI
Intercept	430694.58	6969.52	61.80	<.0001	416931.74	444457.42
Site 2	-3208.16	6977.73	-0.46	0.6463	-16987.19	10570.87
Site 2×treatment	-55297.77	9205.26	-6.01	<0.0001	-73475.55	-37119.99
Site 3×treatment	-98553.96	18921.63	-5.21	<0.0001	-135918.82	-61189.10
Sex[Female]	-13518.75	4001.87	-3.38	0.0009	-21421.31	-5616.19

Table A16: Buffering and amplification effects observed in host plant microsite climatic data. Thermal offsets are calculated from the difference between macroclimatic and microclimatic records. Negative values indicate thermal buffering effects (microclimate cooler than macroclimate), and positive values, mean ground level thermal amplification (microclimate warmer than macroclimate).

Microsite	Site	Thermal offset (°C)	Std err	Lower 95CI	Upper 95CI	Montane-to-lowland ratio
Closed	Lowland (sites 1 and 2)	-0.79	0.32	-1.42	-0.15	6.58
	Mid-elevation (sites 3 and 4)	-5.20	0.17	-5.55	-4.85	
Open	Lowland (sites 1 and 2)	1.90	0.18	1.54	2.26	1.60
	Mid-elevation (sites 3 and 4)	3.04	0.28	2.49	3.58	

Table A17: Summary of the OLS model for the experiment analysing the effect of thermal treatment, family, and larval weight on thermal death time (TDT).

Model fit: $R^2 = 0.81$, $P < 0.0001$				
Variable	df	Sum of squares	F ratio	P
Thermal treatment	1	6.108	117.796	<0.0001
Family	5	1.067	4.115	0.0033
Larval weight	1	0.502	9.674	0.0031

A.2 Phenotypic biomarkers of climatic stress

A phenotypic biomarker is a trait or measurable characteristic that is objectively measured and evaluated as an indication of the biological state of an organism or a specific biological process (Colin et al., 2016; Group, 2001).

We hypothesise that phenotypic biomarkers of thermal stress on insect performance should present a critical trait value beyond which negative effects on larval performance tend to occur in natural populations (Fig. A14a). This critical trait value (P^*) should be in turn associated to a threshold value of thermal stress (T^*). In the range of studied stressful temperatures, it would be a desirable feature that the phenotypic biomarker responds linearly to temperature variation (as in Fig. A14). In thermally buffered sites, we would expect the observation of biomarker values higher than P^* (Fig. A14). In the next section we develop a simple mathematical model for a formal definition of the T^* value. This model also illustrates how T^* values may be modified in specific field locations by thermal buffering effects, larval behaviour and host plant quality.

A.2.1 A simple model integrating thermal effects on survival and fecundity, habitat and behavioural thermal buffering, and host plant quality effects

Thermal performance curves can be described by Gaussian, quadratic, Weibull, or exponentially modified gaussian functions (Angilletta, 2006). In the case of quadratic functions, insect performance functions such as survival (S) and fecundity (F) can be described as:

$$S = aT - bT^2 + k_1 \quad (\text{A.1})$$

$$F = cT - dT^2 + k_2 \quad (\text{A.2})$$

Fecundity and survival functions are often maximised at intermediate temperatures (Kingsolver and Huey, 2008). In Eqs. A.1 and A.2, parameters a and c describe positive effects of temperature on survival and fecundity, respectively. b and d describe negative effects of warm temperatures on organism performance. The available empirical evidence indicates that thermal conditions can differently affect fecundity and survival functions. For example, for insect model species such as *Drosophila melanogaster* optimal temperatures for insect fecundity are higher than for survival (Kingsolver and Huey, 2008). Fig. A15 and the parameters in Table A18 A simulate this case.

Survival and fecundity are key determinants of population growth. For example, the instantaneous growth rate of a population growing exponentially according to equals to:

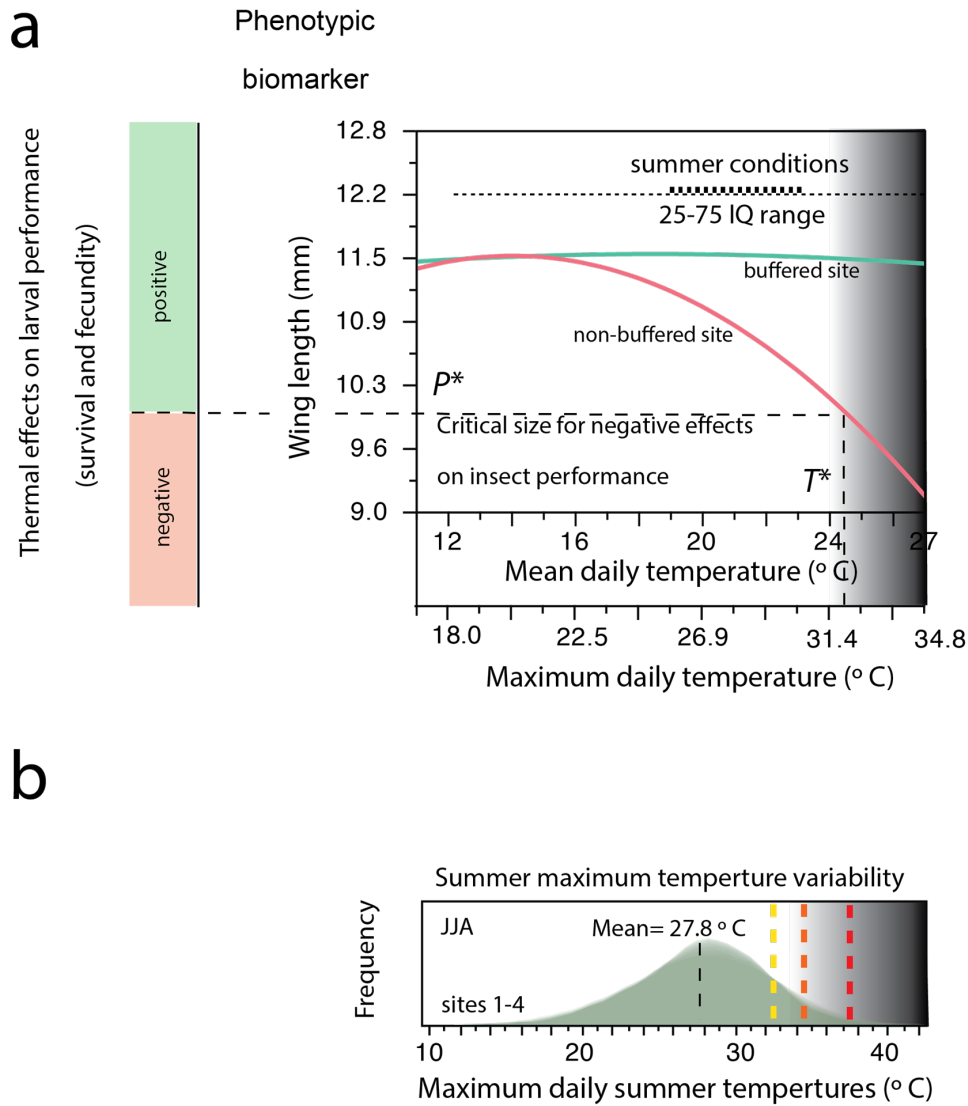


Figure A14: (a) Conceptual figure for the definition of phenotypic biomarkers of climatic stress. (b) Observed variation of maximum daily temperatures in sites 1-4. Experimental TDT and TAB thermal thresholds are illustrated (yellow, orange, and red lines, see Fig. A10 for detailed definitions).

$$\frac{dN}{dT} = rN$$

where r is the sum of instantaneous survival rate per individual (s) and the instantaneous birth rate per individual (ϕ):

$$r = s + \phi$$

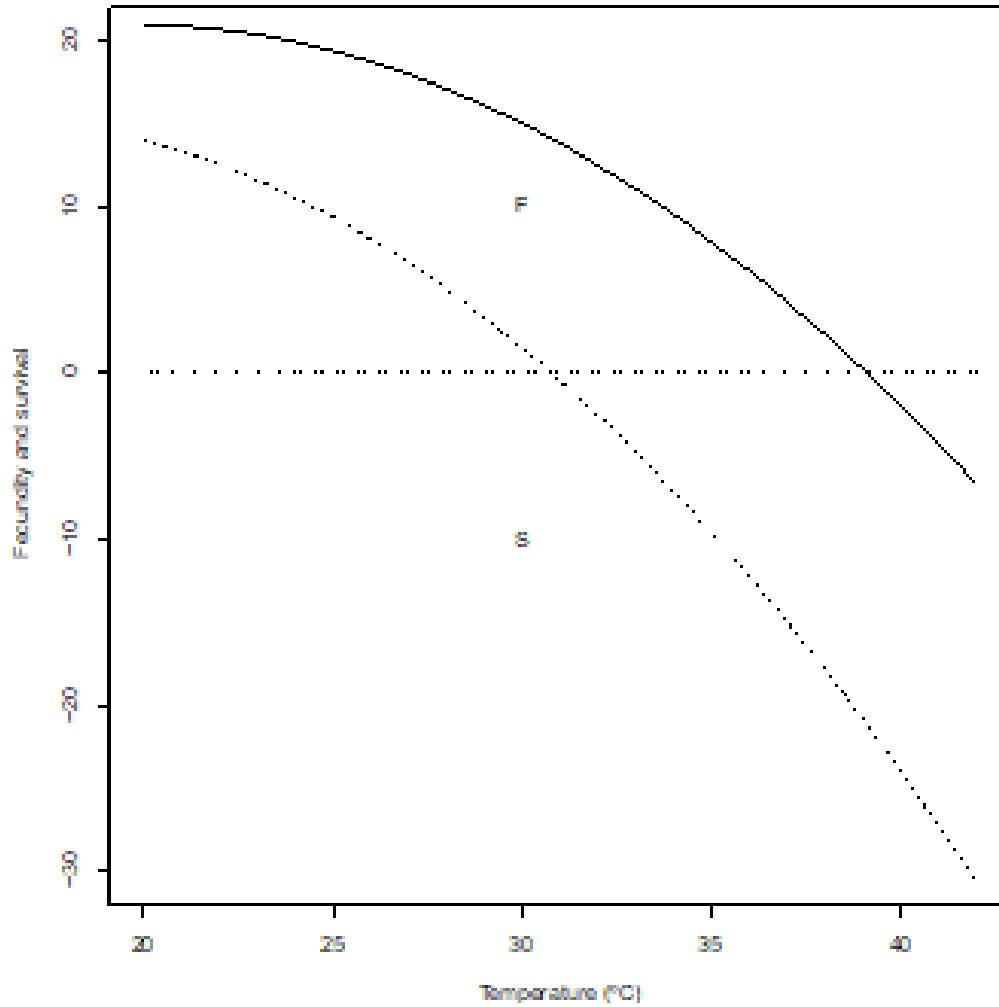


Figure A15: A plot of Eqs. A.1 and A.2. The parameters are specified in Table A18.

We could hypothesise that phenotypic traits linearly associated with temperature such as body mass and wing length might act as biomarkers of negative effects on insect performance only beyond a threshold temperature (T^*).

Negative effects on population growth should be observed when $r \leq 0$. In the Eqs. A.1 and A.2, if we assume that constants k_1 and $k_2 = 0$, the threshold temperature causing negative effects on butterfly demographic performance would equal to:

$$T^* = \frac{a + c}{b + d} \quad (\text{A.3})$$

As illustrated in Fig. A16, setting the parameters specified in the Table A18, T^* would

Table A18: Parameter values in Fig. A15

Parameter	Value
a	2.15
b	0.055
c	2.00
d	0.065
k_1	0
k_2	0

equal to 34.6 °C.

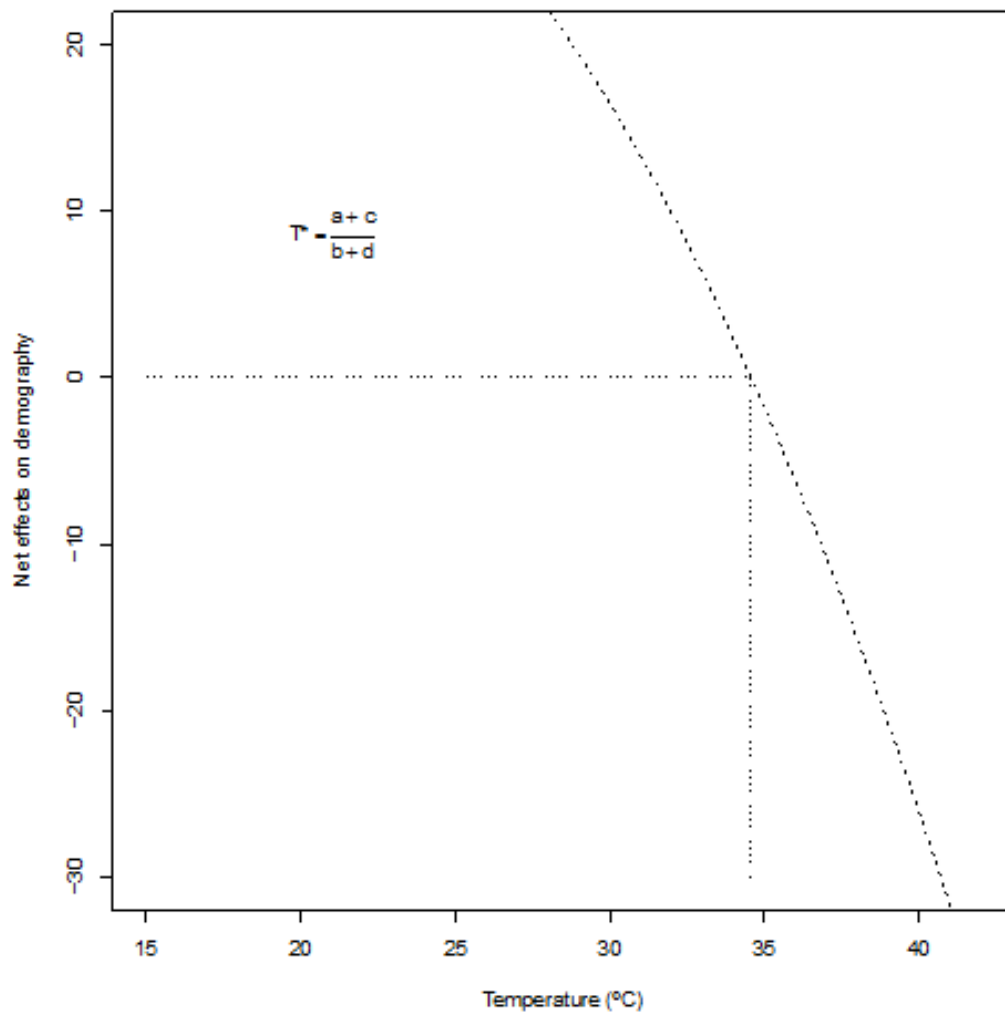


Figure A16: Simulated threshold temperature (T^*) for negative effects on demography applying quadratic thermal performance functions (Eqs. A.1 and A.2).

Table A19: Parameter values in Fig. A17

Parameter	Value
a	2.15
b	0.055
c	2.00
d	0.065
k_1	0
k_2	0
e	0.003
f	0.003

Modelling the effects of habitat and behavioural thermal buffering

Habitat and behavioural buffering can reduce the impacts of extremely warm environmental temperatures on insect survival functions. In this simple model, we could model the positive effects of habitat and behavioural buffering on survival with the parameters e and f :

$$S = aT - bT^2 + eT^2 + fT^2 + k_1 \quad (\text{A.4})$$

The positive effects of habitat and behavioural buffering would then increase the threshold temperature T^* for the observation of negative effects on insect performance. Fig. A17 and the parameters in Table A19 A simulate this case.

In this case T^* would equal to:

$$T^* = \frac{a + c}{b + d - e - f}$$

Note that negative effects of habitat thermal amplification could be modelled setting the coefficient e as a negative value.

Modelling the additional effects of host plant quality and thermal stress

Similarly, we could hypothesise that reduced host plant quality due to summer drought and thermally induced advanced plant phenology would negatively impact the survival curve. Butterfly larvae increase host plant consumption in thermally stressful conditions, balancing water and energy losses due to thermal stress. Reduced host plant quality during summer drought could therefore significantly alter the organism water balance and

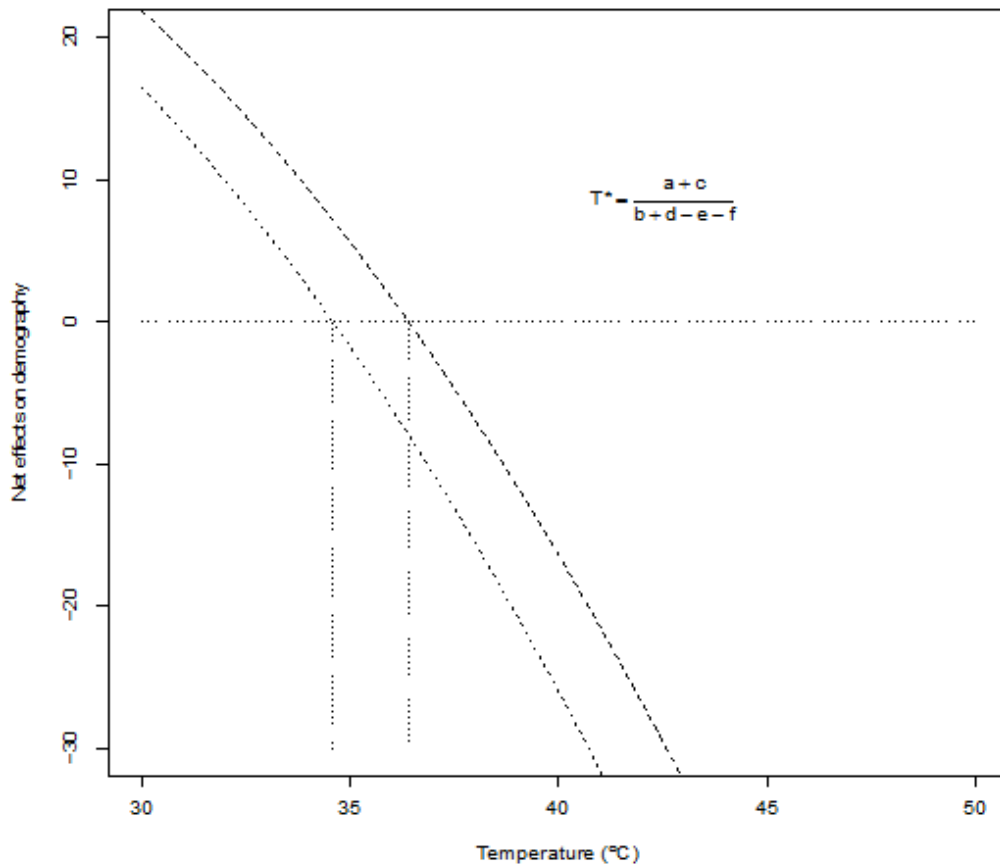


Figure A17: A simulation of the observed change in the threshold temperature (T^*) for negative effects on butterfly performance. Due to the positive effects habitat and behavioural buffering on insect survival (parameters e and f in Eq. A.4 and Table A19) the critical temperature T^* increases from 34.6 °C (simulation without buffering, left curve) to 36.4 °C (with habitat and behavioural buffering effects, right curve). This simulation illustrates how habitat and behavioural buffering change critical threshold environmental temperatures, protecting in this way insects from the effects of extreme temperatures. Because body size and wing length are linearly related to environmental temperatures during growth, in thermally buffered populations we would expect to observe larger individuals when exposed to the same maximum daily temperatures, due to larger T^* values in buffered sites.

the metabolic costs associated to thermal stress. We could model these negative effects on survival introducing an additional parameter (g):

$$S = aT - bT^2 + eT^2 + fT^2 - gT^2 + k_1 \tag{A.5}$$

and T^* would equal in this example to:

$$T^* = \frac{a + c}{b + d - e - f + g}$$

Setting the following parameters (Table A20, $g = 0.01$), reduced host plant quality would imply more negative impacts on larval performance of high summer temperatures, and the critical value for negative effects (T^*) would be reduced from 36.4 °C to 33.46 °C in this example (Fig. A18). In a similar way, the negative effects of leaf surface thermal amplification could be modelled adding an additional parameter to the model (h).

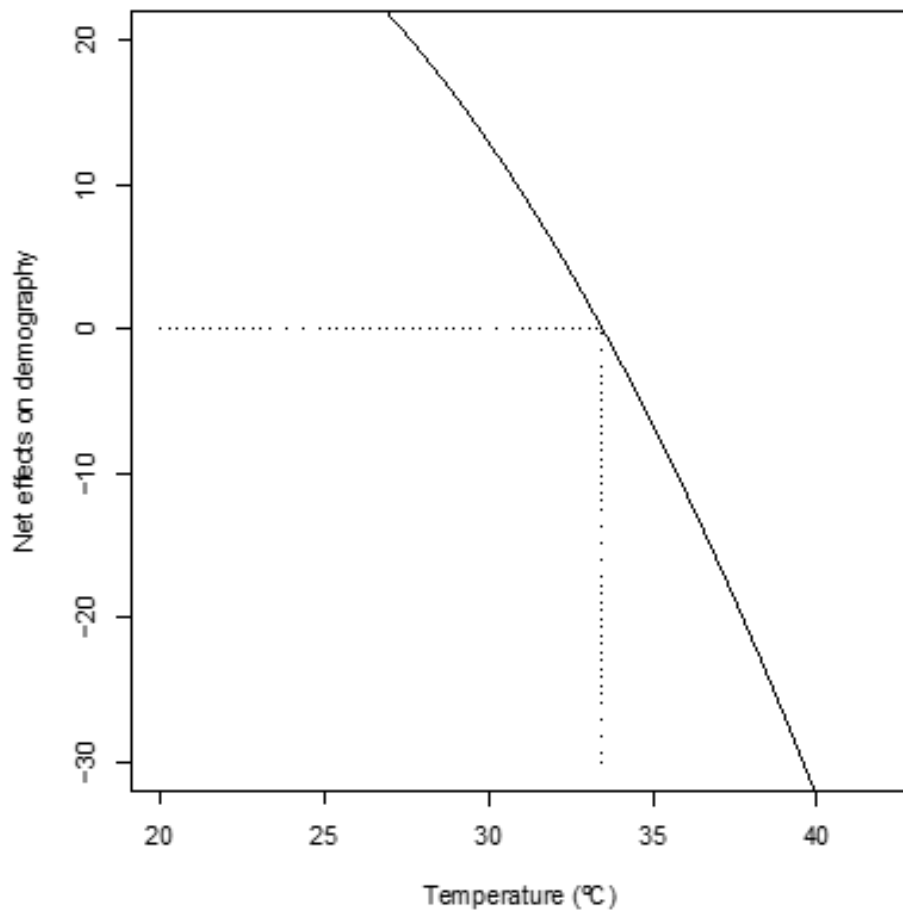


Figure A18: A simulation of the observed change in the threshold temperature (T^*) for negative effects on butterfly performance based on Eq. A.5 and the parameters from Table A20.

Table A20: Parameter values in Fig. A18

Parameter	Value
a	2.15
b	0.055
c	2.00
d	0.065
k_1	0
k_2	0
e	0.003
f	0.003
g	0.01

Appendix B

Chapter 4 - Supporting materials

B.1 Characterisation of the host-plant microhabitats from open–closed ecotones. Measurement and analysis of the vegetation cover and classification of microhabitats according to their degree of closure.

We have termed *open–closed ecotones* the areas where open habitats contact with closed habitats and the transition zones in between, which present diverse microhabitats differing in their degree of closure. The present study assessed whether microhabitat variation across ecotones generated interspecific differences in thermal exposure, thermal mortality, and host-plant condition of two closely-related butterflies. For this reason, we measured vegetation cover in each microsite of host plant monitoring, which represented the different microhabitats from open–closed ecotones. Measurements of vegetation cover considered, on the one hand, the canopy that shrubs and trees provided and, on the other, the ground cover by herbaceous plants, as both vegetal layers could influence microenvironmental conditions of the studied host plants (medium-size herbs). The measurements were repeated each monitoring day in order to additionally assess the temporal dynamics of vegetation cover in each microsite.

Shrubs and trees' influence on each microsite was assessed through the measurement of the canopy closure (i.e. “the proportion of the sky hemisphere obscured by vegetation when viewed from a single point”; Jennings, 1999). Canopy closure is supposed to be more tightly associated with light and microclimatic conditions at the understory than canopy cover, which just takes into account the vertical projection of tree crowns on the floor (Jennings, 1999). The method of measurement consisted in visually estimating the percent area occupied by the canopy, assigning it to one of the cover classes defined by Daubenmire (1959) —0–5%, 5–25%, 25–50%, 50–75%, 75–95%, and 95–100%— and taking its midpoint. The ocular estimation was conducted in each one of the vertical and the

four cardinal directions, separating shrubs from trees. For the four cardinal directions, total canopy closure was then calculated as the mean of shrub closure and tree closure, as no overlapping between these two vegetal layers was assumed to occur. Because trees and shrub layers were considered to overlap in the vertical projection, the maximum of the two canopy closure values was taken as total canopy closure in this case. Finally, canopy closure in each microsite was calculated as the mean value of canopy closure in the five directions.

The herbaceous layer was characterised both as herbaceous ground cover and as mean herb height. Herbaceous cover was estimated by the point-intercept method. A rope with 15 knots separated by distances of 50 cm was randomly placed in the host plant microsite. For each knot, we annotated whether it contacted an herbaceous plant or, contrarily, if it had fallen on bare soil. Herbaceous cover was then calculated as the relative frequency of knots covered by herbs. In addition, height of herbs (cm) was also measured in the herbaceous plants contacted with the rope (or in the nearest herb in case the knot fell on bare soil) and the mean of the height of these 15 individuals was then calculated.

Data analyses were conducted with R version 3.6.1 (R Core Team, 2019). They were based on a careful examination of canopy closure, herbaceous cover, and herbs height data including both analyses of spatial variation between microsities in each study site (ANOVA and post-hoc Tukey test) and the assessment of their temporal dynamics (LOESS). Combining this information with field observations during the monitoring period, we finally classified the host-plant microsities into four microhabitat types: closed (C), semi-closed (SC), semi-open (SO), and open (O). Photographs of the different microhabitat types for each site can be found in Fig. B2. The main results of the analyses of vegetation cover are shown in Fig. B3. More open microhabitats (i.e. open and semi-open) were characterised by presenting a mean canopy closure of the whole monitoring period inferior to 50%. Because shrubs and trees had a sparser distribution there, the herbaceous layer was considered to be more determining for these microhabitats. Semi-open microhabitat categories were then assigned to open areas (such as fields or path margins) with taller herbs and higher herbaceous cover (Fig. B3). Microhabitats more integrated in the forested and shrubby areas of the open–closed ecotones presented values of mean canopy closure greater than 50%. Among them, those that tended to reach inferior values of maximum canopy closure (Fig. B3d) or reached them later (Fig. B3b) were classified as semi-closed microhabitats to differentiate them from the closed microhabitat category.

During the census of oviposition behaviour we weren't able to characterise microhabitat closure with this degree of detail, so we decided to integrate semi-closed and semi-open microhabitats in a unique category (intermediate canopy closure).

B.2 Supplementary tables

Table B1: Information on the installed standalone data loggers.

Site	Microhabitat	Sensor code	First year	Last year
Mid-elevation	C	s12	2014	2018
	SC	s14	2014	2017
	SC	s15	2014	2017
	SO	s1	2017	2018
	SO	s3	2014	2017
	O	s6	2014	2018
	O	s7	2014	2017
Lowland	C	s11	2017	2018
	C	s13	2014	2017
	SC	s2	2017	2018
	SO	s4	2017	2018
	SO	s5	2017	2018
	O	s8	2017	2018
	O	s9	2017	2018
O	s10	2017	2018	

Table B2: Summary of all the variables measured in the field. When not specified, sample size refers to the number of plants (or leaves × plants) sampled in each microsite and monitoring day.

Type	Variable	Sample size	Measured species (site)	Period of measurement
Oviposition behaviour	1. Microhabitat selected to oviposit, time of the day, and egg position	139 ovipositions from 43 females	<i>P. napi</i> & <i>P. rapae</i> (both sites)	Summer 2017 (site 2, 2 days) & summer 2018 (site 1, 4 days)
	Microclimatic conditions	2. Foliar temperature during oviposition (underside)	67 leaves	
3. Microhabitat air temperature (at 25 cm height)		15 data loggers	(both sites)	2014–2018 (hourly)
4. Soil temperature (10 cm depth)		3	<i>A. petiolata</i> (site 1) & <i>L. draba</i> (site 2)	March–October 2017 (every two weeks)
5. Soil surface temperature (exposed to and protected from sun)				
6. Air temperature above the host plant (1 m height)				
7. Foliar temperature (upper and underside)		3 × 3		
8. Soil moisture		3		
Host plant		9. Phenological stage		
	10. Stem length	3		
	11. Foliar length	3 × 3		
	12. Foliar width			
	13. Foliar chlorophyll content	3 × 3		
	14. Foliar fresh weight	3 × 3		
15. Foliar dry weight				
16. Foliar water content				
17. Foliar density				
	18. Number of fruits	90 plants		June 2017 (once)

Table B3: Number of larvae used in the heat tolerance experiments for each static thermal treatment (44, 42, and 40 °C), site, species, and family line. Mean \pm standard deviation of larval initial weight (in mg) is also shown

Site	Species	Family	Total	44 °C	42 °C	40 °C
Mid-elevation site			97	39	38	20
	<i>P. napi</i>		31	15	16	0
		A	7	7	0	0
		B	6	2	4	0
		C	3	0	3	0
		D	15	6	9	0
	<i>P. rapae</i>		66	24	22	20
		E	8	8	0	0
		F	1	0	0	1
		G	19	6	7	6
		H	14	5	5	4
		I	24	5	10	9
Lowland site			113	40	33	40
	<i>P. napi</i>		58	20	18	20
		J	5	5	0	0
		K	27	5	5	17
		L	5	5	0	0
		M	10	5	5	0
		N	4	0	3	1
		O	7	0	5	2
	<i>P. rapae</i>		55	20	15	20
		P	15	5	5	5
		Q	13	5	3	5
		R	2	0	2	0
		S	15	5	5	5
		T	10	5	0	5
TOTAL			210	79	71	60
	<i>P. napi</i>					
		N	89	35	34	20
		(mean \pm sd [mg])	(103 \pm 37)	(96 \pm 48)	(108 \pm 30)	(105 \pm 22)
	<i>P. rapae</i>					
		N	121	44	37	40
		(mean \pm sd [mg])	(99 \pm 41)	(104 \pm 45)	(106 \pm 36)	(86 \pm 38)

Table B4: Oviposition behavior. Census effort (estimated as the total time employed to census) and number of observations are summarised for each study site. O: open microhabitat, SO: semi-open microhabitat, SC: semi-closed microhabitat, and C: closed microhabitat.

Location	Microhabitat	Census duration (min)	<i>P. napi</i> eggs (females)	<i>P. rapae</i> eggs (females)
Mid-elevation population	C	579	3 (3)	0 (0)
	SC+SO	924	46 (11)	0 (0)
	O	494	4 (3)	10 (5)
	TOTAL	1997	53 (17)	10 (5)
Lowland population	C	1895	0 (0)	1 (1)
	SC+SO	2705	11 (10)	3 (3)
	O	620	0 (0)	61 (7)
	TOTAL	5220	11 (10)	65 (11)
		7217	64 (27)	75 (16)

B.3 Supplementary figures

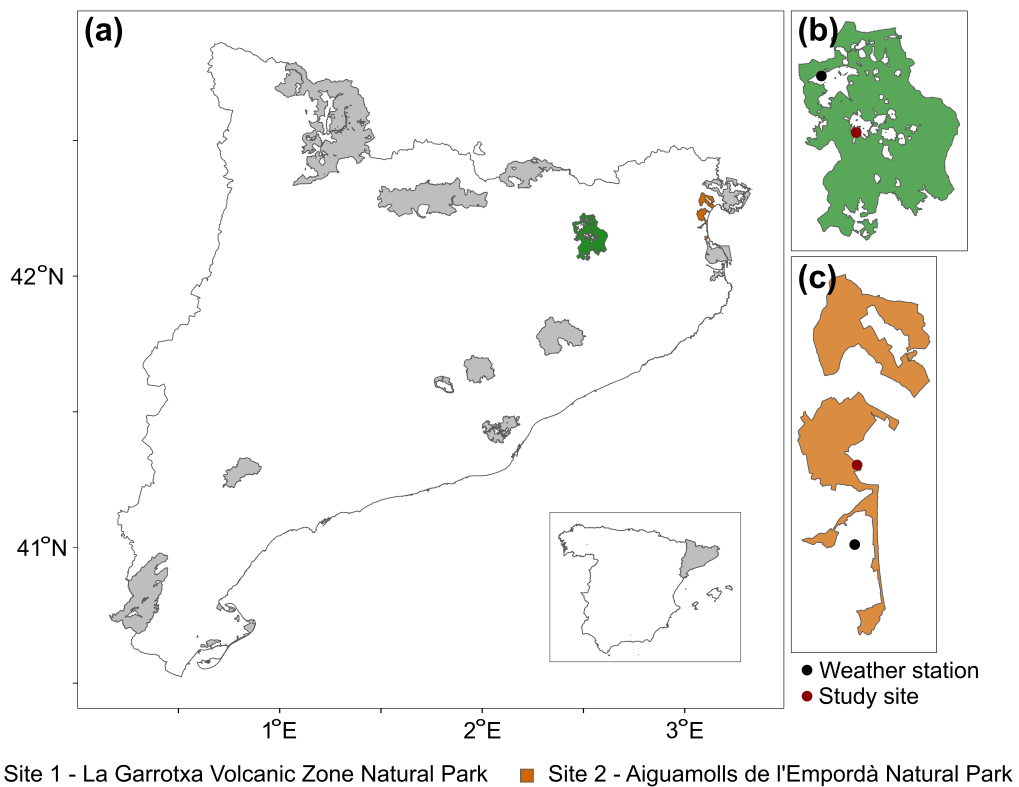


Figure B1: Geographic distribution of the studied areas. (a) Protected Natural Parks from Catalonia (NE Spain, inner panel). The mid-elevation site 1 is located in La Garrotxa Volcanic Zone Natural Park (green) and the lowland site 2 is located in Aiguamolls de l'Empordà Natural Park (orange). Grey areas correspond to the other Natural Parks. (b, c) Location of the two monitored cohorts of host plants (dark red point) and the nearest meteorological stations (black point) in site 1 (b) and site 2 (c).

Mid-elevation site



Lowland site



Figure B2: Photographs of the landscape mosaic of the two study sites and the different microhabitat types of host plant growth present in open–closed ecotones. (a) Mid-elevation site. La Garrotxa Volcanic Zone Natural Park. Landscape view (October). (b) Closed microhabitat from mid-elevation site during October. (c) Semi-closed microhabitat from the mid-elevation site during October. (d) Semi-open microhabitat from the mid-elevation site during October. The monitoring campaign was conducted before the fence that can be observed in the photograph was placed. Tall herbs like those that appear in the right side of the fence covered a much greater area. (e) Open microhabitat from the mid-elevation site during October. In the ecotone between the forest margin and the path, shrubs and trees covered less than 50% of the microhabitat and ground was sparsely covered by short and medium-sized herbs exposing *Alliaria petiolata* to sunlight conditions. (f) Non-flowering first-year rosettes of *A. petiolata* that persisted in the mid-elevation site after the fructification of the second-year individuals. The photograph was taken during October. In the next spring, during the growing season, these rosettes will complete their life cycle. (g) Lowland site. Aiguamolls de l’Empordà Natural Park. Landscape view. Early spring (March). (h) Closed microhabitat from the lowland site during June. (Legend continues on next page).

(Continuation of legend from Fig. B2). Senescent individuals of the host plant *Lepidium draba* could be detected in the ground before achieving a reproductive stage. (i) Semi-closed microhabitat from the lowland site during May. Low light microconditions inhibited sexual maturation of *L. draba* individuals, which presented an unusual vine-like growth form. (j) Semi-open microhabitat of the lowland site during March. *Lepidium draba* was still in the vegetative stage. (k) Open microhabitat from the lowland site during May with *L. draba* individuals at their fruiting stage. (l) *L. draba* resprouts emerging from subterranean rhizomes during midsummer (August) in an open microhabitat from the lowland site. Photograph g was taken by Jofre Carnicer; the rest, by Maria Vives-Inglá.

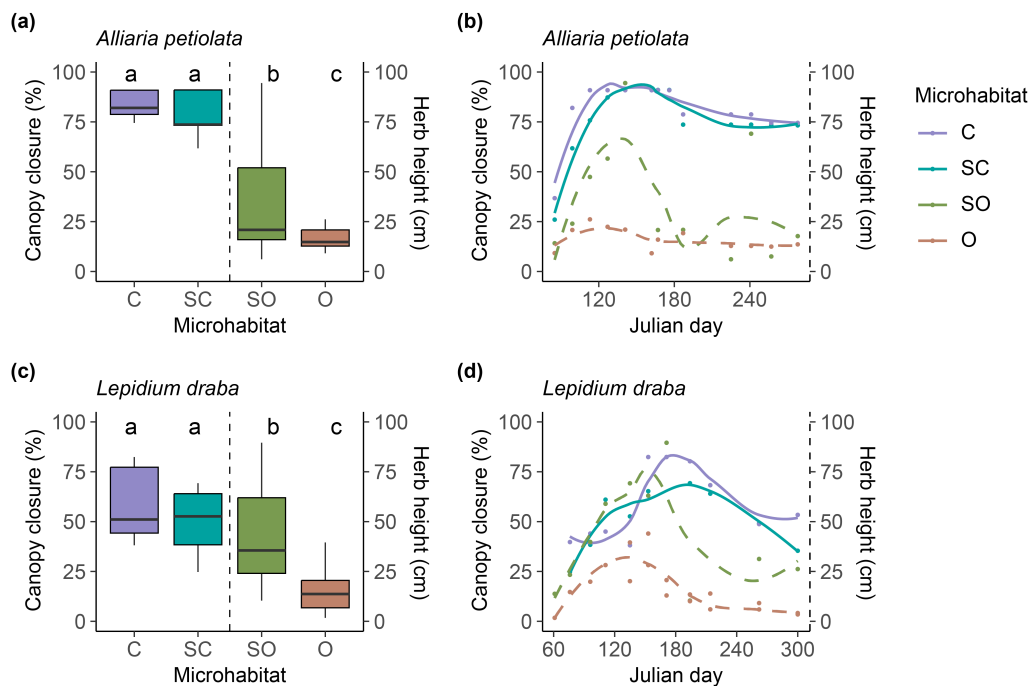


Figure B3: Spatial and temporal variation of the vegetation cover in different microhabitat types defined in open–closed ecotones. (a, c) An ANOVA test comparing canopy closure percentage between closed and semi-closed microhabitats juxtaposed to an ANOVA test comparing mean herb height between semi-open and open microhabitats in the study sites of *Alliaria petiolata* (mid-elevation site 1, a) and *Lepidium draba* (lowland site 2, c). (b, d) Temporal dynamics of canopy closure (solid curves, C and SC microhabitats) and mean herb height (dashed curves, O and SO microhabitats) in the mid-elevation site 1 (b) and lowland site 2 (d). More details can be consulted in Section B.1

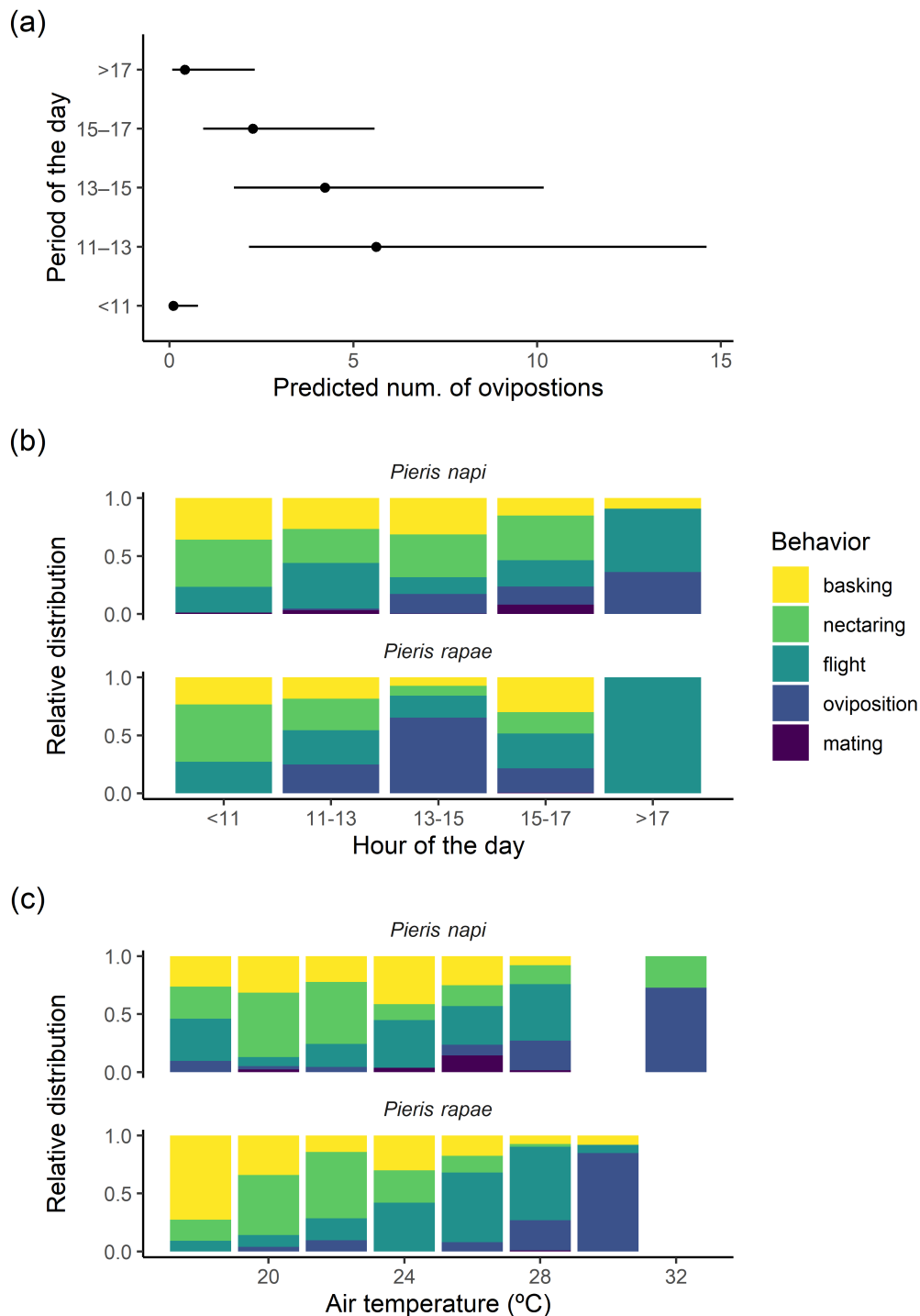


Figure B4: (a) Predicted distribution of ovipositions during the day in the GLMM (model 1). The results are in line with previous observations of *Pieris napi* and *P. rapae* ovipositing behaviour (Hern et al., 1996; Petersen, 1954). (b) Relative distribution of different behaviours recorded during the oviposition censuses along the day. Different types of behaviours were counted and divided by the census effort (i.e. behaviours were measured as hourly rates). Dorsal and lateral basking and nectaring were more frequently observed in the first half of the day, while ovipositing behaviours were more common in the noon and in the afternoon (specially for *P. napi*). (Legend continues on next page).

(Continuation of legend from Fig. B4). (c) Relative distribution of behaviours recorded during the oviposition censuses at different air temperatures (measured with a thermocouple at least once every 45-min census). When air temperatures > 25 °C, we observed a decrease of basking and nectaring behaviours and female butterflies shifted to ovipositing behaviours. We did not record a decrease in the total activity (total number of behaviours) of the butterflies in the warm periods of the day. These species are able to avoid heat stresses and thermoregulate by changing the position or orientation of the wings in relation to the incoming radiation, or simply by moving to fresher areas. Thermoregulation of these species has indeed been studied for long (e.g. Kingsolver, 1987, 1988; Kingsolver and Wiernasz, 1987, 1991) and it is influenced by multiple processes that modify the heat budget of the butterflies at different levels. Some key traits for the butterfly heat budget are fixed during the development of previous stages (e.g. seasonal polyphenism in the wing melanism and plastic changes in size, Carnicer et al., 2019). After pupation and adult emergence, butterflies can adjust incoming radiation and convective and conductive heat fluxes with different types of basking and thermoregulative movements.

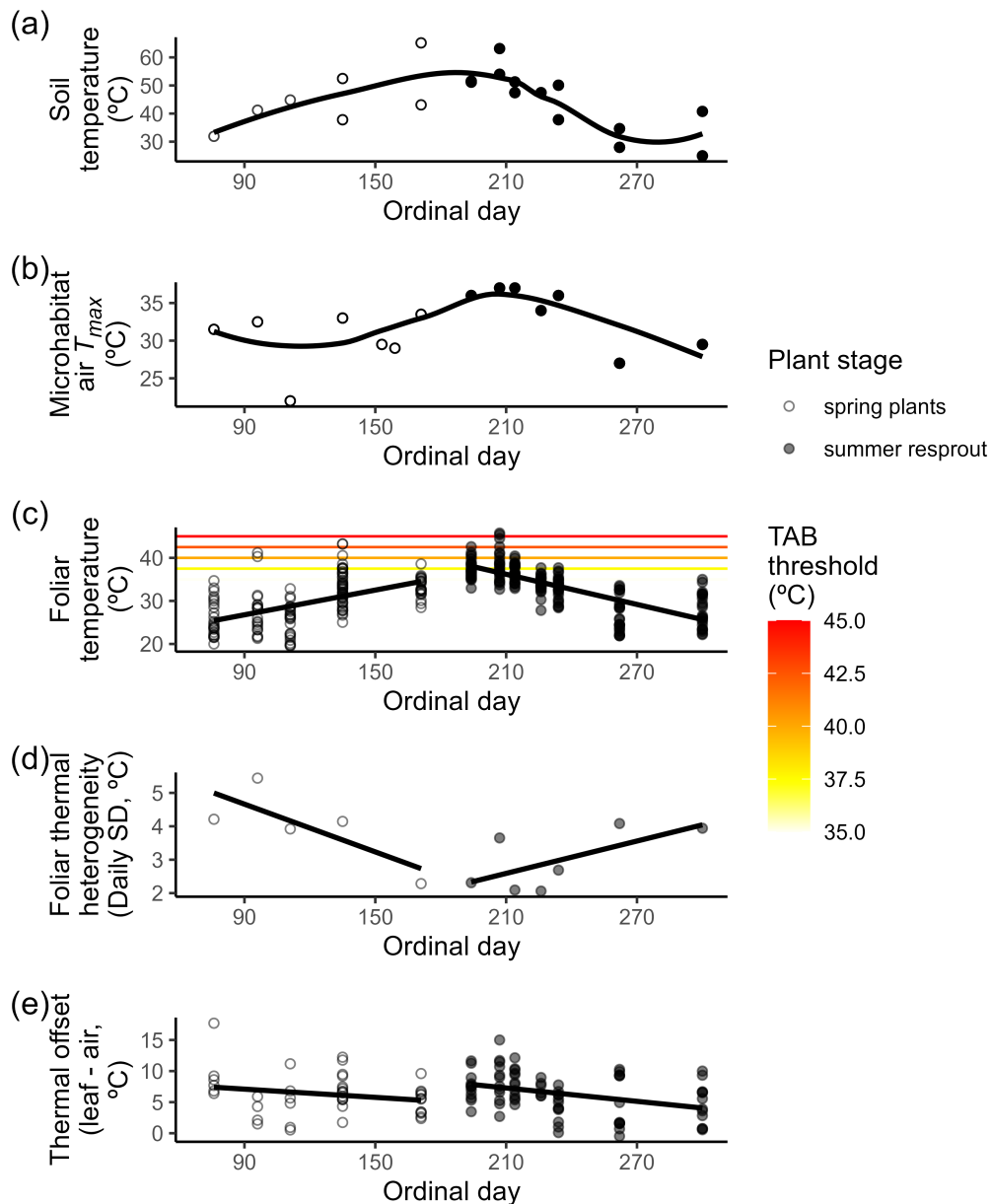


Figure B5: Seasonal variation of the microclimate in the open microhabitat of the lowland site. (a) soil temperature. (b) Daily maximum temperature measured with data loggers. (c) Foliar temperature at the upper side. (d) Spatial variability of the thermal records performed at the foliar level in the same day. (e) Thermal difference between the leaf upper side and the air at 1 m above. Empty dots correspond to plants that develop and fully complete their life cycle during spring, while full dots represent new resprouts that emerge during summer. Coloured lines indicate the different thermal thresholds used in the predictions of thermal mortality.

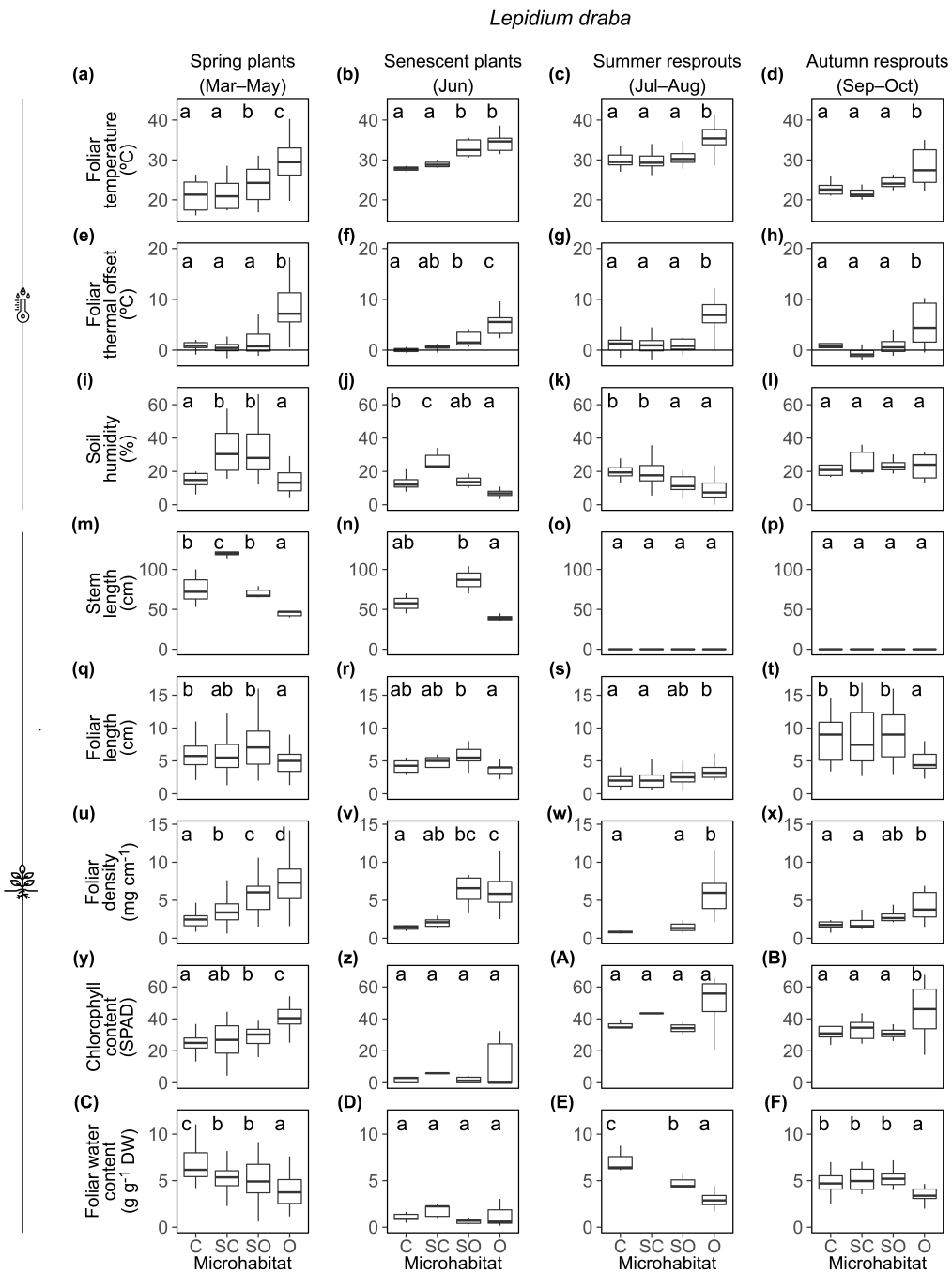


Figure B6: Seasonal variation of the spatial patterns of variation across open-closed ecotones of the lowland site. (a-l) microclimatic conditions. (m-F) *Lepidium draba* traits. C, closed; SC, semi-closed; SO, semi-open; and O, open microhabitats. Different lower case letters indicate significant differences of the response variable between the corresponding microhabitat types in the Tukey HSD test. The horizontal solid lines in the panels e-h indicate foliar temperatures equal to air temperatures above the host plant at 1 m height. Positive values correspond to foliar thermal amplification phenomena, whereas negative values imply thermal cooling effects. Because of the small number and size of midsummer resprouts in the semi-closed microhabitat, no foliar sample was taken to weight (w and E), and foliar chlorophyll measurement was achieved in just one occasion (A).

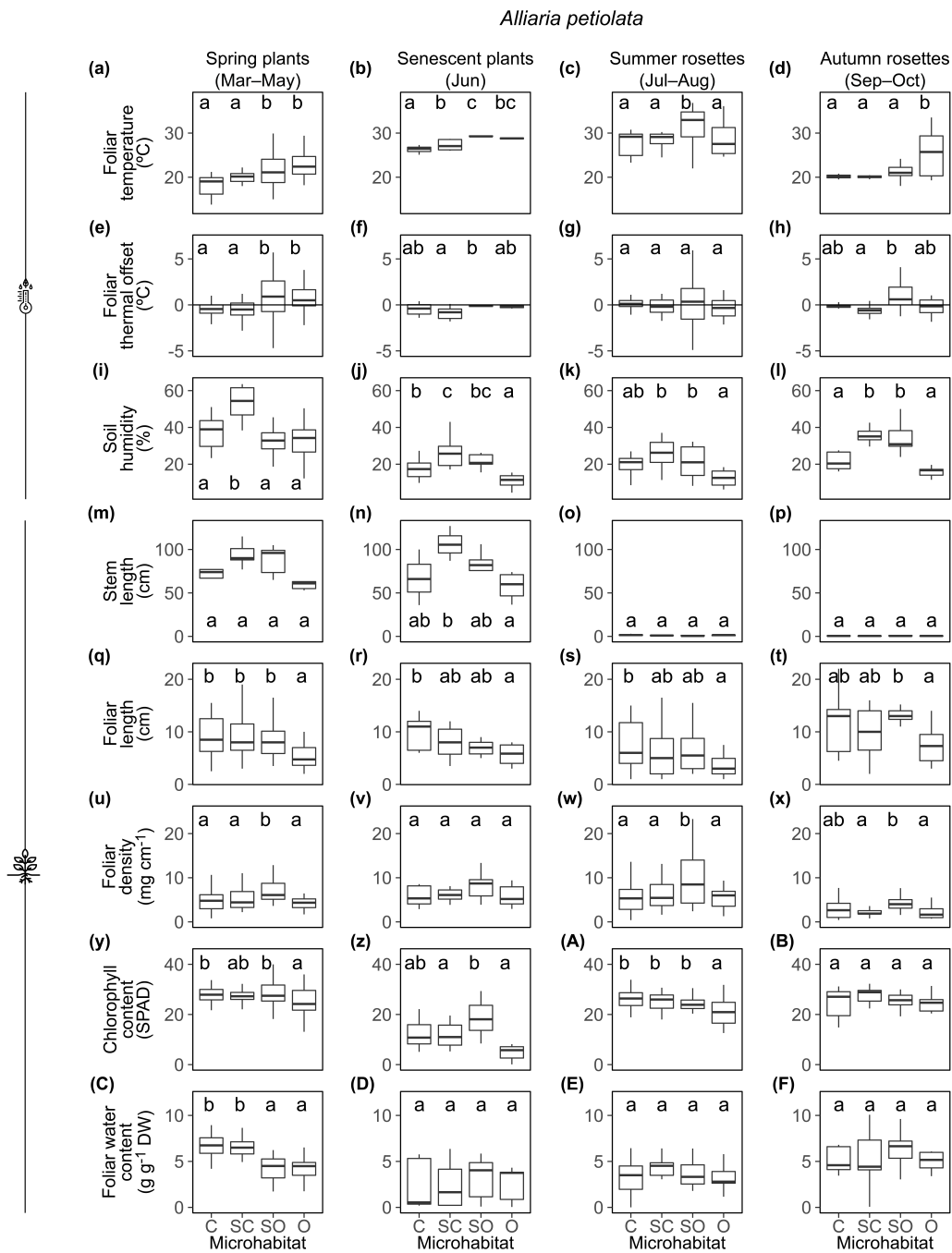


Figure B7: Seasonal variation of the spatial patterns of variation across open-closed ecotones of the mid-elevation site. (a-l) microclimatic conditions. (m-F) *Alliaria petiolata* traits. C, closed; SC, semi-closed; SO, semi-open; and O, open microhabitats. Different lower case letters indicate significant differences of the response variable between the corresponding microhabitat types in the Tukey HSD test. The horizontal solid lines in the panels e-h indicate foliar temperatures equal to air temperatures above the host plant at 1 m height. Positive values correspond to foliar thermal amplification phenomena, whereas negative values indicate foliar cooling effects.

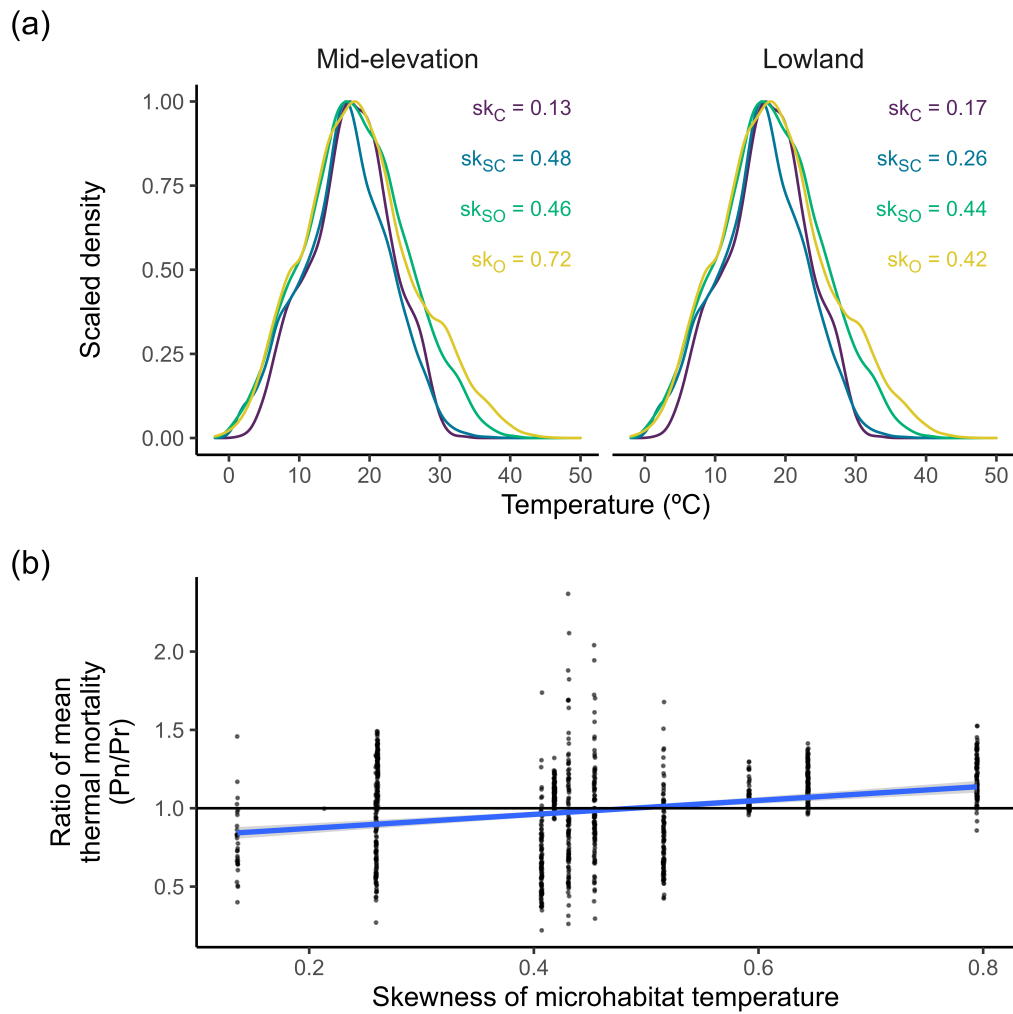


Figure B8: Distribution of the air temperatures measured with the data-loggers in different microhabitats from the mid-elevation and lowland sites (a). Mean daily skewness for all microhabitats is also shown and its linear relationship with the ratio of mean thermal mortality during development between *P. napi* and *P. rapae* ($P < 0.0001$, $R^2 = 0.07$; b).

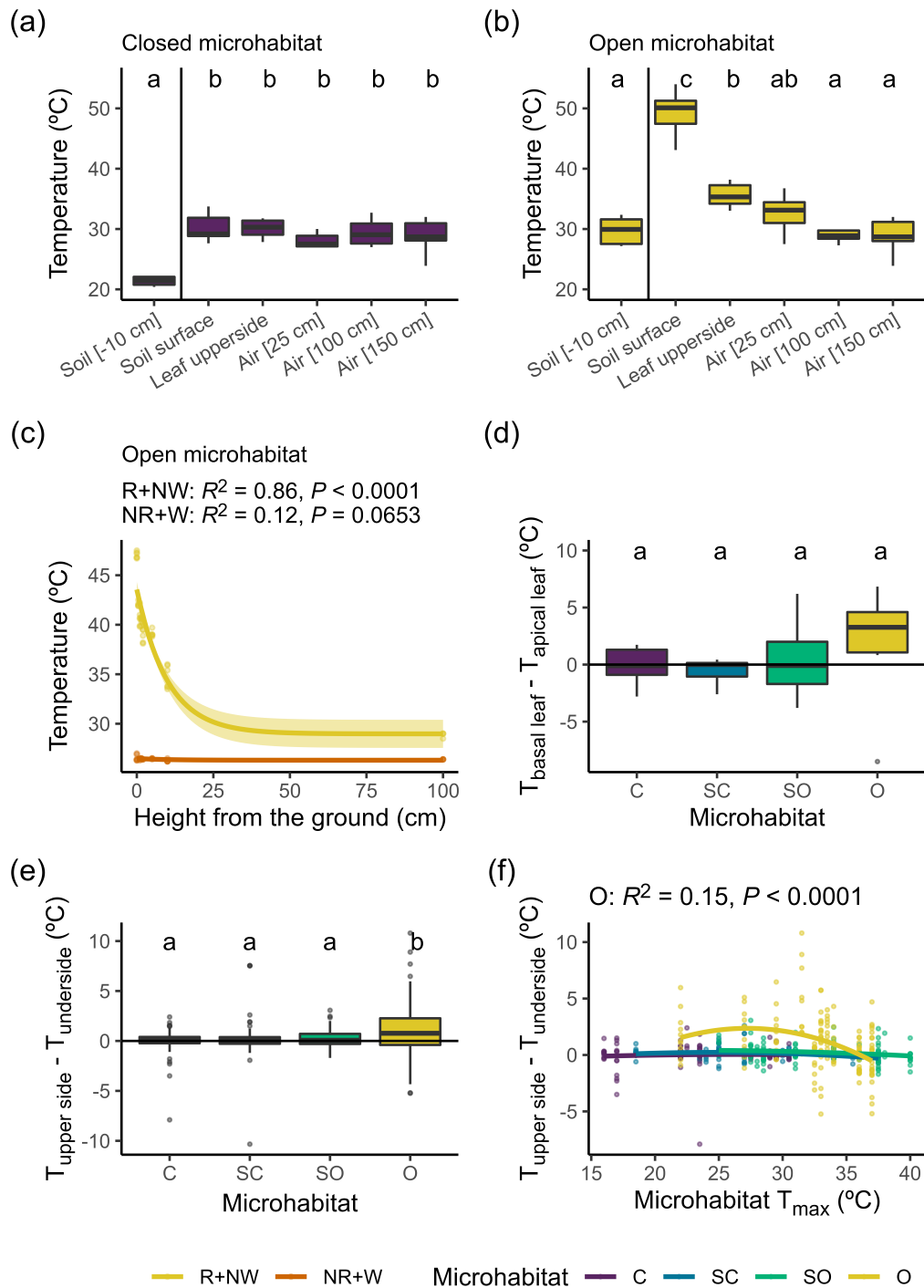


Figure B9: Thermal heterogeneity at fine scales in the lowland site. (a and b) Thermal values recorded during the host-plant monitoring campaign at different surfaces and heights in a closed (a) and open (b) microhabitats. These include soil temperature at 10 cm depth; soil surface exposed to radiation (b) or not (a); foliar upper side; microhabitat air temperature recorded with the data logger during the 2-h period of host plant monitoring; air temperature recorded above the host plant at 1 m height; and macroclimatic daily maximum temperatures recorded at 150 cm height by a nearby weather station (Fig. B1). (Legend continues on next page).

(Continuation of legend from Fig. B9). (c) Temperatures measured at different heights (i.e. 0, 0.5, 1, 1.5, 2, 5, 10, 100 cm) in one microspot exposed to full solar radiation (yellow) and one shaded microspot (orange) of the open microhabitat on 12 July. A hyperbolic sine function was fitted following Geiger (1950). R, solar radiation; NR, shade; W, wind; and NW, without wind conditions. (d and e) Thermal differences between the basal and apical leaves (d) and the upper and the underside of each leaf (e) in each microhabitat type. (f) Thermal differences between the foliar upper and underside against the daily maximum temperature recorded with the data logger. A 2-degree polynomial curve was fitted in the open microhabitat, evidencing that underside cooling effects (Fig. 4.3e) are only produced when leaves are exposed to radiation, and water and thermal conditions allow foliar evapotranspiration.

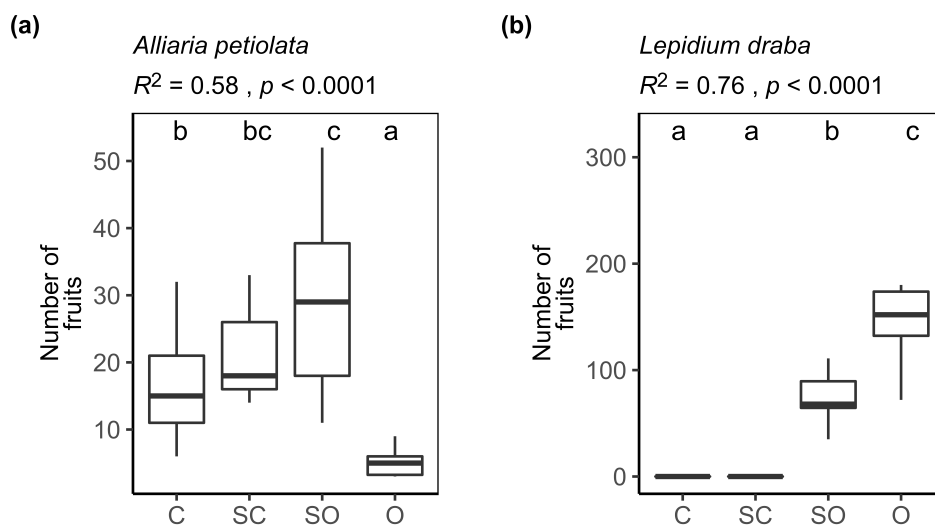


Figure B10: Reproductive output of the host plants across the open–closed ecotones. Different letters indicate significant differences of the response variable between the microhabitat types in the Tukey HSD test. Outliers are not shown. C, closed; SC, semi-closed; SO, semi-open; and O, open microhabitat

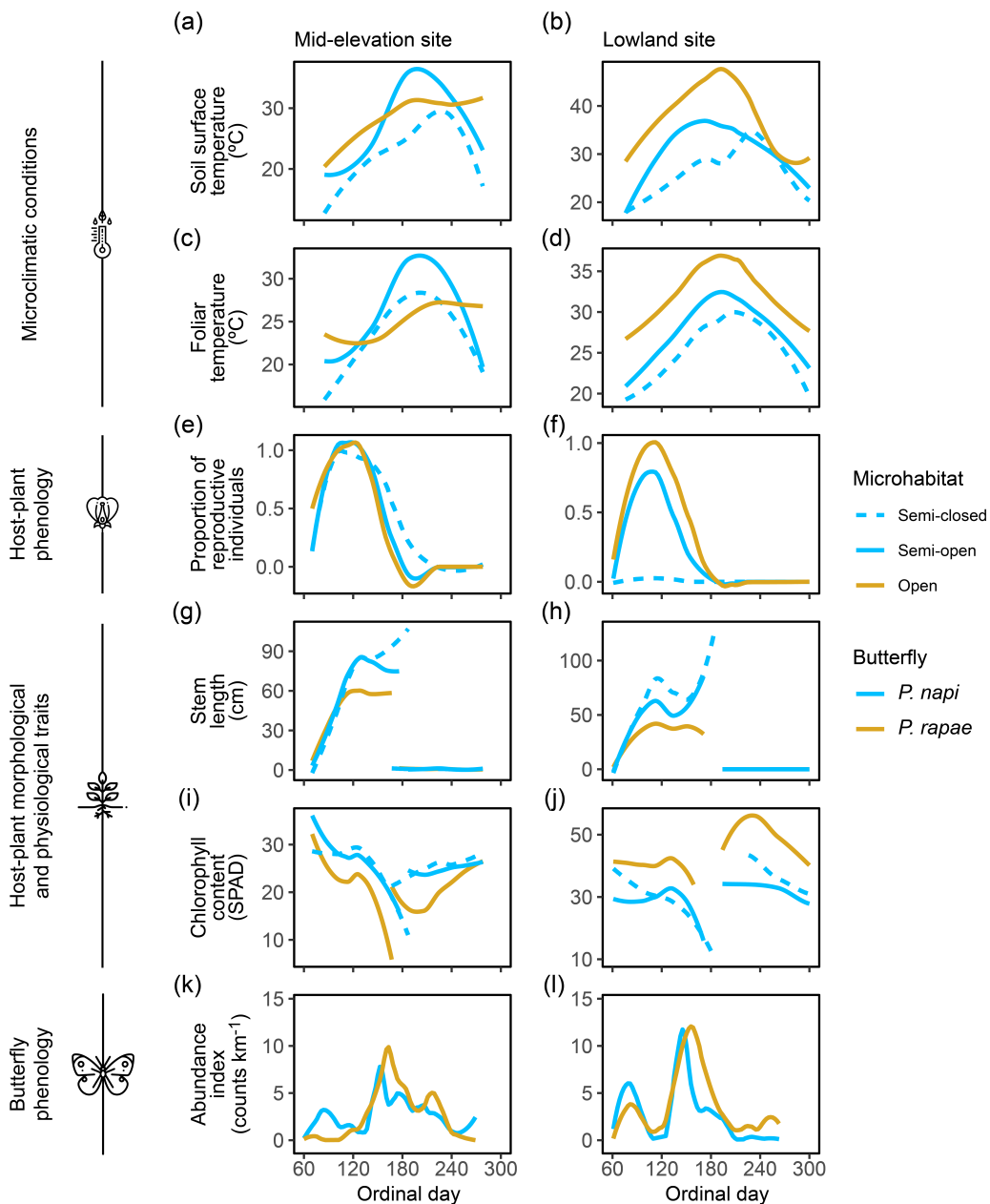


Figure B11: Seasonal dynamics of microclimatic conditions (a–d), host-plant phenological (e and f), and morphological and physiological traits (g–j), and butterfly phenology (k and l). We assessed plant phenological status by classifying 15 individuals of each species in one of four phenological stages: early vegetative (spring rosettes and young shoots before budding), reproductive (plants with buds, flowers, and/or fruits), senescent, and late vegetative (late *A. petiolata* seedlings and *L. draba* resprouts emerging in summer). The assessment of host-plant morphological and physiological traits separated individuals into those that emerged and developed in early spring (spring plants) and those that emerged since June (summer rosettes and resprouts). *Pieris napi* and *P. rapae* phenologies were obtained from the data of the transects of the Catalan Butterfly Monitoring Scheme located at both study sites. Icons used in this figure were made by Freepik from flaticon.com.

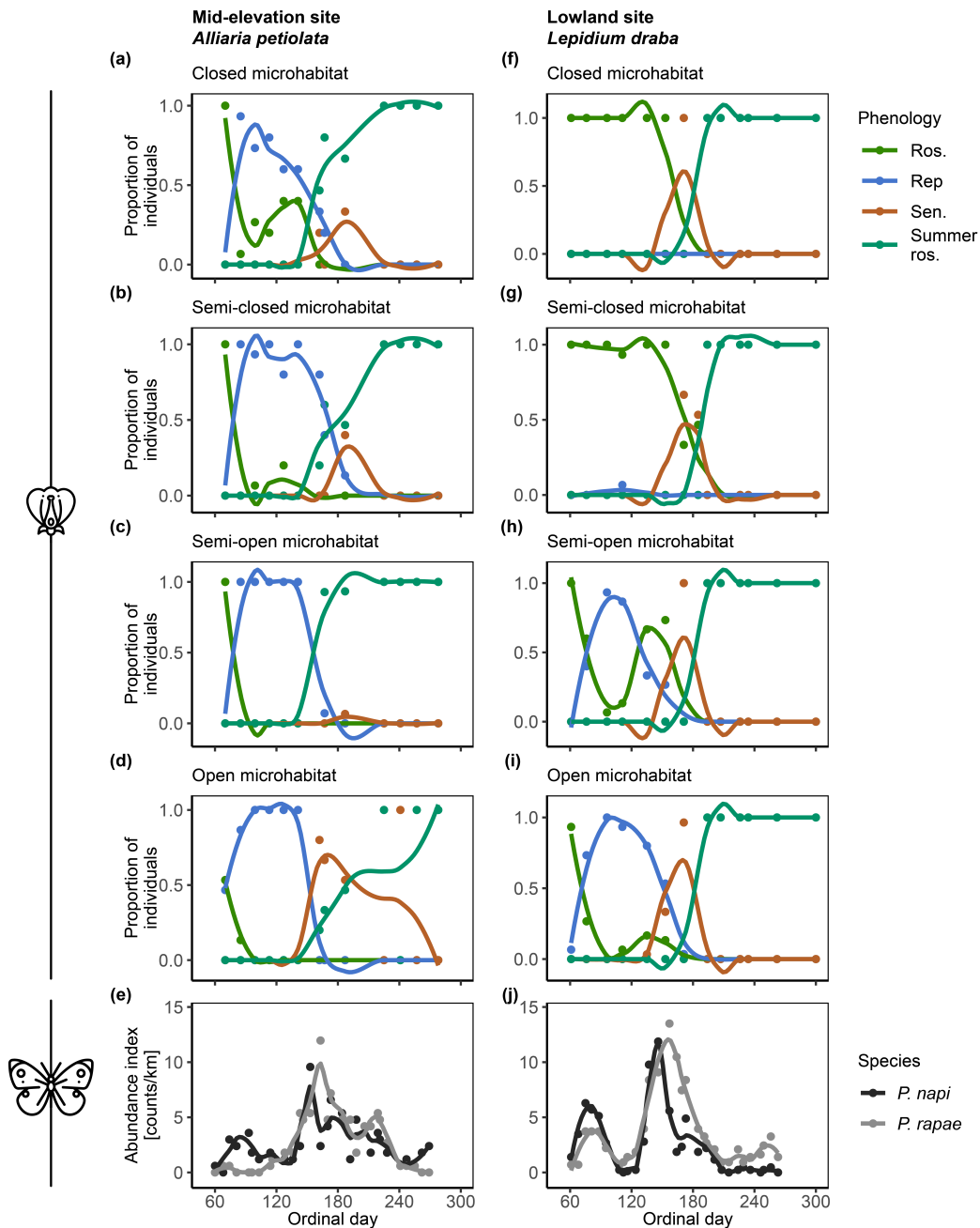


Figure B12: Butterfly and host-plant phenology in the two study sites. Phenological progress of the host-plant individuals growing in different microhabitats across the open–closed ecotones in the mid-elevation site (a–d) and the lowland site (f–i). We assessed plant phenological status by classifying 15 individuals of each species in one of four phenological stages: early vegetative (spring rosettes and young shoots before budding), reproductive (plants with buds, flowers, and/or fruits), senescent, and late vegetative (late *A. petiolata* seedlings and *L. draba* resprouts emerging in summer). *Pieris napi* and *P. rapae* phenologies (e and j) were obtained from the data of the transects of the Catalan Butterfly Monitoring Scheme located at both study sites. Ros: spring rosettes and young shoots before budding; rep: reproductive plants with buds, flowers and/or fruits; sen: senescent plants; summer ros: summer rosettes of *A. petiolata* and midsummer resprouts of *L. draba*.

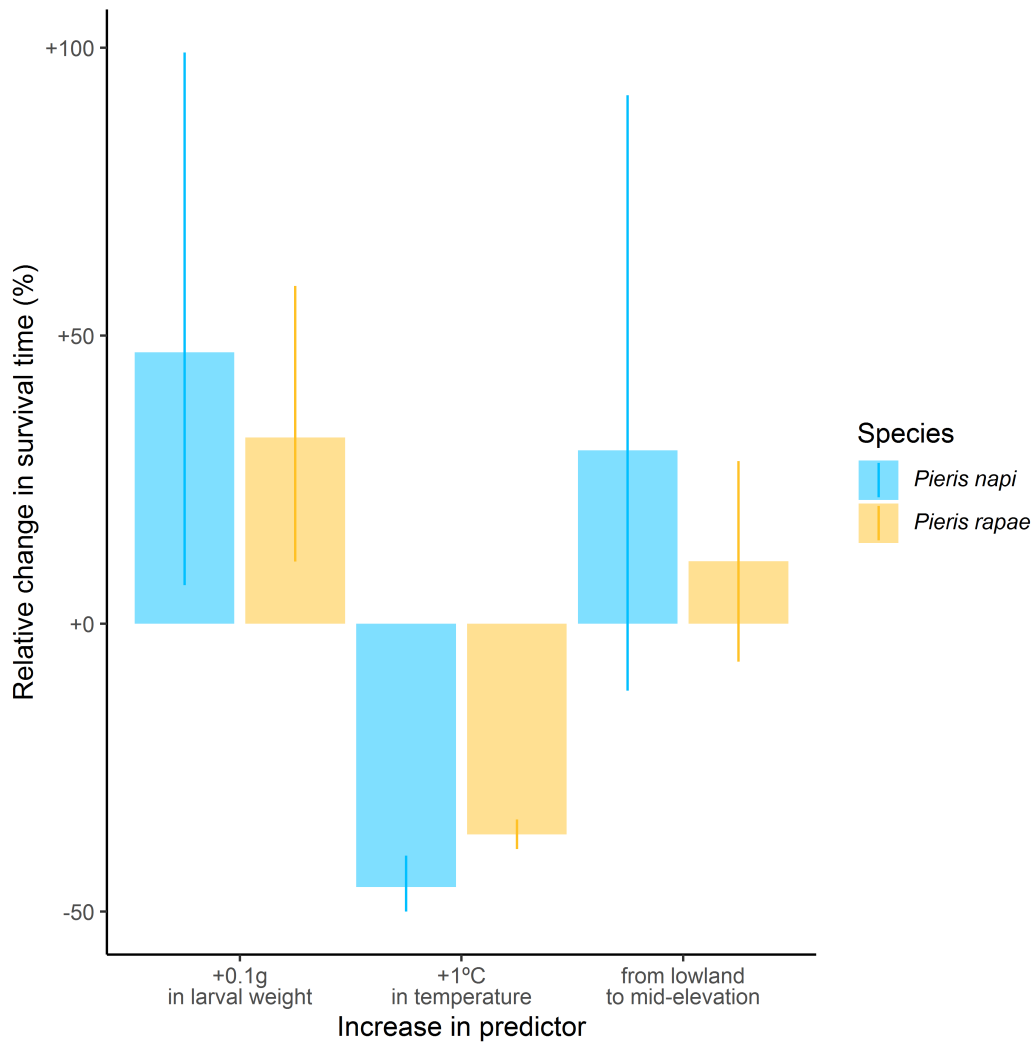


Figure B13: Effect sizes of larval weight, temperature, and population on larval survival time in the linear mixed models (Table 4.2). The mean effects were calculated from the estimated coefficients in the linear mixed models, while the lines represent the predicted interval of the effects calculated from the bounds of the 95% confidence intervals of the coefficients. Larval weights in the experiment ranged from 0.02 g to 0.199 g. Therefore, an increase of 0.1 g (rather than an increase of 1 g) represents an observable situation.

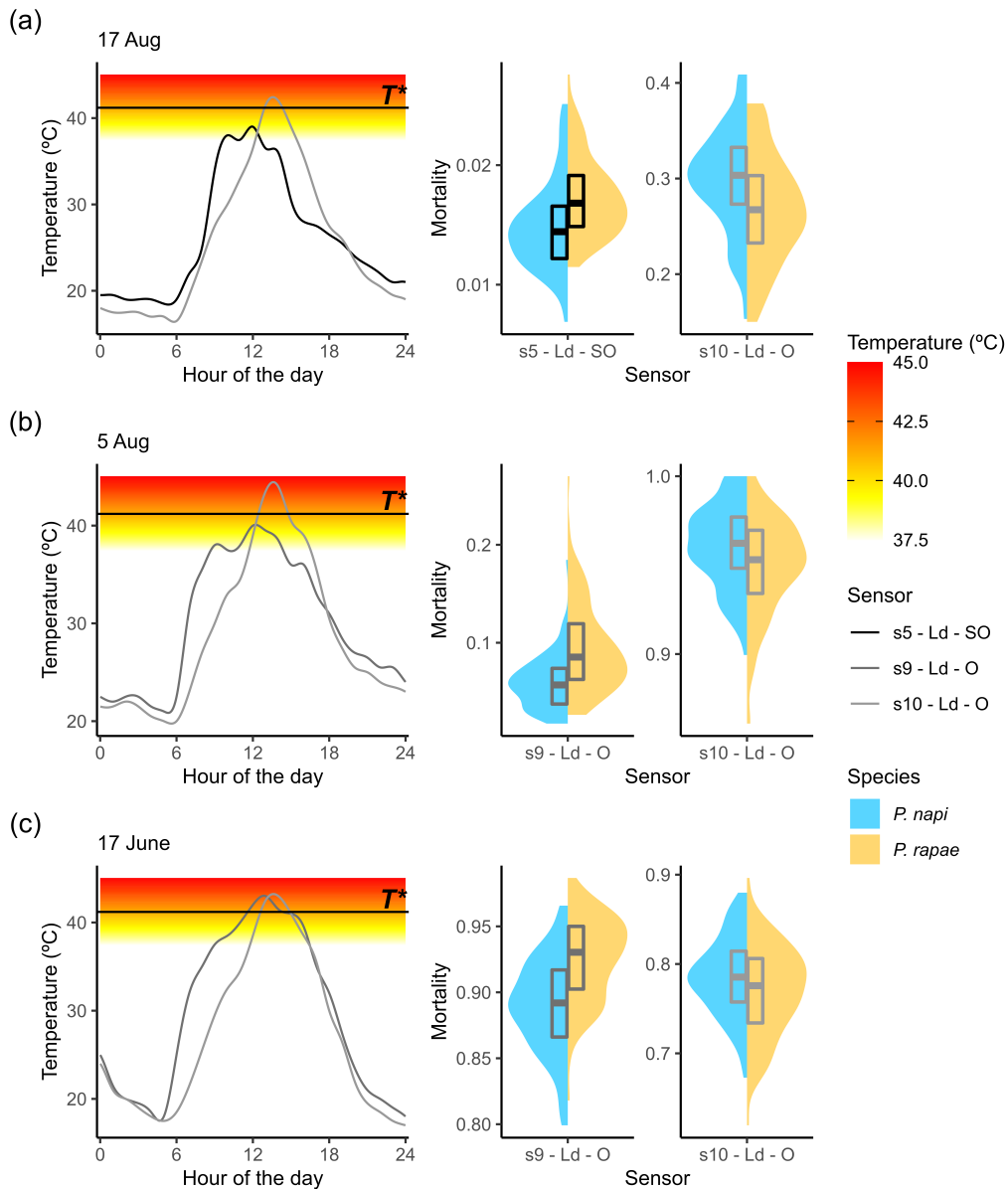


Figure B14: Opposing costs to larval survival of chronic and acute thermal stresses. In the left part of each panel, temperatures recorded in one semi-open (s5, in black) and two open microhabitats (s9 and s10, in dark and light grey respectively) in the lowland site during three summer days (a–c). In the right part of each panel, associated predicted mortality in the 100 bootstrap replicates during these days in these microhabitats. Blue and orange areas represent the density functions of the bootstrapped thermal mortality for *P. napi* and *P. rapae* respectively. The lower and upper limits of the boxes represent the 1st and the 3rd quartiles of thermal mortality and, their inner line, the median. (a) On 17 August, temperatures in the s10 open microhabitat presented a more extreme but shorter heat challenge (acute stress), surpassing the thermal threshold from which *P. rapae* is more tolerant than *P. napi* (i.e. $T^* = 41.2$ °C). Higher thermal mortalities were consequently recorded there for *P. napi*. In contrast, the long exposure at subextreme temperatures (chronic stress) in the s5 semi-open microhabitat was deadlier for *P. rapae*. (b) Similarly, on 5 August, the two compared open microhabitats posed contrasting heat challenges, and provoked opposed thermal mortalities between the species. (Legend continues on next page).

(Continuation of legend from Fig. B14). However, temperatures in s10 reached more extreme values (reddish zone) than on 17 August, producing very high thermal mortalities for both species, although slightly inferior for *P. rapae*. (c) On 17 June temperatures reached similar extreme values and produced very high thermal mortalities in both microsites. However, interspecific differences in thermal mortality were more notorious in s9, likely associated with the longer exposure to subextreme temperatures (chronic stress, yellowish zone) that mainly affects *P. rapae*.)

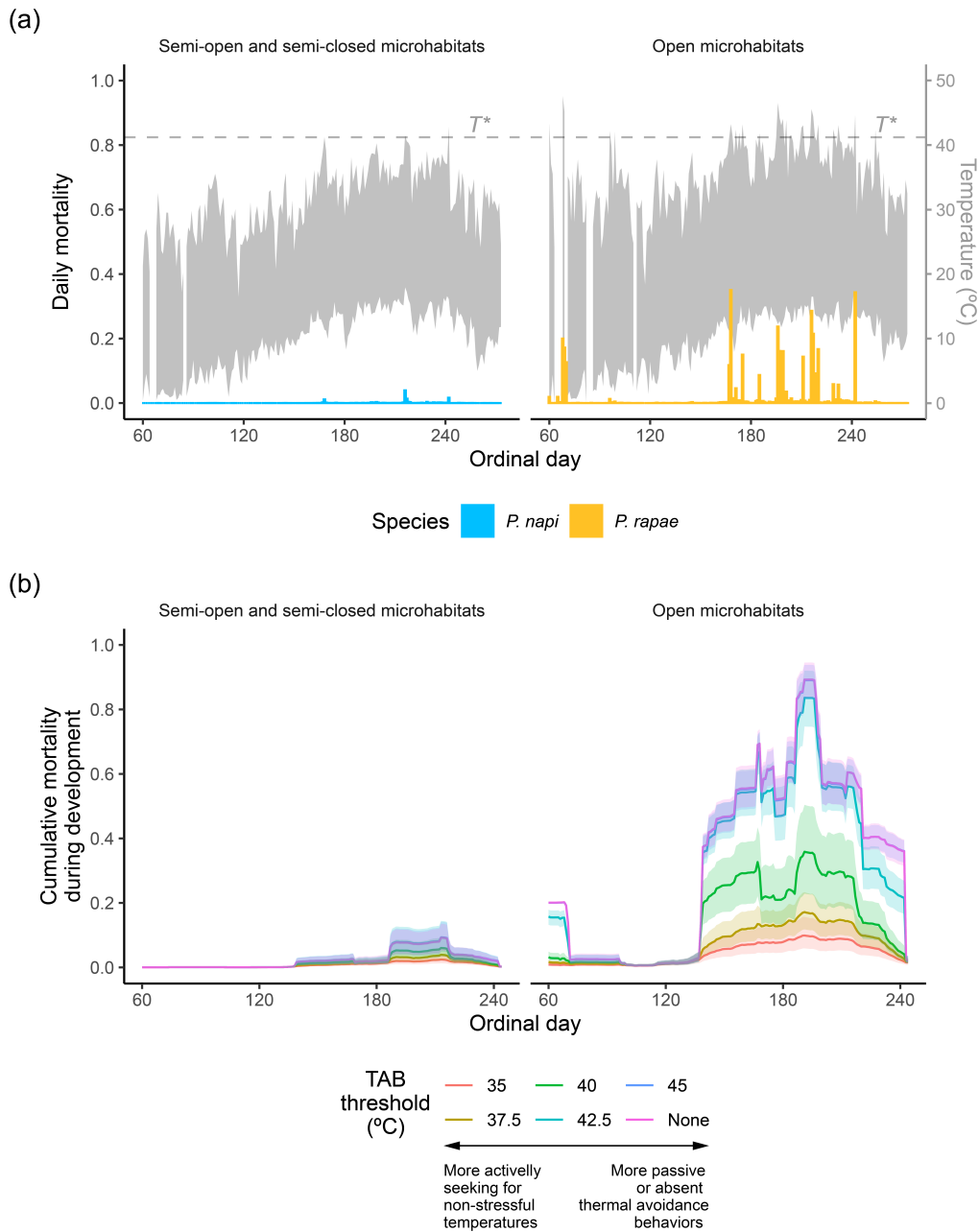


Figure B15: (a) Seasonal cycle of the estimated daily mortality of *P. napi* (blue) and *P. rapae* (yellow) predicted under the annual thermal regime (grey) of the microhabitats selected by each species to oviposit. The value of daily mortality corresponds to the average of the daily mortalities predicted under the thermal profiles of each data logger and bootstrap replicate. The represented thermal regime comprises the temperatures between the mean values of daily minimum and daily maximum temperatures of all the data loggers included in each microhabitat type. The grey dashed line corresponds to the temperature from which *P. rapae* is more tolerant than *P. napi* (T^*). (b) Seasonal cycle of the cumulative mortality during development (i.e. 30 days). Mean values and 95% confidence interval of all the thermal profiles and bootstrap replicates included in each microhabitat category are shown. The procedure was repeated including the effect of larval thermal avoidance behaviours (TAB) on realised thermal exposure. TAB were simulated truncating the thermal profiles for specific threshold values: 35, 37.5, 40, 42.5, 45 °C.)

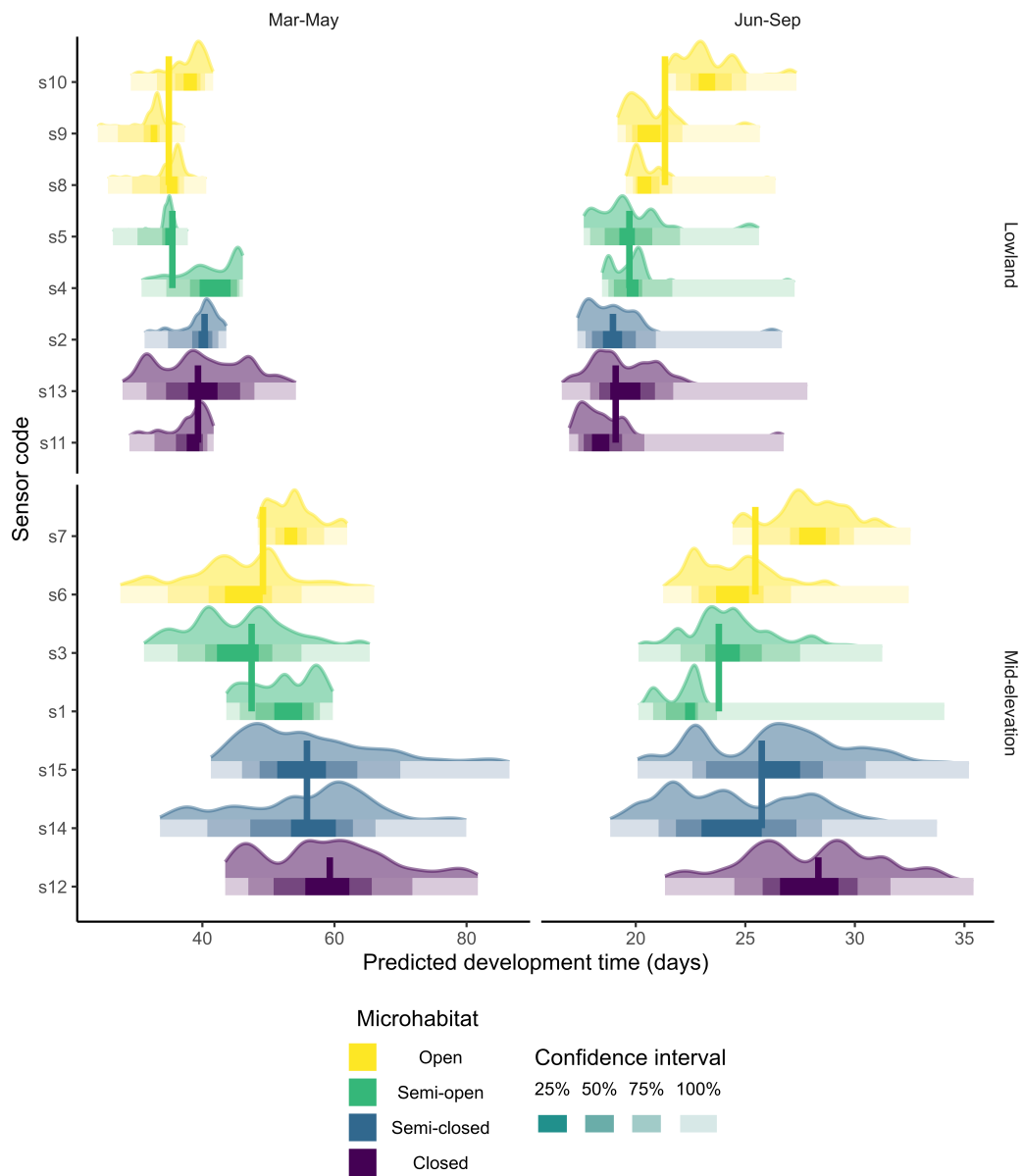


Figure B16: Predicted development times for *Pieris napi* in the studied microhabitat types in spring (left) and summer (right) following the methods presented in von Schmalensee et al. (2021a) and adapting the associated scripts (von Schmalensee et al., 2021b). von Schmalensee et al. (2021a) show how development times in fluctuating thermal regimes can be accurately predicted from the summation of the development rates at different temperatures, when nonlinear thermal performance curves and microclimatic data at high temporal resolution are used. Here we take the thermal performance curve for development rate (days^{-1}) fitted in their study on a population of *P. napi* to predict the development times of the species based on the microclimatic series recorded in our study system at hourly resolution. Thus, the predictions are only calculated for *P. napi* and assume that thermal performance curves of development rates are conserved between the Swedish and the Catalan populations (i.e. there is no local adaptation). These supplementary results are only shown to illustrate how microclimatic exposure could determine development times and are not used in subsequent analyses of thermal mortality. The vertical, solid lines indicate the median of the predicted development times for each season, site, and microhabitat type. Horizontal, shaded bars represent the prediction interval of developmental time at different percentages. Shaded areas correspond to the density functions of the development time estimated with each data logger.



Appendix C

Chapter 5 - Supporting materials

C.1 Supplementary figures and tables

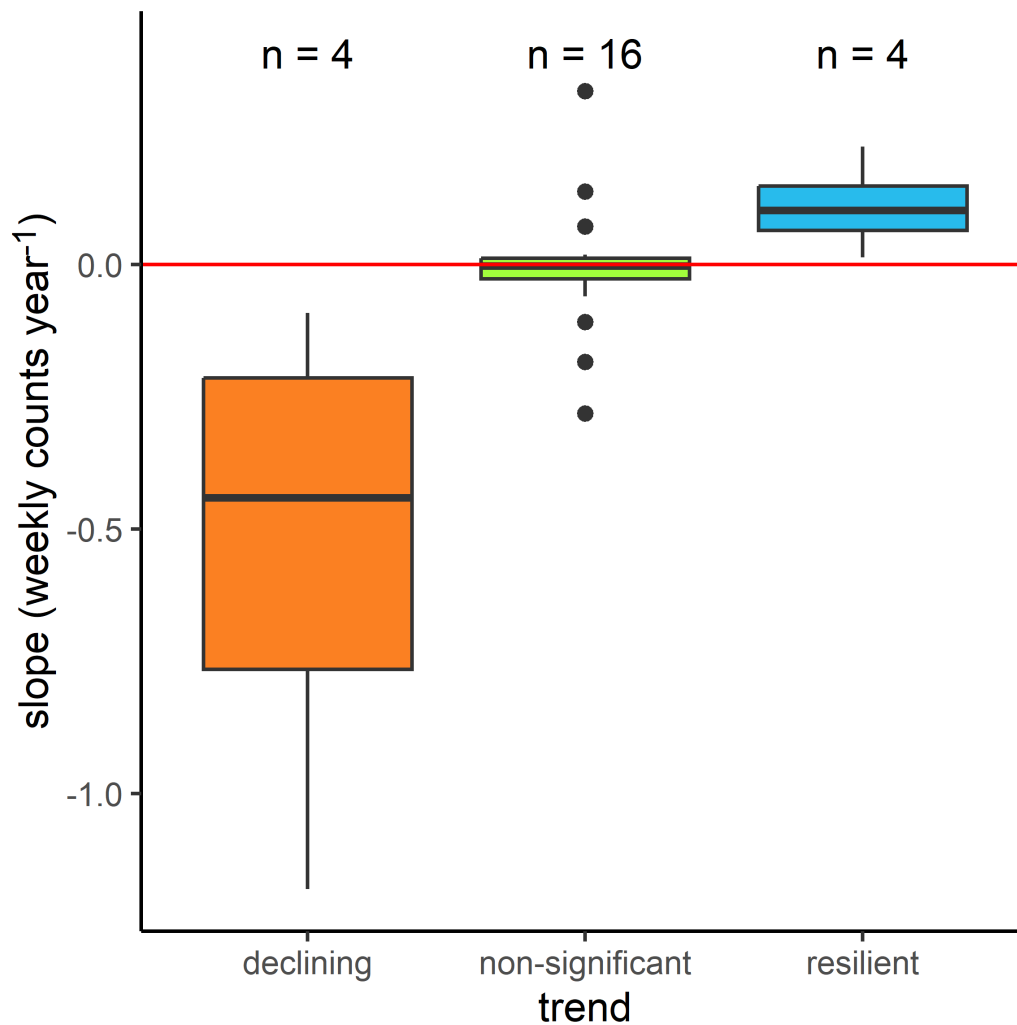


Figure C1: Mosaic of demographic trends of *Pieris napi* in the north-east of the Iberian Peninsula during 1993–2016 for 24 populations of the Catalan Butterfly Monitoring Scheme (CBMS). Weekly counts of adult butterflies were summed for each population and year, and then divided by the number of sampling weeks (around 30 sampling weeks per year). We fitted a general linear model on the standardised weekly counts against year in those sites that had 10 or more years of data, and then extracted the predicted slope (i.e. the multiannual trend of the population). Non-significant trends include those populations where the *P*-value of the slope was > 0.1.

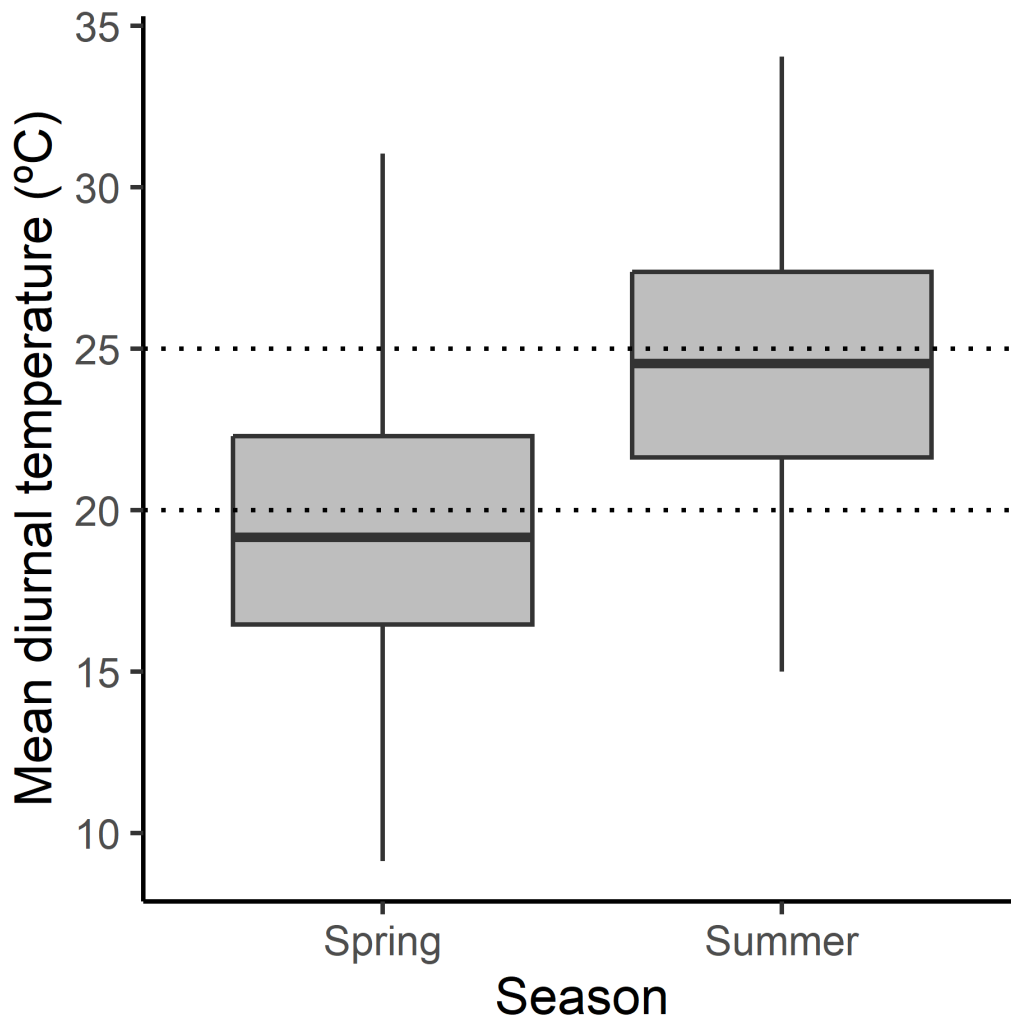


Figure C2: Mean microclimatic temperatures recorded during the day (from 8 to 20h) at the microsites where ovipositing females and larval development have been detected. Specifically, at intermediately covered microhabitats from B1 and B2 populations, such as the margins of paths and irrigation canals partially sheltered by the surrounding vegetation. The dotted lines indicate the two thermal treatments applied in the growth chamber experiments, which are representative of the median microclimatic temperatures recorded in spring and summer. We used the vital rates estimated from the experiments conducted at 20 °C to build the spring transition matrix, and the vital rates estimated from the 25-°C experiments for the summer matrices.

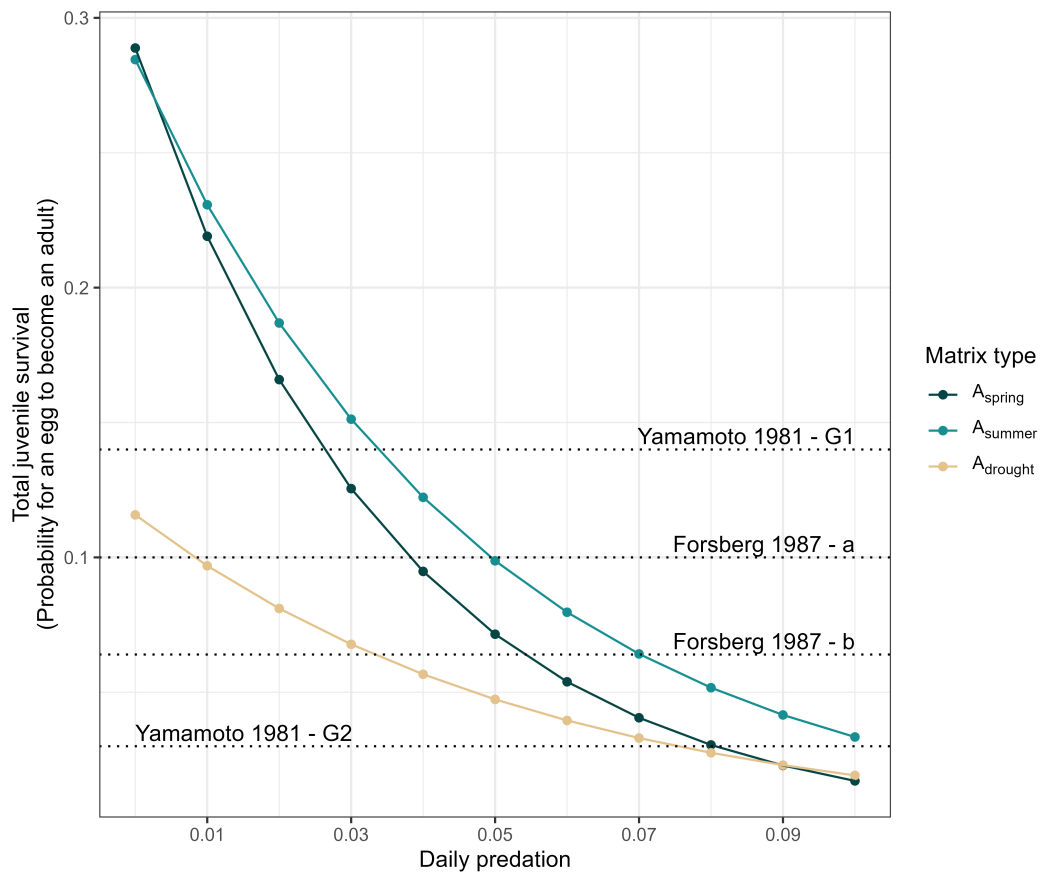


Figure C3: Total probability of juvenile survival (from egg to adult emergence) with increasing daily predation rates from predators and parasitoids in the different transition matrices (A). We performed the simulations with a 5% daily predation rate, obtaining total juvenile survival similar to those estimated in the field for *Pieris napi* in Forsberg (1987) (i.e. central, dotted, horizontal lines). A lower daily predation rate (~3.5%) and a higher daily predation rate (~%) would result in a total juvenile survival similar to the values observed for the spring (G1) and summer (G2) generations respectively in Yamamoto (1981) (lower and higher, dotted, horizontal lines).

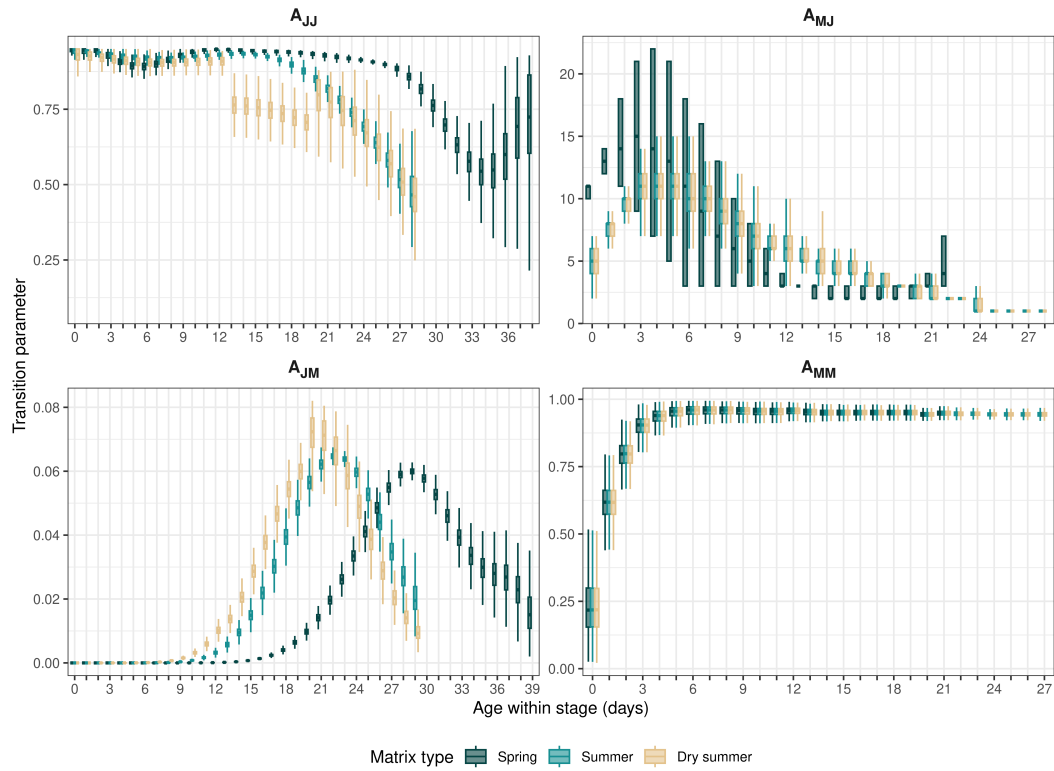


Figure C4: Parameters compounding the four submatrices (A_{JJ} , A_{MJ} , A_{JM} , and A_{MM}) of the three different transition matrices (A_{spring} , A_{summer} , and $A_{drought}$). Boxplots summarise the values obtained for each age-*within*-stage group in the whole set of bootstrap simulations. Outliers are not shown.

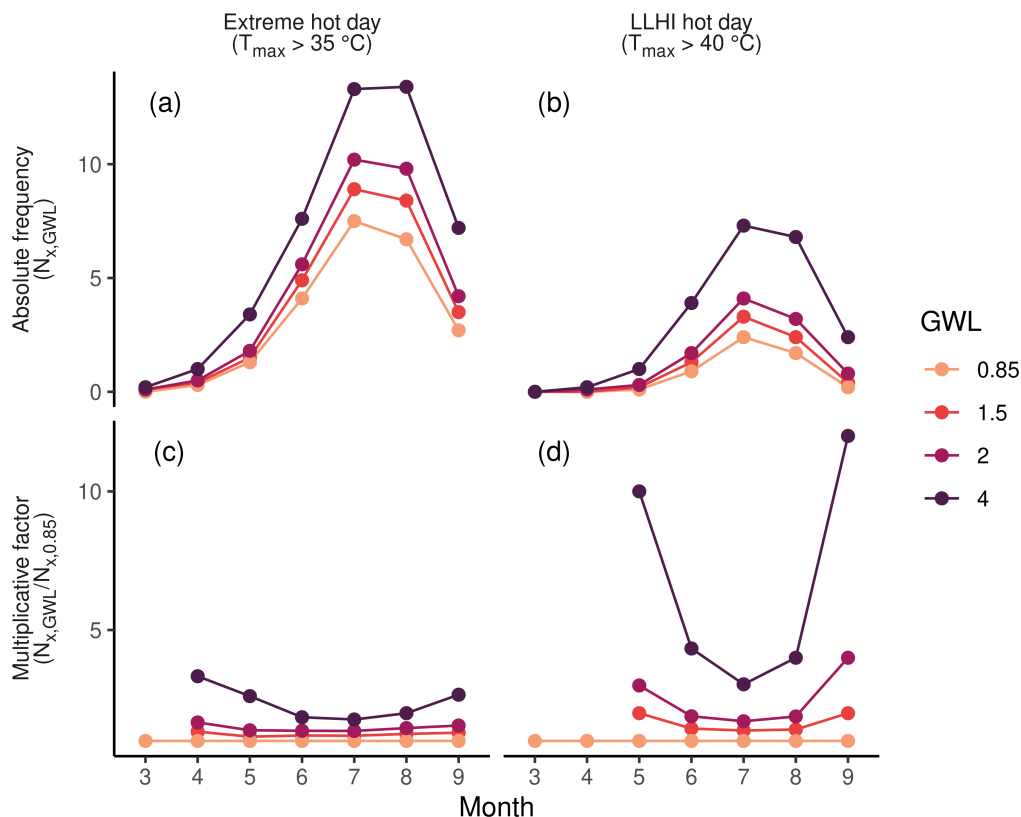


Figure C5: Frequency of extreme heat events in macroclimatic scenarios with increasing global warming levels (GWL = 0.85, 1.5, 2, and 4 °C). (a, b) Predicted number of days exceeding 35 °C and 40 °C, respectively. Predictions correspond to the IPCC projections with the CMIP6 model without bias adjustment for the Mediterranean region (Gutiérrez et al., 2021; IPCC, 2021; Iturbide et al., 2021). (c, d) Factor of increase in the frequency of extreme ($T_{max} > 35$ °C) and LLHI ($T_{max} > 40$ °C) hot days, respectively, calculated as the ratio between the predicted number of extreme days in a particular GWL and the predicted number of extreme days in the current, GWL-0.85 global warming scenario (i.e. the values in a and b panels). Based on these multiplicative factors, we calculated the microclimatic daily probability of occurrence of an extreme day and a LLHI day applied in our simulations (see Appendix C.3). Note that according to the IPCC projections, LLHI hot days are expected to increase relatively more than less harmful extreme heat events (i.e. higher multiplicative factors for LLHI events), especially at warmer scenarios (GWL = 4 °C).

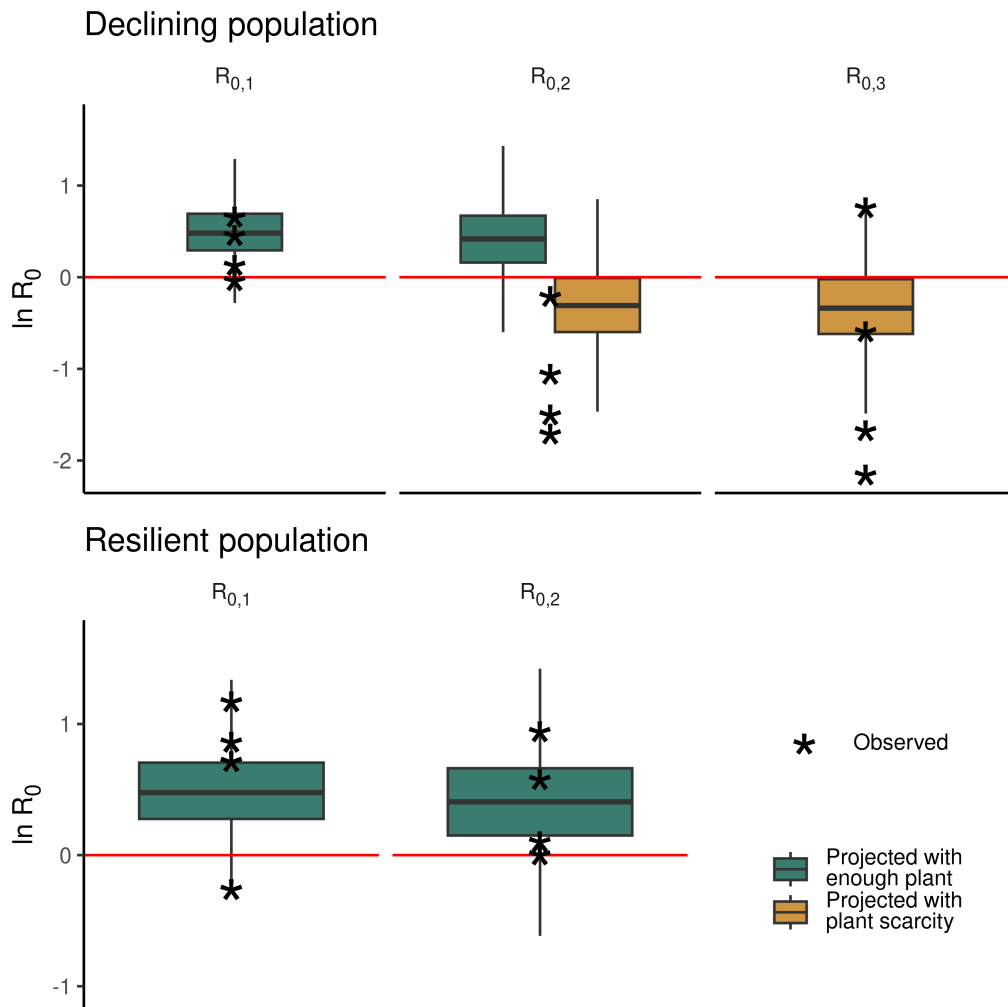


Figure C6: Supplementary validation of the model. We conducted a complementary set of simulations to reinforce the validation of the matrix population model and test the hypothesis that drought-induced plant scarcity is currently driving the declines of the lowland population. We used the thermal series extracted from the microclimatic sensors between 2014–2017 installed in the field (see Appendix C.2) to project the transition between consecutive generations. Simulations were thus conducted with a fixed series of heat events based on the daily Tmax recorded by the sensor. Each fixed series corresponded to one year, transition period, and field microclimatic sensor. We performed 500 replicates on each series bootstrapping the projection matrix (A) as in the main set of simulations (see Appendices C.2 and C.3). For the net reproductive rate capturing the production of the drought-sensitive key generation of the declining population ($R_{0,2}$), we repeated the projections with enough plant availability (green boxplot) and drought-induced plant scarcity (ochre boxplot). Green and brown boxplots thus indicate the results of the simulated data (MPM model), while asterisks represent the R_0 calculated from field data for the years 2014–2017. Note that when asterisks fall inside the predicted range of R_0 they support the MPM validation. Notably, observed $R_{0,2}$ during 2014–2017 are better predicted with the projections of drought-induced plant scarcity. Field monitoring during 2017 confirmed that host plants had already died off at the beginning of June (i.e. just after the peak of the 2nd generation and the subsequent production of the key 3rd generation) (Vives-Inglá et al., 2020).

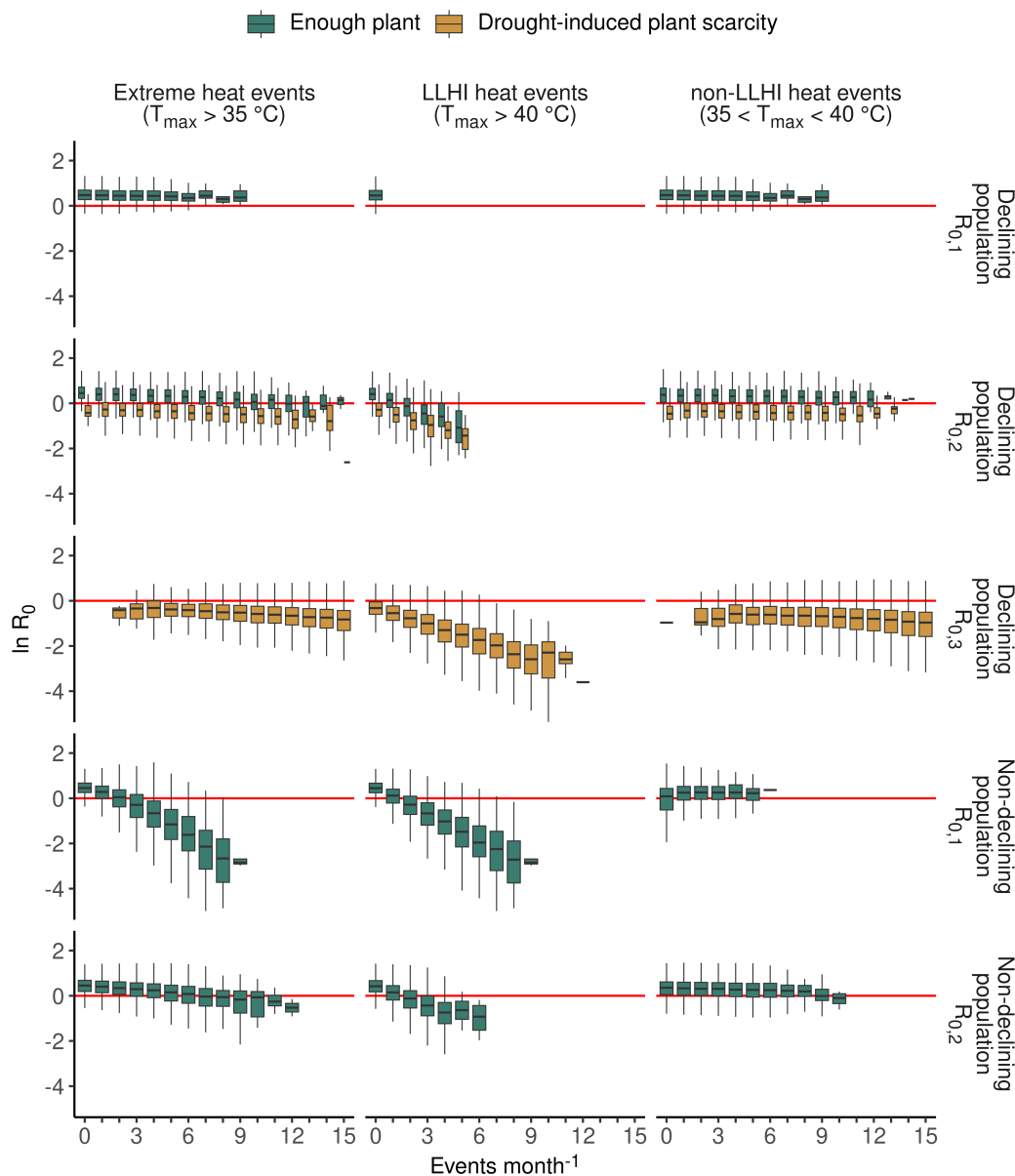


Figure C7: The key role of LLHI heat events in driving negative net reproductive rates ($R_0 < 1$). The boxplots represent the logarithm of the predicted R_0 in all the simulations having the same number of extreme heat events (left), LLHI heat events (centre), or non-LLHI heat events (right) occurring during the first 30 days of the simulation. The lower and upper hinges of the box represent the 1st and the 3rd quartiles respectively (Q_1, Q_3); its inner line, the median; and the length of the box, the $IQR = Q_3 - Q_1$. Lower whisker represents the smallest value $\geq Q_1 - 1.5 \times IQR$; and the upper whisker, the biggest value $\leq Q_3 + 1.5 \times IQR$. Outliers are not shown.

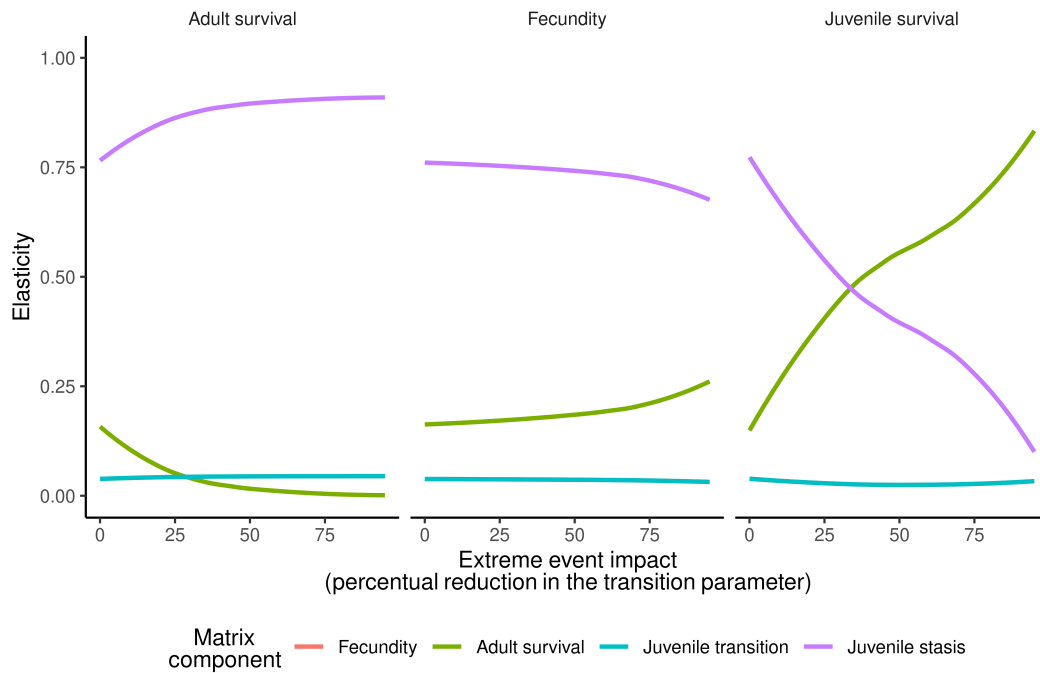


Figure C8: Effects on the calculated elasticities for each matrix component of increasing extreme events impacts on different vital rates. A theoretical extreme event impact was included in the transition matrices by multiplying the affected parameter —adult survival (left), fecundity (centre), or the juvenile parameters(right)— by $1 - \text{impact}$. The elasticities of the finite rate of population increase (λ_{day}) to all the parameters of the modified matrix were then calculated and summed for each matrix component: juvenile stasis (A_{JJ} , purple), juvenile transition (A_{JM} , blue), adult fecundity (A_{MJ} , red), and adult survival (A_{MM} , green). The elasticity values for adult fecundity (red) cannot be seen because they fully overlapped with juvenile transition (blue). The elasticities for the three different transition matrices (A_{spring} , A_{summer} , and $A_{drought}$) are represented together. Juvenile stasis (i.e. the transition probabilities that a juvenile survives and remains in this stage) remains the matrix component with the highest relative contribution to population growth for almost all theoretical extreme event impacts. The only case where we would find a higher relative contribution of adult survival over juveniles would be in extreme events reducing daily juvenile survival by more than 25%. In our main simulations, such extreme impacts only occur on very exceptional occasions (i.e. an extreme LLHI hot day with maximum microclimatic temperatures over 42 °C), having no influence on the overall elasticity patterns reported in our study.

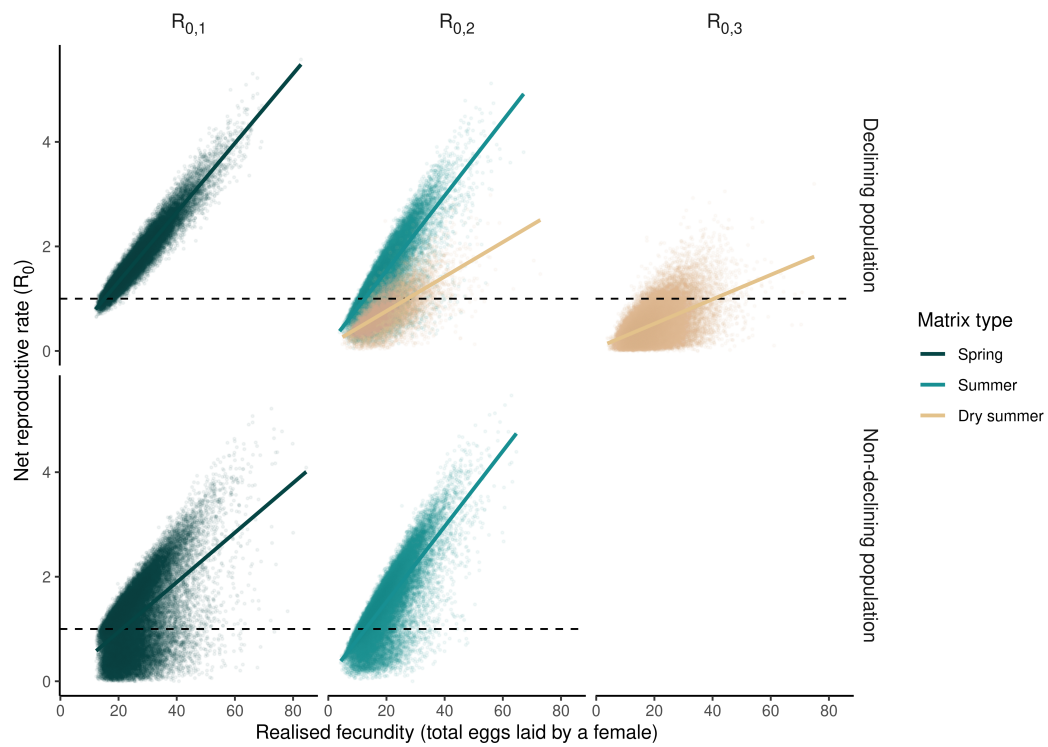


Figure C9: Predicted net reproductive rates (R_0) at increasing simulated fecundities. We calculated the realised fecundity from all the bootstrapped matrices by multiplying the fecundity values at each adult age by the probability of a newly-emerged adult to survive until that age. From the sum of the resulting values, we obtained the realised fecundity and related it with the R_0 predicted in the simulation conducted with the corresponding transition matrix. Notably, R_0 is more tightly linked to the realised fecundity in the simulations with a low frequency of extreme events (e.g. $R_{0,1}$ of the declining population and $R_{0,2}$ of the non-declining population). In contrast, the relation is looser when extreme events are more severe and frequent (e.g. dry summer simulations and simulations with $R_0 < 1$).

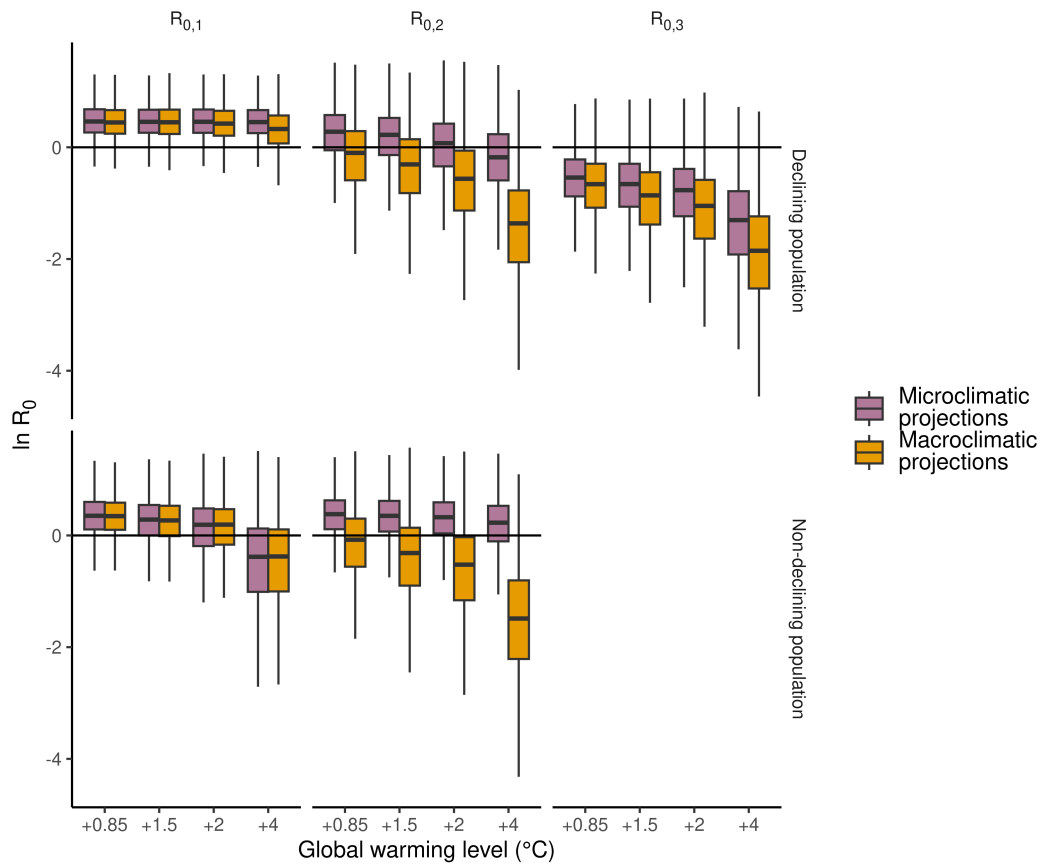


Figure C10: Comparison of the predicted R_0 values considering (pink) or omitting (orange) local microclimatic buffering effects on extreme heat events. The main set of simulations was conducted at a microclimatic scale (i.e. correcting the projected increase of macroclimatic heat events by the probability of occurrence of a microclimatic heat event estimated from field microclimatic records). To assess the importance of microclimatic buffering effects on predicted R_0 , we conducted an additional set of simulations at a macroclimatic scale (i.e. without the microclimatic correction of the frequency of macroclimatic heat events projected by the IPCC, see Appendix C.3.3).

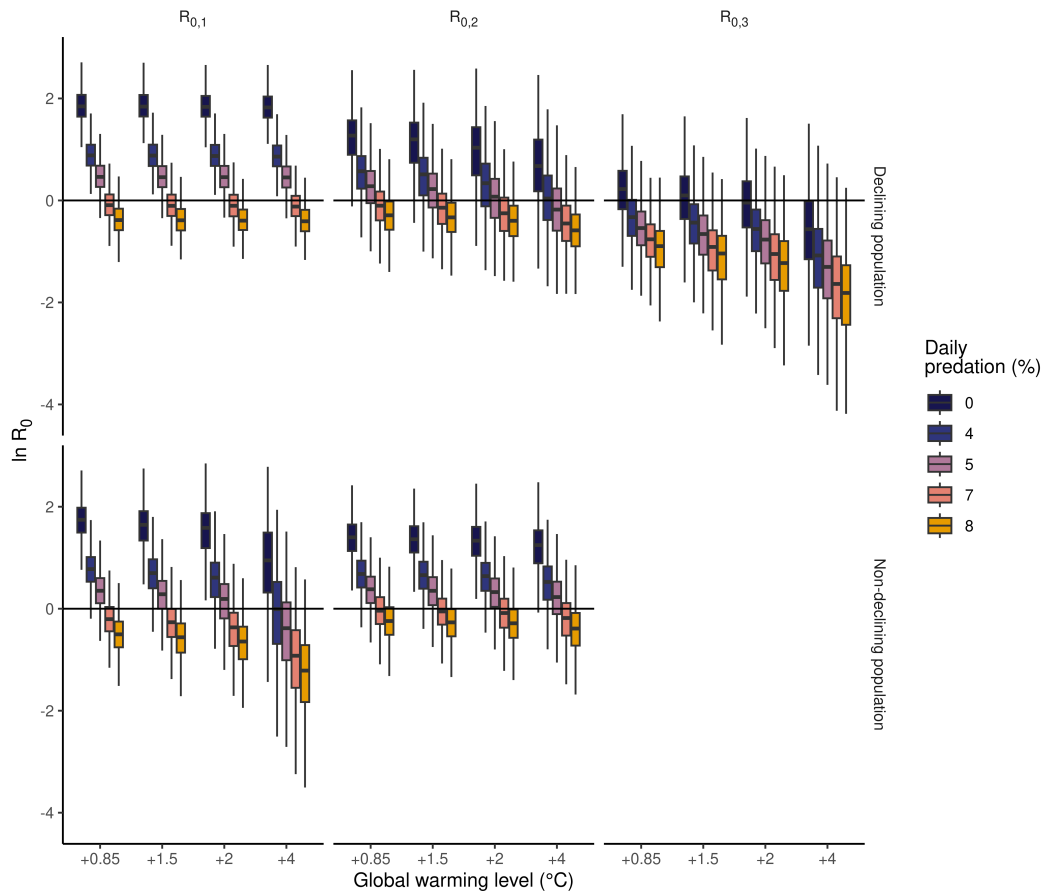


Figure C11: Predicted R_0 values at increasing daily rates of parasitism and predation of juvenile stages. The main set of simulations was conducted assuming a daily predation rate of 5% (pink) and was complemented with simulations without predation pressure (0% daily predation) and three other daily predation rates also aligned with field observations (Fig. C3). As expected, increasing daily predatory rates led to lower predicted values for R_0 . Yet, predicted patterns of population declines were qualitatively similar: more severe declines were reported at increasing global warming levels ($^{\circ}\text{C}$) associated with the nonlinear increase of LLHI heat events. The only simulation set with qualitatively different results was the no predation scenario—a highly unrealistic scenario—, where declining R_0 ($\ln R_0 < 0$) were very rare.

Table C1: Probability of occurrence of the different types of extreme events in the simulations. P_{35} and P_{40} in the $\text{GWL} = +0.85^\circ\text{C}$ correspond to the daily probability of occurrence of an extremely hot day and a LLHI hot day, respectively, estimated from the microclimatic temperature series recorded in partially-sheltered microhabitats in the field (the usual microhabitats of *Pteris napa*). P_{35} and P_{40} in the future scenarios are calculated by multiplying the probabilities of occurrence in the current scenario by the predicted factor of increase of extreme event frequency in the IPCC projections (Gutiérrez et al., 2021; IPCC, 2021; Iturbide et al., 2021). $P_{drought}$ correspond to the frequency of 1-in-10-year soil moisture drought for the June to August period predicted by the IPCC (IPCC, 2021; Seneviratne et al., 2021). See Appendix C.3 for further details.

Extreme type	Population	Net reproductive rate	Months	Probability of an extreme event (P)			
				$\text{GWL} = +0.85^\circ\text{C}$	$\text{GWL} = +1.5^\circ\text{C}$	$\text{GWL} = 2^\circ\text{C}$	$\text{GWL} = +4^\circ\text{C}$
P_{35} Extreme hot day $T_{max} > 35^\circ\text{C}$	Declining	$R_{0,1}$	April–May	0.025	0.030	0.036	0.069
		$R_{0,2}$	June–July	0.121	0.144	0.165	0.218
		$R_{0,3}$	July–August	0.34	0.415	0.479	0.64
	Non-declining	$R_{0,1}$	May–June	0.041	0.049	0.057	0.085
		$R_{0,2}$	July–August	0.065	0.079	0.091	0.122
		$R_{0,1}$	April–May	$3.18\text{E-}09$	$6.36\text{E-}09$	$1.27\text{E-}08$	$3.82\text{E-}08$
P_{40} LLHI hot day $T_{max} > 40^\circ\text{C}$	Declining	$R_{0,2}$	June–July	0.008	0.011	0.013	0.026
		$R_{0,3}$	July–August	0.042	0.058	0.074	0.143
		$R_{0,1}$	May–June	0.017	0.026	0.034	0.084
	Non-declining	$R_{0,2}$	July–August	0.009	0.013	0.016	0.031
		$R_{0,1}$	April–May	0	0	0	0
		$R_{0,2}$	June–July	0.2	0.25	0.4	0.6
$P_{drought}$ Dry summer	Declining	$R_{0,3}$	July–August	1	1	1	1
		$R_{0,1}$	May–June	0	0	0	0
		$R_{0,2}$	July–August	0	0	0	0
	Non-declining	$R_{0,1}$	May–June	0	0	0	0
		$R_{0,2}$	July–August	0	0	0	0
		$R_{0,1}$	April–May	0	0	0	0

Table C2: Summary of the larval ages when host plants were limited experimentally, the subsequent period where we evaluated the impact of plant scarcity on larval survival, and the MPM survival values (\hat{j}_x) modified to include the impacts of plant scarcity following Eq. (C.3)

Age cohort	Ages of individuals when plant scarcity started in the experiment	Ages where we evaluated the effects of plant scarcity in the experiment	Modified values of \hat{j}_x in the MPM
first week	6 and 7 days old	6–14 days old	$\hat{j}_1 - \hat{j}_1 \mathfrak{B}$
second week	12, 13, and 15 days old	12–21 days old	$\hat{j}_{14} - \hat{j}_{20}$
third week	17, 18, and 19 days old	17–28 days old	$\hat{j}_{21} - \hat{j}_m$

Table C3: Summary of the transition matrices applied in the simulations for each population and generation.

Population	Elevation	Observed demographic trend	Transition period	Matrix applied
B _I	Lowland	Declining	From the first to the second generation ($R_{0,1}$)	A_{spring}
			From the second to the third generation ($R_{0,2}$)	A_{summer} and $A_{drought}$
			From the third to the fourth generation ($R_{0,3}$)	$A_{drought}$
B _I	Montane	Non-declining	From the first to the second generation ($R_{0,1}$)	A_{spring}
			From the second to the third generation ($R_{0,2}$)	A_{summer}

C.2 MPM parametrisation

C.2.1 Model structure

We built an *age-within-stage* matrix population model (MPM) for the butterfly *Pieris napi* following the structure proposed by Kerr et al. (2020). Individuals were classified into juveniles (eggs, larvae and pupae) and adults, and subdivided by their age in days. Therefore, the transition matrix of the model (A) was compounded by four submatrices (Eq. (C.1)):

$$A = \begin{pmatrix} A_{JJ} & A_{MJ} \\ A_{JM} & A_{MM} \end{pmatrix},$$

$$A = \begin{pmatrix} 0 & 0 & \dots & 0 & 0 & f_1 & f_2 & \dots & f_{a-1} & f_a \\ j_1(1-e_1)(1-k) & 0 & \dots & 0 & 0 & 0 & 0 & \dots & 0 & 0 \\ 0 & j_2(1-e_2)(1-k) & \dots & 0 & 0 & 0 & 0 & \dots & 0 & 0 \\ \dots & \dots & \dots & \dots & \dots & \dots & \dots & \dots & \dots & \dots \\ 0 & 0 & \dots & j_{m-1}(1-e_{m-1})(1-k) & 0 & 0 & 0 & \dots & 0 & 0 \\ j_1e_1(1-k) & j_2e_2(1-k) & \dots & j_{m-1}e_{m-1}(1-k) & j_me_m(1-k) & 0 & 0 & \dots & 0 & 0 \\ 0 & 0 & \dots & 0 & 0 & s_1 & 0 & \dots & 0 & 0 \\ 0 & 0 & \dots & 0 & 0 & 0 & s_2 & \dots & 0 & 0 \\ \dots & \dots & \dots & \dots & \dots & \dots & \dots & \dots & \dots & \dots \\ 0 & 0 & \dots & 0 & 0 & 0 & 0 & \dots & s_{a-1} & 0 \end{pmatrix}$$

(C.1)

A_{JJ} represents juveniles surviving but not transitioning to adults (i.e. juvenile stasis submatrix, in pink); A_{JM} , juvenile surviving and transitioning to adults (juvenile transition submatrix, in green); A_{MM} , adult survival (in orange); A_{MJ} , adult fecundity (in blue); and m and a the maximum age of juvenile maturation and maximum adult longevity, respectively. As the species produces several generations per year, we built two separate transition matrices representing spring (A_{spring}) and summer generations (A_{summer}) to capture the differences in the mean microclimatic conditions and vital rates during their development. All the analyses to parametrise the model and the subsequent demographic projections were performed in the R environment version 4.3.0 (R Core Team, 2023).

C.2.2 Juvenile vital rates and growth chamber experiments

We parameterised A_{JJ} and A_{JM} submatrices with data from three intensively-studied populations of *Pieris napi* in the north-east of the Iberian Peninsula (Carnicer et al., 2019; Peñuelas et al., 2017; Vives-Inglà et al., 2020, 2023). One of them is a declining population from a coastal wetland (42.225 °N, 3.092 °E, population B1), while the other two correspond to more montane and climatically-buffered populations. One of the two montane populations is located at mid elevations (503 m.a.s.l, 42.145 °N, 2.511 °E, B2), and the other, at higher altitudes, in the Pyrenees (2000 m.a.s.l, 42.454 °N, 1.766 °E, B3).

We calculated the parameters of A_{JJ} and A_{JM} from the experimental estimates of juvenile survival rates (j_x) and the probability of pupal eclosion (e_x , the probability of transition from the juvenile to the adult stage conditioned on juvenile surviving). To estimate these two vital rates (j_x, e_x), we conducted a growth chamber experiment (GCE) with 151 juveniles of *Pieris napi*. We captured 11 females from populations B1 and B3, and reared their offspring in growth chambers (Ibercex Ltd, Spain) programmed at 13:11 L:D and a constant temperature. Captured females were kept in individual cages with abundant host plant and nectar sources to allow oviposition. As butterflies laid eggs, we moved them individually in separate small plates with abundant and fresh host plants, and placed them in a growth chamber at 20 °C (78 eggs) or 25 °C (73 eggs), depending on the treatment. These two treatments represent the mean microclimatic conditions recorded during spring (20 °C) and summer (25 °C) at the microhabitats where larvae of these populations have been detected (Fig. C2). Eggs were followed three times a week across their life cycle until the adults emerged (end of the pupal stage) or until the juveniles died. Appropriate humidity conditions and fresh host-plant availability were checked and maintained regularly.

To calculate juvenile survival rates (j_x) at a daily resolution, we first counted how many juveniles were still alive for each age (in days) and treatment (observed N_x). Then, we fitted a polynomial function on the juvenile counts against age using the *glm* function of the *stats* R package, and applied a generalised linear model (GLM) with a Poisson error distribution and a log link function. We used a 13-degree polynomial function for the juveniles reared at 20 °C and a 5-degree polynomial curve in the case of the juveniles

reared at 25 °C. These corresponded to the polynomial curves with the lowest degree that were significantly different in likelihood ratio tests from the inferior degree curves while maintaining a monotonically declining function (and thus avoiding increases in N_x with time) (Kerr et al., 2020). We then used the predicted daily curve of N_x to calculate juvenile survival rates (j_x) following Eq. (C.2):

$$j_x = \frac{N_{x+1}}{N_x} \quad (\text{C.2})$$

In the field, juveniles are exposed to very high predation rates from predators and specific parasitoids, which we couldn't estimate with the data from the growth chamber experiments (GCE). To account for juvenile predation, we applied a mortality factor homogeneously to all j_x values. Concretely, we multiplied j_x by 0.95 to obtain similar probabilities for an egg to become an adult to those reported in the field (Fig. C3; Cappuccino and Kareiva, 1985; Doak et al., 2006; Forsberg, 1987; Keeler et al., 2006; Yamamoto, 1981).

We estimated the mean time of pupal eclosion by fitting a Poisson family, log-link GLM on the age of the pupae before becoming an adult, and calculated the probability of juvenile eclosion conditioned on surviving (e_x) at each age by considering a Poisson distribution with the estimated mean age as its λ . Data from both model populations and the eleven females was pooled together because no significant contributions were found for these factors.

Direct impacts of extreme heat events

We integrated the direct impacts of extreme heat events on the MPM through the experimental nonlinear responses in heat-induced mortality shown by *P. napi* (TDT curves; Carnicer et al., 2019; Rezende et al., 2014; Vives-Inгла et al., 2023). In previous studies, we calculated the thermally-induced mortality of B1 and B2 populations combining experimental estimates of heat tolerance of the species and its microclimatic exposure recorded in the field (Carnicer et al., 2019; Vives-Inгла et al., 2023). To estimate the heat tolerance, we captured 10 females from the two populations and reared their offspring in controlled conditions (22 °C, 13:11 L:D). We conducted a static assay of heat tolerance with 89 reared larvae, which consisted in submerging the larvae (inside plastic vials) in a water bath programmed at 40, 42, or 44 °C and recording their time of death. With this information, we built a thermal death time curve (TDT curve) for the species. TDT curves describe the decrease in the critical temperature that individuals can tolerate with the logarithm of the time of exposure (Rezende et al., 2014).

We recorded heat exposure in the field by installing, in each population, six standalone data loggers (EL-USB-2-LCD, Lascar Electronics, UK) in different microsites where ovipositing females are usually detected (i.e. intermediately-covered microhabitats, such

as the margins of paths and irrigation canals partially sheltered by the surrounding vegetation; Vives-Inгла et al., 2023). The sensors were programmed to record temperature ($^{\circ}\text{C}$) and relative humidity (%) at an hourly resolution, and were placed 25 cm above the soil protected from direct solar radiation. To calculate the thermal mortality derived from field microclimatic exposure during a day with usual temperatures ($T_{max} < 35^{\circ}\text{C}$), extremely non-LLHI hot event ($35^{\circ}\text{C} < T_{max} < 40^{\circ}\text{C}$), and a low-likelihood high-impact (LLHI) heat event ($T_{max} > 40^{\circ}\text{C}$), we randomly selected 240 days of each type from the microclimatic records. We then applied a dynamical model that integrates, across each recorded day, the infinitesimal changes that the fluctuating microclimatic temperatures produce in the survival probability based on the TDT curve of the species (Rezende et al., 2020a,b; Vives-Inгла et al., 2023). Specifically, we first estimated the daily thermal microclimatic profile at 1-min resolution by linear interpolation between hourly measurements, and the TDT curves of the species for all the values of survival probability ranging from 0 to 1 by 0.001. From this relationship between survival, time and temperatures (i.e. survival-specific TDT curves), we calculated the maximum daily mortality by summing up the infinitesimal decreases in survival associated with the concatenation of 1-min thermal exposures throughout the day. A more detailed mathematical description of the dynamical model can be found in Rezende et al. (2020a,b); Vives-Inгла et al. (2022, 2023). Finally, to allow the prediction of thermal mortality from a single temperature value (each daily T_{max}) in the simulations, we fitted a logistic function on the thermal mortality predicted with the dynamic model ($k = 1 - \text{daily survival}$) against daily microclimatic temperature (T_{max}) using a generalised linear model with a binomial error distribution and a logit link function.

Indirect impacts of extreme summer drought

We integrated the impacts of extreme summer drought on the MPM through their influence on host-plant availability and the associated indirect effects on insect juvenile survival (j_x) and maturation (e_x). To estimate these indirect effects, we conducted a complementary growth chamber experiment under the same summer microclimatic conditions (25°C , 13:11 L:D), but limited host-plant availability. We repeated the same procedure described above with 161 larvae raised from 8 females captured in populations B1 and B2. We provided abundant and fresh host plants to the larvae until the 20th day of the experiment, when we stopped the replacement of host plants for one week, exposing the larvae to a food shortage.

The impacts of drought-induced food stress might change with juvenile age and stage (e.g. between early and larval instars) (Salgado and Saastamoinen, 2019). For this reason, we analysed the effects of the food shortage on juvenile survival in different age cohorts. We classified juveniles into individuals that were on their first, second, or third week of development when food shortage started, and assessed the effects of plant scarcity during their subsequent week of development (Table C2). Again, we counted how many individuals were still alive at each daily age and regressed the daily counts against age (in days)

by fitting a GLM with a Poisson error distribution and a log link function. Best fits corresponded to the 1-degree linear model, resulting in a constant survival probability per age group. To estimate juvenile survival in conditions of plant scarcity ($j_{x,drought}$) from these constant rates, we repeated the same procedure with the data obtained in the GCE under control conditions (i.e. enough host plant) and calculated the same constant survival rates per age group. We finally obtained $j_{x,drought}$ as follows:

$$j_{x,drought} = j_{x,summer} \frac{w_{\lfloor \frac{x}{7} \rfloor, drought}}{w_{\lfloor \frac{x}{7} \rfloor, summer}} \quad (C.3)$$

where x is the juvenile age (in days); $j_{x,summer}$ corresponds to j_x calculated with Eq. (C.2) for the GCE at 25 °C and enough host plant, and $w_{\lfloor \frac{x}{7} \rfloor}$, to the constant survival probabilities corresponding to their age group in conditions of food stress ($w_{\lfloor \frac{x}{7} \rfloor, drought}$) or enough host plant ($w_{\lfloor \frac{x}{7} \rfloor, summer}$).

The curves of $j_{x,summer}$ and $j_{x,drought}$ are shown in Fig. 5.2 of the main document (panel b1). Juveniles that were in their second week of development were the most affected by the food shortage. This might be due to earlier larvae having inferior food demands in absolute terms, and to last-stage larvae advancing their pupation as a response to plant scarcity. Earlier pupations due to low food availability have been observed for this species before (von Schmalensee et al., 2021a) and were also observed in this GCE. This phenological effect was also introduced in the MPM by calculating the difference in the mean age of pupation between the GCE with enough host plant and the GCE with host-plant scarcity, subtracting this difference from λ and recalculating e_x with this new λ (see above).

C.2.3 Adult vital rates

We obtained adult vital rates from published literature on *Pieris napi*. For adult fecundity, we extracted with the *metaDigitise* R package (Pick et al., 2019) the daily quantity of eggs laid by females of this model species directly from the figures of different scientific papers published on the subject (Friberg et al., 2015; Larsdotter-Mellström et al., 2010; Ohsaki, 1980; Välimäki et al., 2006; Wiklund et al., 1993). Extracted data included quantifications from females at different conditions (both in the field and the laboratory), mating systems (monandrous and polyandrous females), and development pathways (diapausing and directly-developing females). We estimated the daily fecundities of the spring matrix with the extracted values from diapausing females by fitting a 3-degree polynomial function of the daily egg count against age (in days) with the *glmTMB* function of the *glmTMB* R package (Brooks et al., 2017a). For the summer matrices, we used the extracted values from directly-developing females and fitted a 5-degree polynomial function. Again, polynomial terms were added in a stepwise fashion and kept if they differed significantly in likelihood ratio tests from the preceding model (Kerr et al.,

2020). We fitted the polynomial curves with generalised linear mixed models (GLMM), adding the original source and mating system of the females as random factors, and using a log link function and a negative binomial II error distribution to account for overdispersion in the data (Brooks et al., 2017a).

For adult survival, we extracted with the *metaDigitise* R package the daily values and the associated 95% confidence interval estimated in the MPM that Kerr et al. (2020) built for *Pieris oleracea*, a very close species to *P. napi* (formerly a subspecies), with a very similar ecology (Bowden, 1979; Chew and Watt, 2006).

The final matrices (A_{spring} and A_{summer}) were 63-dimensional and 59-dimensional, respectively. These dimensions corresponded to the sum of the maximum juvenile and adult longevities (m and a) detected in the different treatments of the GCE ($m = 40$ days in the 20 °C treatment, and $m = 30$ days in the 25 °C treatment) and the bibliographic fecundity values ($a = 23$ days for diapausing females, and $a = 29$ days for directly-developing females). We guaranteed that the resulting matrices were primitive, irreducible, and ergodic (Otto and Day, 2011; Stott et al., 2010). The values of the parameters finally compounding the transition matrices can be found in Fig. C4.

C.3 Demographic projections

C.3.1 Population projections

We projected *P. napi* populations under multiple regimes of extreme events with the *project* function of the *popdemo* R package, version 1.3-1 (Stott et al., 2012). These corresponded to the seasonal conditions that the different generations experienced in the observational period (1993–2018) and three different climatic scenarios of global warming. The simulated extreme events included extremely dry summers, extremely hot days ($T_{max} > 35$ °C), low-likelihood, high-impact hot days ($T_{max} > 40$ °C), and compound hot-dry events when two of these events coincided in time. The projections started with an initial vector of 1 recently-emerged adult (i.e. n_0 with 1 adult of age 1, and 0 individuals of the other stages) and lasted 70 days to give enough time to the simulated population to complete the whole life cycle at least once.

The seasonal conditions that we simulated corresponded to the periods of transition between consecutive generations. To simulate the first transition (i.e. the growth and development of the second generation after the first peak of adults that emerge from winter diapause), the model took May–June conditions in the mid-elevation population B2 ($R_{0,1}$ in the left panel of Fig. 5.2a). For the lowland population (B1), this same transition considered April–May conditions, as the phenology of these populations typically goes faster, with adults emerging and starting to breed earlier ($R_{0,1}$ in the right panel of Fig. 5.2a). The development of these generations were simulated with the spring matrix (A_{spring}). For the development of the third generation from the second flying peak, we

considered July–August conditions for the non-declining mid-elevation population, but June to mid-July conditions for the declining population B1 ($R_{0,2}$ in the corresponding panels). After this summer generation, the lowland declining population can produce another generation during mid-July and August conditions ($R_{0,3}$ in the right panel of Fig. 5.2a).

As summarised in Table C3, we simulated $R_{0,2}$ of the non-declining mid-elevation population with the summer matrix (A_{summer}); $R_{0,3}$ of the declining population with the dry summer matrix ($A_{drought}$); and $R_{0,2}$ of the declining population with either A_{summer} or $A_{drought}$ depending on the probability of occurrence of a dry summer ($P_{drought}$). We defined these seasonal scenarios in agreement with our observations in the field (Carnicer et al., 2019; Vives-Inгла et al., 2020, 2023). While the host plant used in the mid-elevation population B2 usually stays green during the whole year (*Alliaria petiolata*), the species used in the lowland population B1 (*Lepidium draba* and *Brassica nigra*) withers during summer, exposing late generations to a period of food shortage. Thus, the late-summer generation of the declining population ($R_{0,3}$) faces drought-induced plant scarcity every year, while the preceding generation ($R_{0,2}$) only faces plant scarcity in very dry summers, which induce an earlier decay of the host plants. Crucially, our field observations point to drought-induced earlier decays of the host plants as the process driving the demographic declines in these populations (Carnicer et al., 2019; Vives-Inгла et al., 2020, 2023).

We simulated these seasonal regimes of extreme events in four different scenarios of global warming (GWL-0.85, GWL-1.5, GWL-2, and GWL-4). These included an scenario GWL-0.85 of an increase in mean global surface air temperatures of +0.85 °C relative to 1850–1900 (i.e. global warming level, GWL), corresponding to the increase recorded during 1995–2014, matching the field demographic series (Chen et al., 2021; IPCC, 2021). The other three corresponded to future scenarios. Two of them were in line with the Paris Agreement goals (i.e. GWL-1.5 and GWL-2), and the other consisted in a high-emissions scenario with no climate policies (GWL-4). For each climatic scenario and seasonal transitions between generations (i.e. 4 scenarios \times 5 transitions), we performed 10,000 projections to account for the environmental stochasticity in the occurrence of extreme events. To account also for the variation and uncertainty in the estimated vital rates in each projected replicate, we built a transition matrix sampling directly from the physiological data (nonparametric bootstrap). Specifically, for the parameters in A_{JJ} and A_{JM} , we sampled with replacement from GCE data the same amount of individuals monitored in the experiments. For the parameters in A_{MJ} , we sampled with replacement from the bibliographic database of daily fecundities until we obtained a database with the same amount of bibliographic inputs as the original database. Finally, for the parameters in A_{MM} , we sampled the daily values of adult survival from a normal distribution with the logit-transformed mean daily adult survival estimated from Kerr et al. (2020) as its mean, and the standard deviation calculated from the logit-transformed lower value of its 95% confidence interval. The sampled value of adult survival was then back-transformed using a logistic function (expit scale). The primitivity, irreducibility, and ergodicity of all the bootstrapped matrices was checked with the *popdemo* package (Stott et al., 2010, 2012).

Extreme heat events

Heat events were simulated on a daily basis. At each time step, a day with usual maximum temperatures ($T_{max} < 35\text{ }^{\circ}\text{C}$), an extremely hot event ($T_{max} > 35\text{ }^{\circ}\text{C}$), or an LLHI hot event ($T_{max} > 40\text{ }^{\circ}\text{C}$) could be simulated depending on the probabilities of event occurrence (P_{35} and P_{40}). For the simulations at current global warming levels (GWL-0.85), these probabilities of occurrence were calculated from the field microclimatic records taken in the larval growth microhabitats of B1 and B2 populations (see Appendix C.2.2). For each type of heat event (i.e. extremely hot day or LLHI hot day), we estimated their probability of occurrence by fitting a GLM with a Binomial error distribution and logit link function on the daily occurrence of the event (1 if happened, 0 if not) against the population (B1 or B2), the seasonal period as described above, and their interaction. We used the predicted values of the two GLMs as P_{35} and P_{40} for present-day simulations.

For the simulations at future global warming levels (GWL1.5, GWL-2, and GWL-4), we calculated P_{35} and P_{40} based on the projections compiled by the IPCC (Gutiérrez et al., 2021; IPCC, 2021; Iturbide et al., 2021; Seneviratne et al., 2021). For these three global warming levels, we obtained the projected number of days surpassing 35 and 40 °C in the Mediterranean area at a monthly resolution from the CMIP6 models without bias adjustment of the Interactive Atlas of the IPCC-WG1 (Gutiérrez et al., 2021; Iturbide et al., 2021). We translated these macroclimatic projections to microclimatic estimates of P_{35} and P_{40} at different scenarios of global warming following this equation:

$$P_{x,GWL} = P_{x,0.85} \frac{N_{x,GWL}}{N_{x,0.85}} \quad (\text{C.4})$$

where x is the type of heat event (surpassing 35 or 40 °C); $P_{x,GWL}$, the probability of occurrence of the heat event at a microclimatic scale for the projected GWL (GWL = 0.85 °C in the current scenario); and $N_{x,GWL}$, the number of days for each type of event projected at a macroclimatic scale. The ratio of the number of extremely hot days in future IPCC scenarios against the current scenario ($\frac{N_{x,GWL}}{N_{x,0.85}}$) was particularly high for LLHI events in GWL-4 scenario ($\frac{N_{40,4}}{N_{40,0.85}}$), capturing the expected non-proportional increase in P_{40} relative to P_{35} with GWL (Fig. C5 and Table C1) (IPCC, 2021; Seneviratne et al., 2021; Simolo and Corti, 2022; Vogel et al., 2020).

At each daily time step, we randomly sampled one number from a binomial distribution with P_{35} as the probability of success. If 1 was sampled (i.e. an extremely heat event occurred), we sampled a new number from another binomial distribution with $\frac{P_{40}}{P_{35}}$ as the probability of success to decide whether the extreme heat event was a LLHI event (another 1 sampled), or not (a 0 sampled). The algorithm then sampled the maximum temperature of that simulated day (T_{max}) from a uniform distribution (between 17 and 35 °C in the case of days with usual temperatures, 35–40 °C for non-LLHI extremely

hot events, and 40–45 °C for LLHI hot events). Based on this T_{max} , the algorithm calculated thermal mortality (k) using the logistic model fitted on experimental data (see Appendix C.2.2) and multiplied by $1 - k$ the rates of the juvenile submatrices (A_{JJ} and A_{JM} , Eq. (C.1)).

Extreme drought

We simulated drought at a seasonal scale in all the projections of the late-summer generation in the declining population, and some of the projections of the midsummer generation depending on $P_{drought}$ (see Table C3 for a summary) We obtained the probability of occurrence of a dry summer from the estimates of 1-in-10 year soil moisture droughts in the Iberian peninsula published in the 6th Assessment Report of the IPCC (IPCC, 2021; Seneviratne et al., 2021). The definition of a 1-in-10 year soil moisture drought (i.e. $P_{drought} = 0.1$) was based on the period between 1850 and 1900, and estimated to have already increased by 2 during 1995–2014 (GWL-0.85), and to increase by 2.5, 4 and 6 in the GWL-1.5, GWL-2 and GWL-4 scenarios, respectively (Table C1).

Projections of dry summers used the corresponding transition matrix ($A_{drought}$), which also affected the juvenile submatrices (A_{JJ} and A_{JM}). Concurrent dry summers with extremely hot days ($T_{max} > 35$ °C) were considered compound hot-dry events and were simulated by multiplying the corresponding thermal factor ($1 - k$) on $A_{drought}$ (Eq. (C.1)).

C.3.2 Net reproductive rates

To have an estimate of the population performance in the different seasonal and climatic scenarios, we calculated the transient net reproductive rate (R_0) for each bootstrap replicate. Net reproductive rates represent the mean lifetime production of offspring per female of the population, and give a rate of demographic increase per generation and an indicator of population persistence ($R_0 > 1$ for growing populations, and $R_0 < 1$ for declining ones) (Caswell, 2009). Based on its classical definition (Caswell, 2009; Lotka, 1934; Rhodes, 1940), we approximated the transient R_0 as the sum of all adult individuals of age 1 produced in the simulated population until the end of the first generation (the shaded areas of the population curves in Fig. 5.2b3). This calculation corresponds to the expected lifetime offspring production of the adult of age 1 compounding the population at the beginning of the simulation. To estimate the end of the first simulated generation, we defined an algorithm heuristically. This algorithm found the day when the simulated abundance of adults of age 1 started to rise again after a previous decline. At the same time, the algorithm also ignored eventual abrupt changes in abundance associated with episodes of high thermal mortality that were not reflecting the emergence of a new subsequent generation.

The algorithm correctly detected around 98% of the generation endings. The replicates with an incorrect determination of the end of the generation were associated with

very anomalous patterns of adult abundance. In these rare cases, the resulting R_0 was extremely high because the algorithm put the ending of the first generation after 50 days of simulation or did not find any valid ending, and they were thus excluded for the subsequent analyses.

We used the predicted R_0 for three different objectives. First, we compared the predicted R_0 in current levels of global warming (GWL-0.85) with the observed R_0 calculated from the demographic series of the model populations in the field. This was done in order to validate our MPM and give mechanistic support to the hypothesis that summer drought is currently driving population declines. Then, we used the predicted R_0 of the future scenarios to forecast the performance of the population in different global warming levels and the associated regimes of extreme climatic events. The predicted R_0 were additionally used to quantify and compare the impacts of extremely hot days, LLHI hot days, droughts and their combined effects.

Observed R_0

The two model populations that we use to validate our MPM (B1 and B2) are part of the Catalan Butterfly Monitoring Scheme (CBMS, www.catalanbms.org). This provides standardised, weekly counts of the adult butterflies of the species detected along a fixed transect from March to September since 1993. From this data, we calculated observed R_0 in each year by summing all the weekly counts during one flying peak of adults and dividing it by the sum of counts during the preceding flying peak. We defined each flying peak with constant and static periods across all the years. The first flying period included the counts during March and April; the second, May and June counts; the third, all the rest of the counts in the resilient B2, but just July counts in the declining B1; and the fourth was only calculated for B1 and included August and September counts. We also calculated the interannual growth rates (λ_{annual}) by summing all the counts in one year and dividing it by the counts of the preceding year. If hot and dry extreme summer events are driving the declines of the decreasing population, we expect that at least these summer generations show $R_0 < 1$.

C.3.3 Additional simulations

The influence of microclimatic buffering effects on predicted R_0

We performed an additional set of simulations excluding local microclimatic buffering effects (Carnicer et al., 2019; Vives-Inгла et al., 2023) and simulating only the projected increase in macroclimatic extreme events predicted by the IPCC (Gutiérrez et al., 2021; IPCC, 2021; Iturbide et al., 2021). The simulations were conducted as described in Appendices C.2 and C.3 but calculating the probability of occurrence of an extreme heat events ($P_{x,GWL}$) as:

$$P_{x,GWL} = \frac{N_{x,GWL}}{period} \quad (C.5)$$

where x is the type of heat macroclimatic event (surpassing 35 or 40 °C); *period*, the duration in days considered for a particular period of transition between generations (i.e. 61 or 62 depending on the included months); and $N_{x,GWL}$, the number of days for each type of event projected by the IPCC during the corresponding generation period (Fig. C5).

These simulations provided complementary results that confirmed the key role of local microclimate in the mitigation of macroclimatic thermal extremes (Fig. C10).

Varying predator and parasitoid pressures

In order to evaluate the importance of the predatory pressure assumed in our main set of simulations (i.e., a daily predation rate of 5% of the juveniles), we repeated the simulations as explained in Appendices C.2 and C.3 but using different daily predation rates. We selected daily predation rates producing similar probabilities for an egg to become an adult to those reported in different field studies for *P. napi* (Fig. C3; Forsberg, 1987; Yamamoto, 1981) and added an additional scenario without predation. The results of this additional set of simulations can be found in Fig. C11.



Bibliography

- I. M. Aalberg Haugen, D. Berger, and K. Gotthard. The evolution of alternative developmental pathways: footprints of selection on life-history traits in a butterfly. *Journal of Evolutionary Biology*, 25(7):1377–1388, 2012. ISSN 1420-9101. doi: 10.1111/j.1420-9101.2012.02525.x.
- M. Abarca and R. Spahn. Direct and indirect effects of altered temperature regimes and phenological mismatches on insect populations. *Current Opinion in Insect Science*, 47: 67–74, 2021. ISSN 2214-5745. doi: 10.1016/j.cois.2021.04.008.
- H. D. Adams, G. A. Barron-Gafford, R. L. Minor, A. A. Gardea, L. P. Bentley, D. J. Law, D. D. Breshears, N. G. McDowell, and T. E. Huxman. Temperature response surfaces for mortality risk of tree species with future drought. *Environmental Research Letters*, 12(11):115014, 2017. ISSN 1748-9326. doi: 10.1088/1748-9326/aa93be.
- E. T. Addicott, E. P. Fenichel, M. A. Bradford, M. L. Pinsky, and S. A. Wood. Toward an improved understanding of causation in the ecological sciences. *Frontiers in Ecology and the Environment*, 20(8):474–480, 2022. ISSN 1540-9309. doi: 10.1002/fee.2530.
- E. Ali, W. Cramer, J. Carnicer, E. Georgopoulou, N. Hilmi, G. Le Cozannet, and P. Lionello. Cross-Chapter Paper 4: Mediterranean Region. In H.-O. Pörtner, D. C. Roberts, M. Tignor, E. S. Poloczanska, K. Mintenbeck, A. Alegría, M. Craig, S. Langsdorf, S. Löschke, V. Möller, A. Okem, and B. Rama, editors, *Climate Change 2022: Impacts, Adaptation and Vulnerability. Contribution of Working Group II to the Sixth Assessment Report of the Intergovernmental Panel on Climate Change*, pages 2233–2272. Cambridge University Press, Cambridge, UK and New York, USA, 2022. ISBN 978-1-00-932584-4. doi: 10.1017/9781009325844.
- C. D. Allen, A. K. Macalady, H. Chenchouni, D. Bachelet, N. McDowell, M. Vennetier, T. Kitzberger, A. Rigling, D. D. Breshears, E. H. T. Hogg, P. Gonzalez, R. Fensham, Z. Zhang, J. Castro, N. Demidova, J.-H. Lim, G. Allard, S. W. Running, A. Semerci, and N. Cobb. A global overview of drought and heat-induced tree mortality reveals emerging climate change risks for forests. *Forest Ecology and Management*, 259(4): 660–684, 2010. ISSN 0378-1127. doi: 10.1016/j.foreco.2009.09.001.
- S. L. Althaus, M. R. Berenbaum, J. Jordan, and D. A. Shalmon. No buzz for bees: Media coverage of pollinator decline. *Proceedings of the National Academy of Sciences*, 118(2): e2002552117, 2021. ISSN 0027-8424, 1091-6490. doi: 10.1073/pnas.2002552117.

- W. R. L. Anderegg, A. Flint, C.-y. Huang, L. Flint, J. A. Berry, F. W. Davis, J. S. Sperry, and C. B. Field. Tree mortality predicted from drought-induced vascular damage. *Nature Geoscience*, 8(5):367–371, 2015a. ISSN 1752-0908. doi: 10.1038/ngeo2400.
- W. R. L. Anderegg, J. A. Hicke, R. A. Fisher, C. D. Allen, J. Aukema, B. Bentz, S. Hood, J. W. Lichstein, A. K. Macalady, N. McDowell, Y. Pan, K. Raffa, A. Sala, J. D. Shaw, N. L. Stephenson, C. Tague, and M. Zeppel. Tree mortality from drought, insects, and their interactions in a changing climate. *New Phytologist*, 208(3):674–683, 2015b. ISSN 1469-8137. doi: 10.1111/nph.13477.
- W. R. L. Anderegg, T. Klein, M. Bartlett, L. Sack, A. F. A. Pellegrini, B. Choat, and S. Jansen. Meta-analysis reveals that hydraulic traits explain cross-species patterns of drought-induced tree mortality across the globe. *Proceedings of the National Academy of Sciences*, 113(18):5024–5029, 2016. doi: 10.1073/pnas.1525678113.
- S. C. Anderson, T. A. Branch, A. B. Cooper, and N. K. Dulvy. Black-swan events in animal populations. *Proceedings of the National Academy of Sciences*, 114(12):3252–3257, 2017. doi: 10.1073/pnas.1611525114.
- M. J. Angilletta. Estimating and comparing thermal performance curves. *Journal of Thermal Biology*, 31(7):541–545, 2006. ISSN 0306-4565. doi: 10.1016/j.jtherbio.2006.06.002.
- M. J. Angilletta. *Thermal adaptation: a theoretical and empirical synthesis*. Oxford University Press Inc., New York, NY, 2009. ISBN 978-0-19-857087-5.
- Annisa, S. Chen, N. C. Turner, and W. A. Cowling. Genetic Variation for Heat Tolerance During the Reproductive Phase in *Brassica rapa*. *Journal of Agronomy and Crop Science*, 199(6):424–435, 2013. ISSN 1439-037X. doi: 10.1111/jac.12034.
- S. Arif and M. A. MacNeil. Predictive models aren't for causal inference. *Ecology Letters*, 25(8):1741–1745, 2022. ISSN 1461-0248. doi: 10.1111/ele.14033.
- S. Ashton, D. Gutiérrez, and R. J. Wilson. Effects of temperature and elevation on habitat use by a rare mountain butterfly: Implications for species responses to climate change. *Ecological Entomology*, 34(4):437–446, 2009. ISSN 03076946. doi: 10.1111/j.1365-2311.2008.01068.x.
- D. Atkinson. Temperature and Organism Size—A biological Law for Ectotherms? *Advances in Ecological Research*, 25(January 1994):1–58, 1994. ISSN 0065-2504. doi: 10.1016/S0065-2504(08)60212-3.
- D. Atkinson and R. M. Sibly. Why are organisms usually bigger in colder environments? Making sense of a life history puzzle. *Trends in Ecology & Evolution*, 12(6):235–239, 1997. ISSN 0169-5347. doi: 10.1016/S0169-5347(97)01058-6.
- C. S. Awmack and S. R. Leather. Host Plant Quality and Fecundity in Herbivorous Insects. *Annual Review of Entomology*, 47(1):817–844, 2002. doi: 10.1146/annurev.ento.47.091201.145300.

- C. Azpiazu, J. Bosch, E. Viñuela, P. Medrzycki, D. Teper, and F. Sgolastra. Chronic oral exposure to field-realistic pesticide combinations via pollen and nectar: effects on feeding and thermal performance in a solitary bee. *Scientific Reports*, 9(1):13770, 2019. ISSN 2045-2322. doi: 10.1038/s41598-019-50255-4.
- Y. M. Bar-On, R. Phillips, and R. Milo. The biomass distribution on Earth. *Proceedings of the National Academy of Sciences*, 115(25):6506–6511, 2018. doi: 10.1073/pnas.1711842115.
- A. Bastos, S. Sippel, D. Frank, M. D. Mahecha, S. Zaehle, J. Zscheischler, and M. Reichstein. A joint framework for studying compound ecoclimatic events. *Nature Reviews Earth & Environment*, 4:1–18, 2023. ISSN 2662-138X. doi: 10.1038/s43017-023-00410-3.
- D. Bates, M. Mächler, B. Bolker, and S. Walker. Fitting Linear Mixed-Effects Models Using lme4. *Journal of Statistical Software*, 67(1):1–48, 2015. doi: 10.18637/jss.v067.i01.
- S. S. Bauerfeind and K. Fischer. Increased temperature reduces herbivore host-plant quality. *Global Change Biology*, 19(11):3272–3282, 2013a. ISSN 13541013. doi: 10.1111/gcb.12297.
- S. S. Bauerfeind and K. Fischer. Testing the plant stress hypothesis: stressed plants offer better food to an insect herbivore. *Entomologia Experimentalis et Applicata*, 149(2):148–158, 2013b. ISSN 1570-7458. doi: <https://doi.org/10.1111/eea.12118>.
- S. S. Bauerfeind and K. Fischer. Integrating temperature and nutrition – environmental impacts on an insect immune system. *Journal of insect physiology*, 64:14–20, 2014a. ISSN 1879-1611. doi: 10.1016/j.jinsphys.2014.03.003.
- S. S. Bauerfeind and K. Fischer. Simulating climate change: temperature extremes but not means diminish performance in a widespread butterfly. *Population Ecology*, 56(1):239–250, 2014b. ISSN 1438-3896. doi: 10.1007/s10144-013-0409-y.
- S. Beguería and S. M. Vicente-Serrano. SPEI: Calculation of the Standardised Precipitation-Evapotranspiration Index, 2017. URL <https://cran.r-project.org/package=SPEI>.
- N. L. Bennett, P. M. Severns, C. Parmesan, and M. C. Singer. Geographic mosaics of phenology, host preference, adult size and microhabitat choice predict butterfly resilience to climate warming. *Oikos*, 124(1):41–53, 2015. ISSN 16000706. doi: 10.1111/oik.01490.
- D. Benyamini. Pupal summer diapause in Chilean *Pieris brassicae* (Linnaeus, 1758) (Lepidoptera, Pieridae). *Nota Lepidopterologica*, 18(3):184–192, 1996. ISSN 03427536.
- J. Bergström and C. Wiklund. Effects of size and nuptial gifts on butterfly reproduction: can females compensate for a smaller size through male-derived nutrients? *Behavioral Ecology and Sociobiology*, 52(4):296–302, 2002. ISSN 0340-5443, 1432-0762. doi: 10.1007/s00265-002-0512-0.

- E. Bevacqua, C. De Michele, C. Manning, A. Couasnon, A. F. S. Ribeiro, A. M. Ramos, E. Vignotto, A. Bastos, S. Blesić, F. Durante, J. Hillier, S. C. Oliveira, J. G. Pinto, E. Ragno, P. Rivoire, K. Saunders, K. van der Wiel, W. Wu, T. Zhang, and J. Zscheischler. Guidelines for Studying Diverse Types of Compound Weather and Climate Events. *Earth's Future*, 9(11):e2021EF002340, 2021. ISSN 2328-4277. doi: 10.1029/2021EF002340.
- S. Bewick, R. S. Cantrell, C. Cosner, and W. F. Fagan. How Resource Phenology Affects Consumer Population Dynamics. *The American Naturalist*, 187(2):151–166, 2015. ISSN 0003-0147. doi: 10.1086/684432.
- J. Bielby, G. M. Mace, O. R. P. Bininda-Emonds, M. Cardillo, J. L. Gittleman, K. E. Jones, C. D. L. Orme, and A. Purvis. The Fast-Slow Continuum in Mammalian Life History: An Empirical Reevaluation. *The American Naturalist*, 169(6):748–757, 2007. ISSN 0003-0147. doi: 10.1086/516847.
- W. D. Bigelow. The logarithmic nature of thermal death time curves. *The Journal of Infectious Diseases*, 29(5):528–536, 1921. ISSN 0022-1899. doi: 10.1093/infdis/29.5.528.
- W. D. Bigelow and J. R. Esty. The Thermal Death Point in Relation to Time of Typical Thermophilic Organisms. *The Journal of Infectious Diseases*, 27(6):602–617, 1920. ISSN 0022-1899. doi: 10.1093/infdis/27.6.602.
- C. J. Bissoondath and C. Wiklund. Effect of Male Mating History and Body Size on Ejaculate Size and Quality in Two Polyandrous Butterflies, *Pieris napi* and *Pieris rapae* (Lepidoptera: Pieridae). *Functional Ecology*, 10:457–464, 1996. doi: 10.2307/2389938.
- A. J. Bladon, M. Lewis, E. K. Bladon, S. J. Buckton, S. Corbett, S. R. Ewing, M. P. Hayes, G. E. Hitchcock, R. Knock, C. Lucas, A. McVeigh, R. Menéndez, J. M. Walker, T. M. Fayle, and E. C. Turner. How butterflies keep their cool: Physical and ecological traits influence thermoregulatory ability and population trends. *Journal of Animal Ecology*, 89(11):2440–2450, 2020. ISSN 1365-2656. doi: 10.1111/1365-2656.13319.
- C. L. Boggs. The fingerprints of global climate change on insect populations. *Current Opinion in Insect Science*, 17:69–73, 2016. ISSN 22145745. doi: 10.1016/j.cois.2016.07.004.
- C. L. Boggs and D. W. Inouye. A single climate driver has direct and indirect effects on insect population dynamics. *Ecology Letters*, 15(5):502–508, 2012. ISSN 1461023X. doi: 10.1111/j.1461-0248.2012.01766.x.
- S. Bonelli, L. P. Casacci, F. Barbero, C. Cerrato, L. Dapporto, V. Sbordoni, S. Scalercio, A. Zilli, A. Battistoni, C. Teofili, C. Rondinini, and E. Balletto. The first red list of Italian butterflies. *Insect Conservation and Diversity*, 11(5):506–521, 2018. ISSN 1752-4598. doi: 10.1111/icad.12293.
- S. R. Bowden. Subspecific variation in butterflies: adaptation and dissected polymorphism in *Pieris (Artogeia)* (Pieridae). *Journal of the Lepidopterists' Society*, 33(2):77–111, 1979.

- W. E. Bradshaw and C. M. Holzapfel. Genetic shift in photoperiodic response correlated with global warming. *Proceedings of the National Academy of Sciences*, 98(25):14509–14511, 2001. doi: 10.1073/pnas.241391498.
- I. Bramer, B. J. Anderson, J. J. Bennie, A. J. Bladon, P. De Frenne, D. L. Hemming, R. A. Hill, M. R. Kearney, C. Körner, A. H. Korstjens, J. Lenoir, I. M. D. Maclean, C. D. Marsh, M. D. Morecroft, R. Ohlemüller, H. D. Slater, A. J. Suggitt, F. Zellweger, and P. K. Gillingham. Advances in Monitoring and Modelling Climate at Ecologically Relevant Scales. *Advances in Ecological Research*, 58:101–161, 2018. ISSN 0065-2504. doi: 10.1016/BS.AEER.2017.12.005.
- B. Braschler, S. L. Chown, and G. A. Duffy. Sub-critical limits are viable alternatives to critical thermal limits. *Journal of Thermal Biology*, 101:103106, 2021. ISSN 03064565. doi: 10.1016/j.jtherbio.2021.103106.
- N. J. Briscoe, S. D. Morris, P. D. Mathewson, L. B. Buckley, M. Jusup, O. Levy, I. M. D. Maclean, S. Pincebourde, E. A. Riddell, J. A. Roberts, R. Schouten, M. W. Sears, and M. R. Kearney. Mechanistic forecasts of species responses to climate change: The promise of biophysical ecology. *Global Change Biology*, 29(6):1451–1470, 2023. ISSN 1365-2486. doi: 10.1111/gcb.16557.
- J. F. Brodie, O. E. Helmy, J. Mohd-Azlan, A. Granados, H. Bernard, A. J. Giordano, and E. Zipkin. Models for assessing local-scale co-abundance of animal species while accounting for differential detectability and varied responses to the environment. *Biotropica*, 50(1):5–15, 2018. ISSN 1744-7429. doi: 10.1111/btp.12500.
- M. Brooks, E., K. Kristensen, K. J. van Benthem, A. Magnusson, C. Berg, W., A. Nielsen, H. J. Skaug, M. Mächler, and B. M. Bolker. glmmTMB Balances Speed and Flexibility Among Packages for Zero-inflated Generalized Linear Mixed Modeling. *The R Journal*, 9(2):378, 2017a. ISSN 2073-4859. doi: 10.32614/RJ-2017-066.
- S. J. Brooks, A. Self, G. D. Powney, W. D. Pearse, M. Penn, and G. L. Paterson. The influence of life history traits on the phenological response of British butterflies to climate variability since the late-19th century. *Ecography*, 40(10):1152–1165, 2017b. ISSN 16000587. doi: 10.1111/ecog.02658.
- J. H. Brown and A. Kodric-Brown. Turnover Rates in Insular Biogeography: Effect of Immigration on Extinction. *Ecology*, 58(2):445–449, 1977. ISSN 0012-9658. doi: 10.2307/1935620.
- J. L. Brunner, S. L. LaDeau, M. Killilea, E. Valentine, M. Schierer, and R. S. Ostfeld. Off-host survival of blacklegged ticks in eastern North America: A multistage, multiyear, multisite study. *Ecological Monographs*, 93(3):e1572, 2023. ISSN 1557-7015. doi: 10.1002/ecm.1572.
- L. B. Buckley. Temperature-sensitive development shapes insect phenological responses to climate change. *Current Opinion in Insect Science*, 52:100897, 2022. ISSN 2214-5745. doi: 10.1016/j.cois.2022.100897.

BIBLIOGRAPHY

- L. B. Buckley and R. B. Huey. How extreme temperatures impact organisms and the evolution of their thermal tolerance. *Integrative and Comparative Biology*, 56(1):98–109, 2016. ISSN 15577023. doi: 10.1093/icb/icw004.
- L. B. Buckley and J. G. Kingsolver. The demographic impacts of shifts in climate means and extremes on alpine butterflies. *Functional Ecology*, 26(4):969–977, 2012. ISSN 1365-2435. doi: 10.1111/j.1365-2435.2012.01969.x.
- L. B. Buckley, M. C. Urban, M. J. Angilletta, L. G. Crozier, L. J. Rissler, and M. W. Sears. Can mechanism inform species' distribution models? *Ecology Letters*, 13(8):1041–1054, 2010. ISSN 1461-0248. doi: 10.1111/j.1461-0248.2010.01479.x.
- L. B. Buckley, E. Carrington, M. E. Dillon, C. García-Robledo, S. B. Roberts, J. L. Wegrzyn, and M. C. Urban. Characterizing biological responses to climate variability and extremes to improve biodiversity projections. *PLOS Climate*, 2(6):e0000226, 2023a. ISSN 2767-3200. doi: 10.1371/journal.pclm.0000226.
- L. B. Buckley, B. A. B. Ortiz, I. Caruso, A. John, O. Levy, A. V. Meyer, E. A. Riddell, Y. Sakairi, and J. L. Simonis. TrenchR: An R package for modular and accessible microclimate and biophysical ecology. *PLOS Climate*, 2(8):e0000139, 2023b. ISSN 2767-3200. doi: 10.1371/journal.pclm.0000139.
- R. Caillon, C. Suppo, J. Casas, H. A. Woods, and S. Pincebourde. Warming decreases thermal heterogeneity of leaf surfaces: implications for behavioural thermoregulation by arthropods. *Functional Ecology*, 28(6):1449–1458, 2014. ISSN 1365-2435. doi: <https://doi.org/10.1111/1365-2435.12288>.
- P. Capdevila, B. Hereu, J. L. Riera, and C. Linares. Unravelling the natural dynamics and resilience patterns of underwater Mediterranean forests: insights from the demography of the brown alga *Cystoseira zosteroides*. *Journal of Ecology*, 104(6):1799–1808, 2016. ISSN 1365-2745. doi: <https://doi.org/10.1111/1365-2745.12625>.
- N. Cappuccino and P. Kareiva. Coping with a Capricious Environment: A Population Study of a Rare Pierid Butterfly. *Ecology*, 66(1):152–161, 1985. ISSN 00129658. doi: 10.2307/1941315.
- J. Carnicer, M. Coll, M. Ninyerola, X. Pons, G. Sanchez, and J. Peñuelas. Widespread crown condition decline, food web disruption, and amplified tree mortality with increased climate change-type drought. *Proceedings of the National Academy of Sciences*, 108(4):1474–1478, 2011. ISSN 0027-8424. doi: 10.1073/pnas.1010070108.
- J. Carnicer, L. Brotons, C. Stefanescu, and J. Peñuelas. Biogeography of species richness gradients: linking adaptive traits, demography and diversification. *Biological Reviews*, 87(2):457–479, 2012. ISSN 14647931. doi: 10.1111/j.1469-185X.2011.00210.x.
- J. Carnicer, A. Barbeta, D. Sperlich, M. Coll, and J. Penuelas. Contrasting trait syndromes in angiosperms and conifers are associated with different responses of tree growth to temperature on a large scale. *Frontiers in Plant Science*, 4, 2013a. ISSN 1664-462X.

- J. Carnicer, C. Stefanescu, R. Vila, V. Dincă, X. Font, and J. Peñuelas. A unified framework for diversity gradients: The adaptive trait continuum. *Global Ecology and Biogeography*, 22(1):6–18, 2013b. ISSN 1466822X. doi: 10.1111/j.1466-8238.2012.00762.x.
- J. Carnicer, C. W. Wheat, M. Vives-Inгла, A. Ubach, C. Domingo-Marimón, S. Nylin, C. Stefanescu, R. Vila, C. Wiklund, and J. Peñuelas. Evolutionary responses of invertebrates to global climate change: The role of life-history trade-offs and multidecadal climate shifts. In S. N. Johnson and H. Jones, editors, *Global Climate Change and Terrestrial Invertebrates*, pages 319–348. John Wiley & Sons, Ltd, Chichester, UK, first edition, 2017. ISBN 978-1-119-07089-4. doi: 10.1002/9781119070894.ch16.
- J. Carnicer, C. Stefanescu, M. Vives-Inгла, C. López, S. Cortizas, C. W. Wheat, R. Vila, J. Llusà, and J. Peñuelas. Phenotypic biomarkers of climatic impacts on declining insect populations: A key role for decadal drought, thermal buffering and amplification effects and host plant dynamics. *Journal of Animal Ecology*, 88:376–391, 2019. ISSN 13652656. doi: 10.1111/1365-2656.12933.
- J. Carnicer, M. Vives-Inгла, L. Blanquer, X. Méndez-Camps, C. Rosell, S. Sabaté, E. Gutiérrez, T. Sauras, J. Peñuelas, and A. Barbeta. Forest resilience to global warming is strongly modulated by local-scale topographic, microclimatic and biotic conditions. *Journal of Ecology*, 109(9):3322–3339, 2021. ISSN 1365-2745. doi: 10.1111/1365-2745.13752.
- J. Carnicer, J. Sala-García, M. Vives-Inгла, V. Dincă, and R. Vila. Phylogeography and diversification of the *Pieris napi* species group, 2023.
- H. Caswell. *Matrix population models: construction, analysis, and interpretation*. Sinauer Associates, Sunderland (Mass.), 2nd ed. edition, 2001. ISBN 0-87893-096-5.
- H. Caswell. Stage, age and individual stochasticity in demography. *Oikos*, 118(12):1763–1782, 2009. ISSN 1600-0706. doi: 10.1111/j.1600-0706.2009.17620.x.
- P. B. Cavers, M. I. Heagy, and R. F. Kokron. The biology of Canadian weeds. 35. *Alliaria petiolata* (M. Bieb.) Cavara and Grande. *Canadian Journal of Plant Science*, 59(1):217–229, 1979. doi: 10.4141/cjps79-029.
- D. Chen, M. Rojas, B. H. Samset, K. Cobb, A. Diongue-Niang, P. Edwards, S. Emori, S. H. Faria, E. Hawkins, P. Hope, P. Huybrechts, M. Meinshausen, S. K. Mustafa, G.-K. Plattner, and A. M. Tréguier. Framing, context, and methods. In V. Masson-Delmotte, P. Zhai, A. Pirani, S. L. Connors, C. Péan, S. Berger, N. Caud, Y. Chen, L. Goldfarb, M. I. Gomis, M. Huang, K. Leitzell, E. Lonnoy, J. B. R. Matthews, T. K. Maycock, T. Waterfield, Ö. Yelekçi, R. Yu, and B. Zhou, editors, *Climate Change 2021: The Physical Science Basis. Contribution of Working Group I to the Sixth Assessment Report of the Intergovernmental Panel on Climate Change*, pages 147–286. Cambridge University Press, Cambridge, United Kingdom and New York, NY, USA, 2021. doi: 10.1017/9781009157896.001.
- F. S. Chew and W. B. Watt. The green-veined white (*Pieris napi* L.), its Pierine relatives, and the systematics dilemmas of divergent character sets (Lepidoptera, Pieridae).

- Biological Journal of the Linnean Society*, 88(3):413–435, 2006. ISSN 1095-8312. doi: <https://doi.org/10.1111/j.1095-8312.2006.00630.x>.
- F. J. Clissold and S. J. Simpson. Temperature, food quality and life history traits of herbivorous insects. *Current Opinion in Insect Science*, 11:63–70, 2015. ISSN 2214-5745. doi: [10.1016/j.cois.2015.10.011](https://doi.org/10.1016/j.cois.2015.10.011).
- H. Cochard. A new mechanism for tree mortality due to drought and heatwaves. *Peer Community Journal*, 1, 2021. ISSN 2804-3871. doi: [10.24072/pcjournal.45](https://doi.org/10.24072/pcjournal.45).
- N. Colin, C. Porte, D. Fernandes, C. Barata, F. Padrós, M. Carrassón, M. Monroy, O. Cano-Rocabayera, A. de Sostoa, B. Piña, and A. Maceda-Veiga. Ecological relevance of biomarkers in monitoring studies of macro-invertebrates and fish in Mediterranean rivers. *Science of The Total Environment*, 540:307–323, 2016. ISSN 0048-9697. doi: [10.1016/j.scitotenv.2015.06.099](https://doi.org/10.1016/j.scitotenv.2015.06.099).
- P. Colom, A. Traveset, D. Carreras, and C. Stefanescu. Spatio-temporal responses of butterflies to global warming on a Mediterranean island over two decades. *Ecological Entomology*, 46(262-272), 2021. ISSN 1365-2311. doi: <https://doi.org/10.1111/een.12958>.
- P. Colom, M. Ninyerola, X. Pons, A. Traveset, and C. Stefanescu. Phenological sensitivity and seasonal variability explain climate-driven trends in Mediterranean butterflies. *Proceedings of the Royal Society B: Biological Sciences*, 289(1973):20220251, 2022. doi: [10.1098/rspb.2022.0251](https://doi.org/10.1098/rspb.2022.0251).
- S. R. Connolly, S. A. Keith, R. K. Colwell, and C. Rahbek. Process, Mechanism, and Modeling in Macroecology. *Trends in Ecology & Evolution*, 32(11):835–844, 2017. ISSN 01695347. doi: [10.1016/j.tree.2017.08.011](https://doi.org/10.1016/j.tree.2017.08.011).
- G. R. Coope, A. S. Wilkins, J. H. Lawton, and R. M. May. The response of insect faunas to glacial-interglacial climatic fluctuations. *Philosophical Transactions of the Royal Society of London. Series B: Biological Sciences*, 344(1307):19–26, 1997. doi: [10.1098/rstb.1994.0046](https://doi.org/10.1098/rstb.1994.0046).
- H. V. Cornell, B. A. Hawkins, and M. E. Hochberg. Towards an empirically-based theory of herbivore demography. *Ecological Entomology*, 23(3):340–349, 1998. ISSN 0307-6946. doi: [10.1046/j.1365-2311.1998.00140.x](https://doi.org/10.1046/j.1365-2311.1998.00140.x).
- S. P. Courtney. The Ecology of Pierid Butterflies: Dynamics and Interactions. *Advances in Ecological Research*, 15:51–131, 1986. ISSN 0065-2504. doi: [10.1016/S0065-2504\(08\)60120-8](https://doi.org/10.1016/S0065-2504(08)60120-8).
- M. S. Crossley, O. M. Smith, L. L. Berry, R. Phillips-Cosio, J. Glassberg, K. M. Holman, J. G. Holmquest, A. R. Meier, S. A. Varriano, M. R. McClung, M. D. Moran, and W. E. Snyder. Recent climate change is creating hotspots of butterfly increase and decline across North America. *Global Change Biology*, 27(12):2702–2714, 2021. ISSN 1365-2486. doi: <https://doi.org/10.1111/gcb.15582>.

- P. J. Curran, J. L. Dungan, and H. L. Gholz. Exploring the relationship between reflectance red edge and chlorophyll content in slash pine. *Tree Physiology*, 7:33–48, 1990. ISSN 0829-318X, 1758-4469. doi: 10.1093/treephys/7.1-2-3-4.33.
- R. J. Curtis, T. M. Brereton, R. L. H. Dennis, C. Carbone, and N. J. B. Isaac. Butterfly abundance is determined by food availability and is mediated by species traits. *Journal of Applied Ecology*, 52(6):1676–1684, 2015. ISSN 13652664. doi: 10.1111/1365-2664.12523.
- L. Dapporto and R. L. H. Dennis. The generalist-specialist continuum: Testing predictions for distribution and trends in British butterflies. *Biological Conservation*, 157: 229–236, 2013. ISSN 00063207. doi: 10.1016/j.biocon.2012.09.016.
- E. S. Darling and I. M. Côté. Quantifying the evidence for ecological synergies. *Ecology Letters*, 11(12):1278–1286, 2008. ISSN 1461-0248. doi: 10.1111/j.1461-0248.2008.01243.x.
- R. F. Daubenmire. A canopy-coverage method of vegetational analysis. *Northwest Science*, 33:43–64, 1959.
- K. J. Davis. Managed culls mean extinction for a marine mammal population when combined with extreme climate impacts. *Ecological Modelling*, 473:110122, 2022. ISSN 0304-3800. doi: 10.1016/j.ecolmodel.2022.110122.
- K. T. Davis, S. Z. Dobrowski, Z. A. Holden, P. E. Higuera, and J. T. Abatzoglou. Microclimatic buffering in forests of the future: the role of local water balance. *Ecography*, 42(1):1–11, 2019. ISSN 0906-7590. doi: 10.1111/ecog.03836.
- T. P. Dawson, S. T. Jackson, J. I. House, I. C. Prentice, and G. M. Mace. Beyond Predictions: Biodiversity Conservation in a Changing Climate. *Science*, 332(6025):53–58, 2011. ISSN 0036-8075, 1095-9203. doi: 10.1126/science.1200303.
- O. de Bolós and J. Vigo. *Flora dels Països Catalans, II*. Barcino, Barcelona, first edition, 1990. ISBN ISBN 978-84-7226-620-9.
- M. De Cáceres, M. Mencuccini, N. Martin-StPaul, J.-M. Limousin, L. Coll, R. Poyatos, A. Cabon, V. Granda, A. Forner, F. Valladares, and J. Martínez-Vilalta. Unravelling the effect of species mixing on water use and drought stress in Mediterranean forests: A modelling approach. *Agricultural and Forest Meteorology*, 296:108233, 2021. ISSN 0168-1923. doi: 10.1016/j.agrformet.2020.108233.
- P. De Frenne, F. Rodríguez-Sánchez, D. A. Coomes, L. Baeten, G. Verstraeten, M. Vellend, M. Bernhardt-Romermann, C. D. Brown, J. Brunet, J. Cornelis, G. Decocq, H. Dierschke, O. Eriksson, F. S. Gilliam, R. Hedl, T. Heinken, M. Hermy, P. Hommel, M. A. Jenkins, D. L. Kelly, K. J. Kirby, F. J. G. Mitchell, T. Naaf, M. Newman, G. Peterken, P. Petrik, J. Schultz, G. Sonnier, H. Van Calster, D. M. Waller, G.-R. Walther, P. S. White, K. D. Woods, M. Wulf, B. J. Graae, and K. Verheyen. Microclimate moderates plant responses to macroclimate warming. *Proceedings of the National Academy of Sciences*, 110(46):18561–18565, 2013. ISSN 0027-8424. doi: 10.1073/pnas.1311901110.

- P. De Frenne, F. Zellweger, F. Rodríguez-Sánchez, B. R. Scheffers, K. Hylander, M. Luoto, M. Vellend, K. Verheyen, and J. Lenoir. Global buffering of temperatures under forest canopies. *Nature Ecology and Evolution*, 3(5):744–749, 2019. ISSN 2397334X. doi: 10.1038/s41559-019-0842-1.
- P. De Frenne, J. Lenoir, M. Luoto, B. R. Scheffers, F. Zellweger, J. Aalto, M. B. Ashcroft, D. M. Christiansen, G. Decocq, K. D. Pauw, S. Govaert, C. Greiser, E. Gril, A. Hampe, T. Jucker, D. H. Klings, I. A. Koelemeijer, J. J. Lembrechts, R. Marrec, C. Meeussen, J. Ogée, V. Tyystjärvi, P. Vangansbeke, and K. Hylander. Forest microclimates and climate change: Importance, drivers and future research agenda. *Global Change Biology*, 27(11):2279–2297, 2021. ISSN 1365-2486. doi: <https://doi.org/10.1111/gcb.15569>.
- A. Degut, K. Fischer, M. Quque, F. Criscuolo, P. Michalik, and M. Beaulieu. Irreversible impact of early thermal conditions: an integrative study of developmental plasticity linked to mobility in a butterfly species. *Journal of Experimental Biology*, 225(3): jeb243724, 2022. ISSN 0022-0949. doi: 10.1242/jeb.243724.
- J. P. Dempster. The Control of *Pieris rapae* with DDT. I. The Natural Mortality of the Young Stages of *Pieris*. *The Journal of Applied Ecology*, 4(2):485, 1967. ISSN 00218901. doi: 10.2307/2401350.
- J. P. Dempster. The Natural Control of Populations of Butterflies and Moths. *Biological Reviews*, 58(3):461–481, 1983. ISSN 1469-185X. doi: 10.1111/j.1469-185X.1983.tb00396.x.
- R. L. H. Dennis. *Butterflies and climate change*. Manchester University Press, Manchester New York, 1993. ISBN 978-0-7190-3505-0 978-0-7190-4033-7.
- R. L. H. Dennis. *A resource-based habitat view for conservation: butterflies in the British landscape*. John Wiley & Sons, Ltd, West Sussex, first edition, 2010. ISBN 978-1-4051-9945-2.
- C. A. Deutsch, J. J. Tewksbury, R. B. Huey, K. S. Sheldon, C. K. Ghalambor, D. C. Haak, and P. R. Martin. Impacts of climate warming on terrestrial ectotherms across latitude. *Proceedings of the National Academy of Sciences*, 105(18):6668–6672, 2008. ISSN 0027-8424. doi: 10.1073/pnas.0709472105.
- S. E. Diamond, C. A. Penick, S. L. Pelini, A. M. Ellison, N. J. Gotelli, N. J. Sanders, and R. R. Dunn. Using Physiology to Predict the Responses of Ants to Climatic Warming. *Integrative and Comparative Biology*, 53(6):965–974, 2013. ISSN 1540-7063. doi: 10.1093/icb/ict085.
- L. V. Dicks, T. D. Breeze, H. T. Ngo, D. Senapathi, J. An, M. A. Aizen, P. Basu, D. Buchori, L. Galetto, L. A. Garibaldi, B. Gemmill-Herren, B. G. Howlett, V. L. Imperatriz-Fonseca, S. D. Johnson, A. Kovács-Hostyánszki, Y. J. Kwon, H. M. G. Latorff, T. Lungharwo, C. L. Seymour, A. J. Vanbergen, and S. G. Potts. A global-scale expert assessment of drivers and risks associated with pollinator decline. *Nature Ecology & Evolution*, 5:1453–1461, 2021. ISSN 2397-334X. doi: 10.1038/s41559-021-01534-9.

- R. K. Didham, Y. Basset, C. M. Collins, S. R. Leather, N. A. Littlewood, M. H. M. Menz, J. Müller, L. Packer, M. E. Saunders, K. Schönrogge, A. J. A. Stewart, S. P. Yanoviak, and C. Hassall. Interpreting insect declines: seven challenges and a way forward. *Insect Conservation and Diversity*, 13(2):103–114, 2020. ISSN 1752-4598. doi: 10.1111/icad.12408.
- M. E. Dillon, H. A. Woods, G. Wang, S. B. Fey, D. A. Vasseur, R. S. Telemeco, K. E. Marshall, and S. Pincebourde. Life in the frequency domain: The biological impacts of changes in climate variability at multiple time scales. *Integrative and Comparative Biology*, 56(1):14–30, 2016. ISSN 15577023. doi: 10.1093/icb/icw024.
- P. Doak, P. Kareiva, and J. Kingsolver. Fitness consequences of choosy oviposition for a time-limited butterfly. *Ecology*, 87(2):395–408, 2006. ISSN 0012-9658. doi: 10.1890/05-0647.
- C. Domingo-Marimón. *Contributions to the knowledge of the multitemporal spatial patterns of the Iberian Peninsula droughts from a Geographic Information Science perspective*. PhD thesis, Universitat Autònoma de Barcelona, 2016.
- I. Donoso, C. Stefanescu, A. Martínez-Abraín, and A. Traveset. Phenological asynchrony in plant–butterfly interactions associated with climate: a community-wide perspective. *Oikos*, 125(10):1434–1444, 2016. ISSN 16000706. doi: 10.1111/oik.03053.
- H. Douville, K. Raghavan, J. Renwick, R. Allan, P. Arias, M. Barlow, R. Cerezo-Mota, A. Cherchi, T. Gan, J. Gergis, D. Jiang, A. Khan, W. Pokam Mba, D. Rosenfeld, J. Tierney, and O. Zolina. Water Cycle Changes. In V. Masson-Delmotte, P. Zhai, A. Pirani, S. Connors, C. Péan, S. Berger, N. Caud, Y. Chen, L. Goldfarb, M. Gomis, M. Huang, K. Leitzell, E. Lonnoy, J. Matthews, T. Maycock, T. Waterfield, O. Yelekçi, R. Yu, and B. Zhou, editors, *Climate Change 2021: The Physical Science Basis. Contribution of Working Group I to the Sixth Assessment Report of the Intergovernmental Panel on Climate Change*, pages 1055–1210. Cambridge University Press, Cambridge, United Kingdom and New York, NY, USA, 2021. doi: 10.1017/9781009157896.010.
- F. Duchenne, E. Porcher, J.-B. Mihoub, G. Lois, and C. Fontaine. Controversy over the decline of arthropods: a matter of temporal baseline? *Peer Community Journal*, 2, 2022. ISSN 2804-3871. doi: 10.24072/pcjournal.131.
- G. A. Duffy, B. W. Coetzee, C. Janion-Scheepers, and S. L. Chown. Microclimate-based macrophysiology: implications for insects in a warming world. *Current Opinion in Insect Science*, 11:84–89, 2015. ISSN 22145745. doi: 10.1016/j.cois.2015.09.013.
- S. Díaz. A fabric of life view of the world. *Science*, 375(6586):1204–1204, 2022. doi: 10.1126/science.abp8336.
- S. Díaz, J. Kattge, J. H. C. Cornelissen, I. J. Wright, S. Lavorel, S. Dray, B. Reu, M. Kleyer, C. Wirth, I. Colin Prentice, E. Garnier, G. Bönlisch, M. Westoby, H. Poorter, P. B. Reich, A. T. Moles, J. Dickie, A. N. Gillison, A. E. Zanne, J. Chave, S. Joseph Wright, S. N. Sheremet'ev, H. Jactel, C. Baraloto, B. Cerabolini, S. Pierce, B. Shipley,

- D. Kirkup, F. Casanoves, J. S. Joswig, A. Günther, V. Falczuk, N. Rüger, M. D. Mahecha, and L. D. Gorné. The global spectrum of plant form and function. *Nature*, 529(7585):167–171, 2016. ISSN 1476-4687. doi: 10.1038/nature16489.
- S. Díaz, J. Settele, E. S. Brondízio, H. T. Ngo, J. Agard, A. Arneeth, P. Balvanera, K. A. Brauman, S. H. M. Butchart, K. M. A. Chan, L. A. Garibaldi, K. Ichii, J. Liu, S. M. Subramanian, G. F. Midgley, P. Miloslavich, Z. Molnár, D. Obura, A. Pfaff, S. Polasky, A. Purvis, J. Razzaque, B. Reyers, R. R. Chowdhury, Y.-J. Shin, I. Visseren-Hamakers, K. J. Willis, and C. N. Zayas. Pervasive human-driven decline of life on Earth points to the need for transformative change. *Science*, 366(6471):eaax3100, 2019. doi: 10.1126/science.aax3100.
- P. R. Ehrlich, D. D. Murphy, M. C. Singer, C. B. Sherwood, R. R. White, and I. L. Brown. Extinction, reduction, stability and increase: The responses of checkerspot butterfly (*Euphydryas*) populations to the California drought. *Oecologia*, 46(1):101–105, 1980. ISSN 0029-8549. doi: 10.1007/BF00346973.
- S. A. Elias. Insects and Climate Change. *BioScience*, 41(8):552–559, 1991. ISSN 0006-3568. doi: 10.2307/1311608.
- S. P. Ellner and J. Guckenheimer. *Dynamic Models in Biology*. Princeton University Press, Princeton, NJ, 2006. ISBN 978-0-691-12589-3.
- E. K. Engelhardt, M. F. Biber, M. Dolek, T. Fartmann, A. Hochkirch, J. Leidinger, F. Löffler, S. Pinkert, D. Poniatowski, J. Voith, M. Winterholler, D. Zeuss, D. E. Bowler, and C. Hof. Consistent signals of a warming climate in occupancy changes of three insect taxa over 40 years in central Europe. *Global Change Biology*, 28(13):3998–4012, 2022. ISSN 1365-2486. doi: 10.1111/gcb.16200.
- M. Espeland, K. Aagaard, T. Balstad, and K. Hindar. Ecomorphological and genetic divergence between lowland and montane forms of the *Pieris napi* species complex (Pieridae, Lepidoptera). *Biological Journal of the Linnean Society*, 92(4):727–745, 2007.
- J. H. Everitt, A. J. Richardson, and H. W. Guasman. Leaf Reflectance-Nitrogen-Chlorophyll Relations in Buffelgrass. *Photogrammetric Engineering and Remote Sensing*, 51(4):463–466, 1985.
- C. Finn, F. Grattarola, and D. Pincheira-Donoso. More losers than winners: investigating Anthropocene defaunation through the diversity of population trends. *Biological Reviews*, 98(5):1732–1748, 2023. ISSN 1469-185X. doi: 10.1111/brv.12974.
- K. Fischer and K. Fiedler. Response of the copper butterfly *Lycaena tityrus* to increased leaf nitrogen in natural food plants: evidence against the nitrogen limitation hypothesis. *Oecologia*, 124(2):235–241, 2000. ISSN 1432-1939. doi: 10.1007/s004420000365.

- V. Flo, J. Bosch, X. Arnan, C. Primante, A. M. M. González, H. Barril-Graells, and A. Rodrigo. Yearly fluctuations of flower landscape in a Mediterranean scrubland: Consequences for floral resource availability. *PLOS ONE*, 13(1):e0191268, 2018. ISSN 1932-6203. doi: 10.1371/journal.pone.0191268.
- D. T. T. Flockhart, J.-B. Pichancourt, D. R. Norris, and T. G. Martin. Unravelling the annual cycle in a migratory animal: breeding-season habitat loss drives population declines of monarch butterflies. *Journal of Animal Ecology*, 84(1):155–165, 2015. ISSN 1365-2656. doi: <https://doi.org/10.1111/1365-2656.12253>.
- B. Fontaine, B. Bergerot, I. Le Viol, and R. Julliard. Impact of urbanization and gardening practices on common butterfly communities in France. *Ecology and Evolution*, 6(22):8174–8180, 2016. ISSN 20457758. doi: 10.1002/ece3.2526.
- M. L. Forister, V. Novotny, A. K. Panorska, L. Baje, Y. Basset, P. T. Butterill, L. Cizek, P. D. Coley, F. Dem, I. R. Diniz, P. Drozd, M. Fox, A. E. Glassmire, R. Hazen, J. Hrcek, J. P. Jahner, O. Kaman, T. J. Kozubowski, T. A. Kursar, O. T. Lewis, J. Lill, R. J. Marquis, S. E. Miller, H. C. Morais, M. Murakami, H. Nickel, N. A. Pardikes, R. E. Ricklefs, M. S. Singer, A. M. Smilanich, J. O. Stireman, S. Villamarín-Cortez, S. Vodka, M. Volf, D. L. Wagner, T. Walla, G. D. Weiblen, and L. A. Dyer. The global distribution of diet breadth in insect herbivores. *Proceedings of the National Academy of Sciences*, 112(2):442–447, 2015. doi: 10.1073/pnas.1423042112.
- M. L. Forister, B. Cousens, J. G. Harrison, K. Anderson, J. H. Thorne, D. Waetjen, C. C. Nice, M. De Parsia, M. L. Hladik, R. Meese, H. van Vliet, and A. M. Shapiro. Increasing neonicotinoid use and the declining butterfly fauna of lowland California. *Biology Letters*, 12(8):20160475, 2016. ISSN 1744-9561. doi: 10.1098/rsbl.2016.0475.
- M. L. Forister, J. A. Fordyce, C. C. Nice, J. H. Thorne, D. P. Waetjen, and A. M. Shapiro. Impacts of a millennium drought on butterfly faunal dynamics. *Climate Change Responses*, 5(1):3, 2018. ISSN 2053-7565. doi: 10.1186/s40665-018-0039-x.
- J. Forsberg. Size discrimination among conspecific hostplants in two pierid butterflies; *Pieris napi* L. and *Pontia daplidice* L. *Oecologia*, 72(1):52–57, 1987. ISSN 0029-8549, 1432-1939. doi: 10.1007/BF00385044.
- J. Forsberg and C. Wiklund. Mating in the afternoon: Time-saving in courtship and remating by females of a polyandrous butterfly *Pieris napi* L. *Behavioral Ecology and Sociobiology*, 25(5):349–356, 1989. ISSN 0340-5443, 1432-0762. doi: 10.1007/BF00302992.
- J. Forster, A. G. Hirst, and D. Atkinson. Warming-induced reductions in body size are greater in aquatic than terrestrial species. *Proceedings of the National Academy of Sciences*, 109(47):19310–19314, 2012. doi: 10.1073/pnas.1210460109.
- A. Francis and S. I. Warwick. The biology of Canadian weeds. 3. *Lepidium draba* L., *L. chalepense* L., *L. appelianum* Al-Shehbaz. *Canadian Journal of Plant Science*, 88(2):379–401, 2008. ISSN 00084220. doi: 10.4141/CJPS07100.

- O. Franken, M. Huizinga, J. Ellers, and M. P. Berg. Heated communities: large inter- and intraspecific variation in heat tolerance across trophic levels of a soil arthropod community. *Oecologia*, 186(2):311–322, 2018. ISSN 1432-1939. doi: 10.1007/s00442-017-4032-z.
- M. Friberg and C. Wiklund. Host preference variation cannot explain microhabitat differentiation among sympatric *Pieris napi* and *Pieris rapae* butterflies. *Ecological Entomology*, 44(4):571–576, 2019. ISSN 0307-6946. doi: 10.1111/een.12728.
- M. Friberg, M. Olofsson, D. Berger, B. Karlsson, and C. Wiklund. Habitat choice precedes host plant choice - niche separation in a species pair of a generalist and a specialist butterfly. *Oikos*, 117(9):1337–1344, 2008. ISSN 00301299. doi: 10.1111/j.0030-1299.2008.16740.x.
- M. Friberg, J. Dahlerus, and C. Wiklund. Strategic larval decision-making in a bivoltine butterfly. *Oecologia*, 169(3):623–635, 2012. ISSN 00298549. doi: 10.1007/s00442-011-2238-z.
- M. Friberg, D. Posledovich, and C. Wiklund. Decoupling of female host plant preference and offspring performance in relative specialist and generalist butterflies. *Oecologia*, 178(4):1181–1192, 2015. ISSN 00298549. doi: 10.1007/s00442-015-3286-6.
- M. Gamelon, V. Grøtan, A. L. K. Nilsson, S. Engen, J. W. Hurrell, K. Jerstad, A. S. Phillips, O. W. Røstad, T. Slagsvold, B. Walseng, N. C. Stenseth, and B.-E. Sæther. Interactions between demography and environmental effects are important determinants of population dynamics. *Science Advances*, 3(2):e1602298, 2017. doi: 10.1126/sciadv.1602298.
- R. A. Garcia, M. Cabeza, C. Rahbek, and M. B. Araújo. Multiple Dimensions of Climate Change and Their Implications for Biodiversity. *Science*, 344(6183):1247579, 2014. doi: 10.1126/science.1247579.
- E. García-Barros, M. L. Munguira, C. Stefanescu, and A. V. Moreno. *Fauna Ibérica. Vol. 37: Lepidoptera: Papilionoidea*. Consejo Superior de Investigaciones Científicas, Madrid, 1 edition, 2013. ISBN 978-84-00-09726-4.
- A. García-Berro, V. Talla, R. Vila, H. K. Wai, D. Shipilina, K. G. Chan, N. E. Pierce, N. Backström, and G. Talavera. Migratory behaviour is positively associated with genetic diversity in butterflies. *Molecular Ecology*, 32(3):560–574, 2023. ISSN 1365-294X. doi: 10.1111/mec.16770.
- S. X. Ge, Z. H. Jiang, J. Q. Wang, K. Song, C. Zhang, and S. J. Hu. A revision of the *Pieris napi*-complex (Lepidoptera: Pieridae) and similar species with distribution in China. *Arthropod Systematics & Phylogeny*, 81:257–287, 2023. ISSN 1864-8312, 1863-7221. doi: 10.3897/asp.81.e85191.
- R. Geiger. *The climate near the ground*. Harvard University Press, Cambridge, 2nd edition, 1950.

- M. Gibbs and H. Van Dyck. Reproductive plasticity, oviposition site selection, and maternal effects in fragmented landscapes. *Behavioral Ecology and Sociobiology*, 64(1):1–11, 2009. ISSN 0340-5443. doi: 10.1007/s00265-009-0849-8.
- F. Giorgi. Climate change hot-spots. *Geophysical Research Letters*, 33(8):L08707, 2006. ISSN 0094-8276. doi: 10.1029/2006GL025734.
- T. N. Grainger, A. Senthilnathan, P.-J. Ke, M. A. Barbour, N. T. Jones, J. P. DeLong, S. P. Otto, M. I. O'Connor, K. E. Coblenz, N. Goel, J. Sakarchi, M. C. Szojka, J. M. Levine, and R. M. Germain. An Empiricist's Guide to Using Ecological Theory. *The American Naturalist*, 199(1):1–20, 2022. ISSN 0003-0147, 1537-5323. doi: 10.1086/717206.
- K. Grant, J. Kreyling, L. F. H. Dienstbach, C. Beierkuhnlein, and A. Jentsch. Water stress due to increased intra-annual precipitation variability reduced forage yield but raised forage quality of a temperate grassland. *Agriculture, Ecosystems & Environment*, 186: 11–22, 2014. ISSN 0167-8809. doi: 10.1016/j.agee.2014.01.013.
- C. Greiser, L. von Schmalensee, O. Lindestad, K. Gotthard, and P. Lehmann. Microclimatic variation affects developmental phenology, synchrony and voltinism in an insect population. *Functional Ecology*, 36(12):3036–3048, 2022. ISSN 1365-2435. doi: 10.1111/1365-2435.14195.
- E. Gril, F. Spicher, C. Greiser, M. B. Ashcroft, S. Pincebourde, S. Durrieu, M. Nicolas, B. Richard, G. Decocq, R. Marrec, and J. Lenoir. Slope and equilibrium: A parsimonious and flexible approach to model microclimate. *Methods in Ecology and Evolution*, 14(3):885–897, 2023. ISSN 2041-210X. doi: 10.1111/2041-210X.14048.
- B. D. W. Group. Biomarkers and surrogate endpoints: Preferred definitions and conceptual framework. *Clinical Pharmacology & Therapeutics*, 69(3):89–95, 2001. ISSN 1532-6535. doi: 10.1067/mcp.2001.113989.
- S. Gulev, P. Thorne, J. Ahn, F. Dentener, C. Domingues, S. Gerland, D. Gong, D. Kaufman, H. Nnamchi, J. Quaas, J. Rivera, S. Sathyendranath, S. Smith, B. Trewin, K. von Schuckmann, and R. Vose. Changing State of the Climate System. In V. Masson-Delmotte, P. Zhai, A. Pirani, S. Connors, C. Péan, S. Berger, N. Caud, Y. Chen, L. Goldfarb, M. Gomis, M. Huang, K. Leitzell, E. Lonnoy, J. Matthews, T. Maycock, T. Waterfield, O. Yelekçi, R. Yu, and B. Zhou, editors, *Climate Change 2021: The Physical Science Basis. Contribution of Working Group I to the Sixth Assessment Report of the Intergovernmental Panel on Climate Change*, pages 287–422. Cambridge University Press, Cambridge, United Kingdom and New York, NY, USA, 2021. doi: 10.1017/9781009157896.004.
- Y. M. Guo, N. C. Turner, S. Chen, M. N. Nelson, K. H. M. Siddique, and W. A. Cowling. Genotypic Variation for Tolerance to Transient Drought During the Reproductive Phase of *Brassica rapa*. *Journal of Agronomy and Crop Science*, 201(4):267–279, 2015. ISSN 1439-037X. doi: 10.1111/jac.12107.

- E. J. Gustafson. When relationships estimated in the past cannot be used to predict the future: using mechanistic models to predict landscape ecological dynamics in a changing world. *Landscape Ecology*, 28(8):1429–1437, 2013. ISSN 1572-9761. doi: 10.1007/s10980-013-9927-4.
- J. M. Gutiérrez, R. G. Jones, G. T. Narisma, L. M. Alves, M. Amjad, I. V. Gorodetskaya, M. Grose, N. A. B. Klutse, S. Krakovska, D. Martínez-Castro, L. O. Mearns, S. H. Mernild, T. Ngo-Duc, B. van den Hurk, and J.-H. Yoon. Atlas. In V. Masson-Delmotte, P. Zhai, A. Pirani, S. L. Connors, C. Péan, S. Berger, N. Caud, Y. Chen, L. Goldfarb, M. I. Gomis, M. Huang, K. Leitzell, E. Lonnoy, J. B. R. Matthews, T. K. Maycock, T. Waterfield, O. Yelekçi, R. Yu, and B. Zhou, editors, *Climate Change 2021: The Physical Science Basis. Contribution of Working Group I to the Sixth Assessment Report of the Intergovernmental Panel on Climate Change*. Cambridge University Press, Cambridge, UK and New York, USA, 2021.
- F. Günter, M. Beaulieu, M. Brunetti, L. Lange, A. Schmitz Ornés, and K. Fischer. Latitudinal and altitudinal variation in ecologically important traits in a widespread butterfly. *Biological Journal of the Linnean Society*, 128(3):742–755, 2019. ISSN 0024-4066. doi: 10.1093/biolinnean/blz133.
- F. Günter, M. Beaulieu, K. Franke, N. Toshkova, and K. Fischer. Clinal variation in investment into reproduction versus maintenance suggests a ‘pace-of-life’ syndrome in a widespread butterfly. *Oecologia*, 193(4):1011–1020, 2020a. ISSN 1432-1939. doi: 10.1007/s00442-020-04719-4.
- F. Günter, M. Beaulieu, K. F. Freiberg, I. Welzel, N. Toshkova, A. Žagar, T. Simčič, and K. Fischer. Genotype-environment interactions rule the response of a widespread butterfly to temperature variation. *Journal of Evolutionary Biology*, 33(7):920–929, 2020b. ISSN 1420-9101. doi: 10.1111/jeb.13623.
- J. C. Habel, A. Segerer, W. Ulrich, O. Torchyk, W. W. Weisser, and T. Schmitt. Butterfly community shifts over two centuries. *Conservation biology: the journal of the Society for Conservation Biology*, 30(4):754–762, 2016. ISSN 15231739. doi: 10.1111/cobi.12656.
- J. C. Habel, M. J. Samways, and T. Schmitt. Mitigating the precipitous decline of terrestrial European insects: Requirements for a new strategy. *Biodiversity and Conservation*, 28(6):1343–1360, 2019a. ISSN 1572-9710. doi: 10.1007/s10531-019-01741-8.
- J. C. Habel, W. Ulrich, N. Biburger, S. Seibold, and T. Schmitt. Agricultural intensification drives butterfly decline. *Insect Conservation and Diversity*, 12(4):289–295, 2019b. ISSN 1752-4598. doi: 10.1111/icad.12343.
- J. D. Hadfield. MCMC Methods for Multi-Response Generalized Linear Mixed Models: The MCMCglmm R Package. *Journal of Statistical Software*, 33:1–22, 2010. ISSN 1548-7660. doi: 10.18637/jss.v033.i02.
- N. G. Hairston, F. E. Smith, and L. B. Slobodkin. Community Structure, Population Control, and Competition. *The American Naturalist*, 94(879):421–425, 1960. ISSN 0003-0147, 1537-5323. doi: 10.1086/282146.

- C. A. Halsch, A. M. Shapiro, J. A. Fordyce, C. C. Nice, J. H. Thorne, D. P. Waetjen, and M. L. Forister. Insects and recent climate change. *Proceedings of the National Academy of Sciences*, 118(2):e2002543117, 2021. ISSN 0027-8424, 1091-6490. doi: 10.1073/pnas.2002543117.
- I. Hanski. *Metapopulation ecology*. Oxford series in ecology and evolution. Oxford University Press, Oxford; New York, 1999. ISBN 978-0-19-854066-3 978-0-19-854065-6.
- J. A. Harvey, R. Heinen, R. Gols, and M. P. Thakur. Climate change-mediated temperature extremes and insects: From outbreaks to breakdowns. *Global Change Biology*, 26(12):6685–6701, 2020. ISSN 1365-2486. doi: <https://doi.org/10.1111/gcb.15377>.
- J. A. Harvey, K. Tougeron, R. Gols, R. Heinen, M. Abarca, P. K. Abram, Y. Basset, M. Berg, C. Boggs, J. Brodeur, P. Cardoso, J. G. de Boer, G. R. De Snoo, C. Deacon, J. E. Dell, N. Desneux, M. E. Dillon, G. A. Duffy, L. A. Dyer, J. Ellers, A. Espíndola, J. Fordyce, M. L. Forister, C. Fukushima, M. J. G. Gage, C. García-Robledo, C. Gely, M. Gobbi, C. Hallmann, T. Hance, J. Harte, A. Hochkirch, C. Hof, A. A. Hoffmann, J. G. Kingsolver, G. P. A. Lamarre, W. F. Laurance, B. Lavandero, S. R. Leather, P. Lehmann, C. Le Lann, M. M. López-Uribe, C.-S. Ma, G. Ma, J. Moiroux, L. Monticelli, C. Nice, P. J. Ode, S. Pincebourde, W. J. Ripple, M. Rowe, M. J. Samways, A. Sentis, A. A. Shah, N. Stork, J. S. Terblanche, M. P. Thakur, M. B. Thomas, J. M. Tylianakis, J. Van Baaren, M. Van de Pol, W. H. Van der Putten, H. Van Dyck, W. C. E. P. Verberk, D. L. Wagner, W. W. Weisser, W. C. Wetzel, H. A. Woods, K. A. G. Wyckhuys, and S. L. Chown. Scientists' warning on climate change and insects. *Ecological Monographs*, 93(1):e1553, 2023. ISSN 1557-7015. doi: 10.1002/ecm.1553.
- J. L. Hayes. The Population Ecology of a Natural Population of the Pierid Butterfly *Colias alexandra*. *Oecologia*, 49(2):188–200, 1981.
- R. Heinen, R. Gols, and J. A. Harvey. Black and Garlic mustard plants are highly suitable for the development of two native pierid butterflies. *Environmental Entomology*, 45(3):671–676, 2016. ISSN 19382936. doi: 10.1093/ee/nvw024.
- C. Held and H. R. Spieth. First evidence of pupal summer diapause in *Pieris brassicae* L.: the evolution of local adaptedness. *Journal of Insect Physiology*, 45:587–598, 1999.
- A. Hern, G. Edwards-Jones, and R. G. McKinlay. A review of the pre-oviposition behaviour of small cabbage white butterfly, *Pieris rapae* (Lepidoptera: Pieridae). *Annals of Applied Biology*, 128(2):349–371, 1996. ISSN 0003-4746. doi: 10.1111/j.1744-7348.1996.tb07328.x.
- S. Herrando, N. Titeux, L. Brotons, M. Anton, A. Ubach, D. Villero, E. García-Barros, M. L. Munguira, C. Godinho, and C. Stefanescu. Contrasting impacts of precipitation on Mediterranean birds and butterflies. *Scientific Reports*, 9(1):5680, 2019. ISSN 2045-2322. doi: 10.1038/s41598-019-42171-4.
- S. Herrando-Pérez. Climate change heats matrix population models. *Journal of Animal Ecology*, 82(6):1117–1119, 2013. ISSN 1365-2656. doi: 10.1111/1365-2656.12146.

- G. M. Hill, A. Y. Kawahara, J. C. Daniels, C. C. Bateman, and B. R. Scheffers. Climate change effects on animal ecology: butterflies and moths as a case study. *Biological Reviews*, 96(5):2113–2126, 2021. ISSN 1464-7931, 1469-185X. doi: 10.1111/brv.12746.
- J. A. Hill, P. Rastas, E. A. Hornett, R. Neethiraj, N. L. Clark, N. I. Morehouse, M. de la Paz Celorio-Mancera, J. Carnicer, H. Dirksen, C. Meslin, N. Keehnen, P. Pruischer, K. Sikkink, M. Vives-Inglá, H. Vogel, C. Wiklund, A. Woronik, C. L. Boggs, S. Nylin, and C. W. Wheat. Unprecedented reorganization of holocentric chromosomes provides insights into the enigma of lepidopteran chromosome evolution. *Science Advances*, 5(6):eaau3648, 2019. ISSN 2375-2548. doi: 10.1126/sciadv.aau3648.
- B. J. Hindle, C. L. Kerr, S. A. Richards, and S. G. Willis. Topographical variation reduces phenological mismatch between a butterfly and its nectar source. *Journal of Insect Conservation*, 19(2):227–236, 2015. ISSN 15729753. doi: 10.1007/s10841-014-9713-x.
- A. A. Hoffmann, S. L. Chown, and S. Clusella-Trullas. Upper thermal limits in terrestrial ectotherms: how constrained are they? *Functional Ecology*, 27(4):934–949, 2013. ISSN 1365-2435. doi: 10.1111/j.1365-2435.2012.02036.x.
- J. K. Hoover and J. A. Newman. Tritrophic interactions in the context of climate change: a model of grasses, cereal Aphids and their parasitoids. *Global Change Biology*, 10(7):1197–1208, 2004. ISSN 1365-2486. doi: 10.1111/j.1529-8817.2003.00796.x.
- R. B. Huey and M. R. Kearney. Dynamics of death by heat. *Science*, 369(6508):1163–1163, 2020. doi: 10.1126/science.abe0320.
- R. B. Huey and J. G. Kingsolver. Climate Warming, Resource Availability, and the Metabolic Meltdown of Ectotherms. *The American Naturalist*, 194(6):E140–E150, 2019. ISSN 0003-0147. doi: 10.1086/705679.
- T. T. Høye, S. Loboda, A. M. Koltz, M. A. K. Gillespie, J. J. Bowden, and N. M. Schmidt. Nonlinear trends in abundance and diversity and complex responses to climate change in Arctic arthropods. *Proceedings of the National Academy of Sciences*, 118(2):e2002557117, 2021. ISSN 0027-8424, 1091-6490. doi: 10.1073/pnas.2002557117.
- IPCC. *Climate Change 2021: The Physical Science Basis. Contribution of Working Group I to the Sixth Assessment Report of the Intergovernmental Panel on Climate Change*, volume In Press. Cambridge University Press, Cambridge, United Kingdom and New York, NY, USA, 2021. doi: 10.1017/9781009157896.
- M. Iturbide, J. Fernández, J. M. Gutiérrez, J. Bedia, E. Cimadevilla, J. Díez-Sierra, R. Manzanás, A. Casanueva, J. Baño-Medina, J. Milovac, S. Herrera, A. S. Cofiño, D. San Martín, M. García-Díez, M. Hauser, D. Huard, and Ö. Yelekçi. Repository supporting the implementation of FAIR principles in the IPCC-WGI Atlas, 2021. URL <https://github.com/IPCC-WG1/Atlas>.
- J. Jacobs. *Ecology and Management of Whitetop (Cardaria draba (L.) Desv.)*. U.S. Department of Agriculture, Natural Resources Conservation Service, 2007.

- H. Jactel, J. Koricheva, and B. Castagneyrol. Responses of forest insect pests to climate change: not so simple. *Current Opinion in Insect Science*, 35:103–108, 2019. ISSN 2214-5745. doi: 10.1016/j.cois.2019.07.010.
- D. H. Janzen and W. Hallwachs. Perspective: Where might be many tropical insects? *Biological Conservation*, 233:102–108, 2019. ISSN 0006-3207. doi: 10.1016/j.biocon.2019.02.030.
- P. Jaureguiberry, N. Titeux, M. Wiemers, D. E. Bowler, L. Coscieme, A. S. Golden, C. A. Guerra, U. Jacob, Y. Takahashi, J. Settele, S. Díaz, Z. Molnár, and A. Purvis. The direct drivers of recent global anthropogenic biodiversity loss. *Science Advances*, 8(45): eabm9982, 2022. doi: 10.1126/sciadv.abm9982.
- S. Jennings. Assessing forest canopies and understorey illumination: canopy closure, canopy cover and other measures. *Forestry*, 72(1):59–74, 1999. ISSN 0015-752X. doi: 10.1093/forestry/72.1.59.
- S. Jenouvrier and M. E. Visser. Climate change, phenological shifts, eco-evolutionary responses and population viability: toward a unifying predictive approach. *International Journal of Biometeorology*, 55(6):905–919, 2011. ISSN 1432-1254. doi: 10.1007/s00484-011-0458-x.
- S. Jenouvrier, H. Caswell, C. Barbraud, M. Holland, J. Stroeve, and H. Weimerskirch. Demographic models and IPCC climate projections predict the decline of an emperor penguin population. *Proceedings of the National Academy of Sciences*, 106(6):1844–1847, 2009. doi: 10.1073/pnas.0806638106.
- S. Jenouvrier, M. Holland, J. Stroeve, M. Serreze, C. Barbraud, H. Weimerskirch, and H. Caswell. Projected continent-wide declines of the emperor penguin under climate change. *Nature Climate Change*, 4(8):715–718, 2014. ISSN 1758-6798. doi: 10.1038/nclimate2280.
- S. Jenouvrier, C. Péron, and H. Weimerskirch. Extreme climate events and individual heterogeneity shape life-history traits and population dynamics. *Ecological Monographs*, 85(4):605–624, 2015. ISSN 1557-7015. doi: 10.1890/14-1834.1.
- A. Jentsch, J. Kreyling, and C. Beierkuhnlein. A new generation of climate-change experiments: events, not trends. *Frontiers in Ecology and the Environment*, 5(7):365–374, 2007. ISSN 1540-9295. doi: 10.1890/1540-9295(2007)5[365:ANGOCE]2.0.CO;2.
- J. M. Jeschke and H. Kokko. The roles of body size and phylogeny in fast and slow life histories. *Evolutionary Ecology*, 23(6):867–878, 2009. ISSN 1573-8477. doi: 10.1007/s10682-008-9276-y.
- V. Johansson, O. Kindvall, J. Askling, and M. Franzén. Extreme weather affects colonization–extinction dynamics and the persistence of a threatened butterfly. *Journal of Applied Ecology*, 57(6):1068–1077, 2020. ISSN 1365-2664. doi: 10.1111/1365-2664.13611.

- S. N. Johnson and H. Jones. *Global climate change and terrestrial invertebrates*. Wiley Blackwell, Chichester, UK Hoboken, NJ, 2017. ISBN 978-1-119-07087-0 978-1-119-07082-5 978-1-119-07089-4.
- R. E. Jones, J. R. Hart, and G. D. Bull. Temperature, size, and egg production in the cabbage butterfly, *Pieris rapae* L. *Australian Journal of Zoology*, 30(1968):223–232, 1982. doi: <https://doi.org/10.1071/ZO9820223>.
- T. Jucker, T. D. Jackson, F. Zellweger, T. Swinfield, N. Gregory, J. Williamson, E. M. Slade, J. W. Phillips, P. R. L. Bittencourt, B. Blonder, M. J. W. Boyle, M. D. F. Ellwood, D. Hemprich-Bennett, O. T. Lewis, R. Matula, R. A. Senior, A. Shenkin, M. Svátek, and D. A. Coomes. A Research Agenda for Microclimate Ecology in Human-Modified Tropical Forests. *Frontiers in Forests and Global Change*, 2, 2020. ISSN 2624-893X.
- L. B. Jørgensen, H. Malte, M. Ørsted, N. A. Klahn, and J. Overgaard. A unifying model to estimate thermal tolerance limits in ectotherms across static, dynamic and fluctuating exposures to thermal stress. *Scientific Reports*, 11(1):12840, 2021. ISSN 2045-2322. doi: 10.1038/s41598-021-92004-6.
- L. B. Jørgensen, M. Ørsted, H. Malte, T. Wang, and J. Overgaard. Data from: Extreme escalation of heat failure rates in ectotherms with global warming, 2022a. URL <https://zenodo.org/record/6979789>.
- L. B. Jørgensen, M. Ørsted, H. Malte, T. Wang, and J. Overgaard. Extreme escalation of heat failure rates in ectotherms with global warming. *Nature*, 611(7934):93–98, 2022b. ISSN 1476-4687. doi: 10.1038/s41586-022-05334-4.
- A. Kaiser, T. Merckx, and H. Van Dyck. The Urban Heat Island and its spatial scale dependent impact on survival and development in butterflies of different thermal sensitivity. *Ecology and Evolution*, 6(12):4129–4140, 2016. ISSN 2045-7758. doi: 10.1002/ece3.2166.
- A. Kaitala and C. Wiklund. Polyandrous Female Butterflies Forage for Matings. *Behavioral Ecology and Sociobiology*, 35:385–388, 1994.
- P. Kaitaniemi, K. Ruohomäki, V. Ossipov, E. Haukioja, and K. Pihlaja. Delayed induced changes in the biochemical composition of host plant leaves during an insect outbreak. *Oecologia*, 116(1):182–190, 1998. ISSN 1432-1939. doi: 10.1007/s004420050578.
- B. Karlsson and A. Johansson. Seasonal polyphenism and developmental trade-offs between flight ability and egg laying in a pierid butterfly. *Proceedings of the Royal Society B: Biological Sciences*, 275(1647):2131–2136, 2008. ISSN 14712970. doi: 10.1098/rspb.2008.0404.
- B. Karlsson and C. Wiklund. Butterfly life history and temperature adaptations; dry open habitats select for increased fecundity and longevity. *Journal of Animal Ecology*, 74(1): 99–104, 2005. ISSN 00218790. doi: 10.1111/j.1365-2656.2004.00902.x.

- B. Karlsson, O. Leimar, and C. Wiklund. Unpredictable environments, nuptial gifts and the evolution of sexual size dimorphism in insects: an experiment. *Proceedings of the Royal Society B: Biological Sciences*, 264(1381):475–479, 1997. doi: 10.1098/rspb.1997.0068.
- M. Kaspari, N. A. Clay, J. Lucas, S. P. Yanoviak, and A. Kay. Thermal adaptation generates a diversity of thermal limits in a rainforest ant community. *Global Change Biology*, 21(3):1092–1102, 2015. ISSN 1365-2486. doi: <https://doi.org/10.1111/gcb.12750>.
- A. Kause, V. Ossipov, E. Haukioja, K. Lempa, S. Hanhimäki, and S. Ossipova. Multiplicity of biochemical factors determining quality of growing birch leaves. *Oecologia*, 120(1):102–112, 1999. ISSN 1432-1939. doi: 10.1007/s004420050838.
- M. R. Kearney. MicroclimOz – A microclimate data set for Australia, with example applications. *Austral Ecology*, 44(3):534–544, 2019. ISSN 1442-9993. doi: 10.1111/aec.12689.
- M. R. Kearney and W. P. Porter. NicheMapR – an R package for biophysical modelling: the microclimate model. *Ecography*, 40(5):664–674, 2017. ISSN 16000587. doi: 10.1111/ecog.02360.
- M. R. Kearney and W. P. Porter. NicheMapR – an R package for biophysical modelling: the ectotherm and Dynamic Energy Budget models. *Ecography*, 43(1):85–96, 2020. ISSN 1600-0587. doi: 10.1111/ecog.04680.
- M. R. Kearney, W. P. Porter, C. Williams, S. Ritchie, and A. A. Hoffmann. Integrating biophysical models and evolutionary theory to predict climatic impacts on species' ranges: The dengue mosquito *Aedes aegypti* in Australia. *Functional Ecology*, 23(3):528–538, 2009a. ISSN 02698463. doi: 10.1111/j.1365-2435.2008.01538.x.
- M. R. Kearney, R. Shine, and W. P. Porter. The potential for behavioral thermoregulation to buffer "cold-blooded" animals against climate warming. *Proceedings of the National Academy of Sciences*, 106(10):3835–3840, 2009b. ISSN 0027-8424. doi: 10.1073/pnas.0808913106.
- M. R. Kearney, J. Deutscher, J. D. Kong, and A. A. Hoffmann. Summer egg diapause in a matchstick grasshopper synchronizes the life cycle and buffers thermal extremes. *Integrative Zoology*, 13(4):437–449, 2018. ISSN 1749-4877. doi: <https://doi.org/10.1111/1749-4877.12314>.
- M. S. Keeler, F. S. Chew, B. C. Goodale, and J. M. Reed. Modelling the impacts of two exotic invasive species on a native butterfly: Top-down vs. bottom-up effects. *Journal of Animal Ecology*, 75(3):777–788, 2006. ISSN 00218790. doi: 10.1111/j.1365-2656.2006.01098.x.
- A. Kempel, E. Allan, M. M. Gossner, M. Jochum, J. B. Grace, and D. A. Wardle. From bottom-up to top-down control of invertebrate herbivores in a retrogressive chronosequence. *Ecology Letters*, 26(3):411–424, 2023. ISSN 1461-0248. doi: 10.1111/ele.14161.

- J. Kemppinen, J. J. Lembrechts, K. Van Meerbeek, J. Carnicer, N. I. Chardon, Nathalie Isabelle, P. Kardol, J. Lenoir, D. Liu, I. Maclean, J. Pergl, P. Saccone, R. A. Senior, T. Shen, S. Słowińska, V. Vandvik, J. von Oppen, J. Aalto, B. Aylew, O. Bates, C. Bertelsmeier, R. Bertrand, R. Beugnon, J. Borderieux, J. Bruna, L. Buckley, J. Bujan, A. Casanova-Katny, D. M. Christiansen, F. Collart, E. De Lombaerde, K. De Pauw, L. Depauw, M. Di Musciano, R. Díaz Borrego, J. Díaz-Calafat, D. Ellis-Soto, R. Esteban, G. Fálthammar de Jong, E. Gallois, M. B. Garcia, L. Gillerot, C. Greiser, E. Gril, S. Haesen, A. Hampe, P.-O. Hedwall, G. Hes, H. Hespanhol, R. Hoffrén, K. Hylander, B. Jiménez-Alfaro, T. Jucker, D. Klinges, J. Kolstela, M. Kopecký, B. Kovács, E. E. Maeda, F. Máliš, M. Man, C. Mathiak, E. Meineri, I. Naujokaitis-Lewis, I. Nijs, S. Normand, M. Nuñez, A. Orczewska, P. Peña-Aguilera, S. Pincebourde, R. Plichta, S. Quick, D. Renault, L. Ricci, T. Rissanen, L. Segura-Hernández, F. Selvi, J. M. Serra-Diaz, L. Soifer, F. Spicher, J.-C. Svenning, A. Tamian, A. Thomaes, M. Thoonen, B. Trew, S. Van de Vondel, L. van den Brink, P. Vangansbeke, S. Verdonck, M. Vitkova, M. Vives-Inglá, L. von Schmalensee, R. Wang, J. Wild, J. Williamson, F. Zellweger, X. Zhou, E. J. Zuza, and P. De Frenne. Microclimate, an inseparable part of ecology and biogeography. 2023. doi: 10.5281/ZENODO.7973314.
- N. Z. Kerr, E. E. Crone, and F. S. Chew. Life history trade-offs are more pronounced for a noninvasive, native butterfly compared to its invasive, exotic congener. *Population Ecology*, 62(1):119–133, 2020. ISSN 1438-3896. doi: 10.1002/1438-390X.12035.
- H. M. Kharouba, J. M. M. Lewthwaite, R. Guralnick, J. T. Kerr, and M. Vellend. Using insect natural history collections to study global change impacts: challenges and opportunities. *Philosophical Transactions of the Royal Society B: Biological Sciences*, 374(1763):20170405, 2018. doi: 10.1098/rstb.2017.0405.
- J. Kingsolver. The Well-Tempered Biologist. *The American Naturalist*, 174(6):755–768, 2009. ISSN 0003-0147. doi: 10.1086/648310.
- J. G. Kingsolver. Thermal and Hydric Aspects of Environmental Heterogeneity in the Pitcher Plant Mosquito. *Ecological Monographs*, 49(4):357–376, 1979. ISSN 00129615. doi: 10.2307/1942468.
- J. G. Kingsolver. Thermoregulation and Flight in Colias Butterflies: Elevational Patterns and Mechanistic Limitations. *Ecology*, 64(3):534–545, 1983. ISSN 1939-9170. doi: 10.2307/1939973.
- J. G. Kingsolver. Evolution and Coadaptation of Thermoregulatory Behavior and Wing Pigmentation Pattern in Pierid Butterflies. *Evolution*, 41(3):472, 1987. ISSN 00143820. doi: 10.2307/2409250.
- J. G. Kingsolver. Thermoregulation, Flight, and the Evolution of Wing Pattern in Pierid Butterflies: The Topography of Adaptive Landscapes. *American Zoologist*, 28(3):899–912, 1988.

- J. G. Kingsolver. Weather and the Population Dynamics of Insects: Integrating Physiological and Population Ecology. *Physiological Zoology*, 62(2):314–334, 1989. ISSN 0031-935X. doi: 10.1086/physzool.62.2.30156173.
- J. G. Kingsolver. Feeding, Growth, and the Thermal Environment of Cabbage White Caterpillars, *Pieris rapae* L. *Physiological and Biochemical Zoology*, 73(5):621–628, 2000. ISSN 1522-2152. doi: 10.1086/317758.
- J. G. Kingsolver and L. B. Buckley. Climate variability slows evolutionary responses of *Colias* butterflies to recent climate change. *Proceedings of the Royal Society B: Biological Sciences*, 282(1802):20142470, 2015. doi: 10.1098/rspb.2014.2470.
- J. G. Kingsolver and L. B. Buckley. Evolution of plasticity and adaptive responses to climate change along climate gradients. *Proceedings of the Royal Society B: Biological Sciences*, 284(1860):20170386, 2017. ISSN 0962-8452. doi: 10.1098/rspb.2017.0386.
- J. G. Kingsolver and R. Gomulkiewicz. Environmental Variation and Selection on Performance Curves. *Integrative and Comparative Biology*, 43(3):470–477, 2003. ISSN 1540-7063. doi: 10.1093/icb/43.3.470.
- J. G. Kingsolver and R. B. Huey. Size, temperature, and fitness: three rules. *Evolutionary Ecology Research*, 10:251–268, 2008.
- J. G. Kingsolver and D. C. Wiernasz. Dissecting Correlated Characters: Adaptive Aspects of Phenotypic Covariation in Melanization Pattern of *Pieris* Butterflies. *Evolution*, 41(3):491, 1987. ISSN 00143820. doi: 10.2307/2409251.
- J. G. Kingsolver and D. C. Wiernasz. Seasonal Polyphenism in Wing-Melanin Pattern and Thermoregulatory Adaptation in *Pieris* Butterflies. *The American Naturalist*, 137(6):816–830, 1991.
- J. G. Kingsolver, J. G. Shlichta, G. J. Ragland, and K. R. Massie. Thermal reaction norms for caterpillar growth depend on diet. *Evolutionary Ecology Research*, 8(4):703–715, 2006. ISSN 15220613.
- J. G. Kingsolver, H. A. Woods, L. B. Buckley, K. A. Potter, H. J. MacLean, and J. K. Higgins. Complex life cycles and the responses of insects to climate change. *Integrative and Comparative Biology*, 51(5):719–732, 2011. ISSN 15407063. doi: 10.1093/icb/icro15.
- J. T. O. Kirk. *Light and Photosynthesis in Aquatic Ecosystems*. Cambridge University Press, Cambridge, 2 edition, 1994. doi: 10.1017/CBO9780511623370.
- S. M. Kivelä, B. Svensson, A. Tiwe, and K. Gotthard. Thermal plasticity of growth and development varies adaptively among alternative developmental pathways. *Evolution*, 69(9):2399–2413, 2015. ISSN 15585646. doi: 10.1111/evo.12734.
- S. M. Kivelä, M. Friberg, C. Wiklund, and K. Gotthard. Adaptive developmental plasticity in a butterfly: mechanisms for size and time at pupation differ between diapause and direct development. *Biological Journal of the Linnean Society*, 122(1):46–57, 2017. ISSN 0024-4066. doi: 10.1093/biolinnean/blx047.

- M. Klockmann and K. Fischer. Effects of temperature and drought on early life stages in three species of butterflies: Mortality of early life stages as a key determinant of vulnerability to climate change? *Ecology and Evolution*, 7(24):10871–10879, 2017. ISSN 20457758. doi: 10.1002/ece3.3588.
- M. Klockmann, F. Günter, and K. Fischer. Heat resistance throughout ontogeny: body size constrains thermal tolerance. *Global Change Biology*, 23(2):686–696, 2017a. ISSN 13652486. doi: 10.1111/gcb.13407.
- M. Klockmann, F. Kleinschmidt, and K. Fischer. Carried over: Heat stress in the egg stage reduces subsequent performance in a butterfly. *PLOS ONE*, 12(7):e0180968, 2017b. ISSN 1932-6203. doi: 10.1371/journal.pone.0180968.
- E. Klop, B. Omon, and M. F. WallisDeVries. Impact of nitrogen deposition on larval habitats: the case of the Wall Brown butterfly *Lasiommata megera*. *Journal of Insect Conservation*, 19(2):393–402, 2015. ISSN 15729753. doi: 10.1007/s10841-014-9748-z.
- D. N. Koons, S. Pavard, A. Baudisch, and C. Jessica E. Metcalf. Is life-history buffering or lability adaptive in stochastic environments? *Oikos*, 118(7):972–980, 2009. ISSN 00301299, 16000706. doi: 10.1111/j.1600-0706.2009.16399.x.
- P. E. Kriedemann. Photosynthesis in vine leaves as a function of light intensity, temperature, and leaf age. *VITIS - Journal of Grapevine Research*, 7(3):213–213, 1968. ISSN 2367-4156. doi: 10.5073/vitis.1968.7.213-220.
- J. Kuczyk, C. Müller, and K. Fischer. Plant-mediated indirect effects of climate change on an insect herbivore. *Basic and Applied Ecology*, 53:100–113, 2021. ISSN 1439-1791. doi: 10.1016/j.baae.2021.03.009.
- H. Larsdotter-Mellström, M. Friberg, A. K. Borg-Karlson, R. Murtazina, M. Palm, and C. Wiklund. Seasonal polyphenism in life history traits: Time costs of direct development in a butterfly. *Behavioral Ecology and Sociobiology*, 64(9):1377–1383, 2010. ISSN 03405443. doi: 10.1007/s00265-010-0952-x.
- P. Lehmann, P. Pruischer, D. Posledovich, M. Carlsson, R. Käkälä, P. Tang, S. Nylin, C. W. Wheat, C. Wiklund, and K. Gotthard. Energy and lipid metabolism during direct and diapause development in a pierid butterfly. *The Journal of Experimental Biology*, 219(19):3049–3060, 2016. ISSN 0022-0949. doi: 10.1242/jeb.142687.
- P. Lehmann, W. Van Der Bijl, S. Nylin, C. W. Wheat, and K. Gotthard. Timing of diapause termination in relation to variation in winter climate. *Physiological Entomology*, 42(3):232–238, 2017. ISSN 13653032. doi: 10.1111/phen.12188.
- P. Lehmann, P. Pruischer, V. Košťál, M. Moos, P. Šimek, S. Nylin, R. Agren, L. Väre, C. Wiklund, C. W. Wheat, and K. Gotthard. Metabolome dynamics of diapause in the butterfly *Pieris napi*: distinguishing maintenance, termination and post-diapause phases. *The Journal of Experimental Biology*, 221(2):jeb169508, 2018. ISSN 0022-0949. doi: 10.1242/jeb.169508.

- P. Lehmann, T. Ammunét, M. Barton, A. Battisti, S. D. Eigenbrode, J. U. Jepsen, G. Kalinkat, S. Neuvonen, P. Niemelä, J. S. Terblanche, B. Økland, and C. Björkman. Complex responses of global insect pests to climate warming. *Frontiers in Ecology and the Environment*, 18(3):141–150, 2020. ISSN 1540-9309. doi: 10.1002/fee.2160.
- J. J. Lembrechts, J. Lenoir, B. R. Scheffers, and P. D. Frenne. Designing countrywide and regional microclimate networks. *Global Ecology and Biogeography*, 30(6):1168–1174, 2021a. ISSN 1466-8238. doi: <https://doi.org/10.1111/geb.13290>.
- J. J. Lembrechts, J. van den Hoogen, J. Aalto, M. B. Ashcroft, P. De Frenne, J. Kumpinen, M. Kopecký, M. Luoto, I. M. D. Maclean, T. W. Crowther, J. J. Bailey, S. Haesen, D. H. Klings, P. Niittynen, B. R. Scheffers, K. Van Meerbeek, P. Aartsma, O. Abdalaze, M. Abedi, R. Aerts, N. Ahmadian, A. Ahrends, J. M. Alatalo, J. M. Alexander, C. Nina Allonsius, J. Altman, C. Ammann, C. Andres, C. Andrews, J. Ardö, N. Arriga, A. Arzac, V. Aschero, R. L. Assis, J. Johann Assmann, M. Y. Bader, K. Bahalkeh, P. Barančok, I. C. Barrio, A. Barros, M. Barthel, E. W. Basham, M. Bauters, M. Bazzichetto, L. Belelli Marchesini, M. C. Bell, J. C. Benavides, J. Luis Benito Alonso, B. J. Berauer, J. W. Bjerke, R. G. Björk, M. P. Björkman, K. Björnsdóttir, B. Blonder, P. Boeckx, J. Boike, S. Bokhorst, B. N. S. Brum, J. Bruna, N. Buchmann, P. Buysse, J. Luís Camargo, O. C. Campoe, O. Candan, R. Canessa, N. Cannone, M. Carbognani, J. Carnicer, A. Casanova-Katny, S. Cesarz, B. Chojnicki, P. Choler, S. L. Chown, E. F. Cifuentes, M. Čiliak, T. Contador, P. Convey, E. J. Cooper, E. Cremonese, S. R. Curasi, R. Curtis, M. Cutini, C. Johan Dahlberg, G. N. Daskalova, M. Angel de Pablo, S. Della Chiesa, J. Dengler, B. Deronde, P. Descombes, V. Di Cecco, M. Di Musciano, J. Dick, R. D. Dimarco, J. Dolezal, E. Dorrepaal, J. Dušek, N. Eisenhauer, L. Eklundh, T. E. Erickson, B. Erschbamer, W. Eugster, R. M. Ewers, D. A. Exton, N. Fanin, F. Fazlioglu, I. Feigenwinter, G. Fenu, O. Ferlian, M. Rosa Fernández Calzado, E. Fernández-Pascual, M. Finckh, R. Finger Higgins, T. G. W. Forte, E. C. Freeman, E. R. Frei, E. Fuentes-Lillo, R. A. García, M. B. García, C. Géron, M. Gharun, D. Ghosn, K. Gigauri, A. Gobin, I. Goded, M. Goeckede, F. Gottschall, K. Goulding, S. Govaert, B. Jessen Graae, S. Greenwood, C. Greiser, A. Grelle, B. Guénard, M. Guglielmin, J. Guillemot, P. Haase, S. Haider, A. H. Halbritter, M. Hamid, A. Hammerle, A. Hampe, S. V. Haugum, L. Hederová, B. Heinesch, C. Helfter, D. Hepenstrick, M. Herberich, M. Herbst, L. Hermanutz, D. S. Hik, R. Hoffrén, J. Homeier, L. Hörtnagl, T. T. Høye, F. Hrbacek, K. Hylander, H. Iwata, M. Antoni Jackowicz-Korczynski, H. Jactel, J. Järveoja, S. Jastrzębowski, A. Jentsch, J. J. Jiménez, I. S. Jónsdóttir, T. Jucker, A. S. Jump, R. Juszczak, R. Kanka, V. Kašpar, G. Kazakis, J. Kelly, A. A. Khuroo, L. Klemedtsson, M. Klisz, N. Kljun, A. Knohl, J. Kobler, J. Kollár, M. M. Kotowska, B. Kovács, J. Kreyling, A. Lamprecht, S. I. Lang, C. Larson, K. Larson, K. Laska, G. le Maire, R. I. Leihy, L. Lens, B. Liljebladh, A. Lohila, J. Lorite, B. Loubet, J. Lynn, M. Macek, R. Mackenzie, E. Magliulo, R. Maier, F. Malfasi, F. Máliš, M. Man, G. Manca, A. Manco, T. Manise, P. Manolaki, F. Marciniak, R. Matula, A. Clara Mazzolari, S. Medinets, V. Medinets, C. Meeussen, S. Merinero, R. de Cássia Guimarães Mesquita, K. Meusburger, F. J. R. Meysman, S. T. Michaletz, A. Milbau, D. Moiseev, P. Moiseev, A. Mondoni, R. Monfries, L. Mon-

- tagnani, M. Moriana-Armendariz, U. Morra di Cella, M. Mörsdorf, J. R. Mosedale, L. Muffler, M. Muñoz-Rojas, J. A. Myers, I. H. Myers-Smith, L. Nagy, M. Nardino, I. Naujokaitis-Lewis, E. Newling, L. Nicklas, G. Niedrist, A. Niessner, M. B. Nilsson, S. Normand, M. D. Noretto, Y. Nouvellon, M. A. Nuñez, R. Ogaya, J. Ogée, J. Okello, J. Olejnik, J. Eivind Olesen, Ø. Opedal, S. Orsenigo, A. Palaj, T. Pampuch, A. V. Panov, M. Pärtel, A. Pastor, A. Pauchard, H. Pauli, M. Pavelka, W. D. Pearce, M. Peichl, L. Pellissier, R. M. Penczykowski, J. Penuelas, M. Petit Bon, A. Petraglia, S. S. Phartyal, G. K. Phoenix, C. Pio, A. Pitacco, C. Pitteloud, R. Plichta, F. Porro, M. Portillo-Estrada, J. Poulénard, R. Poyatos, A. S. Prokushkin, R. Puchalka, M. Puşcaş, D. Radujković, K. Randall, A. Ratier Backes, S. Remmele, W. Remmers, D. Renault, A. C. Risch, C. Rixen, S. A. Robinson, B. J. Robroek, A. V. Rocha, C. Rossi, G. Rossi, O. Roupsard, A. V. Rubtsov, P. Saccone, C. Sagot, J. Sallo Bravo, C. C. Santos, J. M. Sarneel, T. Scharnweber, J. Schmeddes, M. Schmidt, T. Scholten, M. Schuchardt, N. Schwartz, T. Scott, J. Seeber, A. Cristina Segalin de Andrade, T. Seipel, P. Semenchuk, R. A. Senior, J. M. Serra-Diaz, P. Sewerniak, A. Shekhar, N. V. Sidenko, L. Siebicke, L. Siegwart Collier, E. Simpson, D. P. Siqueira, Z. Sitková, J. Six, M. Smiljanic, S. W. Smith, S. Smith-Tripp, B. Somers, M. Vedel Sørensen, J. João L. L. Souza, B. Israel Souza, A. Souza Dias, M. J. Spasojevic, J. D. M. Speed, F. Spicher, A. Stanisci, K. Steinbauer, R. Steinbrecher, M. Steinwandter, M. Stemkovski, J. G. Stephan, C. Stiegler, S. Stoll, M. Svátek, M. Svoboda, T. Tagesson, A. J. Tanentzap, F. Tanneberger, J. Theurillat, H. J. D. Thomas, A. D. Thomas, K. Tielbörger, M. Tomaselli, U. Albert Treier, M. Trouillier, P. Dan Turtureanu, R. Tutton, V. A. Tyystjärvi, M. Ueyama, K. Ujházy, M. Ujházyová, D. Uogintas, A. V. Urban, J. Urban, M. Urbaniak, T. Ursu, F. Primo Vaccari, S. Van de Vondel, L. van den Brink, M. Van Geel, V. Vandvik, P. Vangansbeke, A. Varlagin, G. Veen, E. Veenendaal, S. E. Venn, H. Verbeeck, E. Verbruggen, F. G. Verheijen, L. Villar, L. Vitale, P. Vittoz, M. Vives-Ingla, J. von Oppen, J. Walz, R. Wang, Y. Wang, R. G. Way, R. E. M. Wedegärtner, R. Weigel, J. Wild, M. Wilkinson, M. Wilmking, L. Wingate, M. Winkler, S. Wipf, G. Wohlfahrt, G. Xenakis, Y. Yang, Z. Yu, K. Yu, F. Zellweger, J. Zhang, Z. Zhang, P. Zhao, K. Ziemlińska, R. Zimmermann, S. Zong, V. I. Zyryanov, I. Nijs, and J. Lenoir. Global maps of soil temperature. *Global Change Biology*, 28(9):3110–3144, 2021b. ISSN 1354-1013, 1365-2486. doi: 10.1111/gcb.16060.
- M. Lemus-Canovas and J. A. Lopez-Bustins. Assessing internal changes in the future structure of dry-hot compound events: the case of the Pyrenees. *Natural Hazards and Earth System Sciences*, 21(6):1721–1738, 2021. ISSN 1561-8633. doi: 10.5194/nhess-21-1721-2021.
- J. Lenoir, T. Hattab, and G. Pierre. Climatic microrefugia under anthropogenic climate change: implications for species redistribution. *Ecography*, 40(2):253–266, 2017. ISSN 09067590. doi: 10.1111/ecog.02788.
- R. Lenth. emmeans: Estimated Marginal Means, aka Least-Squares Means, 2020. URL <https://cran.r-project.org/package=emmeans>.

- R. Levins. The Strategy of Model Building in Population Biology. *American Scientist*, 54(4):421–431, 1966. ISSN 0003-0996.
- M. Lima, M. A. Previtali, and P. L. Meserve. Climate and small rodent dynamics in semi-arid Chile: the role of lateral and vertical perturbations and intra-specific processes. *Climate Research*, 30(2):125–132, 2006. ISSN 0936-577X, 1616-1572. doi: 10.3354/cro30125.
- P. Lionello and L. Scarascia. The relation between climate change in the Mediterranean region and global warming. *Regional Environmental Change*, 18(5):1481–1493, 2018. ISSN 1436378X. doi: 10.1007/s10113-018-1290-1.
- D. O. Logofet and R. Salguero-Gómez. Novel challenges and opportunities in the theory and practice of matrix population modelling: An editorial for the special feature. *Ecological Modelling*, 443:109457, 2021. ISSN 03043800. doi: 10.1016/j.ecolmodel.2021.109457.
- A. J. Lotka. *Théorie analytique des associations biologiques*. Number pt. 2 in Actualités scientifiques et industrielles. Hermann et cie, Paris, 1934.
- D. Lüdecke, M. S. Ben-Shachar, I. Patil, P. Waggoner, and D. Makowski. performance: An R Package for Assessment, Comparison and Testing of Statistical Models. *Journal of Open Source Software*, 6(60):3139, 2021. doi: 10.21105/joss.03139.
- C.-S. Ma, G. Ma, and S. Pincebourde. Survive a Warming Climate: Insect Responses to Extreme High Temperatures. *Annual Review of Entomology*, 66(1):163–184, 2021. ISSN 0066-4170, 1545-4487. doi: 10.1146/annurev-ento-041520-074454.
- L. Ma, S. R. Conradie, C. L. Crawford, A. S. Gardner, M. R. Kearney, I. M. Maclean, A. E. McKechnie, C.-R. Mi, R. A. Senior, and D. S. Wilcove. Global patterns of climate change impacts on desert bird communities. *Nature communications*, 14(1):211, 2023.
- H. J. MacLean, J. K. Higgins, L. B. Buckley, and J. G. Kingsolver. Geographic divergence in upper thermal limits across insect life stages: does behavior matter? *Oecologia*, 181(1):107–114, 2016. ISSN 00298549. doi: 10.1007/s00442-016-3561-1.
- I. M. D. Maclean, J. P. Duffy, S. Haesen, S. Govaert, P. D. Frenne, T. Vanneste, J. Lenoir, J. J. Lembrechts, M. W. Rhodes, and K. V. Meerbeek. On the measurement of microclimate. *Methods in Ecology and Evolution*, 12(8):1397–1410, 2021. ISSN 2041-210X. doi: 10.1111/2041-210X.13627.
- J. L. Maino, J. D. Kong, A. A. Hoffmann, M. G. Barton, and M. R. Kearney. Mechanistic models for predicting insect responses to climate change. *Current Opinion in Insect Science*, 17:81–86, 2016. ISSN 2214-5745. doi: 10.1016/j.cois.2016.07.006.
- A. H. Malinowska, A. J. Van Strien, J. Verboom, M. F. WallisdeVries, and P. Opdam. No evidence of the effect of extreme weather events on annual occurrence of four groups

- of ectothermic species. *PLoS ONE*, 9(10):1–10, 2014. ISSN 19326203. doi: 10.1371/journal.pone.0110219.
- M. Man, V. Kalčík, M. Macek, J. Brůna, L. Hederová, J. Wild, and M. Kopecký. myClim: Microclimate data handling and standardised analyses in R. *Methods in Ecology and Evolution*, 14(9):2308–2320, 2023. ISSN 2041-210X. doi: 10.1111/2041-210X.14192.
- M. Mantova, S. Herbette, H. Cochard, and J. M. Torres-Ruiz. Hydraulic failure and tree mortality: from correlation to causation. *Trends in Plant Science*, 27(4):335–345, 2022. ISSN 1360-1385. doi: 10.1016/j.tplants.2021.10.003.
- M. Maron, C. A. McAlpine, J. E. M. Watson, S. Maxwell, and P. Barnard. Climate-induced resource bottlenecks exacerbate species vulnerability: a review. *Diversity and Distributions*, 21(7):731–743, 2015. ISSN 1472-4642. doi: 10.1111/ddi.12339.
- W. J. Mattson. Herbivory in Relation to Plant Nitrogen Content. *Annual Review of Ecology and Systematics*, 11(1):119–161, 1980. ISSN 0066-4162. doi: 10.1146/annurev.es.11.110180.001003.
- O. McDermott Long, R. Warren, J. Price, T. M. Brereton, M. S. Botham, and A. M. A. Franco. Sensitivity of UK butterflies to local climatic extremes: which life stages are most at risk? *Journal of Animal Ecology*, 86(1):108–116, 2017. ISSN 1365-2656. doi: 10.1111/1365-2656.12594.
- J. F. McLaughlin, J. J. Hellmann, C. L. Boggs, and P. R. Ehrlich. The route to extinction: population dynamics of a threatened butterfly. *Oecologia*, 132(4):538–548, 2002. ISSN 1432-1939. doi: 10.1007/s00442-002-0997-2.
- Y. Melero, C. Stefanescu, and J. Pino. General declines in Mediterranean butterflies over the last two decades are modulated by species traits. *Biological Conservation*, 201:336–342, 2016. ISSN 00063207. doi: 10.1016/j.biocon.2016.07.029.
- Y. Melero, L. C. Evans, M. Kuussaari, R. Schmucki, C. Stefanescu, D. B. Roy, and T. H. Oliver. Local adaptation to climate anomalies relates to species phylogeny. *Communications Biology*, 5(1):143, 2022. ISSN 2399-3642. doi: 10.1038/s42003-022-03088-3.
- J. Memmott, P. G. Craze, N. M. Waser, and M. V. Price. Global warming and the disruption of plant–pollinator interactions. *Ecology Letters*, 10(8):710–717, 2007. ISSN 1461-0248. doi: <https://doi.org/10.1111/j.1461-0248.2007.01061.x>.
- T. Merckx, M. Serruys, and H. Van Dyck. Anthropogenic host plant expansion leads a nettle-feeding butterfly out of the forest: consequences for larval survival and developmental plasticity in adult morphology. *Evolutionary Applications*, 8(4):363–372, 2015. ISSN 17524571. doi: 10.1111/eva.12249.
- T. Merckx, M. E. Nielsen, J. Heliölä, M. Kuussaari, L. B. Pettersson, J. Pöyry, J. Tiainen, K. Gotthard, and S. M. Kivelä. Urbanization extends flight phenology and leads to local adaptation of seasonal plasticity in Lepidoptera. *Proceedings of the National Academy of Sciences*, 118(40):e2106006118, 2021. doi: 10.1073/pnas.2106006118.

- R. M. Merrill, D. Gutiérrez, O. T. Lewis, J. Gutiérrez, S. B. Díez, and R. J. Wilson. Combined effects of climate and biotic interactions on the elevational range of a phytophagous insect. *Journal of Animal Ecology*, 77(1):145–155, 2008. ISSN 00218790. doi: 10.1111/j.1365-2656.2007.01303.x.
- C. J. E. Metcalf and S. Pavard. Why evolutionary biologists should be demographers. *Trends in Ecology & Evolution*, 22(4):205–212, 2007. ISSN 01695347. doi: 10.1016/j.tree.2006.12.001.
- M. Mingarro, J. P. Cancela, A. Burón-Ugarte, E. García-Barros, M. L. Munguira, H. Romo, and R. J. Wilson. Butterfly communities track climatic variation over space but not time in the Iberian Peninsula. *Insect Conservation and Diversity*, 14(5):647–660, 2021. ISSN 1752-4598. doi: 10.1111/icad.12498.
- A. Mora, A. Wilby, and R. Menéndez. South European mountain butterflies at a high risk from land abandonment and amplified effects of climate change. *Insect Conservation and Diversity*, 2023. ISSN 1752-4598. doi: 10.1111/icad.12676.
- C. Moritz and R. Agudo. The future of species under climate change: resilience or decline? *Science*, 341(6145):504–8, 2013. ISSN 1095-9203. doi: 10.1126/science.1237190.
- W. F. Morris, C. A. Pfister, S. Tuljapurkar, C. V. Haridas, C. L. Boggs, M. S. Boyce, E. M. Bruna, D. R. Church, T. Coulson, D. F. Doak, S. Forsyth, J.-M. Gaillard, C. C. Horvitz, S. Kalisz, B. E. Kendall, T. M. Knight, C. T. Lee, and E. S. Menges. Longevity Can Buffer Plant and Animal Populations Against Changing Climatic Variability. *Ecology*, 89(1):19–25, 2008. ISSN 1939-9170. doi: 10.1890/07-0774.1.
- R. Munns, R. A. James, X. R. R. Sirault, R. T. Furbank, and H. G. Jones. New phenotyping methods for screening wheat and barley for beneficial responses to water deficit. *Journal of Experimental Botany*, 61(13):3499–3507, 2010. ISSN 0022-0957. doi: 10.1093/jxb/erq199.
- W. W. Murdoch. "Community Structure, Population Control, and Competition"-A Critique. *The American Naturalist*, 100(912):219–226, 1966. ISSN 0003-0147, 1537-5323. doi: 10.1086/282415.
- D. D. Murphy, A. E. Launer, and P. R. Ehrlich. The role of adult feeding in egg production and population dynamics of the checkerspot butterfly *Euphydryas editha*. *Oecologia*, 56(2):257–263, 1983. ISSN 1432-1939. doi: 10.1007/BF00379699.
- J. H. Myers. Effect of Physiological Condition of the Host Plant on the Ovipositional Choice of the Cabbage White Butterfly, *Pieris rapae*. *Journal of Animal Ecology*, 54(1): 193–204, 1985.
- K. R. Nail, R. V. Batalden, and K. S. Oberhauser. What's too hot and what's too cold? In K. S. Oberhauser, K. R. Nail, and S. Altizer, editors, *Monarchs in a Changing World: Biology and Conservation of an Iconic Butterfly*, pages 99–108. Cornell University Press, New York, NY, 2015. ISBN 978-0-8014-5559-9.

- S. Nakagawa, P. C. D. Johnson, and H. Schielzeth. The coefficient of determination R^2 and intra-class correlation coefficient from generalized linear mixed-effects models revisited and expanded. *Journal of The Royal Society Interface*, 14(134):20170213, 2017. doi: 10.1098/rsif.2017.0213.
- R. Neethiraj, E. A. Hornett, J. A. Hill, and C. W. Wheat. Investigating the genomic basis of discrete phenotypes using a Pool-Seq-only approach: New insights into the genetics underlying colour variation in diverse taxa. *Molecular Ecology*, 26(19):4990–5002, 2017. ISSN 1365-294X. doi: 10.1111/mec.14205.
- F. Neff, F. Korner-Nievergelt, E. Rey, M. Albrecht, K. Bollmann, F. Cahenzli, Y. Chittaro, M. M. Gossner, C. Martínez-Núñez, E. S. Meier, C. Monnerat, M. Moretti, T. Roth, F. Herzog, and E. Knop. Different roles of concurring climate and regional land-use changes in past 40 years' insect trends. *Nature Communications*, 13(1):7611, 2022. ISSN 2041-1723. doi: 10.1038/s41467-022-35223-3.
- T. Newbold, P. Oppenheimer, A. Etard, and J. J. Williams. Tropical and Mediterranean biodiversity is disproportionately sensitive to land-use and climate change. *Nature Ecology & Evolution*, 4(12):1630–1638, 2020. ISSN 2397-334X. doi: 10.1038/s41559-020-01303-0.
- V. Nguyen, Y. M. Buckley, R. Salguero-Gómez, and G. M. Wardle. Consequences of neglecting cryptic life stages from demographic models. *Ecological Modelling*, 408:108723, 2019. ISSN 0304-3800. doi: 10.1016/j.ecolmodel.2019.108723.
- C. C. Nice, M. L. Forister, J. G. Harrison, Z. Gompert, J. A. Fordyce, J. H. Thorne, D. P. Waetjen, and A. M. Shapiro. Extreme heterogeneity of population response to climatic variation and the limits of prediction. *Global Change Biology*, 25(6):2127–2136, 2019. ISSN 1365-2486. doi: <https://doi.org/10.1111/gcb.14593>.
- M. E. Nielsen, P. Lehmann, and K. Gotthard. Longer and warmer prewinter periods reduce post-winter fitness in a diapausing insect. *Functional Ecology*, 36(5):1151–1162, 2022. ISSN 1365-2435. doi: 10.1111/1365-2435.14037.
- S. Nieto-Sánchez, D. Gutiérrez, and R. J. Wilson. Long-term change and spatial variation in butterfly communities over an elevational gradient: Driven by climate, buffered by habitat. *Diversity and Distributions*, 21(8):950–961, 2015. ISSN 14724642. doi: 10.1111/ddi.12316.
- G. H. Nygren, A. Bergström, and S. Nylin. Latitudinal body size clines in the butterfly *Polyommatus icarus* are shaped by gene-environment interactions. *Journal of Insect Science*, 8(1):47, 2008. ISSN 1536-2442. doi: 10.1673/031.008.4701.
- N. Ohsaki. Comparative population studies of three *Pieris* butterflies, *P. rapae*, *P. melete* and *P. napi*, living in the same area: I. Ecological requirements for habitat resources in the adults. *Researches on Population Ecology*, 20(2):278–296, 1979. ISSN 0034-5466, 1438-390X. doi: 10.1007/BF02512633.

- N. Ohsaki. Comparative population studies of three *Pieris* butterflies, *P. rapae*, *P. melete* and *P. napi*, living in the same area. II. Utilization of patchy habitats by adults through migratory and non-migratory movements. *Population Ecology*, 22(1):163–183, 1980. ISSN 1438-3896. doi: 10.1007/BF02513543.
- N. Ohsaki. Comparative population studies of three *Pieris* butterflies, *P. rapae*, *P. melete* and *P. napi*, living in the same area: III. Difference in the annual generation numbers in relation to habitat selection by adults. *Researches on Population Ecology*, 24:193–210, 1982.
- N. Ohsaki and Y. Sato. Food Plant Choice of *Pieris* Butterflies as a Trade-Off between Parasitoid Avoidance and Quality of Plants. *Ecology*, 75(1):59–68, 1994. ISSN 00129658. doi: 10.2307/1939382.
- N. Ohsaki and Y. Sato. The role of parasitoids in evolution of habitat and larval food plant preference by three *Pieris* butterflies. *Researches on Population Ecology*, 41(1):107–119, 1999. ISSN 0034-5466. doi: 10.1007/PL00011975.
- T. H. Oliver, C. Stefanescu, F. Páramo, T. M. Brereton, and D. B. Roy. Latitudinal gradients in butterfly population variability are influenced by landscape heterogeneity. *Ecography*, 37(9):863–871, 2014. ISSN 16000587. doi: 10.1111/ecog.00608.
- T. H. Oliver, H. H. Marshall, M. D. Morecroft, T. M. Brereton, C. Prudhomme, and C. Huntingford. Interacting effects of climate change and habitat fragmentation on drought-sensitive butterflies. *Nature Climate Change*, 5(August):1–6, 2015. ISSN 1758-678X. doi: 10.1038/nclimate2746.
- M. Ørsted, L. B. Jørgensen, and J. Overgaard. Finding the right thermal limit: a framework to reconcile ecological, physiological and methodological aspects of CT_{max} in ectotherms. *Journal of Experimental Biology*, 225(19):jeb244514, 2022. ISSN 0022-0949. doi: 10.1242/jeb.244514.
- S. P. Otto and T. Day. *A Biologist's Guide to Mathematical Modeling in Ecology and Evolution*. Princeton University Press, Princeton, NJ, 2011. ISBN 978-1-4008-4091-5.
- C. L. Outhwaite, P. McCann, and T. Newbold. Agriculture and climate change are reshaping insect biodiversity worldwide. *Nature*, 605(7908):97–102, 2022. ISSN 1476-4687. doi: 10.1038/s41586-022-04644-x.
- G. Palmer, P. J. Platts, T. M. Brereton, J. W. Chapman, C. Dytham, R. Fox, J. W. Pearce-Higgins, D. B. Roy, J. K. Hill, and C. D. Thomas. Climate change, climatic variation and extreme biological responses. *Philosophical Transactions of the Royal Society B: Biological Sciences*, 372(1723):20160144, 2017. ISSN 14712970. doi: 10.1098/rstb.2016.0144.
- M. Paniw, P. F. Quintana-Ascencio, F. Ojeda, and R. Salguero-Gómez. Accounting for uncertainty in dormant life stages in stochastic demographic models. *Oikos*, 126(6):900–909, 2017. ISSN 1600-0706. doi: 10.1111/oik.03696.

- M. Paniw, D. Z. Childs, K. B. Armitage, D. T. Blumstein, J. G. A. Martin, M. K. Oli, and A. Ozgul. Assessing seasonal demographic covariation to understand environmental-change impacts on a hibernating mammal. *Ecology Letters*, 23(4):588–597, 2020. ISSN 1461-0248. doi: <https://doi.org/10.1111/ele.13459>.
- M. Paniw, D. García-Callejas, F. Lloret, R. D. Bassar, J. Travis, and O. Godoy. Pathways to global-change effects on biodiversity: new opportunities for dynamically forecasting demography and species interactions. *Proceedings of the Royal Society B: Biological Sciences*, 290(1993):20221494, 2023. doi: [10.1098/rspb.2022.1494](https://doi.org/10.1098/rspb.2022.1494).
- D. Pardo, S. Jenouvrier, H. Weimerskirch, and C. Barbraud. Effect of extreme sea surface temperature events on the demography of an age-structured albatross population. *Philosophical Transactions of the Royal Society B: Biological Sciences*, 372(1723):20160143, 2017. doi: [10.1098/rstb.2016.0143](https://doi.org/10.1098/rstb.2016.0143).
- C. Parmesan. Climate and species' range. *Nature*, 382(August):765, 1996.
- C. Parmesan. Ecological and Evolutionary Responses to Recent Climate Change. *Annual Review of Ecology, Evolution, and Systematics*, 37(1):637–669, 2006. ISSN 1543-592X, 1545-2069. doi: [10.1146/annurev.ecolsys.37.091305.110100](https://doi.org/10.1146/annurev.ecolsys.37.091305.110100).
- C. Parmesan. Influences of species, latitudes and methodologies on estimates of phenological response to global warming. *Global Change Biology*, 13(9):1860–1872, 2007. ISSN 1354-1013. doi: [10.1111/j.1365-2486.2007.01404.x](https://doi.org/10.1111/j.1365-2486.2007.01404.x).
- C. Parmesan and M. C. Singer. Mosaics of climatic stress across species' ranges: tradeoffs cause adaptive evolution to limits of climatic tolerance. *Philosophical Transactions of the Royal Society B: Biological Sciences*, 377(1848):20210003, 2022. doi: [10.1098/rstb.2021.0003](https://doi.org/10.1098/rstb.2021.0003).
- C. Parmesan and G. Yohe. A globally coherent fingerprint of climate change impacts across natural systems. *Nature*, 421(6918):37–42, 2003. ISSN 0028-0836. doi: [10.1038/nature01286](https://doi.org/10.1038/nature01286).
- C. Parmesan, N. Ryrholm, C. Stefanescu, J. K. Hill, C. D. Thomas, H. Descimon, B. Huntley, L. Kaila, J. Kullberg, T. Tammaru, W. J. Tennent, J. A. Thomas, and M. S. Warren. Poleward shifts in geographical ranges of butterfly species associated with regional warming. *Nature*, 399(June):579–583, 1999. ISSN 0028-0836. doi: [10.1038/21181](https://doi.org/10.1038/21181).
- C. Parmesan, T. L. Root, and M. R. Willig. Impacts of Extreme Weather and Climate on Terrestrial Biota. *Bulletin of the American Meteorological Society*, 81(3):443–450, 2000. ISSN 0003-0007, 1520-0477. doi: [10.1175/1520-0477\(2000\)081<0443:IOEWAC>2.3.CO;2](https://doi.org/10.1175/1520-0477(2000)081<0443:IOEWAC>2.3.CO;2).
- R. M. Pateman, C. D. Thomas, S. A. Hayward, and J. K. Hill. Macro- and microclimatic interactions can drive variation in species' habitat associations. *Global Change Biology*, 22(2):556–566, 2016. ISSN 13652486. doi: [10.1111/gcb.13056](https://doi.org/10.1111/gcb.13056).

- B. Petersen. Egg-laying and Habitat Selection in some *Pieris* Species (Lep.). *Entomologisk tidskrift*, 75(2-4):194–203, 1954.
- N. Pettorelli, N. A. J. Graham, N. Seddon, M. Maria da Cunha Bustamante, M. J. Lowton, W. J. Sutherland, H. J. Koldewey, H. C. Prentice, and J. Barlow. Time to integrate global climate change and biodiversity science-policy agendas. *Journal of Applied Ecology*, 58(11):2384–2393, 2021. ISSN 1365-2664. doi: 10.1111/1365-2664.13985.
- J. Peñuelas, J. Sardans, I. Filella, M. Estiarte, J. Llusà, R. Ogaya, J. Carnicer, M. Bartrons, A. Rivas-Ubach, O. Grau, G. Peguero, O. Margalef, S. Pla-Rabés, C. Stefanescu, D. Asensio, C. Preece, L. Liu, A. Verger, A. Barbeta, A. Achotegui-Castells, A. Gargallo-Garriga, D. Sperlich, G. Farré-Armengol, M. Fernández-Martínez, D. Liu, C. Zhang, I. Urbina, M. Camino-Serrano, M. Vives-Inglà, B. D. Stocker, M. Balzarolo, R. Guerrieri, M. Peaucelle, S. Marañón-Jiménez, K. Bórnez-Mejías, Z. Mu, A. Descals, A. Castellanos, and J. Terradas. Impacts of global change on Mediterranean forests and their services. *Forests*, 8(12):463, 2017. ISSN 19994907. doi: 10.3390/f8120463.
- J. L. Pick, S. Nakagawa, and D. W. A. Noble. Reproducible, flexible and high-throughput data extraction from primary literature: The `metaDigitise` package. *Methods in Ecology and Evolution*, 10(3):426–431, 2019. ISSN 2041-210X, 2041-210X. doi: 10.1111/2041-210X.13118.
- S. Pincebourde and J. Casas. Multitrophic Biophysical Budgets: Thermal Ecology of an Intimate Herbivore Insect-Plant Interaction. *Ecological Monographs*, 76(2):175–194, 2006. ISSN 0012-9615.
- S. Pincebourde and J. Casas. Narrow safety margin in the phyllosphere during thermal extremes. *Proceedings of the National Academy of Sciences*, 116(12):5588–5596, 2019. ISSN 0027-8424, 1091-6490. doi: 10.1073/pnas.1815828116.
- S. Pincebourde and C. Suppo. The Vulnerability of Tropical Ectotherms to Warming Is Modulated by the Microclimatic Heterogeneity. *Integrative and Comparative Biology*, 56(1):85–97, 2016. ISSN 1540-7063. doi: 10.1093/icb/icw014.
- S. Pincebourde and H. A. Woods. Climate uncertainty on leaf surfaces: The biophysics of leaf microclimates and their consequences for leaf-dwelling organisms. *Functional Ecology*, 26(4):844–853, 2012. ISSN 02698463. doi: 10.1111/j.1365-2435.2012.02013.x.
- S. Pincebourde and H. A. Woods. There is plenty of room at the bottom: microclimates drive insect vulnerability to climate change. *Current Opinion in Insect Science*, 41:63–70, 2020. ISSN 22145745. doi: 10.1016/j.cois.2020.07.001.
- S. Pincebourde, C. C. Murdock, M. Vickers, and M. W. Sears. Fine-scale microclimatic variation can shape the responses of organisms to global change in both natural and urban environments. *Integrative and Comparative Biology*, 56(1):45–61, 2016. ISSN 15577023. doi: 10.1093/icb/icw016.

- S. Pincebourde, M. E. Dillon, and H. A. Woods. Body size determines the thermal coupling between insects and plant surfaces. *Functional Ecology*, 35(7):1424–1436, 2021. ISSN 1365-2435. doi: 10.1111/1365-2435.13801.
- E. Pollard and T. J. Yates. *Monitoring Butterflies for Ecology and Conservation: The British Butterfly Monitoring Scheme*. Chapman & Hall, London, 1 edition, 1993. ISBN 0-412-63460-0.
- X. Pons. MiraMon. Geographical Information System and Remote Sensing Software. Version 4.4, 2002.
- H. Poorter, Ü. Niinemets, N. Ntagkas, A. Siebenkäs, M. Mäenpää, S. Matsubara, and T. Pons. A meta-analysis of plant responses to light intensity for 70 traits ranging from molecules to whole plant performance. *New Phytologist*, 223(3):1073–1105, 2019. ISSN 0028-646X, 1469-8137. doi: 10.1111/nph.15754.
- K. Porter. Eggs and egg-laying. In R. L. H. Dennis, editor, *Ecology of Butterflies in Britain*, pages 46–72. Oxford University Press, Inc., Oxford, 1992.
- W. P. Porter, J. W. Mitchell, W. A. Beckman, and C. B. DeWitt. Behavioral implications of mechanistic ecology: Thermal and behavioral modeling of desert ectotherms and their microenvironment. *Oecologia*, 13(1):1–54, 1973. ISSN 1432-1939. doi: 10.1007/BF00379617.
- D. Posledovich, T. Toftegaard, C. Wiklund, J. Ehrlén, and K. Gotthard. Latitudinal variation in diapause duration and post-winter development in two pierid butterflies in relation to phenological specialization. *Oecologia*, 177(1):181–190, 2015. ISSN 00298549. doi: 10.1007/s00442-014-3125-1.
- K. A. Potter, G. Davidowitz, and H. A. Woods. Insect eggs protected from high temperatures by limited homeothermy of plant leaves. *Journal of Experimental Biology*, 212:3448–3454, 2009. ISSN 0022-0949. doi: 10.1242/jeb.033365.
- K. A. Potter, H. Arthur Woods, and S. Pincebourde. Microclimatic challenges in global change biology. *Global Change Biology*, 19(10):2932–2939, 2013. ISSN 13541013. doi: 10.1111/gcb.12257.
- P. W. Price, R. F. Denno, M. D. Eubanks, D. L. Finke, and I. Kaplan. *Insect Ecology: Behavior, Populations and Communities*. Cambridge University Press, 1 edition, 2011. ISBN 978-0-521-83488-9 978-0-521-54260-9 978-0-511-97538-7. doi: 10.1017/CBO9780511975387.
- P. Pruischer, H. Larsdotter-Mellström, C. Stefanescu, S. Nylin, C. W. Wheat, and K. Gotthard. Sex-linked inheritance of diapause induction in the butterfly *Pieris napi*. *Physiological Entomology*, 42(3):257–265, 2017. ISSN 13653032. doi: 10.1111/phen.12194.
- P. Pruischer, S. Nylin, C. W. Wheat, and K. Gotthard. A region of the sex chromosome associated with population differences in diapause induction contains highly divergent

- alleles at clock genes. *Evolution*, 75(2):490–500, 2021. ISSN 0014-3820, 1558-5646. doi: 10.1111/evo.14151.
- R Core Team. R: A Language and Environment for Statistical Computing, 2019.
- R Core Team. *R: A Language and Environment for Statistical Computing*. R Foundation for Statistical Computing, Vienna, Austria, 2023.
- V. Radchuk, C. Turlure, and N. Schtickzelle. Each life stage matters: The importance of assessing the response to climate change over the complete life cycle in butterflies. *Journal of Animal Ecology*, 82(1):275–285, 2013. ISSN 00218790. doi: 10.1111/j.1365-2656.2012.02029.x.
- P. H. Raven and D. L. Wagner. Agricultural intensification and climate change are rapidly decreasing insect biodiversity. *Proceedings of the National Academy of Sciences*, 118(2): e2002548117, 2021. ISSN 0027-8424, 1091-6490. doi: 10.1073/pnas.2002548117.
- M. Rees and S. P. Ellner. Integral projection models for populations in temporally varying environments. *Ecological Monographs*, 79(4):575–594, 2009. ISSN 1557-7015. doi: <https://doi.org/10.1890/08-1474.1>.
- M. Rees, D. Childs, J. Metcalf, K. Rose, A. Sheppard, and P. Grubb. Seed Dormancy and Delayed Flowering in Monocarpic Plants: Selective Interactions in a Stochastic Environment. *The American Naturalist*, 168(2):E53–E71, 2006. ISSN 0003-0147. doi: 10.1086/505762.
- J. A. A. Renwick and C. D. Radke. Sensory cues in host selection for oviposition by the cabbage butterfly, *Pieris rapae*. *Journal of Insect Physiology*, 34(3):251–257, 1988. ISSN 00221910. doi: 10.1016/0022-1910(88)90055-8.
- E. L. Rezende and F. Bozinovic. Thermal performance across levels of biological organization. *Philosophical Transactions of the Royal Society B: Biological Sciences*, 374(1778): 20180549, 2019. ISSN 0962-8436. doi: 10.1098/rstb.2018.0549.
- E. L. Rezende and M. Santos. Comment on ‘Ecologically relevant measures of tolerance to potentially lethal temperatures’. *Journal of Experimental Biology*, 215(4):702–703, 2012. ISSN 0022-0949. doi: 10.1242/jeb.067835.
- E. L. Rezende, M. Tejedo, and M. Santos. Estimating the adaptive potential of critical thermal limits: methodological problems and evolutionary implications. *Functional Ecology*, 25(1):111–121, 2011. ISSN 1365-2435. doi: 10.1111/j.1365-2435.2010.01778.x.
- E. L. Rezende, L. E. Castañeda, and M. Santos. Tolerance landscapes in thermal ecology. *Functional Ecology*, 28(4):799–809, 2014. ISSN 13652435. doi: 10.1111/1365-2435.12268.
- E. L. Rezende, F. Bozinovic, A. Szilágyi, and M. Santos. Dataset and scripts from: Predicting temperature mortality and selection in natural *Drosophila* populations, 2020a. URL <http://datadryad.org/stash/dataset/doi:10.5061/dryad.stqjq2c1r>.

BIBLIOGRAPHY

- E. L. Rezende, F. Bozinovic, A. Szilágyi, and M. Santos. Predicting temperature mortality and selection in natural *Drosophila* populations. *Science*, 369(6508):1242–1245, 2020b. ISSN 0036-8075, 1095-9203. doi: 10.1126/science.aba9287.
- E. C. Rhodes. Population Mathematics—I. *Journal of the Royal Statistical Society*, 103(1):61–89, 1940. ISSN 2397-2335. doi: 10.1111/j.2397-2335.1940.tb01344.x.
- M. S. Romanov and V. B. Masterov. Low breeding performance of the Steller’s sea eagle (*Haliaeetus pelagicus*) causes the populations to decline. *Ecological Modelling*, 420:108877, 2020. ISSN 0304-3800. doi: 10.1016/j.ecolmodel.2019.108877.
- D. B. Roy and J. A. Thomas. Seasonal variation in the niche, habitat availability and population fluctuations of a bivoltine thermophilous insect near its range margin. *Oecologia*, 134(3):439–444, 2003. ISSN 0029-8549. doi: 10.1007/s00442-002-1121-3.
- D. M. Salcido, M. L. Forister, H. Garcia Lopez, and L. A. Dyer. Loss of dominant caterpillar genera in a protected tropical forest. *Scientific Reports*, 10(1):422, 2020. ISSN 2045-2322. doi: 10.1038/s41598-019-57226-9.
- A. L. Salgado and M. Saastamoinen. Developmental stage-dependent response and preference for host plant quality in an insect herbivore. *Animal Behaviour*, 150:27–38, 2019. ISSN 0003-3472. doi: 10.1016/j.anbehav.2019.01.018.
- M. Santos, L. E. Castañeda, and E. L. Rezende. Making sense of heat tolerance estimates in ectotherms: Lessons from *Drosophila*. *Functional Ecology*, 25(6):1169–1180, 2011. ISSN 02698463. doi: 10.1111/j.1365-2435.2011.01908.x.
- SAS Institute Inc. JMP 10, 2012.
- R. Schmucki, G. Pe’er, D. B. Roy, C. Stefanescu, C. A. Van Swaay, T. H. Oliver, M. Kuussaari, A. J. Van Strien, L. Ries, J. Settele, M. Musche, J. Carnicer, O. Schweiger, T. M. Brereton, A. Harpke, J. Heliölä, E. Kühn, and R. Julliard. A regionally informed abundance index for supporting integrative analyses across butterfly monitoring schemes. *Journal of Applied Ecology*, 53(2):501–510, 2016. ISSN 00218901. doi: 10.1111/1365-2664.12561.
- J. M. Scriber. Limiting effects of low leaf-water content on the nitrogen utilization, energy budget, and larval growth of *Hyalophora cecropia* (Lepidoptera: Saturniidae). *Oecologia*, 28(3):269–287, 1977. ISSN 1432-1939. doi: 10.1007/BF00751605.
- J. M. Scriber and F. Slansky. The Nutritional Ecology of Immature Insects. *Annual Review of Entomology*, 26(1):183–211, 1981. ISSN 0066-4170. doi: 10.1146/annurev.en.26.010181.001151.
- T. R. Seastedt and D. A. Crossley. The Influence of Arthropods on Ecosystems. *BioScience*, 34(3):157–161, 1984. ISSN 0006-3568. doi: 10.2307/1309750.

- S. Seibold, M. M. Gossner, N. K. Simons, N. Blüthgen, J. Müller, D. Ambarlı, C. Ammer, J. Bauhus, M. Fischer, J. C. Habel, K. E. Linsenmair, T. Naus, C. Penone, D. Prati, P. Schall, E.-D. Schulze, J. Vogt, S. Wöllauer, and W. W. Weisser. Arthropod decline in grasslands and forests is associated with landscape-level drivers. *Nature*, 574(7780):671–674, 2019. ISSN 1476-4687. doi: 10.1038/s41586-019-1684-3.
- S. I. Seneviratne, N. Nicholls, D. Easterling, C. M. Goodess, S. Kanae, J. Kossin, Y. Luo, J. Marengo, K. McInnes, M. Rahimi, M. Reichstein, A. Sorteberg, C. Vera, X. Zhang, M. Rusticucci, V. Semenov, L. V. Alexander, S. Allen, G. Benito, T. Cavazos, J. Clague, D. Conway, P. M. Della-Marta, M. Gerber, S. Gong, B. N. Goswami, M. Hemer, C. Huggel, B. van den Hurk, V. V. Kharin, A. Kitoh, A. M. K. Tank, G. Li, S. Mason, W. McGuire, G. J. van Oldenborgh, B. Orłowsky, S. Smith, W. Thiaw, A. Velegarakis, P. Yiou, T. Zhang, T. Zhou, and F. W. Zwiers. Changes in Climate Extremes and their Impacts on the Natural Physical Environment. In C. B. Field, V. Barros, T. F. Stocker, and Q. Dahe, editors, *Managing the Risks of Extreme Events and Disasters to Advance Climate Change Adaptation*, pages 109–230. Cambridge University Press, Cambridge, UK and New York, USA, 1 edition, 2012. ISBN 978-1-107-02506-6 978-1-107-60780-4 978-1-139-17724-5. doi: 10.1017/CBO9781139177245.006.
- S. I. Seneviratne, X. Zhang, M. Adnan, W. Badi, C. Dereczynski, A. Di Luca, S. Ghosh, I. Iskandar, J. Kossin, S. Lewis, F. Otto, I. Pinto, M. Satoh, S. M. Vicente-Serrano, M. Wehner, and B. Zhou. Weather and Climate Extreme Events in a Changing Climate. In V. Masson-Delmotte, P. Zhai, A. Pirani, S. L. Connors, C. Péan, S. Berger, N. Caud, Y. Chen, L. Goldfarb, M. Gomis, M. Huang, K. Leitzell, E. Lonnoy, J. Matthews, T. K. Maycock, T. Waterfield, O. Yelekçi, R. Yu, and B. Zhou, editors, *Climate Change 2021: The Physical Science Basis. Contribution of Working Group I to the Sixth Assessment Report of the Intergovernmental Panel on Climate Change*, pages 1513–1766. Cambridge University Press, Cambridge, UK and New York, USA, 2021.
- R. A. Senior, J. K. Hill, and D. P. Edwards. ThermStats: An R package for quantifying surface thermal heterogeneity in assessments of microclimates. *Methods in Ecology and Evolution*, 10(9):1606–1614, 2019. ISSN 2041-210X. doi: 10.1111/2041-210X.13257.
- M. Shafiei, A. P. Moczek, and H. F. Nijhout. Food availability controls the onset of metamorphosis in the dung beetle *Onthophagus taurus* (Coleoptera: Scarabaeidae). *Physiological Entomology*, 26(2):173–180, 2001. ISSN 1365-3032. doi: 10.1046/j.1365-3032.2001.00231.x.
- A. M. Shapiro. Phenotypic induction in *Pieris napi* L.: role of temperature and photoperiod in a coastal California population. *Ecological Entomology*, 2(3):217–224, 1977. ISSN 13652311. doi: 10.1111/j.1365-2311.1977.tb00884.x.
- A. M. Shapiro. The phenology of *Pieris napi microstriata* (Lepidoptera: Pieridae) during and after de 1975-77 California drought, and its evolutionary significance. *Psyche*, 86(1):1–10, 1979.

BIBLIOGRAPHY

- J. A. Sheridan and D. Bickford. Shrinking body size as an ecological response to climate change. *Nature Climate Change*, 1(8):401–406, 2011. ISSN 1758-6798. doi: 10.1038/nclimate1259.
- D. J. Shure, P. D. Mooreside, and S. M. Ogle. Rainfall Effects on Plant–Herbivore Processes in Anupland Oak Forest. *Ecology*, 79(2):604–617, 1998. ISSN 1939-9170. doi: 10.1890/0012-9658(1998)079[0604:REOPHP]2.0.CO;2.
- C. Simolo and S. Corti. Quantifying the role of variability in future intensification of heat extremes. *Nature Communications*, 13(1):7930, 2022. ISSN 2041-1723. doi: 10.1038/s41467-022-35571-0.
- M. C. Singer and C. Parmesan. Phenological asynchrony between herbivorous insects and their hosts: Signal of climate change or pre-existing adaptive strategy? *Philosophical Transactions of the Royal Society B: Biological Sciences*, 365(1555):3161–3176, 2010. ISSN 14712970. doi: 10.1098/rstb.2010.0144.
- F. Slansky and P. Feeny. Stabilization of the Rate of Nitrogen Accumulation by Larvae of the Cabbage Butterfly on Wild and Cultivated Food Plants. *Ecological Monographs*, 47(2):209–228, 1977.
- C. F. Soo Hoo and G. Fraenkel. The consumption, digestion, and utilization of food plants by a polyphagous insect, *Prodenia eridania* (Cramer). *Journal of Insect Physiology*, 12(6):711–730, 1966. ISSN 0022-1910. doi: 10.1016/0022-1910(66)90116-8.
- P. Soroye, T. Newbold, and J. Kerr. Climate change contributes to widespread declines among bumble bees across continents. *Science*, 367(6478):685–688, 2020. doi: 10.1126/science.aax8591.
- H. R. Spieth. Estivation and hibernation of *Pieris brassicae* (L.) in southern Spain: Synchronization of two complex behavioral patterns. *Population Ecology*, 44(3):273–280, 2002. ISSN 14383896. doi: 10.1007/s101440200031.
- H. R. Spieth and E. Schwarzer. Aestivation in *Pieris brassicae* (Lepidoptera: Pieridae): Implications for parasitism. *European Journal of Entomology*, 98(2):171–176, 2001. ISSN 18028829. doi: 10.14411/eje.2001.032.
- H. R. Spieth, U. Porschmann, and C. Teiwes. The occurrence of summer diapause in the large white butterfly *Pieris brassicae* (Lepidoptera: Pieridae): A geographical perspective. *European Journal of Entomology*, 108(3):377–384, 2011. ISSN 12105759. doi: 10.14411/eje.2011.047.
- J. Spinoni, P. Barbosa, E. Bucchignani, J. Cassano, T. Cavazos, J. H. Christensen, O. B. Christensen, E. Coppola, J. Evans, B. Geyer, F. Giorgi, P. Hadjinicolaou, D. Jacob, J. Katzfey, T. Koenigk, R. Laprise, C. J. Lennard, M. L. Kurnaz, D. Li, M. Llopart, N. McCormick, G. Naumann, G. Nikulin, T. Ozturk, H.-J. Panitz, R. P. d. Rocha, B. Rockel, S. A. Solman, J. Syktus, F. Tangang, C. Teichmann, R. Vautard, J. V. Vogt, K. Winger, G. Zittis, and A. Dosio. Future Global Meteorological Drought Hot Spots:

- A Study Based on CORDEX Data. *Journal of Climate*, 33(9):3635–3661, 2020. ISSN 0894-8755, 1520-0442. doi: 10.1175/JCLI-D-19-0084.1.
- C. Stefanescu. *Coronopus squamatus* (Forssk.) Asch. (Cruciferae), una nova planta nutricia per *Pieris rapae* (L.), *Pieris manni* May. i *Pieris napi* (L.) (Pieridae) als Aiguamolls de l'Empordà, amb notes addicionals sobre altres recursos tròfics. *Butlletí de la Societat Catalana de Lepidopterologia*, 80:26–29, 1997.
- C. Stefanescu. El Butterfly Monitoring Scheme en Catalunya: Los primeros cinco años. *Treballs de la Societat Catalana de Lepidopterologia*, 15:5–48, 2000.
- C. Stefanescu, J. Peñuelas, and I. Filella. Effects of climatic change on the phenology of butterflies in the northwest Mediterranean Basin. *Global Change Biology*, 9:1494–1506, 2003. ISSN 1354-1013. doi: 10.1046/j.1365-2486.2003.00682.x.
- C. Stefanescu, S. Herrando, and F. Páramo. Butterfly species richness in the north-west Mediterranean Basin: the role of natural and human-induced factors. *Journal of Biogeography*, 31(6):905–915, 2004. ISSN 03050270. doi: 10.1111/j.1365-2699.2004.01088.x.
- C. Stefanescu, J. Peñuelas, J. Sardans, and I. Filella. Females of the specialist butterfly *Euphydryas aurinia* (Lepidoptera: Nymphalinae: Melitaeini) select the greenest leaves of *Lonicera implexa* (Caprifoliaceae) for oviposition. *European Journal of Entomology*, 103(3):569–574, 2006. ISSN 12105759. doi: 10.14411/eje.2006.077.
- C. Stefanescu, J. Carnicer, and J. Peñuelas. Determinants of species richness in generalist and specialist Mediterranean butterflies: The negative synergistic forces of climate and habitat change. *Ecography*, 34(3):353–363, 2011a. ISSN 09067590. doi: 10.1111/j.1600-0587.2010.06264.x.
- C. Stefanescu, I. Torre, J. Jubany, and F. Páramo. Recent trends in butterfly populations from north-east Spain and Andorra in the light of habitat and climate change. *Journal of Insect Conservation*, 15(1):83–93, 2011b. ISSN 1366638X. doi: 10.1007/s10841-010-9325-z.
- C. Stefanescu, P. Colom, J. M. Barea-Azcón, D. Horsfield, B. Komac, A. Miralles, M. R. Shaw, A. Ubach, and D. Gutiérrez. Larval parasitism in a specialist herbivore is explained by phenological synchrony and host plant availability. *Journal of Animal Ecology*, 91(5):1010–1023, 2022. ISSN 1365-2656. doi: 10.1111/1365-2656.13689.
- N. C. Stenseth, K.-S. Chan, G. Tavecchia, T. Coulson, A. Mysterud, T. H. Clutton-Brock, and B. T. Grenfell. Modelling non-additive and nonlinear signals from climatic noise in ecological time series: Soay sheep as an example. *Proceedings of the Royal Society B: Biological Sciences*, 271(1552):1985–1993, 2004. ISSN 14712970. doi: 10.1098/rspb.2004.2794.
- N. E. Stork. How Many Species of Insects and Other Terrestrial Arthropods Are There on Earth? *Annual Review of Entomology*, 63(1):31–45, 2018. ISSN 0066-4170, 1545-4487. doi: 10.1146/annurev-ento-020117-043348.

- I. Stott, S. Townley, D. Carslake, and D. J. Hodgson. On reducibility and ergodicity of population projection matrix models. *Methods in Ecology and Evolution*, 1(3):242–252, 2010. ISSN 2041210X. doi: 10.1111/j.2041-210X.2010.00032.x.
- I. Stott, D. J. Hodgson, and S. Townley. popdemo: an R package for population demography using projection matrix analysis. *Methods in Ecology and Evolution*, 3(5): 797–802, 2012. ISSN 2041210X. doi: 10.1111/j.2041-210X.2012.00222.x.
- P. Stoutjesdijk and J. J. Barkman. *Microclimate, Vegetation & Fauna*. KNNV Publishing, 2014. ISBN 978-90-5011-545-2.
- A. J. Suggitt, P. K. Gillingham, J. K. Hill, B. Huntley, W. E. Kunin, D. B. Roy, and C. D. Thomas. Habitat microclimates drive fine-scale variation in extreme temperatures. *Oikos*, 120(1):1–8, 2011. ISSN 00301299. doi: 10.1111/j.1600-0706.2010.18270.x.
- A. J. Suggitt, C. Stefanescu, F. Páramo, T. H. Oliver, B. J. Anderson, J. K. Hill, D. B. Roy, T. M. Brereton, and C. D. Thomas. Habitat associations of species show consistent but weak responses to climate. *Biology Letters*, 8(April):590–593, 2012. doi: 10.1098/rsbl.2012.0112.
- A. J. Suggitt, R. J. Wilson, T. A. August, R. Fox, N. J. B. Isaac, N. A. Macgregor, M. D. Morecroft, and I. M. D. Maclean. Microclimate affects landscape level persistence in the British Lepidoptera. *Journal of Insect Conservation*, 19(2):237–253, 2015. ISSN 15729753. doi: 10.1007/s10841-014-9749-y.
- A. J. Suggitt, P. J. Platts, I. M. Barata, J. J. Bennie, M. D. Burgess, N. Bystrakova, S. J. Duffield, S. R. Ewing, P. K. Gillingham, A. B. Harper, A. J. Hartley, D. L. Hemming, I. M. D. Maclean, K. Maltby, H. H. Marshall, M. D. Morecroft, J. W. Pearce-Higgins, P. Pearce-Kelly, A. B. Phillimore, J. T. Price, A. Pyke, J. E. Stewart, R. Warren, and J. K. Hill. Conducting robust ecological analyses with climate data. *Oikos*, 126(11):1533–1541, 2017. ISSN 16000706. doi: 10.1111/oik.04203.
- A. J. Suggitt, R. J. Wilson, N. J. B. Isaac, C. M. Beale, A. G. Auffret, T. A. August, J. J. Bennie, H. Q. P. Crick, S. J. Duffield, R. Fox, J. J. Hopkins, N. A. Macgregor, M. D. Morecroft, K. J. Walker, and I. M. D. Maclean. Extinction risk from climate change is reduced by microclimatic buffering. *Nature Climate Change*, 8(8):713–717, 2018. ISSN 17586798. doi: 10.1038/s41558-018-0231-9.
- J. M. Sunday, A. E. Bates, M. R. Kearney, R. K. Colwell, N. K. Dulvy, J. T. Longino, and R. B. Huey. Thermal-safety margins and the necessity of thermoregulatory behavior across latitude and elevation. *Proceedings of the National Academy of Sciences*, 111(15): 5610–5615, 2014. ISSN 0027-8424. doi: 10.1073/pnas.1316145111.
- J. Sunde, M. Franzén, P.-E. Betzholtz, Y. Francioli, L. B. Pettersson, J. Pöyry, N. Ryrholm, and A. Forsman. Century-long butterfly range expansions in northern Europe depend on climate, land use and species traits. *Communications Biology*, 6(1):601, 2023. ISSN 2399-3642. doi: 10.1038/s42003-023-04967-z.

- R. T. Sutton. ESD Ideas: a simple proposal to improve the contribution of IPCC WGI to the assessment and communication of climate change risks. *Earth System Dynamics*, 9(4):1155–1158, 2018. ISSN 2190-4979. doi: 10.5194/esd-9-1155-2018.
- N. N. Taleb. *The black swan: the impact of the highly improbable*. Random House, New York, 1st ed edition, 2007. ISBN 978-1-4000-6351-2.
- W. Talloen, S. Van Dongen, H. Van Dyck, and L. Lens. Environmental stress and quantitative genetic variation in butterfly wing characteristics. *Evolutionary Ecology*, 23(3): 473–485, 2009. ISSN 1573-8477. doi: 10.1007/s10682-008-9246-4.
- S. J. Thackeray, T. H. Sparks, M. Frederiksen, S. Burthe, P. J. Bacon, J. R. Bell, M. S. Botham, T. M. Brereton, P. W. Bright, L. Carvalho, T. H. Clutton-Brock, A. Dawson, M. Edwards, J. M. Elliot, R. Harrington, D. Johns, I. D. Jones, J. T. Jones, D. I. Leech, D. B. Roy, W. A. Scott, M. Smith, R. J. Smithers, I. J. Winfield, and S. Wanless. Trophic level asynchrony in rates of phenological change for marine, freshwater and terrestrial environments. *Global Change Biology*, 16(12):3304–3313, 2010. ISSN 13541013. doi: 10.1111/j.1365-2486.2010.02165.x.
- T. Tolman and R. Lewington. *Collins butterfly guide*. Collins, London, 3 edition, 2009. ISBN 978-0-00-727977-7.
- J. Tsuji and L. Coe. Effects of Foliage Color on the Landing Response of *Pieris rapae* (Lepidoptera: Pieridae). *Environmental Entomology*, 43(4):989–994, 2014. ISSN 0046-225X. doi: 10.1603/EN14084.
- M. Tuomaala, A. Kaitala, and R. L. Rutowski. Females show greater changes in wing colour with latitude than males in the green-veined white butterfly, *Pieris napi* (Lepidoptera: Pieridae). *Biological Journal of the Linnean Society*, 107(4):899–909, 2012. ISSN 00244066. doi: 10.1111/j.1095-8312.2012.01996.x.
- C. Turney, A.-G. Ausseil, and L. Broadhurst. Urgent need for an integrated policy framework for biodiversity loss and climate change. *Nature Ecology & Evolution*, 4(8):996–996, 2020. ISSN 2397-334X. doi: 10.1038/s41559-020-1242-2.
- A. Ubach, F. Páramo, C. Gutiérrez, and C. Stefanescu. Vegetation encroachment drives changes in the composition of butterfly assemblages and species loss in Mediterranean ecosystems. *Insect Conservation and Diversity*, 13(2):151–161, 2019. ISSN 1752-458X. doi: 10.1111/icad.12397.
- A. Ubach, F. Páramo, and C. Stefanescu. Heterogeneidad en las respuestas demográficas asociadas al gradiente altitudinal: el caso de las mariposas en el noreste ibérico. *Ecossistemas*, 30(1):2148–2148, 2021. ISSN 1697-2473. doi: 10.7818/ECOS.2148.
- A. Ubach, F. Páramo, M. Prohom, and C. Stefanescu. Weather and butterfly responses: a framework for understanding population dynamics in terms of species' life-cycles and extreme climatic events. *Oecologia*, 199:427–439, 2022. ISSN 1432-1939. doi: 10.1007/s00442-022-05188-7.

BIBLIOGRAPHY

- B. Uhl, M. Wölfling, and C. Bässler. Mediterranean moth diversity is sensitive to increasing temperatures and drought under climate change. *Scientific Reports*, 12(1):14473, 2022. ISSN 2045-2322. doi: 10.1038/s41598-022-18770-z.
- M. C. Urban. Projecting biological impacts from climate change like a climate scientist. *WIREs Climate Change*, 10(4):e585, 2019. ISSN 1757-7799. doi: 10.1002/wcc.585.
- M. C. Urban, G. Bocedi, A. P. Hendry, J. B. Mihoub, G. Pe'er, A. Singer, J. R. Bridle, L. G. Crozier, L. De Meester, W. Godsoe, A. Gonzalez, J. J. Hellmann, R. D. Holt, A. Huth, K. Johst, C. B. Krug, P. W. Leadley, S. C. Palmer, J. H. Pantel, A. Schmitz, P. A. Zollner, and J. M. Travis. Improving the forecast for biodiversity under climate change. *Science*, 353(6304):aad8466, 2016. ISSN 10959203. doi: 10.1126/science.aad8466.
- M. C. Urban, J. M. J. Travis, D. Zurell, P. L. Thompson, N. W. Synes, A. Scarpa, P. R. Peres-Neto, A.-K. Malchow, P. M. A. James, D. Gravel, L. De Meester, C. Brown, G. Bocedi, C. H. Albert, A. Gonzalez, and A. P. Hendry. Coding for Life: Designing a Platform for Projecting and Protecting Global Biodiversity. *BioScience*, 72(1): 91–104, 2022. ISSN 0006-3568. doi: 10.1093/biosci/biab099.
- M. C. Urban, C. P. Nadeau, and S. T. Giery. Using mechanistic insights to predict the climate-induced expansion of a key aquatic predator. *Ecological Monographs*, 93(3): e1575, 2023. ISSN 1557-7015. doi: 10.1002/ecm.1575.
- J. O. S. Valim, N. C. Teixeira, N. A. Santos, M. G. A. Oliveira, and W. G. Campos. Drought-induced acclimatization of a fast-growing plant decreases insect performance in leaf-chewing and sap-sucking guilds. *Arthropod-Plant Interactions*, 10(4):351–363, 2016. ISSN 1872-8847. doi: 10.1007/s11829-016-9440-1.
- E. van Bergen, T. Dallas, M. F. DiLeo, A. Kahilainen, A. L. K. Mattila, M. Luoto, and M. Saastamoinen. The effect of summer drought on the predictability of local extinctions in a butterfly metapopulation. *Conservation Biology*, 34(6):1503–1511, 2020. ISSN 1523-1739. doi: 10.1111/cobi.13515.
- M. van de Pol, S. Jenouvrier, J. H. C. Cornelissen, and M. E. Visser. Behavioural, ecological and evolutionary responses to extreme climatic events: challenges and directions. *Philosophical Transactions of the Royal Society B: Biological Sciences*, 372(1723):20160134, 2017. doi: 10.1098/rstb.2016.0134.
- J. P. van der Sluijs. Insect decline, an emerging global environmental risk. *Current Opinion in Environmental Sustainability*, 46:39–42, 2020. ISSN 1877-3435. doi: 10.1016/j.cosust.2020.08.012.
- R. van Klink, D. E. Bowler, K. B. Gongalsky, A. B. Swengel, A. Gentile, and J. M. Chase. Erratum for the Report “Meta-analysis reveals declines in terrestrial but increases in freshwater insect abundances” by R. Van Klink, D. E. Bowler, K. B. Gongalsky, A. B. Swengel, A. Gentile, J. M. Chase. *Science*, 370(6515):eabf1915, 2020a. doi: 10.1126/science.abf1915.

- R. van Klink, D. E. Bowler, K. B. Gongalsky, A. B. Swengel, A. Gentile, and J. M. Chase. Meta-analysis reveals declines in terrestrial but increases in freshwater insect abundances. *Science*, 368(6489):417–420, 2020b. ISSN 0036-8075, 1095-9203. doi: 10.1126/science.aax9931.
- A. J. van Strien, C. A. M. van Swaay, W. T. van Strien-van Liempt, M. J. Poot, and M. F. WallisDeVries. Over a century of data reveal more than 80% decline in butterflies in the Netherlands. *Biological Conservation*, 234:116–122, 2019. ISSN 0006-3207. doi: 10.1016/J.BIOCON.2019.03.023.
- C. A. M. van Swaay, P. Nowicki, J. Settele, and A. J. van Strien. Butterfly monitoring in Europe: methods, applications and perspectives. *Biodiversity and Conservation*, 17(14):3455–3469, 2008. ISSN 0960-3115. doi: 10.1007/s10531-008-9491-4.
- C. A. M. van Swaay, A. Cuttelod, S. Collins, D. Maes, M. López Munguira, M. Šašić, J. Settele, R. Verovnik, T. Verstrael, M. S. Warren, M. Wiemers, and I. Wynhoff. *European red list of butterflies*. Publications Office of the European Union, Luxembourg, 2010. ISBN 978-92-79-14151-5. doi: 10.2779/83897.
- C. A. M. van Swaay, E. B. Dennis, R. Schmucki, C. Sevilleja, M. Balalaikins, M. S. Botham, N. A. D. Bourn, T. M. Brereton, J. P. Cancela, B. Carlisle, P. Chambers, S. Collins, C. Dopagne, R. Escobés, R. Feldmann, J. M. Fernández-García, B. Fontaine, A. Garcianteparaluceta, C. Harrower, A. Harpke, J. Heliölä, B. Komac, E. Kühn, A. Lang, D. Maes, X. Mestdagh, I. Middlebrook, Y. Monasterio, M. L. Munguira, T. E. Murray, M. Musche, E. Ōunap, F. Páramo, L. B. Pettersson, J. Piqueray, J. Settele, C. Stefanescu, G. Švitra, A. Tiitsaar, R. Verovnik, M. S. Warren, I. Wynhoff, and D. B. Roy. The EU Butterfly Indicator for Grassland species: 1990-2017: Technical Report. Technical report, Butterfly Conservation Europe, 2019.
- R. Vila, C. Stefanescu, and J. M. Sesma. *Guia de les papallones diürnes de Catalunya*. Lynx Edicions, Bellaterra, first edition, 2018. ISBN 978-84-16728-06-0.
- M. Vives-Inгла, C. Stefanescu, J. Sala-Garcia, and J. Carnicer. Plastic and phenological variation of host plants mediates local responses of the butterfly *Pieris napi* to drought in the Mediterranean basin. In C. Stefanescu and T. Lafranchis, editors, *Butterfly and moths in l'Empordà and their response to global change*, volume 12, pages 113–129. Recerca i Territori, 2020.
- M. Vives-Inгла, J. Sala-Garcia, C. Stefanescu, A. Casadó-Tortosa, M. Garcia, J. Peñuelas, and J. Carnicer. mvives-ingla/ecotones: Interspecific differences in microhabitat use expose insects to contrasting thermal mortality, 2022. URL <https://zenodo.org/record/7358091>.
- M. Vives-Inгла, J. Sala-Garcia, C. Stefanescu, A. Casadó-Tortosa, M. Garcia, J. Peñuelas, and J. Carnicer. Interspecific differences in microhabitat use expose insects to contrasting thermal mortality. *Ecological Monographs*, 93(2):e1561, 2023.

- M. M. Vogel, M. Hauser, and S. I. Seneviratne. Projected changes in hot, dry and wet extreme events' clusters in CMIP6 multi-model ensemble. *Environmental Research Letters*, 15(9):094021, 2020. ISSN 1748-9326. doi: 10.1088/1748-9326/ab90a7.
- G. von Arx, E. Graf Pannatier, A. Thimonier, and M. Rebetez. Microclimate in forests with varying leaf area index and soil moisture: potential implications for seedling establishment in a changing climate. *Journal of Ecology*, 101(5):1201–1213, 2013. ISSN 00220477. doi: 10.1111/1365-2745.12121.
- J. von Oppen, J. J. Assmann, A. D. Bjorkman, U. A. Treier, B. Elberling, J. Nabe-Nielsen, and S. Normand. Cross-scale regulation of seasonal microclimate by vegetation and snow in the Arctic tundra. *Global Change Biology*, 28(24):7296–7312, 2022. ISSN 1365-2486. doi: 10.1111/gcb.16426.
- L. von Schmalensee, K. H. Gunnarsdóttir, J. Näslund, K. Gotthard, and P. Lehmann. Thermal performance under constant temperatures can accurately predict insect development times across naturally variable microclimates. *Ecology Letters*, 24:1633–1645, 2021a. ISSN 1461-0248. doi: <https://doi.org/10.1111/ele.13779>.
- L. von Schmalensee, K. Hulda Gunnarsdóttir, J. Näslund, K. Gotthard, and P. Lehmann. Thermal performance under constant temperatures can accurately predict insect development times across naturally variable microclimates, 2021b. URL <http://datadryad.org/stash/dataset/doi:10.5061/dryad.gtht76hm5>.
- L. von Schmalensee, P. Caillault, K. H. Gunnarsdóttir, K. Gotthard, and P. Lehmann. Seasonal specialization drives divergent population dynamics in two closely related butterflies. *Nature Communications*, 14(1):3663, 2023. ISSN 2041-1723. doi: 10.1038/s41467-023-39359-8.
- P. Välimäki, A. Kaitala, and H. Kokko. Temporal patterns in reproduction may explain variation in mating frequencies in the green-veined white butterfly *Pieris napi*. *Behavioral Ecology and Sociobiology*, 61(1):99–107, 2006. ISSN 1432-0762. doi: 10.1007/s00265-006-0240-y.
- P. Välimäki, S. M. Kivelä, L. Jääskeläinen, A. Kaitala, V. Kaitala, and J. Oksanen. Divergent timing of egg-laying may maintain life history polymorphism in potentially multivoltine insects in seasonal environments. *Journal of Evolutionary Biology*, 21(6):1711–1723, 2008. ISSN 1420-9101. doi: 10.1111/j.1420-9101.2008.01597.x.
- D. L. Wagner. Insect Declines in the Anthropocene. *Annual Review of Entomology*, 65(1):457–480, 2020. ISSN 0066-4170. doi: 10.1146/annurev-ento-011019-025151.
- D. L. Wagner, R. Fox, D. M. Salcido, and L. A. Dyer. A window to the world of global insect declines: Moth biodiversity trends are complex and heterogeneous. *Proceedings of the National Academy of Sciences*, 118(2):e2002549117, 2021a. ISSN 0027-8424, 1091-6490. doi: 10.1073/pnas.2002549117.

- D. L. Wagner, E. M. Grames, M. L. Forister, M. R. Berenbaum, and D. Stopak. Insect decline in the Anthropocene: Death by a thousand cuts. *Proceedings of the National Academy of Sciences*, 118(2):e2023989118, 2021b. ISSN 0027-8424, 1091-6490. doi: 10.1073/pnas.2023989118.
- N. Wahlberg, J. Rota, M. F. Braby, N. E. Pierce, and C. W. Wheat. Revised systematics and higher classification of pierid butterflies (Lepidoptera: Pieridae) based on molecular data. *Zoologica Scripta*, 43(6):641–650, 2014. ISSN 1463-6409. doi: 10.1111/zsc.12075.
- A. Wallberg, F. Han, G. Wellhagen, B. Dahle, M. Kawata, N. Haddad, Z. L. P. Simões, M. H. Allsopp, I. Kandemir, P. De la Rúa, C. W. Pirk, and M. T. Webster. A worldwide survey of genome sequence variation provides insight into the evolutionary history of the honeybee *Apis mellifera*. *Nature Genetics*, 46(10):1081–1088, 2014. ISSN 1546-1718. doi: 10.1038/ng.3077.
- M. F. WallisDeVries and C. A. M. van Swaay. A nitrogen index to track changes in butterfly species assemblages under nitrogen deposition. *Biological Conservation*, 212:448–453, 2017. ISSN 00063207. doi: 10.1016/j.biocon.2016.11.029.
- M. S. Warren, E. Pollard, and T. J. Bibby. Annual and Long-Term Changes in a Population of the Wood White Butterfly *Leptidea sinapis*. *Journal of Animal Ecology*, 55(2): 707–719, 1986. ISSN 0021-8790. doi: 10.2307/4749.
- M. S. Warren, D. Maes, C. A. M. van Swaay, P. Goffart, H. Van Dyck, N. A. D. Bourn, I. Wynhoff, D. Hoare, and S. Ellis. The decline of butterflies in Europe: Problems, significance, and possible solutions. *Proceedings of the National Academy of Sciences*, 118(2):e2002551117, 2021. ISSN 0027-8424, 1091-6490. doi: 10.1073/pnas.2002551117.
- M. T. Webster, A. Beaurepaire, P. Neumann, and E. Stolle. Population Genomics for Insect Conservation. *Annual Review of Animal Biosciences*, 11(1):115–140, 2023. ISSN 2165-8102, 2165-8110. doi: 10.1146/annurev-animal-122221-075025.
- N. Wedell, C. Wiklund, and P. A. Cook. Monandry and polyandry as alternative lifestyles in a butterfly. *Behavioral Ecology*, 13(4):450–455, 2002. ISSN 1045-2249. doi: 10.1093/beheco/13.4.450.
- W. W. Weisser and E. Siemann, editors. *Insects and ecosystem function*. Number 173 in Ecological studies. Springer, Berlin, 2007. ISBN 978-3-540-74003-2.
- C. Wiklund and A. Kaitala. Sexual selection for large male size in a polyandrous butterfly: the effect of body size on male versus female reproductive success in *Pieris napi*. *Behavioral Ecology*, 6(1):6–13, 1995. ISSN 1045-2249. doi: 10.1093/beheco/6.1.6.
- C. Wiklund, A. Kaitala, V. Lindfors, and J. Abenius. Polyandry and its effects on female reproduction in the green-veined butterfly (*Pieris napi* L.). *Behavioral Ecology and Sociobiology*, 33:25–33, 1993. doi: 10.1007/BF00164343.

- C. Wiklund, A. Kaitala, and N. Wedell. Decoupling of reproductive rates and parental expenditure in a polyandrous butterfly. *Behavioral Ecology*, 9(1):20–25, 1998. ISSN 1045-2249. doi: 10.1093/beheco/9.1.20.
- J. Wild, M. Kopecký, M. Macek, M. Šanda, J. Jankovec, and T. Haase. Climate at ecologically relevant scales: A new temperature and soil moisture logger for long-term microclimate measurement. *Agricultural and Forest Meteorology*, 268:40–47, 2019. ISSN 0168-1923. doi: 10.1016/j.agrformet.2018.12.018.
- S. E. Williams, L. P. Shoo, J. L. Isaac, A. A. Hoffmann, and G. Langham. Towards an Integrated Framework for Assessing the Vulnerability of Species to Climate Change. *PLOS Biology*, 6(12):e325, 2008. ISSN 1545-7885. doi: 10.1371/journal.pbio.0060325.
- R. J. Wilson, D. Gutiérrez, J. Gutiérrez, D. Martínez, R. Agudo, and V. J. Monserrat. Changes to the elevational limits and extent of species ranges associated with climate change. *Ecology Letters*, 8(11):1138–1146, 2005. ISSN 1461023X. doi: 10.1111/j.1461-0248.2005.00824.x.
- R. J. Wilson, D. Gutiérrez, J. Gutiérrez, and V. J. Monserrat. An elevational shift in butterfly species richness and composition accompanying recent climate change. *Global Change Biology*, 13(9):1873–1887, 2007. ISSN 13541013. doi: 10.1111/j.1365-2486.2007.01418.x.
- J. L. Wolfson. Oviposition response of *Pieris rapae* to environmentally induced variation in *Brassica nigra*. *Entomologia Experimentalis et Applicata*, 27(3):223–232, 1980. ISSN 0013-8703. doi: 10.1111/j.1570-7458.1980.tb02969.x.
- R. A. Wood, M. Crucifix, T. M. Lenton, K. J. Mach, C. Moore, M. New, S. Sharpe, T. F. Stocker, and R. T. Sutton. A Climate Science Toolkit for High Impact-Low Likelihood Climate Risks. *Earth's Future*, 11(4):e2022EF003369, 2023. ISSN 2328-4277. doi: 10.1029/2022EF003369.
- H. A. Woods. Water loss and gas exchange by eggs of *Manduca sexta*: Trading off costs and benefits. *Journal of Insect Physiology*, 56(5):480–487, 2010. ISSN 0022-1910. doi: 10.1016/j.jinsphys.2009.05.020.
- H. A. Woods. Ontogenetic changes in the body temperature of an insect herbivore. *Functional Ecology*, 27(6):1322–1331, 2013. ISSN 1365-2435. doi: 10.1111/1365-2435.12124.
- H. A. Woods, M. E. Dillon, and S. Pincebourde. The roles of microclimatic diversity and of behavior in mediating the responses of ectotherms to climate change. *Journal of Thermal Biology*, 54:86–97, 2015. ISSN 0306-4565. doi: 10.1016/j.jtherbio.2014.10.002.
- H. A. Woods, G. Legault, J. G. Kingsolver, S. Pincebourde, A. A. Shah, and B. G. Larkin. Climate-driven thermal opportunities and risks for leaf miners in aspen canopies. *Ecological Monographs*, 92(4):e1544, 2022. ISSN 1557-7015. doi: 10.1002/ecm.1544.

- I. J. Wright, P. B. Reich, M. Westoby, D. D. Ackerly, Z. Baruch, F. Bongers, J. Cavender-Bares, T. Chapin, J. H. C. Cornelissen, M. Diemer, J. Flexas, E. Garnier, P. K. Groom, J. Gullias, K. Hikosaka, B. B. Lamont, T. Lee, W. Lee, C. Lusk, J. J. Midgley, M.-L. Navas, Ü. Niinemets, J. Oleksyn, N. Osada, H. Poorter, P. Poot, L. Prior, V. I. Pyankov, C. Roumet, S. C. Thomas, M. G. Tjoelker, E. J. Veneklaas, and R. Villar. The worldwide leaf economics spectrum. *Nature*, 428(6985):821–827, 2004. ISSN 1476-4687. doi: 10.1038/nature02403.
- H.-J. Xiao, D. Yang, and F.-S. Xue. Effect of photoperiod on the duration of summer and winter diapause in the cabbage butterfly, *Pieris melete* (Lepidoptera: Pieridae). *European Journal of Entomology*, 103(3):537–540, 2006. ISSN 1210-5759, 1802-8829. doi: 10.14411/eje.2006.071.
- F.-S. Xue, H. G. Kallenborn, and H.-Y. Wei. Summer and winter diapause in pupae of the cabbage butterfly, *Pieris melete* Ménétriés. *Journal of Insect Physiology*, 43(8):701–707, 1997. ISSN 00221910. doi: 10.1016/S0022-1910(97)00053-X.
- M. Yamamoto. Comparison of Population Dynamics of Two Pierid Butterflies, *Pieris rapae crucivora* and *P. napi nesis*, Living in the Same Area and Feeding on the Same Plant in Sapporo, Northern Japan. *Journal of the Faculty of Science, Hokkaido University. Zoology*, 22(3):202–249, 1981. ISSN 0368-2188.
- M. Yamamoto. Microhabitat Segregation in Two Closely Related Pierid Butterflies. *Japanese Journal of Ecology*, 33(3):263–270, 1983. doi: 10.18960/seitai.33.3_263.
- L. H. Yang, E. G. Postema, T. E. Hayes, M. K. Lippey, and D. J. MacArthur-Waltz. The complexity of global change and its effects on insects. *Current Opinion in Insect Science*, 47:90–102, 2021. ISSN 2214-5745. doi: 10.1016/j.cois.2021.05.001.
- F. Zellweger, P. De Frenne, J. Lenoir, D. Rocchini, and D. A. Coomes. Advances in Microclimate Ecology Arising from Remote Sensing. *Trends in Ecology & Evolution*, 34(4):327–341, 2019. ISSN 0169-5347. doi: 10.1016/J.TREE.2018.12.012.
- F. Zellweger, P. De Frenne, J. Lenoir, P. Vangansbeke, K. Verheyen, M. Bernhardt-Römermann, L. Baeten, R. Hédli, I. Berki, J. Brunet, H. Van Calster, M. Chudomelová, G. Decocq, T. Dirnböck, T. Durak, T. Heinken, B. Jaroszewicz, M. Kopecký, F. Máliš, M. Macek, M. Malicki, T. Naaf, T. A. Nagel, A. Ortmann-Ajkai, P. Petřík, R. Pielech, K. Reczyńska, W. Schmidt, T. Standovár, K. Świerkosz, B. Teleki, O. Vild, M. Wulf, and D. Coomes. Forest microclimate dynamics drive plant responses to warming. *Science*, 368(6492):772–775, 2020. ISSN 0036-8075. doi: 10.1126/science.aba6880.
- Z.-Q. Zhang. Animal biodiversity: An update of classification and diversity in 2013. In: Zhang, Z.-Q. (Ed.) *Animal Biodiversity: An Outline of Higher-level Classification and Survey of Taxonomic Richness (Addenda 2013)*. *Zootaxa*, 3703(1):5–11, 2013a. ISSN 1175-5334, 1175-5326. doi: 10.11646/zootaxa.3703.1.3.

BIBLIOGRAPHY

- Z.-Q. Zhang. Phylum Arthropoda. *In*: Zhang, Z.-Q. (Ed.) *Animal Biodiversity: An Outline of Higher-level Classification and Survey of Taxonomic Richness* (Addenda 2013). *Zootaxa*, 3703(1):17–26, 2013b. ISSN 1175-5334. doi: 10.11646/zootaxa.3703.1.6.
- K. Zografou, V. Kati, A. Grill, R. J. Wilson, E. Tzirkalli, L. N. Pamperis, and J. M. Halley. Signals of Climate Change in Butterfly Communities in a Mediterranean Protected Area. *PLoS ONE*, 9(1):e87245, 2014. ISSN 1932-6203. doi: 10.1371/journal.pone.0087245.
- J. Zscheischler, S. Westra, B. J. J. M. van den Hurk, S. I. Seneviratne, P. J. Ward, A. Pitman, A. AghaKouchak, D. N. Bresch, M. Leonard, T. Wahl, and X. Zhang. Future climate risk from compound events. *Nature Climate Change*, 8(6):469–477, 2018. ISSN 1758-6798. doi: 10.1038/s41558-018-0156-3.
- A. F. Zuur, E. N. Ieno, N. J. Walker, A. A. Saveliev, and G. M. Smith. *Mixed Effects Models and Extensions in Ecology with R*. Springer Science+Business Media, New York, 2009. ISBN 978-0-387-87457-9. doi: 10.1007/978-0-387-87458-6.



